NASA Conference Publication 2211

KC-135 Winglet Program Review

Proceedings of a symposium
held at Dryden Flight Research Center
Edwards, California
September 16, 1981

NASA
National Aeronautics
and Space Administration

**Scientific and Technical
Information Branch**

1982

PREFACE

A review of the results of a joint NASA/USAF program to develop and flight test winglets on a KC-135 aircraft was held at the Dryden Flight Research Center on September 16, 1981. This publication is a compilation of the results presented.

CONTENTS

KC-135 WINGLET PROGRAM OVERVIEW

Marvin R. Barber* and David Selegan**

SUMMARY

A joint NASA/USAF program was conducted to accomplish the following objectives:

1. Evaluate the benefits that could be achieved from the application of winglets to KC-135 aircraft.
2. Determine the ability of wind tunnel tests and analytical analysis to predict winglet characteristics.

The program included wind-tunnel development of a test winglet configuration; analytical predictions of the changes to the aircraft resulting from the application of the test winglet; and finally, flight tests of the developed configuration.

Pressure distribution, loads, stability and control, buffet, fuel mileage, and flutter data were obtained to fulfill the objectives of the program.

INTRODUCTION

This paper provides an overview of a joint NASA/USAF effort that resulted in full-scale flight tests of winglets on a KC-135 aircraft. Winglet evolution is traced from concept, through wind-tunnel testing and full-scale flight tests.

The details of the flight tests are emphasized in this paper and serve as an introduction for the flight test result papers that follow in this proceeding.

SYMBOLS

L	Lift Force - lbs
D	Drag Force - lbs
W	Gross Weight - lbs
δ	Ambient Pressure in Standard Atmospheres
M	Mach Number
hp	Pressure Altitude - ft.
C_t	Wing Tip Chord
CRT	Cathode Ray Tube

*NASA Dryden Flight Research Center
**USAF Wright Aeronautical Laboratory

NRT Normal Rated Thrust

Keas Knots Equivalent Airspeed - knots

CONCEPT

Winglets are small, nearly vertical aerodynamic surfaces which are designed to be mounted at the tips of aircraft wings (see figure 1). Winglets are designed with the same careful attention to airfoil shape and local flow conditions as the wing itself. The primary component of the winglet configurations is a large winglet mounted rearward above the wing tip. The "upper surface" of this airfoil is the inboard surface. For some configurations an additional small winglet, mounted forward, below the wing tip, is necessary. The "upper surface" of the airfoil for this lower winglet is the outboard surface.

The winglets operate in the circulation field around the wing tip. Because of the pressure differential between the wing surfaces at the tip, the air flow tends to move outboard along the wing lower surface, around the tip, and inboard along the wing upper surface. This wing-tip vortex produces cross flows at each winglet. Thus the winglets produce large side forces even at low aircraft angles of attack. Since the side force vectors are approximately perpendicular to the local flow, the side forces produced by the winglets have forward (thrust) components (figure 1) which reduce the aircraft induced drag. This is the same principle that enables a sailboat to travel upwind by tacking. For winglets to be fully effective the side forces must be produced as efficiently as possible; therefore, advanced aerodynamic airfoil shapes are used. The side force produced by the winglets, and therefore the thrust produced, is dependent upon the strength of the circulation around the wing tip. Since the circulation strength is a function of the lift loads near the wing tip, winglets are more effective on those aircraft with higher wing loads near the tip.

The near vertical mounting of the winglets enables them to provide their thrust with very little increase in wing root bending. This can be an important design or retrofit consideration.

Theoretical calculations indicate that the aerodynamic benefit would be the same for a given size winglet in either the upper or lower position. However, ground clearance of low-wing jet transports limits the span of the lower winglet, and interference with the upper winglet flow limits the chord length of the lower winglet. Thus, from a practical standpoint for low-wing aircraft, the lower winglet must be relatively small. As a result, for the jet transports being discussed herein, the contributions of the lower winglet to the reduction of drag were relatively small.

As indicated in figure 1, the winglets tend to straighten the air flow thus slightly reducing the wing-tip vortex strength. However, the trailing vortex hazard still exists. The reduction is an indication of an increase in the aircraft efficiency. Winglets are not designed to improve flight safety for trailing aircraft, but to increase aerodynamic efficiency.

FLIGHT PROGRAM DEVELOPMENT

Program Inception and Motivation

The concept of winglets to reduce aircraft drag was developed by NASA/Langley. An empirical investigation of winglets on a DC-10 model was conducted in the NASA/Langley 8-foot transonic tunnel. Results of the investigation indicated a decrease in induced drag of about 15 percent and an overall drag decrease of about 5 percent. These preliminary results and fuel conservation interests were the motivation for application to military vehicles. Subsequently, a Boeing Company analysis of the effects of winglets on the 747 was correlated with wind tunnel data and indicated a drag reduction of approximately 4 percent on the full-scale 747 aircraft.

Based on these early results, a Memorandum of Understanding (MOU) for a joint USAF/NASA Winglet Development Program was developed. Under this MOU, NASA LaRC and the Flight Dynamics Laboratory coordinated the development of a wind tunnel data base relative to the application of winglets to selected Air Force aircraft.

The Boeing Company, under contract to the Air Force, performed an analytical investigation of winglet concepts for the KC-135 and C-141 aircraft and for the purpose of recommending winglet configurations. The analysis addressed the effect of winglets on vehicle aerodynamic characteristics and wing root bending moments. The feasibility of winglets on KC-135 aircraft and wing tip winglets interface moments were also addressed. This effort was supported by NASA/LaRC through wind tunnel tests of selected configurations.

Wind tunnel tests of a NASA/Langley constructed semi-span KC-135 model with winglets were conducted in the NASA/Langley 8-foot transonic tunnel. Results of these tests indicated an 8 percent total drag reduction at cruise flight conditions (M = 0.78, hp = 35,000 ft.).

Subsequently, a full span KC-135 model with winglets was tested in the NASA/LaRC 8 foot transonic tunnel, indicating drag reductions of 6 percent at cruise. This series included off-nominal conditions. Low speed investigations of the winglets effects on the KC-135 with various flap and aileron configurations were completed during the months of July and August 1976.

The results of the wind tunnel tests and anlytical studies are reported in references 1 through 11. In summary, these studies indicate that winglets would reduce KC-135 aircraft drag by 6 to 8 percent. This reduction translated into approximately 37 million gallons of fuel saved per year for the KC-135 fleet.

Based on these results, and the high priority fuel conservation effort within the United States in this time period, the Air Force initiated an Advanced Development Program to build and flight test a set of winglets on a KC-135 aircraft. NASA was eager to participate in a flight test program to obtain full-scale lift and drag data for comparison with the wind tunnel results. Reynolds number effects on the winglets aerodynamic performance was the primary concern in initiating flight and wind tunnel data comparisons. Both agencies objectives, though different, were compatible to a joint program and were formalized in another Memorandum of Understanding that formulated a flight program.

Obviously, both the USAF and NASA were interested in obtaining as much information as possible from the flight program. However, the specific data interests of each organization were slanted differently in some areas. A breakdown of the primary interest of each organization is provided in table I.

The responsibilities of the organizations participating in the joint program are defined in figure 2. The program was under the overall management of the Flight Dynamics Laboratory. They provided the test aircraft, a serviceable set of outer wing panels, and were technically and financially responsible for contracting with the Boeing Military Airplane Company for the design, fabrication and ground test of a set of winglets and modified outer wing panels.

NASA/Dryden was responsible for the flight phase of the program. They instrumented the aircraft, and provided funds, manpower and facilities required for this portion of the program.

The Air Force Flight Test Center provided flight crew and engineering support to the flight test program. They were also responsible for all flight flutter testing and were the onsite Air Force representative during flight testing.

NASA/Langley provided facilities, personnel, and data processing as required to support the winglet wind tunnel tests. They also provided technical support in the design of the flight winglet.

Boeing Military Airplane Company accomplished the design, fabrication, and ground testing of the winglets and provided onsite engineering support during the flight test phase.

The original flight program milestones are shown in figure 3. A contract was awarded to The Boeing Military Airplane Company, Wichita, Kansas, in September 1977. The effort included the design, fabrication and ground testing of a set of winglets and the modification of the outer wing panels to accept the winglets. Preliminary and final design reviews were held at Boeing in February and June 1978, respectively.

In conjunction with the design effort, a low speed flutter test was conducted in January 1978 in the Convair wind tunnel in San Diego. The test results are reported in reference 11. Also in support of the design effort, a limited amount of force and moment and pressure data was obtained in NASA/Langley facilities.

Prior to delivery of the winglets to NASA, Boeing conducted a ground vibration and proof load test on the outer wing panel and winglet. Included in the proof load test was a loads calibration test wherein 12 point loads were applied to the wing.

The winglets and outer wing panels were delivered to NASA/Dryden in May 1979. The outer wing panels were installed by NASA and instrument checkout was completed in July 1979. The first winglet flight was made 24 July 1979. The flight test program was interrupted several times for maintenance problems with the test aircraft. These problems are discussed later in the paper.

Winglet Design and Construction

The winglet geometry was specified by the Government and conformed to Dr. Whitcomb's design criteria as shown in figure 4. The winglet airfoil was a general purpose airfoil and the same airfoil section was used from root to tip. No twist distribution was incorporated into the design. Airfoil coordinates are listed in table II.

The design philosophy was to provide a winglet and outboard wing modification for a flight research program and not oriented to production. The design included the capability to vary the winglet incidence and cant angle on the ground as illustrated in figure 5. A two-spar design was selected for the winglet. This design allowed for a positive positioning of the winglets using fittings with a total of four shear pins per side. The seven different cant/incidence combinations could be obtained by inserting bolts through designated holes in the fittings. Gap cover fairings were provided to assure aerodynamic sealing and smoothness for each setting. The structural arrangement is shown in figure 6.

A new internal structure was designed for the wing tip to transmit the loads from the winglet to the outboard wing. The principal load carrying paths were from the front spar of the winglet to the rear spar of the outboard wing and from the rear spar of the winglet to the outboard wing auxiliary spar. A thin doubler was added to the outboard portion of the outboard wing to prevent skin "oilcanning" in the fuel tank area. All areas were smoothed with aerodynamic sealer and/or fiber glass to maintain smooth contours on the wing and winglet (see figure 7).

The design also included provisions for total removal of the winglet so that baseline airplane data could be obtained. A new tip cap was manufactured for use in baseline testing.

The winglet skin was supported by ribs, placed at 10-inch intervals, from the front spar to the winglet trailing edge. The leading edge was manufactured by nesting two 0.050-inch thick skins bonded together with close out ribs at the winglet tip and root. This approach allowed for minimum tooling since the spars and ribs could be manufactured using numeric control procedures. This approach did require that all loads from the winglet be transferred to the wing tip through the fittings (no loads in skin at the winglet root). It was decided that skin "oilcanning" would be allowed at the limit load, with no "oilcanning" below 50 percent of limit load, which should have provided smooth airfoil contours during testing. The design was verified by proof load testing during which "oilcanning" of the skin was noted between 60 and 80 percent of limit load. Pillowing of the skins during flight testing was found. The pillowing was the result of a combination of the inboard pressure loading on the surface and the compressive loads in the skin. The inboard pressure loads were not considered in the design, nor were they simulated during the proof load testing. Because of pillowing, corrections were required to the aerodynamic drag; however, there was no concern from a loads standpoint as the spars were designed to carry the total load.

Test Airplane

The airplane assigned to the flight test program was a very early model of the KC-135A which had been used for other than normal tanker missions (e.g., zero "g" training missions for the astronauts). It had not received the lower wing reskin (a fleet modification on KC-135 aircraft designed to extend the fatigue life of high time or highly stressed airplanes), and due to its relatively high and unusual usage, the Air Force determined that the airplane should be restricted per the criteria for high time airplanes without the reskin modification. This restriction did not appreciably impact the flutter or performance testing, but did require that all loads data be gathered within a constrained envelope, rather than testing at the limits of the V-n envelope.

To reduce concerns that arose from the lack of a lower wing reskin, splice plates were installed at the airplane's wing root. These splice plates are a standard USAF modification designed to extend an airplane's fatigue life until a lower wing reskin can be accomplished.

A photograph of the test airplane with the flight test nose boom installed is provided in figure 8.

Instrumentation

A broad description of the instrumentation that was used for the various types of measurements that were made (i.e., drag, fuel mileage, loads, etc.) is provided in table III. A detailed definition of all the parameters that were measured as of the last flight is provided in the instrumentation line-up in appendix A. A noseboom was installed for the air data measurements. The boom is evident in figure 8 and the details of its head are shown in figure 9. Longitudinal and normal accelerometers were attached to the angle-of-attack vane to provide a measure of flight path acceleration.

A digital pulse code modulated data acquisition unit with a multiplexing capability was used to acquire the flight data. In its design configuration the data system provided a telemetry capability to Dryden and Air Force Flight Test Center ground stations for real-time data analysis, and an onboard recording capability as a backup in case of telemetry losses. This configuration was acceptable for the flutter testing but proved unacceptable for the performance testing. Tying the performance tests to the Edwards airspace complex in order to allow telemetry to the ground station resulted in constrained flight rates dependent on local weather and ground station scheduling conflicts, and constrained data gathering capability dependent on the length of the Edwards airspace complex. Therefore, after eight attempts to gather performance data via telemetry to the ground based station, the data system was modified to provide an onboard computational capability that enabled breaking the ground link.

A PDP-11 computer was installed on the airplane to provide the needed real-time calculations (i.e. W, W/δ, M, and hp) for performance testing. A CRT and keyboard provided the display and programing capabilities for the computer. A simplified block diagram of the data system in final configuration is provided in figure 10.

FLIGHT PROGRAM

Test Plans

Initial planning laid out 35 flutter, performance, and envelope coverage flights to be conducted in the order of sequence specified in figure 11. Seven winglet configurations were to be tested in an attempt to define the configuration that would provide the best trade-off between winglet-induced performance gains and loads. The strategy was to clear the four configuration corners for flutter and thereby allow performance and envelope coverage flights for the remaining configurations without concern of flutter. The 15° can/4° incidence angle configuration included additional testing because it was the configuration at which wind-tunnel data had been obtained to evaluate stability and control characteristics and buffet boundaries.

A typical performance flight plan is shown in figure 12. Note that it includes not only performance maneuvers but loads and buffet boundaries as well. The scani-valve runs were to obtain pressure distribution data. A typical flutter flight plan is shown in figure 13. These plans nominally allowed for the coverage of two fuel configurations per flight. Envelope coverage flight plans included additional items as follows: roll response, minimum control speed, check climbs, check descents, missed approach characteristics, stability and control maneuvers, and 1g stall approaches.

Upon completion of the testing of the seven winglet configurations, it was planned to obtain data for a baseline configuration which was termed Modified Wing Tips (see figure 11). This terminology resulted from minor external modifications that were made to accomodate the winglet installation.

While the baseline tests were being conducted, it was planned that the USAF would have evaluated sufficient data from the seven winglet configuration tests to enable them to select a configuration that they would most desire to retrofit the KC-135 fleet with. That configuration then would be subjected to additional flutter and performance testing as well as envelope coverage tests.

Test Accomplishments

Figure 14 presents a photograph of the test airplane with the winglets. installed. A complete log of the test airplane's flight activity from the time it arrived at Dryden in December 1977 is provided in table IV. Flight crew checkout training was flown in the spring of 1978. Between May and September 1978, the aircraft was "layed up" while being instrumented. Upon completion of the instrumentation installation it was necessary to take the airplane to Tinker AFB, Oklahoma, for the installation of the wing root splice plates previously referred to. Some airspeed calibration and instrumentation checkout flying was accomplished prior to the delivery of the modified wing tips and winglets to Dryden in May 1979. The winglets were installed and the first winglet flight occurred on July 24, 1979. Per the plan layed out in figure 11, this winglet configuration was 15° cant angle/-2° incidence angle. This configuration required seven flights to complete rather than the planned four and uncovered a "pillowing" of the winglet skins as shown in figure 15. This "pillowing" caused sufficient concern, relative to its effect on the performance of the test

articles, and it was decided to deviate from the test plan and go to the 15° cant angle/-4° incidence angle configuration for the next tests. Wind tunnel, pressure distribution, and lift and drags measurements were available in the 15°/-4° configuration to provide some indication of the effect the pillowing might be causing. The 15°-4° tests were conducted and baseline tests (modified wing tips) immediately thereafter, still giving priority to the question of the effects of the "pillowing". Preliminary analysis indicated that the pillowing was having a small effect on the winglets' performance (approximately 10 percent of the expected gain) but was certainly not masking all of their expected benefit. (A detailed analysis of the winglet skin "pillowing", its causes and effects, is provided in reference 12.)

With the effects of the "pillowing" in hand, other considerations started driving the flight sequencing. The activity was behind schedule because of airplane fuel leaks and instrumentation problems. Therefore, it was decided to go to the 0° cant/-4° configuration and delete the 0°/-2° and 0°/-7.5° configurations. In testing this configuration, less than adequate structural damping occurred at airspeeds greater than the operational flight envelope speeds but less than the dive speeds. The low damping is discussed in detail in references 12 and 13. Also, while testing this configuration a large fuel leak developed that was the result of a crack in the front spar chord at the number 3 engine strut location. The crack in the spar chord has occurred on other airplanes and the source is a bad fatigue detail. Neither the fuel leaks nor the cracked spar cap were due to the installation of winglets. The repair of this wing spar required significant down time, January - July 1980. The need for the onboard computational capability discussed under Instrumentation had become evident and this down time was used to accomplish that modification.

Also during this down time the USAF selected the 15° cant/-4° incidence configuration as the best for fleet retrofit. This selection was primarily driven by the less than adequate structural damping that was found in the 0°/-4° configuration. The retrofit selection is discussed in reference 14.

Upon resuming flight testing in July 1980 the 0° cant/-4° incidence configuration was again checked for flutter to see if the cracked wing spare might have had some effect on that result. Verifying that the cracked wing spar had no effect, the 0°/-4° performance flights were resumed with the onboard computational capability.

During the spar crack repair downtime, a review of the performance data indicated that more data than planned for each configuration would be necessary to sufficiently define the winglet fuel mileage gains. Therefore, the performance data points in the plan were doubled in number. Scatter in the data resulting from weather disturbances was the prime driver of this conclusion. The remainder of the flight activity was devoted to obtaining the 0°/-4 baseline, and 15°/-4 performance data in acceptable quantity and quality as shown in table IV.

CONCLUSIONS

A joint NASA/USAF program was conducted to accomplish the following objectives:

1. Evaluate the benefits that could be achieved from the application of winglets to KC-135 aircraft.

2. Determine the ability of wind tunnel tests and analytical analysis to predict winglet characteristics.

The program included wind-tunnel development of a test winglet configuration; analytical predictions of the changes to the aircraft resulting from the application of the test winglet; and finally, flight tests of the developed configuration.

The pressure distribution, loads, stability and control, buffet, fuel mileage, and flutter data produced fulfilled the objectives of the program.

REFERENCES

1. Whitcomb, Richard T.: A Design Approach and Selected Wind-Tunnel Results at High Subsonic Speeds for Wing-Tip Mounted Winglets. NASA TN D-8260, 1976.

2. Bartlett, Dennis W.; and Patterson, James C., Jr.: NASA Supercritical Wing Technology. CTOL Transport Technology - 1978, NASA CP-2036, Pt. II, 1978, pp. 533-552.

3. Ishimitusu, K. K.; VanDevender, N.; Dodson, R.: Design and Analysis of Winglets for Military Aircraft. USAF AFFDL Technical Report 76-6, 1976.

4. Jacobs, Peter F.; Flechner, Suart G.; and Montoya, Lawrence C.: Effect of Winglets on a First-Generation Jet Transport Wing. I - Longitudinal Aero-dynamic Characteristics of a Semi-Span Model at Subsonic Speeds. NASA TN D-8473, 1977.

5. Ishimitsu, K. K.; Zanton, D. F.: Design and Analysis of Winglets for Military Aircraft; Phase II. USAF AFFDL Technical Report 77-23, 1977.

6. Montoya, Lawrence C.; Flechner, Stuart G.; and Jacobs, Peter F.: Effect of Winglets on a First-Generation Jet Transport Wing. II - Pressure and Spanwise Load Distributions for a Semi-Span Model at High Subsonic Speeds. NASA TN D-8474, 1977.

7. Montoya, Lawrence C.; Jacobs, Peter F.; and Flechner, Stuart G.: Effect of Winglets of a First-Generation Jet Transport Wing. III - Pressure and Spanwise Load Distributions for a Semi-Span Model at Mach 0.30. NASA TN D-8478, 1977.

8. Meyer, Robert R., Jr.: Effect of Winglets on a First-Generation Jet Transport Wing. IV - Stability Characteristics for a Full-Span Model at Mach 0.30. NASA TP-1119, 1978.

9. Jacobs, Peter F.: Effect of Winglets on a First-Generation Jet Transport Wing. V - Stability Characteristics of a Full-Span Wing with a Generalized Fuselage at High Subsonic Speeds. NASA TP-1163, 1978.

10. Flechner, Stuart G.: Effect of Winglets on a First-Generation Jet Transport Wing. VI - Stability Characteristics for a Full-Span Model at Subsonic Speeds. NASA TP-1330, 1979.

11. Schneider, F. C.; and Shoup, G. S.: "KC-135A Winglet Flutter Model Test", Boeing Document D3-11353-1, Boeing Wichita Company, Wichita, Kansas, May 5, 1978.

12. Dodson, R. O.; Ayala, J.; Shurtz, R. M.; and Temanson, G.: KC-135 Winglet Flight Research and Demonstration Program. AFWAL-TR-81-3115; July 1981.

13. Kehoe, Michael W.: KC-135A Winglet Flight Flutter Test Program. USAF, AFFTC-TR-81-4; June 1981.

14. Dodson, R. O.; Ayala, J.; Shurtz, R. M.; et al: KC-135 Winglet Flight Research and Demonstration Program - Trade Study Results. AFWAL-TR-81-3031; May 1981.

TABLE I. - PRIMARY FLIGHT DATA INTERESTS

Data	USAF	NASA
Lift and Drag		X
Fuel Mileage	X	
Loads	X	X
Flutter	X	
Stability and Control	X	
Buffet	X	
Handling Qualities	X	

TABLE II. - AIRFOIL COORDINATES FOR WINGLETS

x/c	z/c for -	
	Upper Surface	Lower Surface
0	0	0
.0020	.0077	-.0032
.0050	.0119	-.0041
.0125	.0179	-.0060
.0250	.0249	-.0077
.0375	.0296	-.0090
.0500	.0333	-.0100
.0750	.0389	-.0118
.1000	.0433	-.0132
.1250	.0469	-.0144
.1500	.0499	-.0154
.1750	.0525	-.0161
.2000	.0547	-.0167
.2500	.0581	-.0175
.3000	.0605	-.0176
.3500	.0621	-.0174
.4000	.0628	-.0168
.4500	.0627	-.0158
.5000	.0618	-.0144
.5500	.0599	-.0122
.5750	.0587	-.0106
.6000	.0572	-.0090
.6250	.0554	-.0071
.6500	.0533	-.0052
.6750	.0508	-.0033
.7000	.0481	-.0015
.7250	.0451	.0004
.7500	.0419	.0020
.7750	.0384	.0036
.8000	.0349	.0049
.8250	.0311	.0060
.8500	.0270	.0065
.8750	.0228	.0064
.9000	.0184	.0059
.9250	.0138	.0045
.9500	.0089	.0021
.9750	.0038	-.0013
1.0000	-.0020	-.0067

TABLE III. - KC-135 WINGLET TEST AIRPLANE INSTRUMENTATION

1. DRAG:

   Engine-Pressures, and RPM's
   Flight Path and Body Axis Accelerometers
   Air Data (M, h_p, α)

2. RANGE:

   Fuel Flows
   Accelerometers
   Air Data (M, h_p, α)

3. LOADS:

   Load and Strain Gages
   Accelerometers
   Air Data (M, h_p, α, β)

4. PRESSURE DISTRIBUTIONS:

   Scanning Pressure Valves
   Reference Pressures
   Air Data (M, h_p, α, β)

5. BUFFET BOUNDARIES:

   Accelerometers
   Air Data (M, h_p, α)

6. STABILITY AND CONTROL:

   Control Positions
   Accelerometers
   Angular - Attitudes, Rates and Accelerations
   Air Data (M, h_p, α, β)

7. FLUTTER:

   Accelerometers
   Air Data (M, h_p, α, β)
   Control Positions

TABLE IV. - KC-135 (3129) FLIGHT LOG

FLIGHT NO.	FLIGHT TIME	DATE	CONFIGURATION	OBJECTIVE
1	1.2	11 Apr 78	Baseline	Crew Checkout
2	2.2	11 Apr 78	Baseline	Crew Checkout
3	2.1	12 Apr 78	Baseine	Crew Checkout
4	1.8	12 Apr 78	Baseline	Crew Checkout
5	2.2	14 Apr 78	Baseline	Crew Checkout
6	2.7	20 Apr 78	Baseline	Crew Checkout
7	3.7	24 Apr 78	Baseline	Crew Checkout
8	4.3	28 Apr 78	Baseline	Crew Checkout
9	2.4	21 Sep 78	Baseline	Airspeed Calibration and Flutter
10	2.5	25 Sep 78	Baseline	Ferry to Tinker AFB
11	0.6	22 Dec 78	Baseline	Check Flight
12	3.3	17 Jan 79	Baseline	Ferry to Edwards AFB
13	3.0	14 Mar 79	Baseline	Airspeed Calibration and Flutter
14	3.8	23 Apr 79	Baseline	Flutter and Instrumentation Checkout
15	3.0	26 Apr 79	Baseline	Instrumentation Checkout
16	2.8	30 Apr 79	Baseline	Instrumentation Checkout
17	2.3	24 Jul 79	15/-2	Airspeed Calibration and Flutter
18	3.5	1 Aug 79	15/-2	Flutter
19	3.8	2 Aug 79	15-2	Airspeed Calibration and Flutter
20	3.8	10 Aug 79	15/-2	Flutter
21	5.4	24 Aug 79	15/-2	Performance
22	2.9	19 Sep 79	15/-2	Performance
23	5.4	21 Sep 79	15/-2	Airspeed Calibration and Performance
24	5.0	26 Oct 79	15/-4	Flutter
25	6.4	2 Nov 79	15/-4	Performance

TABLE IV. - KC-135 (3129) FLIGHT LOG (cont'd)

FLIGHT NO.	FLIGHT TIME	DATE	CONFIGURATION	OBJECTIVE
26	4.0	9 Nov 79	Baseline (Mod Wing Tips)	Flutter
27	6.8	16 Nov 79	Baseline (Mod Wing Tips)	Performance
28	3.6	28 Nov 79	0/-4	Flutter
29	3.3	13 Dec 79	0/-4	Flutter and Performance
30	2.3	16 Jan 80	0/-4	Performance*
31	2.3	17 Jan 80	0/-4	Performance*
32	1.8	31 Jan 80	0/-4	Inflight Fuel Leak Check
33	1.4	15 Jul 80	0/-4	Functional Check Flight
34	2.0	22 Jul 80	0/-4	Flutter
35	7.7	29 Jul 80	0/-4	Performance
36	1.9	1 Aug 80	0/-4	Performance*
37	2.6	4 Aug 80	0/-4	Performance*
38	6.7	8 Aug 80	0/-4	Performance
39	5.0	14 Aug 80	0/-4	Performance
40	1.5	21 Aug 80	Baseline (Mod Wing Tips)	Performance**
41	7.0	25 Aug 80	Baseline (Mod Wing Tips)	Performance
42	6.9	28 Aug 80	Baseline (Mod Wing Tips)	Performance
43	6.3	5 Sep 80	Baseline (Mod Wing Tips)	Performance
44	7.0	9 Sep 80	Baseline (Mod Wing Tips)	Performance
45	6.7	11 Sep 80	Baseline (Mod Wing Tips)	Performance
46	6.9	17 Sep 80	15/-4	Performance
47	7.1	23 Sep 80	15/-4	Performance
48	4.6	25 Sep 80	15/-4	Performance*
49	5.3	3 Oct 80	15/-4	Performance

TABLE IV. - KC-135 (3129) FLIGHT LOG (cont'd)

FLIGHT NO.	FLIGHT TEST	DATE	CONFIGURATION	OBJECTIVE
50	2.7	15 Oct 80	15/-4	Performance*
51	4.6	17 Oct 80	15/-4	Performance
52	7.0	19 Dec 80	15/-4	Performance
53	3.0	23 Dec 80	15/-4	Performance
54	2.0	24 Dec 80	15/-4	Performance**
55	4.8	8 Jan 81	15/-4	Performance

*Flight aborted due to rough air.

**Flight aborted due to computer malfunction.

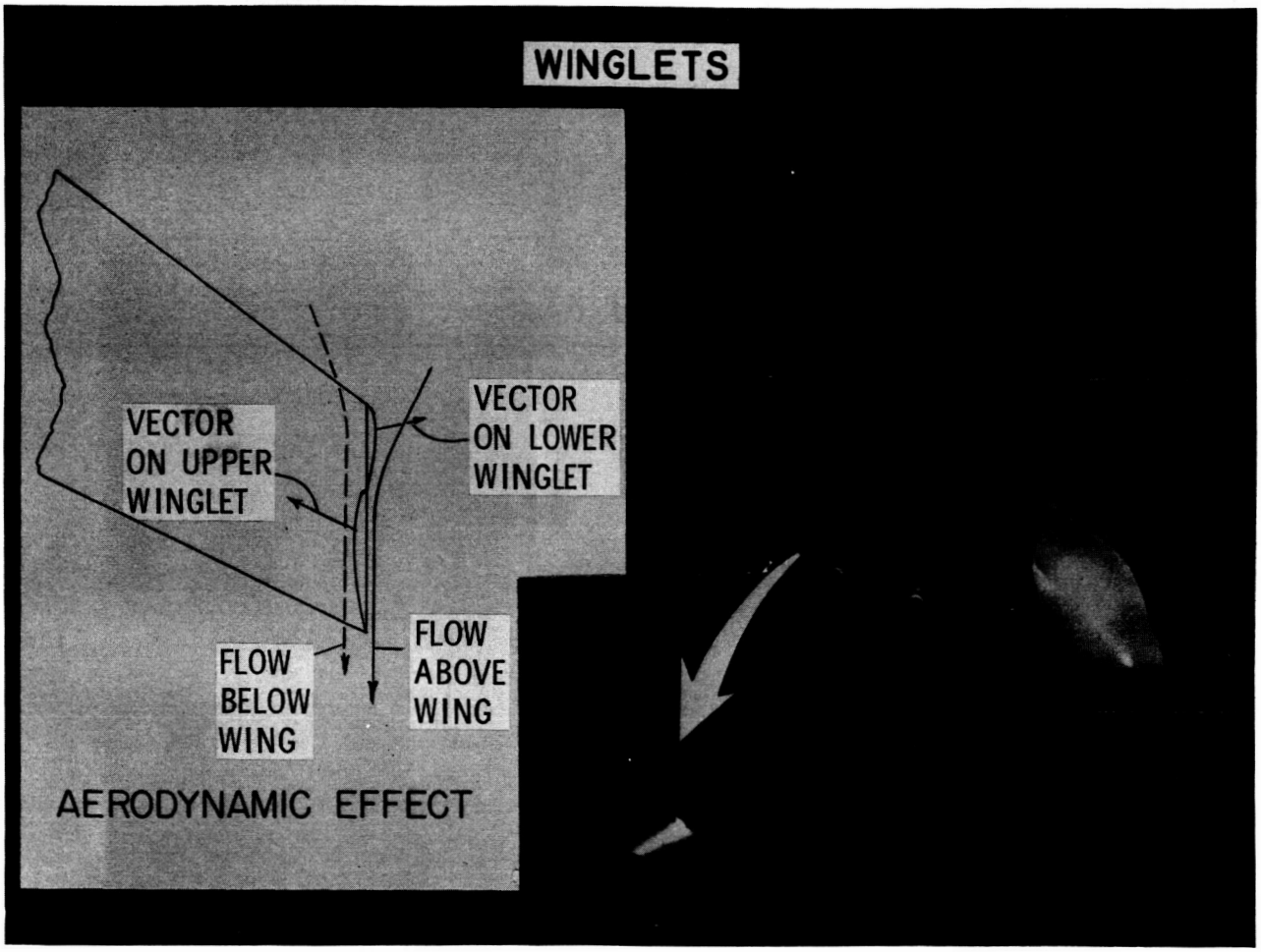

Figure 1. - Aerodynamic effect of winglet

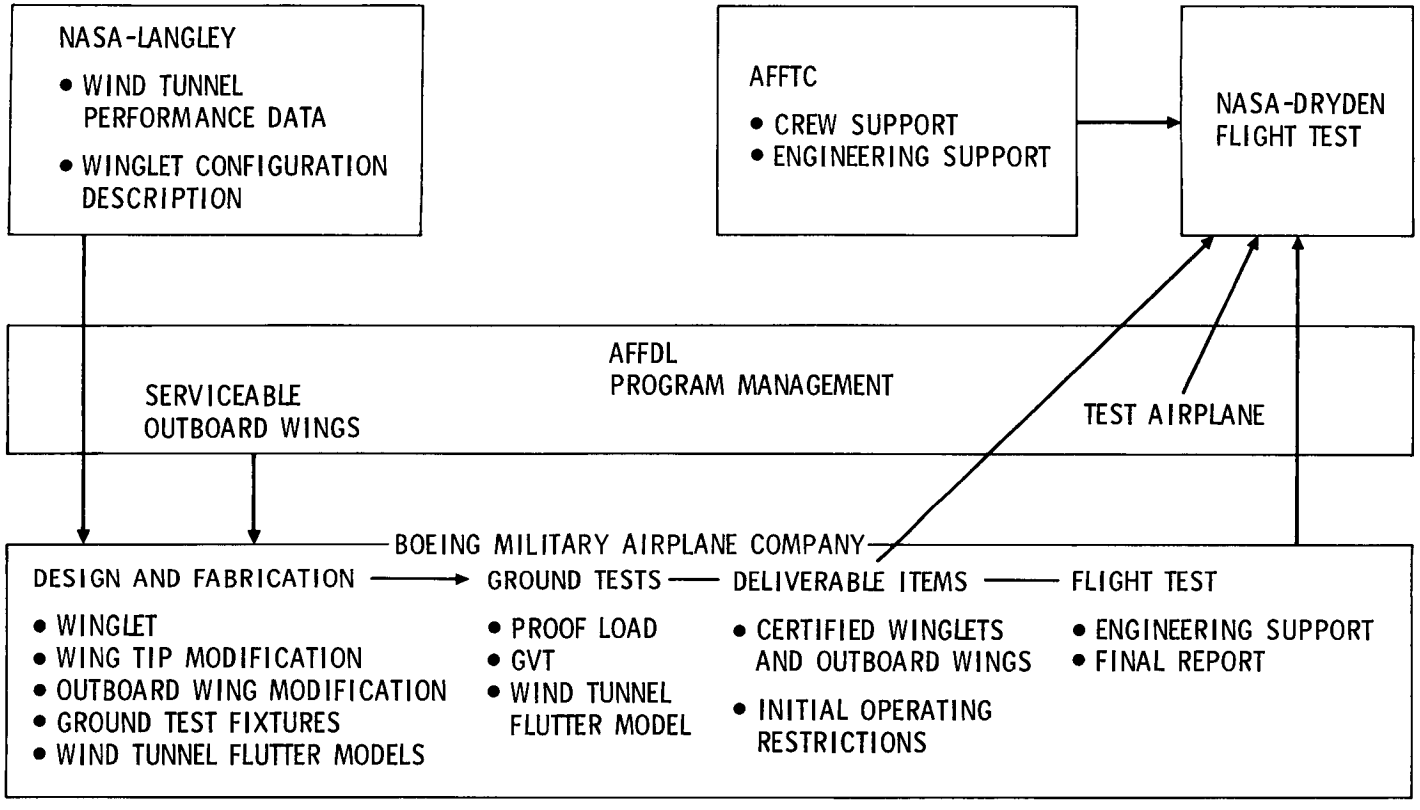

Figure 2. - KC-135 winglet flight research and demonstration program (joint program responsibilities)

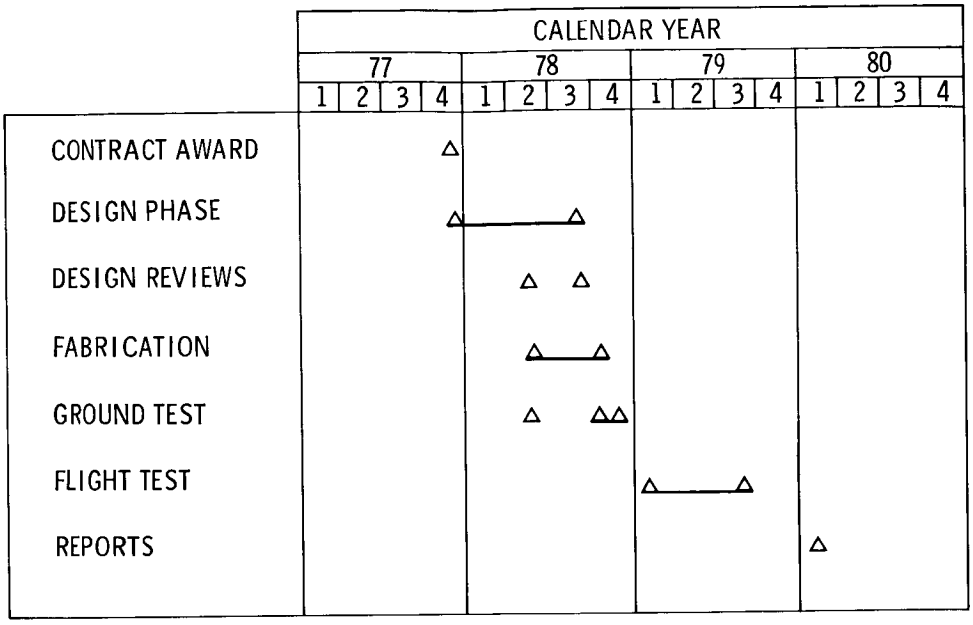

Figure 3. - KC-135 winglet flight research and demonstration program milestones

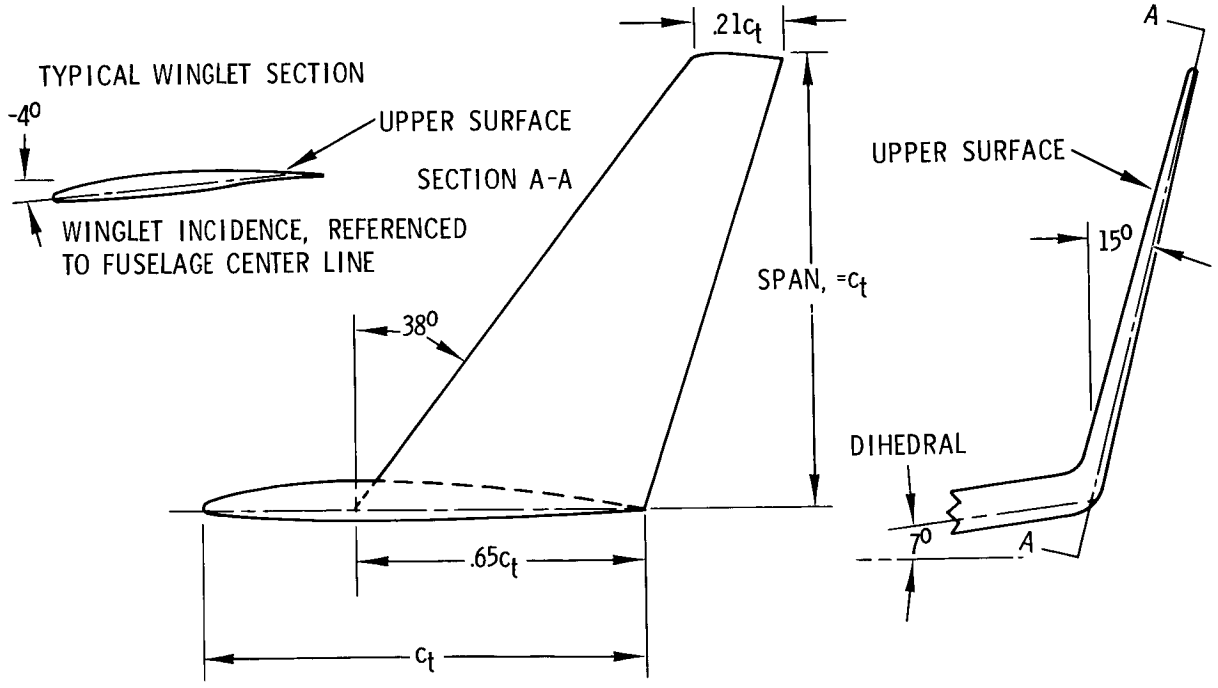

Figure 4. - KC-135 winglet design

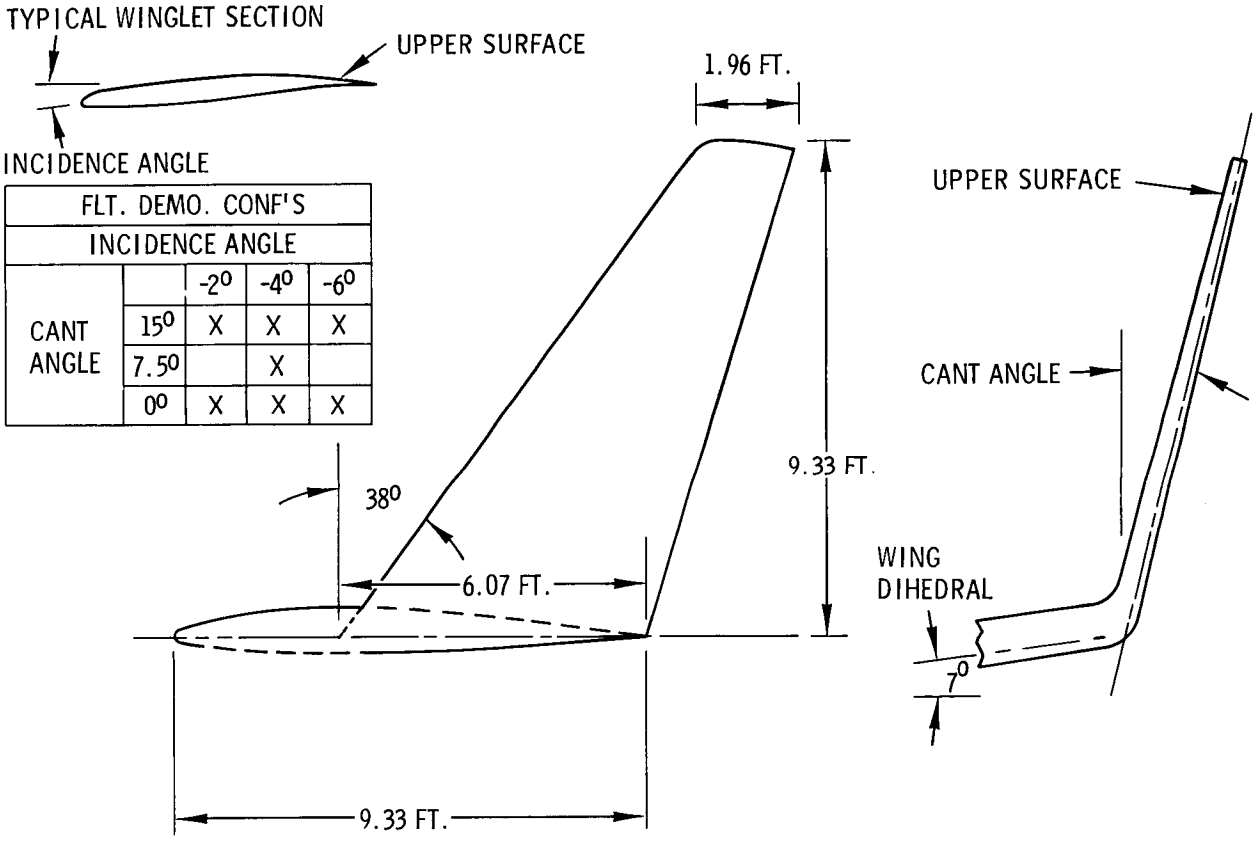

Figure 5. - Winglet geometry

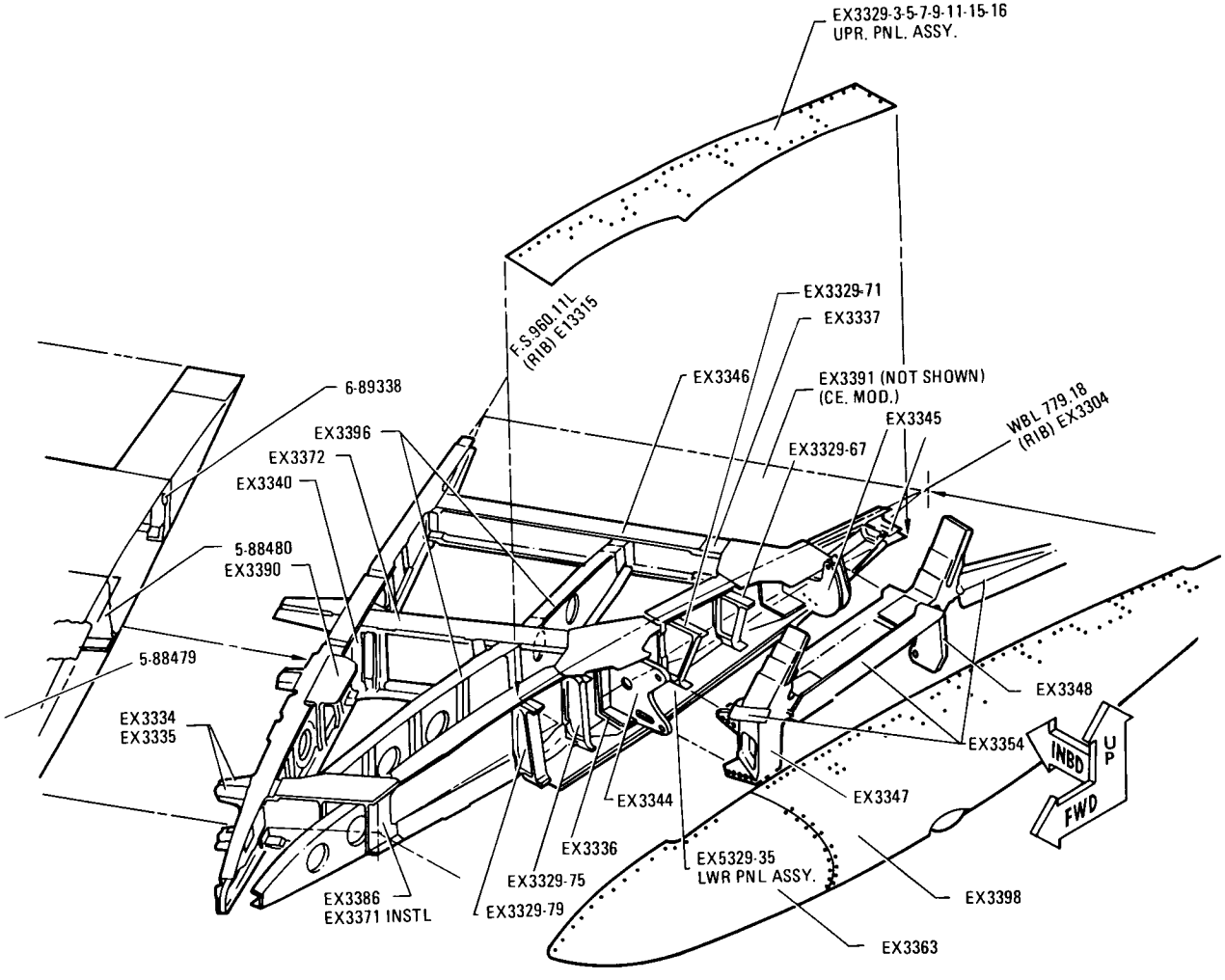

Figure 6. - KC-135 test wingtip structure

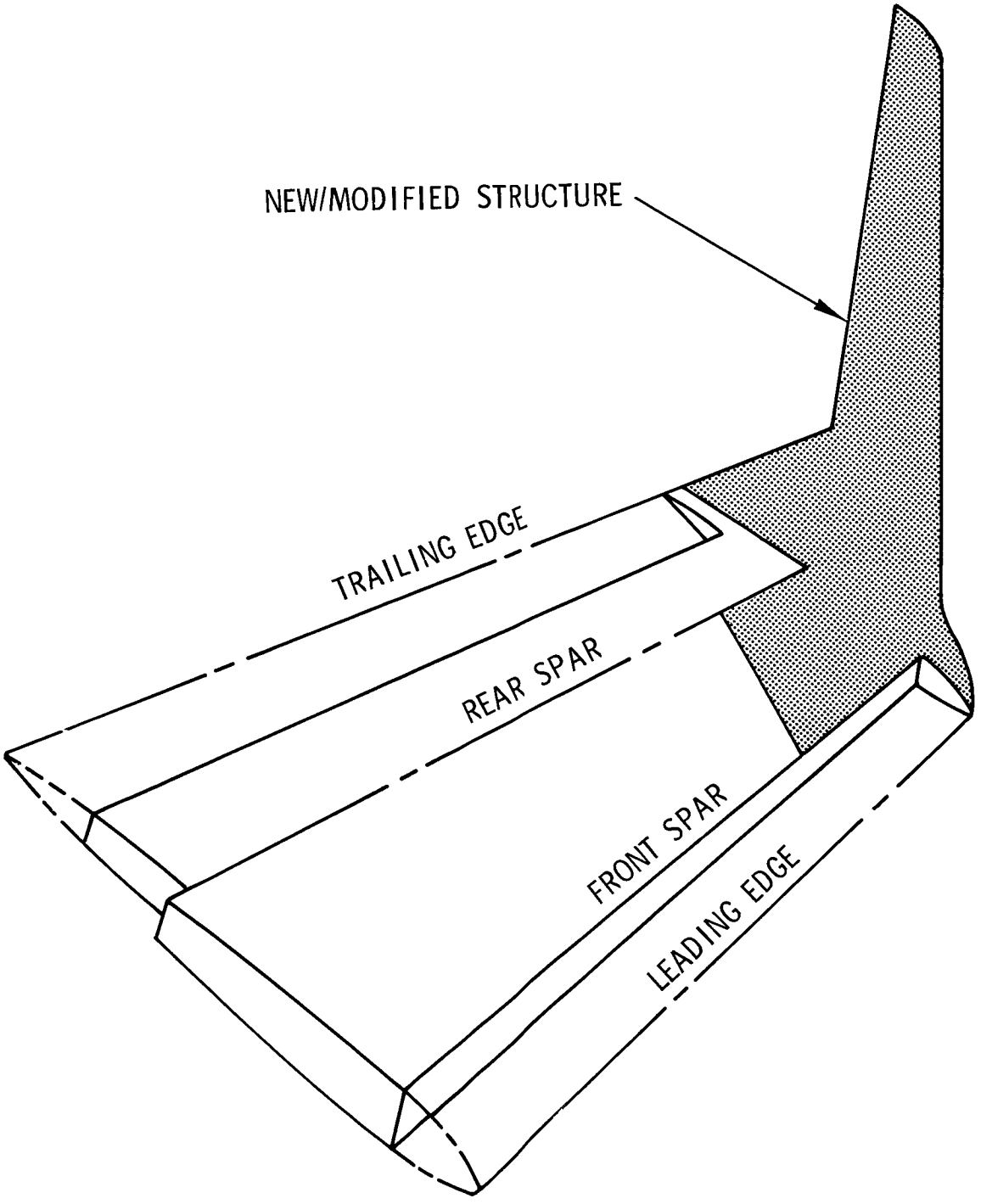

Figure 7. - Outboard wing/winglet arrangements

Figure 8. - KC-135 aircraft in flight

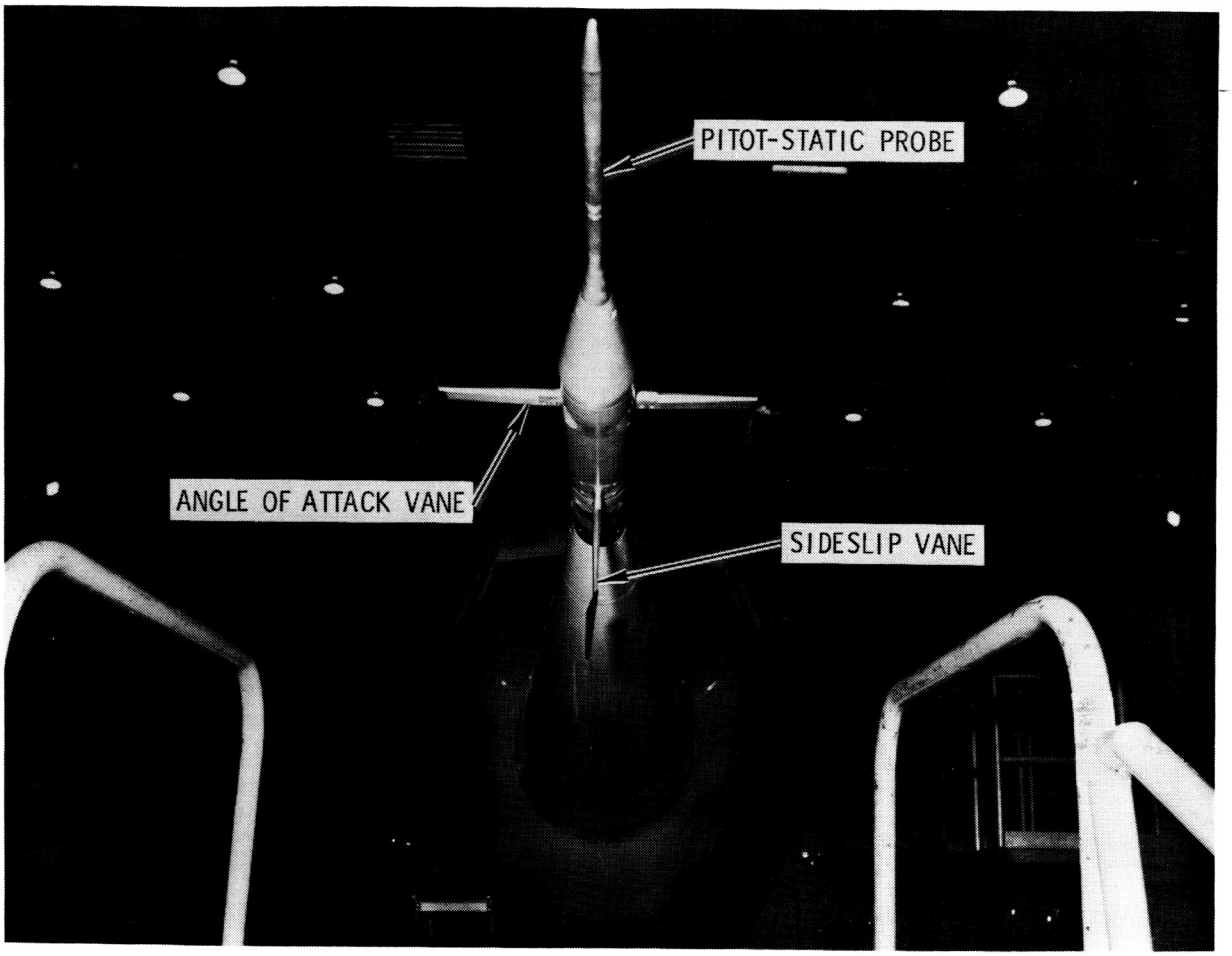

Figure 9. Noseboom instrumentation unit

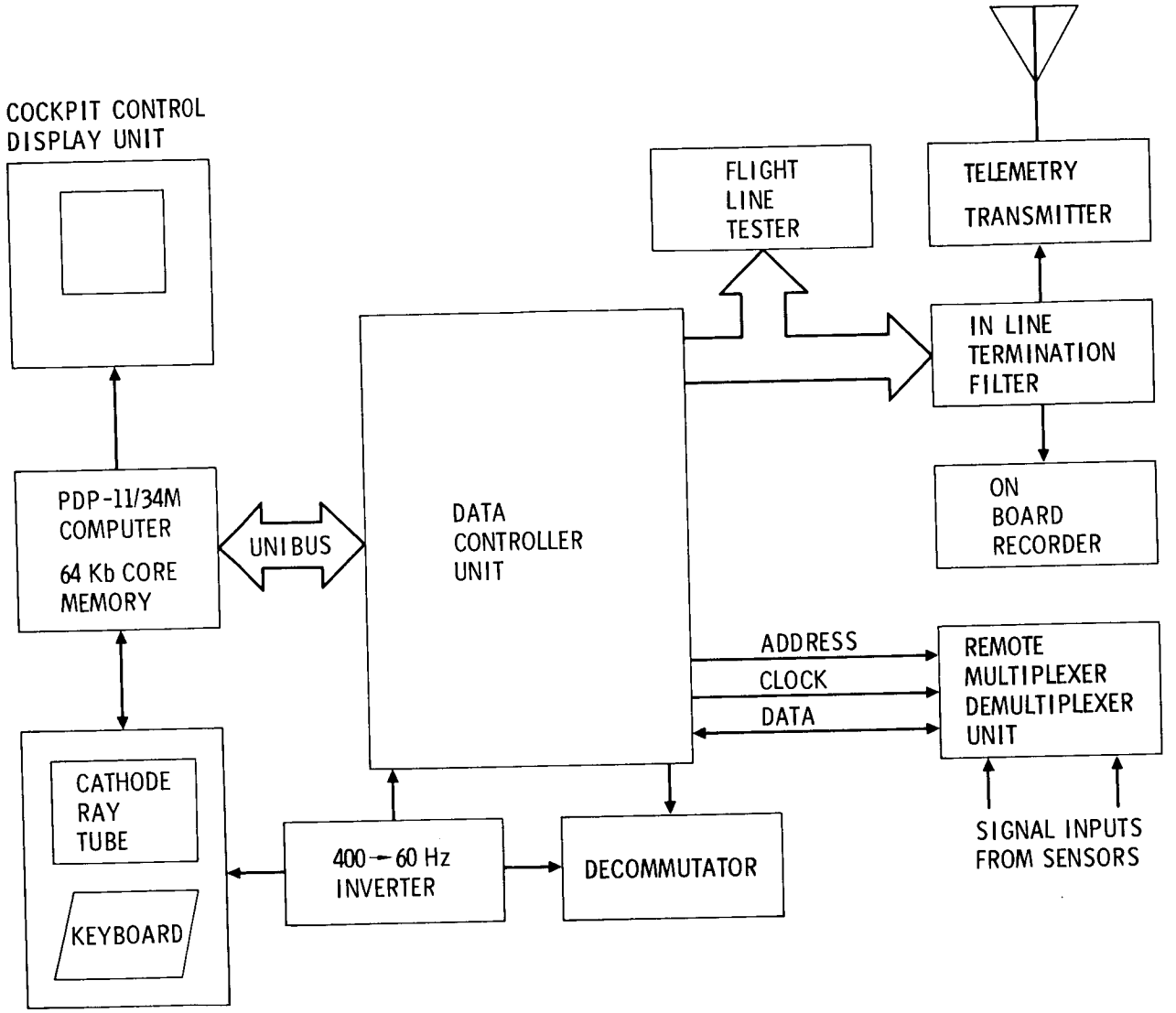

Figure 10. - Computer interactive data system
(simplified block diagram)

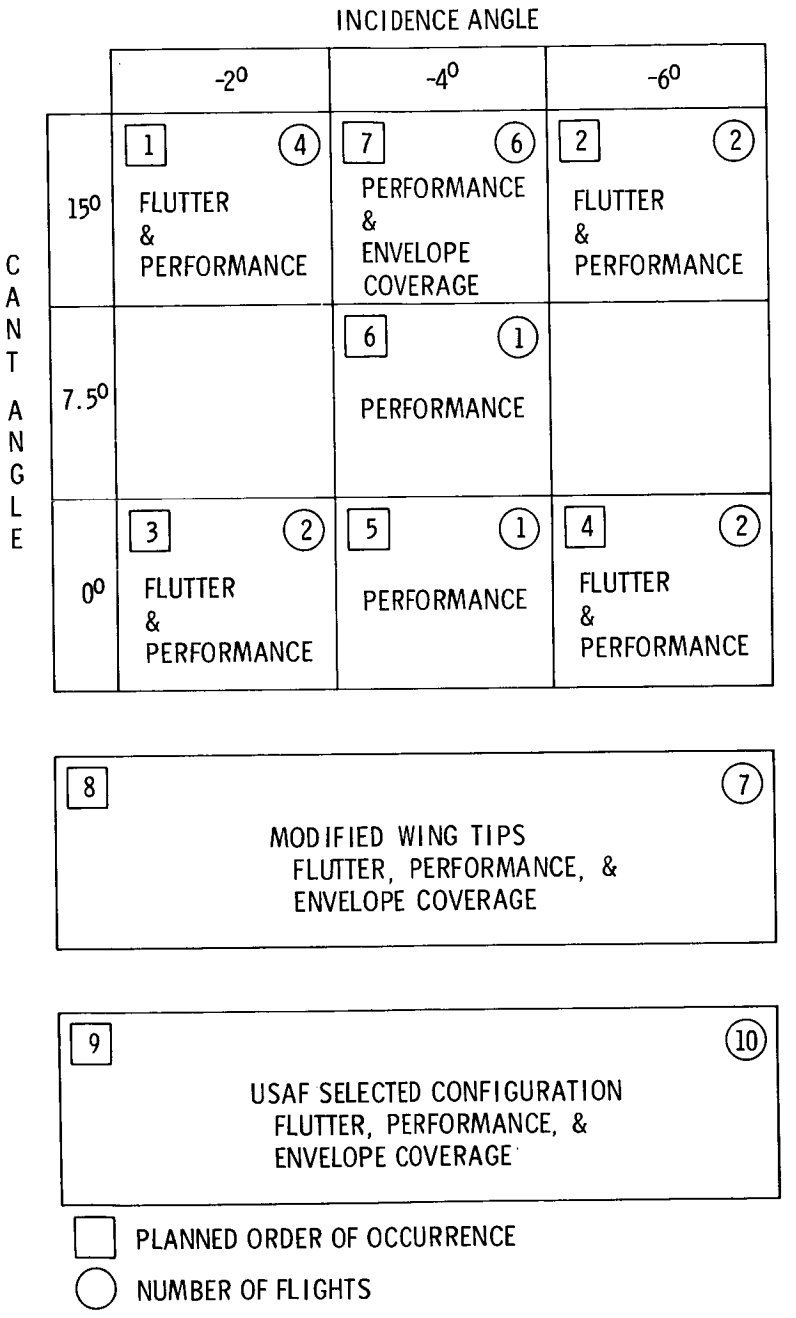

Figure 11. - Planned KC-135 winglet flight sequence

KC-135 WINGLET FLIGHT SEQUENCE

FLIGHT NO. _____ CANT ∠ _____ INCIDENCE ∠ _____

OBJECTIVE	MANEUVER	A/S, M, ALT	WEIGHT	COMMENTS
TAKE OFF PERFORMANCE	HANDBOOK TAKEOFF	FIELD ELEVATION	265,000 LBS, INCLUDING 5,600# WATER	THEODOLITE MEAS. FROM BRAKE RELEASE TO 50 FT.
CRUISE PERFORMANCE W/δ = 1,050,000	SPEED POWER, ACCEL	.82, .80, .78, .75, .72, .70, ACCEL .70, .82, .80, .78 ≃ 35.5K FT.	240,000 LBS	3 MIN STABILIZED POINTS WITH 1 MIN OF SCANI-VALVE AT END OF EACH RUN. WING DEFLECTION PHOTOS DURING RUN ACCEL AT NRT.
CRUISE PERFORMANCE W/δ = 900,000	SPEED POWER, PUSH OVER-PULLUP, AND ACCEL	.82, .80, .78, .75, .72, .70, ACCEL .70 - .82, .80, .78 ≃ 34.5K FT.	220,000 LBS	↓
LOADS	TRIM POINT, STEADY STATE SIDESLIPS (NOISE LEFT AND RIGHT), AND PULLUP-PUSHOVER PULLUP (1.5-. 5-1.5g)	220, 250, 280, 320, 350 KEAS @ 15K	200,000 LBS	SCANI-VALVE DATA AT TRIM POINT AND SIDESLIPS
CRUISE PERFORMANCE W/δ = 800,000	SPEED POWER, AND ACCEL	.82, .80, .78, .75, .72, .70, ACCEL .70 - .82, .80, .78 ≃ 35K FT.	188,000 LBS	3 MIN STABILIZED POINTS WITH 1 MIN OF SCANI-VALVE AT END OF EACH RUN. WING DEFLECTION PHOTOS DURING RUN ACCEL AT NRT.
BUFFET BOUNDARIES	WIND UP TURN TO INITIAL BUFFET (≃ 15 SEC DURATION)	40K @ .60, .70, .80, .84 33K' @ .50 24K' @ .40 15K' @ .33	LESS THAN 170K LBS FWD AND AFT BODY EMPTY	

Figure 12. - KC-135 winglet flight sequence

KC-135 WINGLET FLIGHT SEQUENCE

FLIGHT NO. _____ CANT ∠ _____ INCIDENCE ∠ _____

OBJECTIVE	MANEUVER	A/S, M, ALT	WEIGHT	COMMENTS
TAKE OFF PERFORMANCE	HANDBOOK TAKEOFF	FIELD ELEVATION	252,600 LBS. INCLUDING WATER	THEODOLITE MEAS. FROM BRAKE RELEASE TO 50 FT
FLUTTER CHECKS FUEL CONDITION	2 EACH – ELEV., RUDDER, AND AILERON RAPS	300/.67* 320/.712 340/.754, 350/.775* 360/.795, 370/.815 380/.835, 390/.857*	MAIN AND RESERVE TANKS FULL	*3 AXIS AUTO-PILOT ON AND OFF (ALL OTHER CONDITIONS – AUTO PILOT OFF).
↓	↓	395/.867, 400/.876 405/.887, 410/.897 413/.903, 416/.91 CAS/M @ 21,500'	↓	
FLUTTER CHECKS FUEL CONDITION	2 EACH ELEV., RUDDER, AND AILERON RAPS	300/.67,* 320/.712 340/.754, 350/.775 360/.795, 370/.815 380/.885, 390/.857*	10,000 LBS EACH MAIN TANK RESERVE TANKS EMPTY	*3 AXIS AUTO-PITOT ON AND OFF (ALL OTHER CONDITIONS AUTO PILOT OFF).
↓	↓	395/.867, 400/.876 405/.887, 410/.897 413/.903, 416/.91 CAS/M @ 21,500	↓	

Figure 13. - KC-135 winglet flight sequence

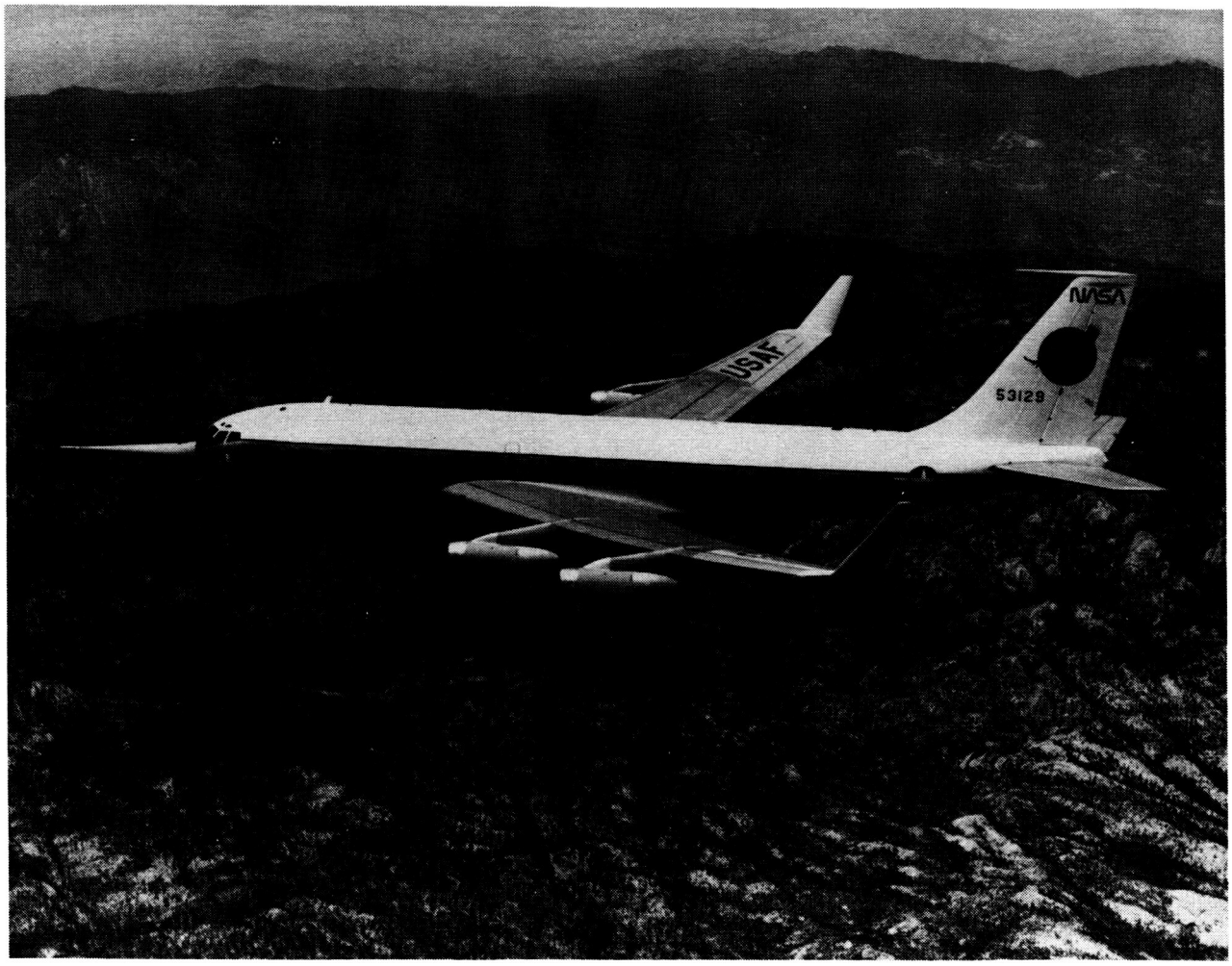

Figure 14. - Test airplane with winglets installed

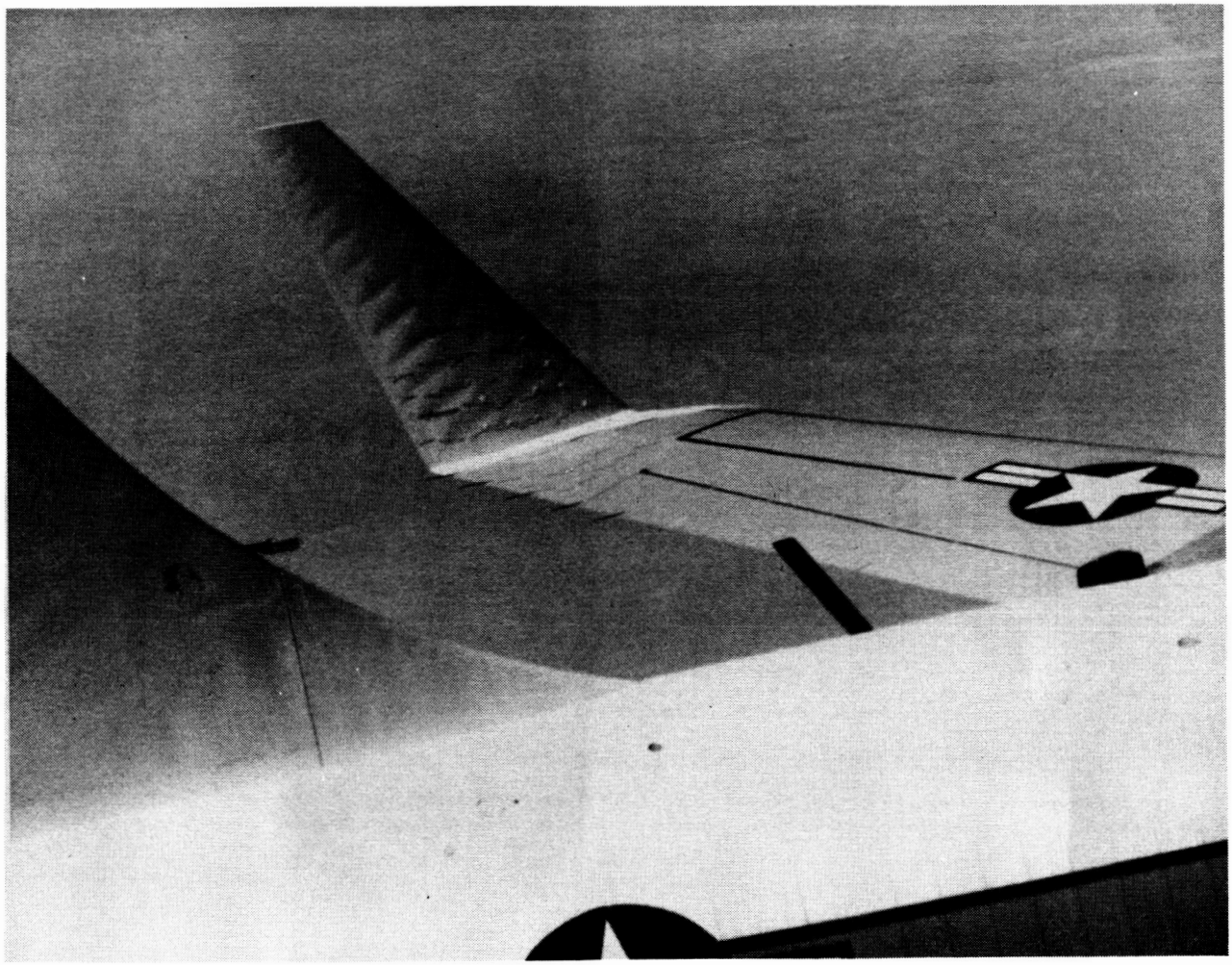

Figure 15. - Winglet inflight with skin "pillowing"

APPENDIX A

TODAY: 01/07/81 FLIGHT INSTRUMENTATION PARAMETER LIST PAGE 1 OF COPY 1
REV: 0 DATE: 7/24/79

VEHICLE: KC-135 WINGLET PROGRAM PCM BIT RATE: 125 KHZ
FLT NO. 054 PROJ INSTR ENGR: GENE KENNER BITS/WORD: 10
SCHED FLT DATE: 12/24/80 WORDS/FRAME: 64
TM FREQ: MHZ S/N FR/DATA CY: 10
PCM SYS/CODE NO. 1-04 FORMAT NO. 1 FBT=BIT1=MSB
PCM SYS MODEL: RMDU MAIN FRAME SYNC WORDS: 00 , 01 , 02

ITM NO.: SYS:	PARMID	CALID	NAME	CALIBRATED DATE	RANGE LOW	RANGE HIGH	ENG UNITS	FRAM: WORD: POS	FRAME: NO.	SAMP: RATE:	COMP: ALG	REF PRESS	VP/TP KP	FILTER PARMID	FREQ	DB	ITM NO.
1:	4FF1***	311 00 000	MAIN FRAME SYNC NO.1 0045 OCT					0:		200:	2000:						1
2:	4FF2***	311 00 001	MAIN FRAME SYNC NO.2 0434 OCT					1:		200:	2000:						2
3:	4FF3***	311 00 002	MAIN FRAME SYNC NO.3 1677 OCT					2:		200:	2000:						3
4:	TD1***	311 00 003	SUB FRAME I.D.COUNTER					3:		200:	2000:						4
5:	AC5LEL	311 05 009	C*: L/H WINGLET LE LONG ACCEL	08/11/80	-5	5	G	4:		195:	4000:				33:	18:	5
6:	AC5LEN	311 05 008	B*: L/H WINGLET LE NORM ACCEL	06/16/80	-10	10	G	5:		195:	4000:				55:	18:	6
7:	SV1P	311 02 010	B*: SCANIVALVE NO 1 PRESS	06/16/80	-3	3	PSID	6:		195:	4000:	SVRP1B			40:	6:	7
8:	SVID1	311 00 007	C*: SCANIVALVE NO 1 ID	03/14/79	1	48	CODE	7:		195:	4000:						8
9:	AC10VEN	311 02 021	D*: VERT FIN LAT ACCEL	02/23/79	-5	5	G	8:		195:	4000:						9
10:	AC10HN	311 02 022	A*: HORIZ STAB ACCEL	11/17/80	-5	5	G	9:		195:	4000:						10
11:	AC4EN	311 02 019	B*: ENGINE 4 NORMAL ACCEL	08/16/80	-5	5	G	10:		195:	4000:				18:	18:	11
12:	AC4EL	311 02 020	D*: ENGINE 4 LATERAL ACCEL	08/16/80	-5	5	G	11:		195:	4000:				18:	18:	12
13:	AC10LAT	311 05 013	A*: AFT BODY LATERAL ACCEL	06/16/80	-1	1	G	12:		195:	4000:				20:	18:	13
14:	AC10NOR	311 05 014	A*: AFT BODY NORMAL ACCEL	06/16/80	-5	5	G	13:		195:	4000:				35:	18:	14
15:	AILL	311 04 019	C*: L/H OUTBD AILERON POS	06/16/80	-15	19	DEG	14:		195:	4000:						15
16:	AILR	311 04 020	D*: R/H OUTBD AILERON POS	06/16/80	-17	17.5	DEG	15:		195:	4000:						16
17:	SV2P	311 02 011	B*: SCANIVALVE NO 2 PRESS	06/16/80	-3	3	PSID	16:		195:	4000:	SVRP0B	VM002		55:	6:	17
18:	SV3P	311 02 012	B*: SCANIVALVE NO 3 PRESS	06/16/80	-3	3	PSID	17:		195:	4000:	SVRP0B	VM002		55:	6:	18
19:	SV4P	311 02 013	B*: SCANIVALVE NO 4 PRESS	06/16/80	-3	3	PSID	18:		195:	4000:	SVRP0B	VM002		55:	6:	19
20:	SV5P	311 02 014	B*: SCANIVALVE NO 5 PRESS	06/16/80	-3	3	PSID	19:		195:	4000:	SVRP0B	VM002		55:	6:	20
21:	SVID2	311 10 101	C*: SCANIVALVE NO 2 ID	07/15/79	1	48	PORT ID	20:		200:	4000:						21
22:	SVID3	311 10 102	A*: SCANIVALVE NO 3 ID	07/15/79	1	48	PORT ID	21:		200:	4000:						22
23:	SVID4	311 09 104	D*: SCANIVALVE NO 4 ID	07/15/79	1	48	PORT ID	22:		200:	4000:						23
24:	SVID5	311 09 102	C*: SCANIVALVE NO 5 ID	07/15/79	1	48	PORT ID	23:		200:	4000:						24
25:	AC7LEN	311 05 001	B*: R/H WINGTIP LE NORM ACCEL	06/16/80	-10	10	G	24:		195:	4000:				55:	18:	25
26:	AC7TEN	311 05 002	A*: R/H WINGTIP TE NORM ACCEL	06/16/80	-10	10	G	25:		195:	4000:				55:	18:	26
27:	AC7LEL	311 05 003	A*: R/H WINGTIP LE LONG ACCEL	06/16/80	-2	2	G	26:		195:	4000:				35:	18:	27
28:	AC6LEN	311 05 004	B*: L/H WINGTIP LE NORM ACCEL	06/16/80	-10	10	G	27:		195:	4000:				55:	18:	28
29:	AC6LEN	311 05 005	A*: R/H WINGLET LE NORM ACCEL	06/16/80	-10	10	G	28:		195:	4000:				55:	18:	29
30:	AC6LEL	311 05 006	D*: R/H WINGLET LE LONG ACCEL	08/12/80	-5	5	G	29:		195:	4000:				37:	18:	30
31:	AC8TEN	311 05 007	A*: R/H WINGLET TE NORM ACCEL	06/16/80	-10	10	G	30:		195:	4000:				55:	18:	31
32:	TCREF	311 02 016	D*: THERMO REF OVEN TEMP	10/01/80	100	180	DEG F	31:		195:	4000:						32
33:	NULL	311 00 032						32:		200:	2000:						33
34:	PHI	311 03 015	A*: ROLL ANGLE	06/16/80	-30	30	DEG	33:		195:	4000:						34
35:	SVRP1B	311 03 001	A*: SCANIVALVE REF PRESS - INBD	06/16/80	0	15	PSIA	34:		195:	4000:				40:	6:	35
36:	SVRP0B	311 03 002	B*: SCANIVALVE REF PRESS - OUTBD	06/16/80	0	15	PSIA	35:		195:	4000:				55:	6:	36
37:	AC98MN	311 05 015	D*: NOSE BOOM NORM ACCEL	02/27/79	-15	15	G	36:		200:	4000:				40:	6:	37
38:	AC7WPN	311 05 016	A*: WING PANEL ACCEL	11/20/79	-80	80	G	37:		195:	4000:				100:	18:	38
39:	AC3EN	311 07 019	B*: ENGINE 3 NORMAL ACCEL	09/08/80	-3	3	G	38:		195:	4000:				18:	18:	39
40:	AC3EL	311 07 020	A*: ENGINE 3 LATERAL ACCEL	08/16/80	-5	5	G	39:		195:	4000:				18:	18:	40
41:	NULL	311 00 040						40:		200:	2000:						41
42:	S1F001*	311 00 041	SUBFRAME 01					41:		195:	1000:						42
43:	S1F002*	311 00 042	SUBFRAME 02					42:		195:	1000:						43
44:	S1F003*	311 00 043	SUBFRAME 03					43:		195:	1000:						44
45:	S1F004*	311 00 044	SUBFRAME 04					44:		195:	1000:						45
46:	S1F005*	311 00 045	SUBFRAME 05					45:		195:	1000:						46
47:	S1F006*	311 00 046	SUBFRAME 06					46:		195:	1000:						47
48:	S1F007*	311 00 047	SUBFRAME 07					47:		195:	1000:						48

TODAY: 01/07/81 FLIGHT INSTRUMENTATION PARAMETER LIST PAGE 2 OF COPY 1
REV: D DATE: 7/24/79

VEHICLE: KC-135 WINGLET PROGRAM
FLT NO. 054 PROJ INSTR ENGR: GENE KENNER
SCHED FLT DATE: 12/24/80
TM FREQ: MHZ S/N
PCM SYS/COM NO. 1-00 FORMAT NO. 1
PCM SYS MODEL: RMDU

PCM BIT RATE: 125 KHZ
BITS/WORD: 16
WORDS/FRAME: 64
FR/DATA CY: 10
FBT=BIT1=MSB
MAIN FRAME SYNC WORDS: 00 , 01 , 02

ITM NO., SYS	PARAMETER ID	CALID	NAME	CALIBRATED DATA	CALIBRATED RANGE LOW	CALIBRATED RANGE HIGH	ENG UNITS	FRAME WORD POS	FRAME NO.	SAMP RATE	COMP ALG	REF PRESS PARMID	VM/TP KP PARMID	FILTER FREQ	FILTER DB	ITM INC. COM
49	S1F009*	311 00 048	SUBFRAME 08					48		195:1000						49
50	S1F009*	311 00 049	SUBFRAME 09					49		195:1000						50
51	S1F010*	311 00 050	SUBFRAME 10					50		195:1000						51
52	S1F011*	311 00 051	SUBFRAME 11					51		195:1000						52
53	S1F012*	311 00 052	SUBFRAME 12					52		195:1000						53
54	S1F013*	311 00 053	SUBFRAME 13					53		195:1000						54
55	S1F014*	311 00 054	SUBFRAME 14					54		195:1000						55
56	S1F015*	311 00 055	SUBFRAME 15					55		195:1000						56
57	S1F016*	311 00 056	SUBFRAME 16					56		195:1000						57
58	S1F017*	311 00 057	SUBFRAME 17					57		195:1000						58
59	S1F018*	311 00 058	SUBFRAME 18					58		195:1000						59
60	S1F019*	311 00 059	SUBFRAME 19					59		195:1000						60
61	S1F020*	311 00 060	SUBFRAME 20					60		195:1000						61
62	S1F021*	311 00 061	SUBFRAME 21					61		195:1000						62
63	S1F022*	311 00 062	SUBFRAME 22					62		195:1000						63
64	S1F023*	311 00 063	SUBFRAME 23					63		195:1000						64

TODAY: 01/07/81 FLIGHT INSTRUMENTATION PARAMETER LIST PAGE 3 OF COPY 1
REV: D DATE: 7/24/79

VEHICLE: KC-135 WINGLET PROGRAM PCM BIT RATE: 125 KHZ
FLT NO. 054 PROJ INSTR ENGR: GENE KENNER BITS/WORD: 10
SCHED FLT DATE: 12/24/80 WORDS/FRAME: 64
TM FREQ: MHZ S/N FR/DATA CY: 10
PCM SYS/COM NO. 1-00 FORMAT NO. 1 FBT=BIT1=MSB
PCM SYS MODEL: RMDU MAIN FRAME SYNC WORDS: 00 , 01 , 02

SCANIVALVE NO. 1

S/V PRESSURE PARMID SV1P S/V REF PRESSURE PARMID SVRP1B S/V PORT ID SVID1
SYS ITEM NO/ER WD POS 7 6 SYS ITEM NO/ER WD POS 35 34 SYS ITEM NO/FR WD POS 8 7

ITEM NO. SYS	PARMID	PARAMETER NAME	PORT ID DEC	PARAMETERS AFFECTED	REMARKS	PORT NO.
7	S1REF01	REF PRESS PORT 01 26% SV 1	1	10	PORTS PER SEC	1
7	R1U00	26 PCT PORT U00	2			2
7	R1U03	26 PCT PORT 03	3			3
7	R1U05	26 PCT PORT 05	4			4
7	R1U15	26 PCT PORT 15	5			5
7	R1U25	26 PCT PORT 25	6			6
7	R1U35	26 PCT PORT 35	7			7
7	R1U45	26 PCT PORT 45	8			8
7	R1U55	26 PCT PORT 55	9			9
7	R1U65	26 PCT PORT 65	10			10
7	R1U75	26 PCT PORT 75	11			11
7	R1U85	26 PCT PORT 85	12			12
7	R1U95	26 PCT PORT 95	13			13
7	R1L03	26 PCT PORT L03	14			14
7	R1L05	26 PCT PORT L05	15			15
7	R1L15	26 PCT PORT L15	16			16
7	R1L250	26 PCT PORT L250	17			17
7	R1L350	26 PCT PORT L350	18			18
7	R1L450	26 PCT PORT L450	19			19
7	R1L550	26 PCT PORT L550	20			20
7	R1L650	26 PCT PORT L650	21			21
7	R1L750	26 PCT PORT 750	22			22
7	R1L950	26 PCT PORT L950	23			23
7	S1REF24	REF PRESS PORT 24	24			24
7	S1SP25	SPARE S.V. PORTS AT 26 PCT	25			25
7	S1SP26	SPARE S.V. PORTS AT 26 PCT	26			26
7	S1SP27	SPARE S.V. PORTS AT 26 PCT	27			27
7	S1SP28	SPARE S.V. PORTS AT 26 PCT	28			28
7	S1SP29	SPARE S.V. PORTS AT 26 PCT	29			29
7	S1SP30	SPARE S.V. PORTS AT 26 PCT	30			30
7	S1SP31	SPARE S.V. PORTS AT 26 PCT	31			31
7	S1SP32	SPARE S.V. PORTS AT 26 PCT	32			32
7	S1SP33	SPARE S.V. PORTS AT 26 PCT	33			33
7	S1SP34	SPARE S.V. PORTS AT 26 PCT	34			34
7	S1SP35	SPARE S.V. PORTS AT 26 PCT	35			35
7	S1SP36	SPARE S.V. PORTS AT 26 PCT	36			36
7	S1SP37	SPARE S.V. PORTS AT 26 PCT	37			37
7	S1SP38	SPARE S.V. PORTS AT 26 PCT	38			38
7	S1SP39	SPARE S.V. PORTS AT 26 PCT	39			39
7	S1SP40	SPARE S.V. PORTS AT 26 PCT	40			40
7	S1SP41	SPARE S.V. PORTS AT 26 PCT	41			41
7	S1SP42	SPARE S.V. PORTS AT 26 PCT	42			42
7	S1SP43	SPARE S.V. PORTS AT 26 PCT	43			43
7	S1SP44	SPARE S.V. PORTS AT 26 PCT	44			44
7	S1SP45	SPARE S.V. PORTS AT 26 PCT	45			45
7	S1SP46	SPARE S.V. PORTS AT 26 PCT	46			46
7	S1SP47	SPARE S.V. PORTS AT 26 PCT	47			47
7	S1SP48	SPARE S.V. PORTS AT 26 PCT	48			48

TODAY: 01/07/81 FLIGHT INSTRUMENTATION PARAMETER LIST PAGE 4 OF COPY 1
REV: D DATE: 7/24/79

VEHICLE: KC-135 WINGLET PROGRAM
FLT NO. 054 PROJ INSTR ENGR: GENE KENNER
SCHED FLT DATE: 12/24/80
TM FREQ: MHZ S/N
PCM SYS/COM NO. 1-0U FORMAT NO. 1
PCM SYS MODEL: RMDU

PCM BIT RATE: 128 KHZ
BITS/WORD: 10
WORDS/FRAME: 64
FR/DATA CY: 10
FBT=BIT1=MSB
MAIN FRAME SYNC WORDS: 00 , 01 , 02

SCANIVALVE NO. 2

S/V PRESSURE PARMID SV2P
SYS ITEM NO/ER WD POS 17 16

S/V REF PRESSURE PARMID SVRP0R
SYS ITEM NO/ER WD POS 36 35

S/V PORT ID SVID2
SYS ITEM NO/ER WD POS 21 2C

ITEM NO. SYS	PARMID	NAME	PORT ID DEC	PARAMETERS AFFECTED / REMARKS	PORT NO.
17	S2REF01	REF PRESSURE PORT 1	1	10 PORTS / SECOND	1
17	R2U00	77 % PORT U00	2		2
17	R2U03	77 % PORT U03	3	20 SAMPLES / PORT	3
17	R2U05	77 % PORT U05	4		4
17	R2U10	77 % PORT U10	5		5
17	R2U15	77 % PORT U15	6		6
17	R2U20	77 % PORT U20	7		7
17	R2U25	77 % PORT U25	8		8
17	R2U30	77 % PORT U30	9		9
17	R2U35	77 % PORT U35	10		10
17	R2U40	77 % PORT U40	11		11
17	R2U45	77 % PORT U45	12		12
17	R2U50	77 % PORT U50	13		13
17	R2U55	77 % PORT U55	14		14
17	R2U60	77 % PORT U60	15		15
17	R2U65	77 % PORT U65	16		16
17	R2U70	77 % PORT U70	17		17
17	R2U75	77 % PORT U75	18		18
17	R2U80	77 % PORT U80	19		19
17	R2U85	77 % PORT U85	20		20
17	R2U90	77 % PORT U90	21		21
17	R2U95	77 % PORT U95	22		22
17	R2L00	77 % PORT L00	23		23
17	R2L05	77 % PORT L05	24		24
17	R2L10	77 % PORT L10	25		25
17	R2L25	77 % PORT L25	26		26
17	R2L30	77 % PORT L30	27		27
17	R2L55	77 % PORT L55	28		28
17	R2L60	77 % PORT L60	29		29
17	R2L80	77 % PORT L80	30		30
17	R2L90	77 % PORT L90	31		31
17	R3U00	92 % PORT U00	32		32
17	R3U01	92 % PORT U01	33		33
17	R3U03	92 % PORT U03	34		34
17	R3U05	92 % PORT U05	35		35
17	R3U10	92 % PORT U10	36		36
17	R3U15	92 % PORT U15	37		37
17	R3U20	92 % PORT U20	38		38
17	R3U25	92 % PORT U25	39		39
17	R3U30	92 % PORT U30	40		40
17	R3U35	92 % PORT U35	41		41
17	R3U40	92 % PORT U40	42		42
17	R3U45	92 % PORT U45	43		43
17	R3U50	92 % PORT U50	44		44
17	R3U60	92 % PORT U60	45		45
17	R3U65	92 % PORT U65	46		46
17	R3U70	92 % PORT U70	47		47
17	S2REF48	REF PRESSURE PORT 48	48		48

TODAY: 01/07/81 FLIGHT INSTRUMENTATION PARAMETER LIST PAGE 5 OF COPY 1
REV: 0 DATE: 7/24/79

VEHICLE: KC-135 WINGLET PROGRAM PCM BIT RATE: 125 KHZ
FLT NO. 354 PROJ INSTR ENGR: GENE KENNER BITS/WORD: 10
SCHED FLT DATE: 12/24/80 WORDS/FRAME: 64
TM FREQ: MHZ S/N FR/DATA CY: 10
PCM SYS/COM NO. 1-00 FORMAT NO. 1 FBT=BIT1=MSB
PCM SYS MODEL: RMDU MAIN FRAME SYNC WORDS: 00 , 01 , 02

SCANIVALVE NO. 3

ITEM NO.	PARAMETER								PORT ID DEC	PARAMETERS AFFECTED		PORT NO.
SYS	PARMID	NAME								REMARKS		
1R	S3REF01	REF PRESS PORT 01							1	10 PORTS PER SEC		1
1R	R3U75	92 PCT	PORT	U75	S.V 3				2			2
1R	R3U80	92 PCT	PORT	80	S.V 3				3	20 SAMPLES PER PORT		3
1R	R3U85	92 PCT	PORT	85	S.V 3				4			4
1R	R3U90	92 PCT	PORT	90	S.V 3				5			5
1R	R3U95	92 PCT	PORT	95	S.V 3				6			6
1R	R3L03	92 PCT	PORT	L03	S.V 3				7			7
1R	R3L05	92 PCT	PORT	L05	S.V 3				8			8
1R	R3L15	92 PCT	PORT	L15	S.V 3				9			9
1R	R3L25	92 PCT	PORT	L25	S.V 3				10			10
1R	R3L35	92 PCT	PORT	L35	S.V 3				11			11
1R	R3L55	92 PCT	PORT	L55	S.V 3				12			12
1R	R3L65	92 PCT	PORT	L65	S.V 3				13			13
1R	R3L85	92 PCT	PORT	L85	S.V 3				14			14
1R	R3L95	92 PCT	PORT	L95	S.V 3				15			15
1R	R4U00	99 PCT	PORT	U00	S.V 3				16			16
1R	R4U01	99 PCT	PORT	U01	S.V 3				17			17
1R	R4U03	99 PCT	PORT	U03	S.V 3				18			18
1R	R4U05	99 PCT	PORT	U05	S.V 3				19			19
1R	R4U10	99 PCT	PORT	U10	S.V 3				20			20
1R	R4U15	99 PCT	PORT	U15	S.V 3				21			21
1R	R4U20	99 PCT	PORT	U20	S.V 3				22			22
1R	R4U25	99 PCT	PORT	U25	S.V 3				23			23
1R	R4U30	99 PCT	PORT	U30	S.V 3				24			24
1R	R4U35	99 PCT	PORT	U35	S.V. 3				25			25
1R	R4U40	99 PCT	PORT	U40	S.V. 3				26			26
1R	R4U45	99 PCT	PORT	U45	S.V. 3				27			27
1R	R4U50	99 PCT	PORT	U50	S.V. 3				28			28
1R	R4U55	99 PCT	PORT	U55	S.V. 3				29			29
1R	R4U60	99 PCT	PORT	U60	S.V. 3				30			30
1R	R4U65	99 PCT	PORT	U65	S.V. 3				31			31
1R	R4U70	99 PCT	PORT	U70	S.V. 3				32			32
1R	R4U75	99 PCT	PORT	U75	S.V. 3				33			33
1R	R4U80	99 PCT	PORT	U80	S.V. 3				34			34
1R	R4U85	99 PCT	PORT	U85	S.V. 3				35			35
1R	R4U90	99 PCT	PORT	U90	S.V. 3				36			36
1R	R4L03	99 PCT	PORT	L03	S.V. 3				37			37
1R	R4L05	99 PCT	PORT	L05	S.V. 3				38			38
1R	R4L15	99 PCT	PORT	L15	S.V. 3				39			39
1R	R4L25	99 PCT	PORT	L25	S.V. 3				40			40
1R	R4L35	99 PCT	PORT	L35	S.V. 3				41			41
1R	R4L45	99 PCT	PORT	L45	S.V. 3				42			42
1R	R4L55	99 PCT	PORT	L55	S.V. 3				43			43
1R	R4L65	99 PCT	PORT	L65	S.V. 3				44			44
1R	R4L75	99 PCT	PORT	L75	S.V. 3				45			45
1R	R4L85	99 PCT	PORT	L85	S.V. 3				46			46
1R	R4L95	99 PCT	PORT	L95	S.V. 3				47			47
1R	S3REF48	REF PRESS PORT 48							48			48

TODAY: 01/07/81 FLIGHT INSTRUMENTATION PARAMETER LIST PAGE 6 OF COPY 1
REV: D DATE: 7/24/79

VEHICLE: KC-135 WINGLET PROGRAM
FLT NO. 054 PROJ INSTR ENGR: GENE KENNER
SCHED FLT DATE: 12/24/80
TM FREQ: MHZ S/N
PCM SYS/CJM NO. 1-00 FORMAT NO. 1
PCM SYS MODEL: RMDU

PCM BIT RATE: 125 KHZ
BITS/WORD: 10
WORDS/FRAME: 64
FR/DATA CY: 10
FBT=BIT1=MSB
MAIN FRAME SYNC WORDS: 00 , 01 , 02

SCANIVALVE NO. 4

ITEM NO.	S/V PRESSURE PARMID	NAME	SV4P	PORT ID DEC	S/V REF PRESSURE PARMID	SVRP08	S/V PORT ID	SVID4
SYS ITEM NO/FR WD POS	19 18				SYS ITEM NO/FR WD POS	36 35	SYS ITEM NO/FR WD POS	23 22
SYS	PARMID	NAME			REMARKS			PORT NO.
19	S4REF01	REFERENCE PRESSURE PORT 1		1	10 PORTS / SECOND			1
19	R5U00	101 % PORT U00		2				2
19	R5U02	101 % PORT 02		3	20 SAMPLES / PORT			3
19	R5U05	101 % PORT 05		4				4
19	R5U15	101 % PORT 15		5				5
19	R5U25	101 % PORT 25		6				6
19	R5U35	101 % PORT 35		7				7
19	R5U45	101 % PORT 45		8				8
19	R5U55	101 % PORT 55		9				9
19	R5U65	101 % PORT 65		10				10
19	R5U75	101 % PORT 75		11				11
19	R5U85	101 % PORT 85		12				12
19	R5U95	101 % PORT 95		13				13
19	R5L02	101 % PORT L02		14				14
19	R5L05	101 % PORT L05		15				15
19	R5L15	101 % PORT L15		16				16
19	R5L25	101 % PORT L25		17				17
19	R5L35	101 % PORT L35		18				18
19	R5L45	101 % PORT L45		19				19
19	R5L55	101 % PORT L55		20				20
19	R5L65	101 % PORT L65		21				21
19	R5L75	101 % PORT L75		22				22
19	R5L85	101 % PORT L85		23				23
19	R5L95	101 % PORT L95		24				24
19	R6U00	103 % PORT U00		25				25
19	R6U02	103 % PORT U02		26				26
19	R6U05	103 % PORT 05		27				27
19	R6U15	103 % PORT U15		28				28
19	R6U25	103 % PORT U25		29				29
19	R6U35	103 % PORT U35		30				30
19	R6U45	103 % PORT U45		31				31
19	R6U55	103 % PORT U55		32				32
19	R6U65	103 % PORT U65		33				33
19	R6U75	103 % PORT U75		34				34
19	R6U85	103 % PORT U85		35				35
19	R6U95	103 % PORT U95		36				36
19	R6L02	103 % PORT L02		37				37
19	R6L05	103 % PORT L05		38				38
19	R6L15	103 % PORT L15		39				39
19	R6L25	103 % PORT L25		40				40
19	R6L35	103 % PORT L35		41				41
19	R6L45	103 % PORT L45		42				42
19	R6L55	103 % PORT L55		43				43
19	R6L65	103 % PORT L65		44				44
19	R6L75	103 % PORT L75		45				45
19	R6L85	103 % PORT L85		46				46
19	R6L95	103 % PORT L95		47				47
19	S4REF48	REFERENCE PRESSURE PORT 48		48				48

VEHICLE: KC-135 WINGLET PROGRAM
FLT NO. 054 PROJ INSTR ENGR: GENE KENNER
SCHED FLT DATE: 12/24/80
TM FREQ: MHZ S/N
PCM SYS/COM NO. 1-00 FORMAT NO. 1
PCM SYS MODEL: RMDU

PCM BIT RATE: 125 KHZ
BITS/WORD: 10
WORDS/FRAME: 64
FR/DATA CY: 10
FBT=BIT1=MSB
MAIN FRAME SYNC WORDS: 00 , 01 , 02

SCANIVALVE NO. 5

S/V PRESSURE PARMID SV5P S/V REF PRESSURE PARMID SVRP08 S/V PORT ID SVID5
SYS ITEM NO/FR WD POS 20 19 SYS ITEM NO/FR WD POS 36 35 SYS ITEM NO/FR WD POS 24 23

ITEM NO. SYS	PARAMETER PARMID	NAME	PORT ID DEC	PARAMETERS AFFECTED REMARKS	PORT NO.
20	S5REF01	REFERENCE PRESSURE PORT 1	1	10 PORTS / SECOND	1
20	R7U00	105 % PORT U00	2		2
20	R7U02	105 % PORT U02	3	20 SAMPLES / PORT	3
20	R7U05	105 % PORT U05	4		4
20	R7U15	105 % PORT U15	5		5
20	R7U25	105 % PORT U25	6		6
20	R7U35	105 % PORT U35	7		7
20	R7U45	105 % PORT U45	8		8
20	R7U55	105 % PORT U55	9		9
20	R7U65	105 % PORT U65	10		10
20	R7U75	105 % PORT U75	11		11
20	R7U85	105 % PORT U85	12		12
20	R7U95	105 % PORT U95	13		13
20	R7L02	105 % PORT L02	14		14
20	R7L05	105 % PORT L05	15		15
20	R7L15	105 % PORT L15	16		16
20	R7L25	105 % PORT L25	17		17
20	R7L35	105 % PORT L35	18		18
20	R7L45	105 % PORT L45	19		19
20	R7L55	105 % PORT L55	20		20
20	R7L65	105 % PORT L65	21		21
20	R7L75	105 % PORT L75	22		22
20	R7L85	105 % PORT L85	23		23
20	R7L95	105 % PORT L95	24		24
20	S5REF25	REFERENCE PRESSURE PORT 25	25		25
20	S5REF26	REFERENCE PRESSURE PORT 26	26		26
20	S5REF27	REFERENCE PRESSURE PORT 27	27		27
20	S5REF28	REFERENCE PRESSURE PORT 28	28		28
20	S5REF29	REFERENCE PRESSURE PORT 29	29		29
20	S5REF30	REFERENCE PRESSURE PORT 30	30		30
20	S5REF31	REFERENCE PRESSURE PORT 31	31		31
20	S5REF32	REFERENCE PRESSURE PORT 32	32		32
20	S5REF33	REFERENCE PRESSURE PORT 33	33		33
20	S5REF34	REFERENCE PRESSURE PORT 34	34		34
20	S5REF35	REFERENCE PRESSURE PORT 35	35		35
20	S5REF36	REFERENCE PRESSURE PORT 36	36		36
20	S5REF37	REFERENCE PRESSURE PORT 37	37		37
20	S5REF38	REFERENCE PRESSURE PORT 38	38		38
20	S5REF39	REFERENCE PRESSURE PORT 39	39		39
20	S5REF40	REFERENCE PRESSURE PORT 40	40		40
20	S5REF41	REFERENCE PRESSURE PORT 41	41		41
20	S5REF42	REFERENCE PRESSURE PORT 42	42		42
20	S5REF43	REFERENCE PRESSURE PORT 43	43		43
20	S5REF44	REFERENCE PRESSURE PORT 44	44		44
20	S5REF45	REFERENCE PRESSURE PORT 45	45		45
20	S5REF46	REFERENCE PRESSURE PORT 46	46		46
20	S5REF47	REFERENCE PRESSURE PORT 47	47		47
20	S5REF48	REFERENCE PRESSURE PORT 48	48		48

TODAY: 01/07/81 FLIGHT INSTRUMENTATION PARAMETER LIST PAGE 8 OF COPY 1

REV: D DATE: 7/24/79

VEHICLE: KC-135 WINGLET PROGRAM PCM BIT RATE: 125 KHZ

FLT NO. 054 PROJ INSTR ENGR: GENE KENNER BITS/WORD: 10

SCHED FLT DATE: 12/24/80 WORDS/FRAME: 64

TM FREQ: MHZ S/N FR/DATA CY: 10

PCM SYS/COM NO. 1-01 FORMAT NO. 1 FRT=BIT1=MSB

PCM SYS MODEL: RNDU MAIN FRAME SYNC WORDS: 00 , 01 , 02

ITM NO. SYS	PARMID	CALID		NAME	DATE	CALIBRATED RANGE LOW	CALIBRATED RANGE HIGH	UNITS	ENG PROCESS	FRAME WORD POS	FRAME NO.	SAMP RATE	COMP ALG	REF PPESS KP	VP/TP PARMID	FILTER FREQ	FILTER QDR	ITM NO. COM
65	FTQT2E	311	07 101	FUEL TOTALIZER ENG 2		0	512	COUNTS		41	0	39:1000						1
66	FTQT2C	311	07 102	OK: FUEL TOTALIZER ENG 2	08/28/78	512	65535	COUNTS		42	0	39:1000			FTQT2F			2
67	RRUD	311	04 017	B*: RUDDER POSITION	06/16/80	-25	25	DEG		43	0	39:4000				55	6	3
68	RRUDTT	311	04 018	B*: RUDDER TRIM TAB POSITION	06/16/80	-21	22.5	DEG		44	0	39:4000				55	6	4
69	FFRD1	311	08 3U1	O*: FUEL FLOW RATE CIC. ENG. 1	06/16/80	0	40	GPM		45	0	39:4000						5
70	SGRT1	311	02 023	: FRONT SPAR BENDING UP SURF						46	0	19.5:4000				55	6	6
71	SGRT2	311	02 024	: FRONT SPAR SHEAR UP SURF						47	0	19.5:4000				55	6	7
72	SGRT3	311	02 025	: FRONT SPAR BENDING UP SURF						48	0	19.5:4000				55	6	8
73	SGRT4	311	02 026	: FRONT SPAR SHEAR UP SURF						49	0	19.5:4000				55	6	9
74	SGRT5	311	02 027	: FRONT SPAR BENDING UP SURF						50	0	19.5:4000				55	6	10
75	SGRT6	311	02 028	: AFT SPAR SHEAR UP SURF						51	0	19.5:4000				55	6	11
76	SGRT7	311	02 029	: AFT SPAR BENDING UP SURF						52	0	19.5:4000				55	6	12
77	PT2E1P1	311	01 001	A*: PT-2 ENGINE 1 PORT 1	06/16/80	-4	4	PSID		53	0	19.5:4000	QPR01C			5	6	13
78	PT2E1P2	311	01 002	AP: PT-2 ENGINE 1 PORT 2	06/16/80	-4	4	PSID		54	0	19.5:4000	QPR01C			5	6	14
79	PT2E1P3	311	01 003	AP: PT-2 ENGINE 1 PORT 3	06/16/80	-4	4	PSID		55	0	19.5:4000	QPR01C			5	6	15
80	PT2E1P4	311	01 004	AP: PT-2 ENGINE 1 PORT 4	06/16/80	-4	4	PSID		56	0	19.5:4000	QPR01C			5	6	16
81	PT2E1P5	311	01 005	AP: PT-2 ENGINE 1 PORT 5	06/16/80	-4	4	PSID		57	0	19.5:4000	QPR01C			5	6	17
82	PT2E1P6	311	01 006	AP: PT-2 ENGINE 1 PORT 6	06/16/80	-4	4	PSID		58	0	19.5:4000	QPR01C			5	6	18
83	PT2E1P7	311	01 007	AP: PT-2 ENGINE 1 PORT 7	11/21/79	-4	4	PSID		59	0	20:4000	QPR01C			5	6	19
84	PT2E1P8	311	01 008	AP: PT-2 ENGINE 1 PORT 8	07/19/80	-4	4	PSID		60	0	19.5:4000	QPR01C			5	6	20
85	PT2E2P1	311	01 009	AP: PT-2 ENGINE 2 PORT 1	06/16/80	-4	4	PSID		61	0	19.5:4000	QPR01C			5	6	21
86	PT2E2P2	311	01 010	AP: PT-2 ENGINE 2 PORT 2	06/16/80	-4	4	PSID		62	0	19.5:4000	QPR01C			5	6	22
87	PT2E2P3	311	01 011	AP: PT-2 ENGINE 2 PORT 3	06/16/80	-4	4	PSID		63	0	19.5:4000	QPR01C			5	6	23
88	FTQT3F	311	07 103	: FUEL TOTALIZER ENG 3		0	512	COUNTS		41	1	39:1000						24
89	FTQT3C	311	08 101	OK: FUEL TOTALIZER ENG 3	08/28/78	512	65535	COUNTS		42	1	39:1000			FTQT3F			25
90	DALLT	311	04 021	D*: L/H INBD AILERON POS	06/16/80	-19.4	16.5	DEG		43	1	39:4000				55	6	26
91	DALRT	311	04 022	G*: R/H INBD AILERON POS	10/30/80	-18.2	19.5	DEG		44	1	39:4000				55	6	27
92	AC13CN	311	05 010	B*: COCKPIT NORMAL ACCEL	08/11/60	-1	3	G		45	1	39:4000				35	18	28
93	SGRT8	311	02 030	: AFT SPAR SHEAR UP SURF						46	1	19.5:4000				55	6	29
94	SGRT9	311	02 031	: AFT SPAR BENDING UP SURF						47	1	19.5:4000				55	6	30
95	SGRT10	311	02 032	: AFT SPAR SHEAR LP SURF						48	1	19.5:4000				55	6	31
96	SGRT11	311	06 013	: AFT BENDING UP SURF						49	1	19.5:4000				55	6	32
97	SGRT12	311	06 014	: FRONT SPAR BENDING LO SURF						50	1	19.5:4000				55	6	33
98	SGRT13	311	06 015	: FRONT SPAR SHEAR LO SURF						51	1	19.5:4000				55	6	34
99	SGRT14	311	06 016	: FRONT SPAR BENDING LO SURF						52	1	19.5:4000				55	6	35
100	PT2E2P4	311	01 012	AP: PT-2 ENGINE 2 PORT 4	06/16/80	-4	4	PSID		53	1	19.5:4000	QPR01C			5	6	36
101	PT2E2P5	311	01 013	PP: PT-2 ENGINE 2 PORT 5	06/16/80	-4	4	PSID		54	1	19.5:4000	QPR01C			5	6	37
102	PT2E2P6	311	01 014	AP: PT-2 ENGINE 2 PORT 6	06/16/80	-4	4	PSID		55	1	19.5:4000	QPR01C			5	6	38
103	PT2E2P7	311	01 015	AP: PT-2 ENGINE 2 PORT 7	06/16/80	-4	4	PSID		56	1	19.5:4000	QPR01C			5	6	39
104	PT2E2P8	311	01 016	AP: PT-2 ENGINE 2 PORT 8	06/16/80	-4	4	PSID		57	1	19.5:4000	QPR01C			5	6	40
105	PT2E3P1	311	01 017	AP: PT-2 ENGINE 3 PORT 1	06/16/80	-4	4	PSID		58	1	19.5:4000	QPR01C			5	6	41
106	PT2E3P2	311	01 018	AP: PT-2 ENGINE 3 PORT 2	06/16/80	-4	4	PSID		59	1	19.5:4000	QPR01C			5	6	42
107	PT2E4P1	311	01 019	AP: PT-2 ENGINE 4 PORT 1	06/16/80	-4	4	PSID		60	1	19.5:4000	QPR01C			5	6	43
108	PT2E4P2	311	01 020	AP: PT-2 ENGINE 4 PORT 2	06/16/80	-4	4	PSID		61	1	19.5:4000	QPR01C			5	6	44
109	PS2E1PA	311	01 021	AP: PS-2 ENGINE 1 PORT A	06/16/80	-6	6	PSID		62	1	19.5:4000	QPR01C			5	6	45
110	PS2E1PB	311	01 022	AP: PS-2 ENG 1 RAKE PORT B	06/16/80	-6	6	PSID		63	1	19.5:4000	QPR01C			5	6	46
111	FTQT4F	311	08 102	: FUEL TOTALIZER ENG 4				COUNTS		41	2	39:1000						47
112	FTQT4C	311	08 103	OK: FUEL TOTALIZER ENG 4	06/28/78	512	65535	COUNTS		42	2	39:1000			FTQT4F			48

VEHICLE: KC-135 WINGLET PROGRAM
FLT NO. 954 PROJ INSTR ENGR: GENE KENNER
SCHED FLT DATE: 12/24/80
TM FREQ: MHZ S/N
PCM SYS/COM NO. 1-01 FORMAT NO. 1
PCM SYS MODEL: RMFU

PCM BIT RATE: 125 KHZ
BITS/WORD: 10
WORDS/FRAME: 64
FR/DATA CY: 10
FBT=BIT1=MSB
MAIN FRAME SYNC WORDS: 00 , 01 , 02

ITM NO./SYS	PARMID	CALID		NAME	CALIBRATED DATE	RANGE LOW	RANGE HIGH	UNITS	ENG WORD POS	FRAME NO.	FRAME RATE	SAMP ALG	COMP PRESS	REF PARMID	VM/TM KP	FILTER PARMID	FREQ	DB	ITM INC. COM
113	D8LCT	311	04 023	A*: L/H INBD AIL CONTROL TAB	06/16/80	-21.5	19.5	DEG	43	2	39	4000					55	6	49
114	D8LPCT	311	04 024	C*: R/H INBD AIL CONTROL TAB	08/16/80	-20	21.5	DEG	44	2	39	4000					55	6	50
115	AZ	311	04 031	B*: C.G. NORMAL ACCEL	06/16/80	-1	3	G	45	2	39	4000					3	18	51
116	SGRT15	311	06 017	: FRONT SPAR LO SURF					46	2	19.5	4000					55	6	52
117	SGRT16	311	06 018	: FRONT SPAR LO SURF					47	2	19.5	4000					55	6	53
118	SGRT17	311	06 019	: AFT SPAR SHEAR LO SURF					48	2	19.5	4000					55	6	54
119	SGRT18	311	06 020	: AFT SPAR BENDING LO SURF					49	2	19.5	4000					55	6	55
120	SGRT19	311	06 021	: AFT SPAR SHEAR LO SURF					50	2	19.5	4000					55	6	56
121	SGRT20	311	06 022	: AFT SPAR BENDING LO SURF					51	2	19.5	4000					55	6	57
122	SGRT21	311	06 023	: AFT SPAR SHEAR LO SURF					52	2	19.5	4000					55	6	58
123	PS2E190	311	01 023	AP: PS-2 ENG 1 RAKE PORT C	06/16/80	-6	6	PSID	53	2	19.5	4000	QPR01C				5	6	59
124	PS2E190	311	01 024	AP: PS-2 ENG 1 RAKE PORT D	06/16/80	-6	6	PSID	54	2	19.5	4000	QPR01C				5	6	60
125	PS2E29A	311	01 025	AP: PS-2 ENG 2 RAKE PORT A	06/16/80	-6	6	PSID	55	2	19.5	4000	QPR01C				5	6	61
126	PS2E29B	311	01 026	AP: PS-2 ENG 2 RAKE PORT B	06/16/80	-6	6	PSID	56	2	19.5	4000	QPR01C				5	6	62
127	PS2E29C	311	01 027	AP: PS-2 ENG 2 RAKE PORT C	06/16/80	-6	6	PSID	57	2	19.5	4000	QPR01C				5	6	63
128	PS2E29D	311	01 028	AP: PS-2 ENG 2 RAKE PORT D	06/16/80	-6	6	PSID	58	2	19.5	4000	QPR01C				5	6	64
129	PS2E39A	311	01 029	AP: PS-2 ENG 3 RAKE PORT A	06/16/80	-6	6	PSID	59	2	19.5	4000	QPR01C				5	6	65
130	PS2E39B	311	01 030	AP: PS-2 ENG 3 RAKE PORT B	06/16/80	-6	6	PSID	60	2	19.5	4000	QPR01C				5	6	66
131	PS2E4PA	311	01 031	AP: PS-2 ENG 4 RAKE PORT A	06/16/80	-6	6	PSID	61	2	19.5	4000	QPR01C				5	6	67
132	PS2E49B	311	01 032	AP: PS-2 ENG 4 RAKE PORT B	06/16/80	-6	6	PSID	62	2	19.5	4000	QPR01C				5	6	68
133	VM003	311	05 019	O*: VOLTAGE MONITOR 10 V	02/16/79	0	10	COUNTS	63	2	20	4000					5	6	69
134	PREF15	311	09 102	: PROP REF PRESS				PSIA	41	3	39	1000							70
135	PREF1C	311	09 103	AK: PROP REF PRESS	06/16/80	0	40	PSIA	42	3	39	1000			QPR01F				71
136	ELV0	311	04 025	F*: R/H ELEVATOR POSITION	06/16/80	-24.5	15	DEG	43	3	39	4000					55	6	72
137	ELVCT	311	04 026	G*: ELEVATOR CONTROL TAB POS	02/20/79	-17.5	23.5	DEG	44	3	39	4000					55	6	73
138	DHSTB	311	04 027	R*: HORZ STAB POSITION	06/16/80	-13.5	.5	DEG	45	3	39	4000					55	6	74
139	SGRT22	311	06 024	: AFT SPAR BENDING LO SURF					46	3	19.5	4000					55	6	75
140	SGWI1	311	06 031	: O/B WING REAR SPAR 779 MAIN					47	3	19.5	4000					55	6	76
141	SGWI2	311	06 032	: O/B WING REAR SPAR 779 SPARE					48	3	19.5	4000					55	6	77
142	SGWT3	311	06 029	: O/B WING AUX SPAR 779 MAIN					49	3	19.5	4000					55	6	78
143	SGWT4	311	06 030	: O/B WING AUX SPAR 779 SPARE					50	3	19.5	4000					55	6	79
144	SGOW1	311	07 001	: O/B WING FR SPAR 745 MAIN					51	3	19.5	4000					55	6	80
145	SGOW2	311	07 002	: O/B WING FR SPAR 745 SPARE					52	3	19.5	4000					55	6	81
146	PT7E10	311	02 001	DP: PT-7 ENG 1 DIFF PRESS	10/21/80	0	40	PSID	53	3	19.5	4000	QPR01C				5	6	82
147	PT7E20	311	02 002	BP: PT-7 ENG 2 DIFF PRESS	10/21/80	0	40	PSID	54	3	19.5	4000	QPR01C				5	6	83
148	PT7E30	311	02 003	BP: PT-7 ENG 3 DIFF PRESS	10/21/80	0	40	PSID	55	3	19.5	4000	QPR01C				5	6	84
149	PT7E40	311	02 004	AP: PT-7 ENG 4 DIFF PRESS	06/16/80	0	40	PSID	56	3	19.5	4000	QPR01C				5	6	85
150	PSRE10	311	02 005	AP: PS-8 ENG 1 DIFF PRESS	06/16/80	-30	30	PSID	57	3	19.5	4000	QPR01C				5	6	86
151	PSRE20	311	02 006	AP: PS-8 ENG 2 DIFF PRESS	06/16/80	-30	30	PSID	58	3	19.5	4000	QPR01C				5	6	87
152	PSRE30	311	02 007	AP: PS-8 ENG 3 DIFF PRESS	06/16/80	-30	30	PSID	59	3	19.5	4000	QPR01C				5	6	88
153	PSRE40	311	02 008	AP: PS-8 ENG 4 DIFF PRESS	06/16/80	-30	30	PSID	60	3	19.5	4000	QPR01C				5	6	89
154	PT8E20	311	02 009	CP: PT-8 ENG 2 DIFF PRESS	10/21/80	0	40	PSID	61	3	19.5	4000	QPR01C				5	6	90
155	ETM01	311	03 006	C*: FUEL TEMP ENGINE 1	10/01/80	0	135	DEG F	62	3	19.5	4000					10	6	91
156	ETM02	311	03 007	C*: FUEL TEMP ENGINE 2	10/01/80	0	135	DEG F	63	3	19.5	4000					10	6	92
157	VTS	311	10 101	: AIRSPEED				KNOTS	41	4	39	1000							93
158	VI	311	10 102	BK: AIRSPEED	08/09/79	0	100	KNOTS	42	4	39	1000			VIF				94
159	AYCEN	311	04 028	B*: C.G. LONG ACCEL SENSITIVE	06/16/80	-.25	.25	G	43	4	39	4000					3	18	95
160	AY	311	04 029	B*: C.G. LONG ACCEL	06/16/80	-1	1	G	44	4	39	4000					3	18	96

TODAY: 01/07/81

FLIGHT INSTRUMENTATION PARAMETER LIST
REV: 0 DATE: 7/24/79

VEHICLE: KC-135 WINGLET PROGRAM
FLT NO. 354
SCHED FLT DATE: 12/24/80
TM FREQ: MHZ S/N
PCM SYS/COM NO. 1-01 FORMAT NO. 1
PCM SYS MODEL: RMDU

PROJ INSTR ENGR: GENE KENNER

PCM BIT RATE: 125 KHZ
BITS/WORD: 10
WORDS/FRAME: 64
FR/DATA CY: 10
FRT=RIT1=MS8
MAIN FRAME SYNC WORDS: 00 , 01 , 02

ITM NO. SYS	PARMID	CALID		PARAMETER NAME	CALIBRATED DATE	LOW	HIGH	ENG UNITS	FRAM WORD POS	FRAME NO.	SAMP RATE	COMP ALG	REF PRESS	VM/TM KP	FILTER PARMID	FREQ	DB	ITM NO.
161	4Y	311	04 030	A*	C.G. LAT ACCEL	06/16/80	-.5	.5	G	45	41 39	4000				55	6	97
162	SGDW3	311	07 005		O/B WING SHR FR SPAR 745-1					46	4	19.5	4000			55	6	98
163	SGDW4	311	07 006		O/B WING SHR FR SPAR 745-2					47	4	19.5	4000			55	6	99
164	SGDW5	311	07 003		O/B WING REAR SPAR 745 MAIN					48	4	19.5	4000			55	6	100
165	SGDW6	311	07 004		O/B WING REAR SPAR 745 SPARE					49	4	19.5	4000			55	6	101
166	SGDW7	311	07 007		O/B WING SHR REAR SPAR 745-1					50	4	19.5	4000			55	6	102
167	SGDW8	311	07 008		O/B WING SHR REAR SPAR 745-2					51	4	19.5	4000			55	6	103
168	SGES5	311	06 001		R/H OUTBD WING PANEL					52	4	19.5	4000			55	6	104
169	ETMP3	311	03 008	C*	FUEL TEMP ENGINE 3	10/01/80	0	135	DEG F	53	4	19.5	4000			10	6	105
170	ETM04	311	03 014	C*	FUEL TEMP ENGINE 4	10/01/80	0	135	DEG F	54	4	19.5	4000			10	6	106
171	EVENTCM	311	02 017	U*	EVENT-DEFLECTION CAMERA	08/30/79	OFF	ON		55	4	19.5	4000					107
172	THETA	311	03 016	A*	PITCH ANGLE	06/16/80	-30	30	DEG	56	4	19.5	4000					108
173	DELP3L	311	05 021	B*	L/H OUTBD FLAP POSITION	06/16/80	0	50	DEG	57	4	19.5	4000			10	6	109
174	DELP3R	311	05 022	U*	R/H OUTBD FLAP POSITION	06/16/80	0	50	DEG	58	4	19.5	4000			10	6	110
175	DELVL	311	05 023	C*	L/H ELEVATOR POSITION	06/16/80	-23.5	15.3	DEG	59	4	19.5	4000			5	6	111
176	BVE1	311	03 009	D*	BLEED VALVE ENG NO 1	02/20/79	0	500	PSIA	60	4	19.5	4000					112
177	BVE2	311	03 010	D*	BLEED VALVE ENG NO 2	02/20/79	0	500	PSIA	61	4	19.5	4000					113
178	BVE3	311	03 011	D*	BLEED VALVE ENG NO 3	02/20/79	0	500	PSIA	62	4	19.5	4000					114
179	BVE4	311	03 012	U*	BLEED VALVE ENG NO 4	02/20/79	0	500	PSIA	63	4	19.5	4000					115
180	SGWR2	311	06 002		WINGLET MOMENT FR SPAR SPARE					46	5	19.5	4000			55	6	116
181	SGWR3	311	06 005		WINGLET SHEAR FR SPAR MAIN					47	5	19.5	4000			55	6	117
182	SGWR4	311	06 006		WINGLET SHEAR FR SPAR SPARE					48	5	19.5	4000			55	6	118
183	SGWR5	311	06 003		WINGLET MOM REAR SPAR MAIN					49	5	19.5	4000			55	6	119
184	SGWR6	311	06 004		WINGLET MOM REAR SPAR SPARE					50	5	19.5	4000			55	6	120
185	SGWR7	311	06 007		WINGLET SHR REAR SPAR MAIN					51	5	19.5	4000			55	6	121
186	SGWR8	311	06 008		WINGLET SHR REAR SPAR SPARE					52	5	19.5	4000			55	6	122
187	EVENT1	311	03 013	D*	PILOT EVENT	02/15/79	OFF	ON		53	5	19.5	4000					123
188	ACGFBAL	311	05 011	E*	FLIGHT PATH LONG ACCEL	06/16/80	-.25	.25	G	54	5	19.5	4000			3	18	124
189	ACGFBAN	311	05 017	A*	FLIGHT PATH NORMAL ACCEL	06/16/80	-3	3	G	55	5	19.5	4000			3	18	125
190	DELLFD	311	05 024	B*	L/H LE FLAP POS OUTBD	06/16/80	0	100	PERCENT	56	5	19.5	4000			10	6	126
191	DELRFD	311	05 025	B*	R/H LE FLAP POS OUTBD	06/16/80	0	100	PERCENT	57	5	19.5	4000			10	6	127
192	TTMP01	311	03 019	D*	TOTAL TEMPERATURE	03/02/79	-70	140	DEG F	58	5	19.5	4000					128
193	EGT1	311	03 020	D*	EXHAUST TOTAL TEMP ENG 1	03/05/79	0	1200	DEG F	59	5	19.5	4000					129
194	EGT2	311	03 021	D*	EXHAUST TOTAL TEMP ENG 2	03/05/79	0	1200	DEG F	60	5	19.5	4000					130
195	EGT3	311	03 022	D*	EXHAUST TOTAL TEMP ENG 3	03/05/79	0	1200	DEG F	61	5	19.5	4000					131
196	EGT4	311	03 023	D*	EXHAUST TOTAL TEMP ENG 4	03/05/79	0	1200	DEG F	62	5	19.5	4000					132
197	VM02	311	05 018		VOLTAGE MONITOR 5V XFCR PWR				COUNTS	63	5	19.5	4000					133
198	SGWR9	311	06 009		WINGLET SHR I/B SKIN MAIN					46	6	19.5	4000			55	6	134
199	SGWR10	311	06 010		WINGLET SHR I/B SKIN SPARE					47	6	19.5	4000			55	6	135
200	SGES2	311	07 021		FATIGUE STRESS GAGE 2					48	6	19.5	4000			55	6	136
201	SGES2A	311	07 022		FATIGUE STRESS GAGE 2A					49	6	19.5	4000			55	6	137
202	SGES3	311	07 023		FATIGUE STRESS GAGE 3					50	6	19.5	4000			55	6	138
203	AXFUS	311	07 029	C*	LG FUSELAGE LONG ACCEL	06/16/80	-1	1	G	51	6	19.5	4000			3	18	139
204	AC13FL	311	07 030	C*	CockPIT LONG ACCEL	06/16/80	-1	1	G	52	6	19.5	4000			3	18	140
205	RPM1	311	03 025	A*	RPM ENG NO 1 N1	06/16/80	0	10000	RPM	53	6	19.5	4000					141
206	RPM2	311	03 026	A*	RPM ENG NO 2 N1	06/16/80	0	10000	RPM	54	6	19.5	4000					142
207	RPM3	311	03 027	A*	RPM ENG NO 3 N1	06/16/80	0	10000	RPM	55	6	19.5	4000					143
208	RPM4	311	03 028	A*	RPM ENG NO 4 N1	06/16/80	0	10000	RPM	56	6	19.5	4000					144

TODAY: 01/07/81 FLIGHT INSTRUMENTATION PARAMETER LIST PAGE 11 OF COPY 1
REV: D DATE: 7/24/79

VEHICLE: KC-135 WINGLET PROGRAM
FLT NO. 054 PROJ INSTR ENGR: GENE KENNEK
SCHED FLT DATE: 12/24/80
TM FREQ: MHZ S/N
PCM SYS/COM NO. 1-01 FORMAT NO. 1
PCM SYS MODEL: RMLU

PCM BIT RATE: 125 KHZ
BITS/WORD: 10
WORDS/FRAME: 64
FR/DATA CY: 10
FBT=BIT1=MSB
MAIN FRAME SYNC WORDS: 00 , 01 , 02

TM1 NO.:PARMID SYS:	CALID	NAME	CALIBRATED DATE	LOW	HIGH	ENG UNITS	WORD:	FRAME NO.	SAMP: RATE:	COMP: ALG	REF PRESS KP :PARMID	VM/TP :PARMID	FILTER :FREQ	ITM :NO. :CON
209:FFR1	311 03 029 A*	FUEL FLOW RATE ENG NO 1	06/16/80	0	3K	GAL/MIN	57	6	19.5	4000				145
210:FFR2	311 03 030 B*	FUEL FLOW RATE ENG NO 2	06/16/80	0	3K	GAL/MIN	58	6	19.5	4000				146
211:FFR3	311 03 031 B*	FUEL FLOW RATE ENG NO 3	06/16/80	0	3K	GAL/MIN	59	6	19.5	4000				147
212:FFR4	311 03 032 B*	FUEL FLOW RATE ENG NO 4	06/16/80	0	3K	GAL/MIN	60	6	19.5	4000				148
213:DPSAFL	311 05 020 A*	SAF TAB POSITION LEFT	07/25/79	-22.0	23.5	DEG	61	6	19.5	4000				149
214:PLA1	311 04 005 A*	POWER LEVER ANGLE ENG NO 1	06/16/80	0	10K	PERCENT	62	6	19.5	4000				150
215:PLA2	311 04 006 A*	POWER LEVER ANGLE ENG NO 2	06/16/80	0	10K	PERCENT	63	6	19.5	4000				151
216:GROSSW	310 RC U01 OK*	GROSS WEIGHT (ANALOG COARSE)	06/16/80	100K	300K	LB	46	7	19.5	4000		GROSSWF		152
217:GROSSWF	310 RC U02 :	GROSS WEIGHT (ANALOG FINE)	06/16/80	100K	300K	LB	47	7	19.5	4000				153
218:WTDTG	310 RC U03 OK*	GROSS WEIGHT (DIG COARSE)	06/16/80	100K	300K	LB	48	7	19.5	4000		WTDIGF		154
219:WTDIGF	310 RC U04 :	GROSS WEIGHT (DIG FINE)	06/16/80	100K	300K	LB	49	7	19.5	4000				155
220:NULL	311 00 507 :		:	:	:		50	7	:20	00				156
221:ACIDLON	311 07 031 A*	AFT BODY LONG ACCEL	06/16/80	-1	1	G	51	7	19.5	4000			3	18 157
222:FFR02	311 08 302 A*	FUEL FLOW RATE DIG. ENG. 2	11/13/80	0	4K	GPM	52	7	19.5	4000				158
223:DSPLO	311 04 001 B*	L/H SPOILER OUTBD POS	06/16/80	0	60	DEG	53	7	19.5	4000			10	6 159
224:DSPLI	311 04 002 B*	L/H SPOILER INBD POS	06/16/80	0	60	DEG	54	7	19.5	4000			10	6 160
225:DSPRO	311 04 003 B*	R/H SPOILER OUTBD POS	06/16/80	0	60	DEG	55	7	19.5	4000			10	6 161
226:DSPRI	311 04 004 B*	R/H SPOILER INBD POS	06/16/80	0	60	DEG	56	7	19.5	4000			10	6 162
227:DFLFLT	311 04 009 B*	L/H LF FLAP POS INBD	06/16/80	0	100	PERCENT	57	7	19.5	4000			10	6 163
228:DFRFLT	311 04 010 B*	R/H LF FLAP POS INBD	06/16/80	0	100	PERCENT	58	7	19.5	4000			10	6 164
229:DFLOLT	311 04 015 C*	L/H FLAP POS INBD	06/16/80	0	50	DEG	59	7	19.5	4000			10	6 165
230:DFLORT	311 04 016 B*	R/H FLAP POS INBD	06/16/80	0	50	DEG	60	7	19.5	4000			10	6 166
231:FFR03	311 08 303 O*	FUEL FLOW RATE DIG. ENG. 3	06/16/80	0	4K	GPM	61	7	19.5	4000				167
232:PLA3	311 04 007 A*	POWER LEVER ANGLE ENG NO 3	06/16/80	0	100	PERCENT	62	7	19.5	4000			10	6 168
233:PLA4	311 04 008 A*	POWER LEVER ANGLE ENG NO 4	06/16/80	0	100	PERCENT	63	7	19.5	4000			10	6 169
234:SGWI5	311 06 025 :	O/B WING FR SPAR 812 MAIN	:	:	:		46	8	19.5	4000			55	6 170
235:SGWI6	311 06 026 :	O/B WING FR SPAR 812 SPARE	:	:	:		47	8	19.5	4000			55	6 171
236:SGWI7	311 06 027 :	O/B WING REAR SPAR 808 MAIN	:	:	:		48	8	19.5	4000			55	6 172
237:SGWI8	311 06 028 :	O/B WING REAR SPAR 808 SPARE	:	:	:		49	8	19.5	4000			55	6 173
238:FTDG1	311 11 401 A*	FUEL TEMP DIG. ENG. 1	07/24/80	0	212	F	50	8	19.5	4000				174
239:FTDG2	311 11 402 A*	FUEL TEMP DIG. ENG. 2	07/24/80	0	212	F	51	8	19.5	4000				175
240:FTDG3	311 11 403 A*	FUEL TEMP DIG. ENG. 3	07/24/80	0	212	F	52	8	19.5	4000				176
241:NULL	311 00 538 :		:	:	:		53	8	:20	00				177
242:NULL	311 00 548 :		:	:	:		54	8	:20	00				178
243:DPSAFR	311 04 011 A*	SAF TAB POS RIGHT	07/15/79	-22	16	DEG	55	8	19.5	4000			6	179
244:PPOL	311 04 012 A*	PEDAL POSITION	06/16/80	-3.5	3.5	IN	56	8	19.5	4000			10	6 180
245:PWHL	311 04 013 A*	WHEEL POSITION	06/16/80	-90	90	DEG	57	8	19.5	4000			10	6 181
246:PCCLM	311 04 014 C*	CONTROL COLUMN POSITION	06/16/80	-10.5	17.0	DEG	58	8	19.5	4000			10	6 182
247:Q	311 03 003 O*	PITCH RATE	02/28/79	-40	40	DEG/SEC	59	8	20	4000			10	6 183
248:P	311 03 004 O*	ROLL RATE	02/28/79	-40	40	DEG/SEC	60	8	20	4000			10	6 184
249:R	311 03 005 O*	YAW RATE	02/28/79	-10	10	DEG/SEC	61	8	20	4000			10	6 185
250:ALPHAT	311 03 017 C*	ANGLE OF ATTACK (BOOM)	06/16/80	-5	18	DEG	62	8	19.5	4000		VM003	10	6 186
251:BETAT	311 03 018 C*	ANGLE OF SIDESLIP (BOOM)	06/16/80	-8	9	DEG	63	8	19.5	4000		VM003	10	6 187
252:FFR1ES	311 05 026 O*	FUEL FLOW RATE SENS ENG 1	06/16/80	0	15	GPM	46	9	19.5	4000				188
253:FFR2ES	311 05 027 O*	FUEL FLOW RATE SENS ENG 2	06/16/80	0	15	GPM	47	9	19.5	4000				189
254:FFR3ES	311 05 028 O*	FUEL FLOW RATE SENS ENG 3	06/16/80	0	15	GPM	48	9	19.5	4000				190
255:FFR4ES	311 05 029 O*	FUEL FLOW RATE SENS ENG 4	06/16/80	0	15	GPM	49	9	19.5	4000				191
256:FTDG4	311 11 404 A*	FUEL TEMP DIG. ENG. 4	07/24/80	0	212	F	50	9	19.5	4000				192

TODAY: 01/07/81 FLIGHT INSTRUMENTATION PARAMETER LIST PAGE 12 OF COPY 1

REV: D DATE: 7/24/79

VEHICLE: KC-135 WINGLET PROGRAM
FLT NO. 354 PROJ INSTR ENGR: GENE KENNER
SCHED FLT DATE: 12/24/80
TM FREQ: MHZ S/N
PCM SYS/COM NO. 1-01 FORMAT NO. 1
PCM SYS MODEL: RMDU

PCM BIT RATE: 125 KHZ
BITS/WORD: 10
WORDS/FRAME: 64
FR/DATA CY: 10
FBT=BIT1=MSB
MAIN FRAME SYNC WORDS: 00 , 01 , 02

ITM NO.	PARMTR SYS	CALID	NAME	CALIBRATED DATE	CALIBRATED RANGE LOW	CALIBRATED RANGE HIGH	ENG UNITS	FRAM WORD POS	FRAME NO.	SAMP RATE	COMP ALG	REF PRESS PARMID	VM/TM KP PARMID	FILTER FREQ	FILTER DB	ITM NO.
257	NULL	311 00 519						51	9	2000						193
258	NULL	311 00 529						52	9	2000						194
259	FTOT1F	311 11 102	FUEL TOTALIZER ENG 1		0	511	COUNTS	53	9	20	1000					195
260	FTOT1C	311 11 103 OK	FUEL TOTALIZER ENG 1	08/28/78	512	65535	COUNTS	54	9	20	1000		FTOT1F			196
261	PCMLLC	311 00 559	PCM LOW LEVEL CAL					55	9		1000					197
262	PCMHLC	311 00 569	PCM HI LEVEL CAL					56	9		1000					198
263	PCMGA	311 00 579	GPA ZERO					57	9		1000					199
264	PCMPS	311 00 589	PCM PWR SUPPLY					58	9		1000					200
265	NULL	311 00 609						59	9	19.5	2000					201
266	FFR04	311 08 304 O	FUEL FLOW RATE DIG. ENG. 4	06/16/80	0	40	GPM	60	9	19.5	4000					202
267	HPI	311 11 101 OK	ALTITUDE	04/04/79	0	80000	FEET	62	9	19.5	1000		HPIF			203
268	HPIF	311 10 103	ALTITUDE				FEET	61	9	19.5	1000					204
269	TAPEON	311 00 963	TAPE ON		0	1		63	9	19.5	4000					205

TODAY: 01/07/81 FLIGHT INSTRUMENTATION PARAMETER LIST PAGE 13 OF COPY 1

REV: D DATE: 7/24/79

VEHICLE: KC-135 WINGLET PROGRAM
FLT NO. 054
SCHED FLT DATE: 12/24/80
TM FREQ: MHZ S/N
PCM SYS/CUM NO. 1-01 FORMAT NO. 1
PCM SYS MODEL: AMDU
PROJ INSTR ENGR: GENE KENNER

PCM BIT RATE: 125 KHZ
BITS/WORD: 10
WORDS/FRAME: 64
FR/DATA CY: 10
FRT=BIT1=MSB
MAIN FRAME SYNC WORDS: 00 , 01 , 02

DIGITAL WORD INFORMATION

ITEM NO. SYS	PARAMID	PARMID	NAME	WORD POSN	FRAME NO.	BIT NO.	BIT DESIGNATION: 0	1	PARAMETERS AFFECTED	REMARKS	ITEM NO. SEQ
260		FTJT1C	FUEL TOTALIZER ENG NO 1	54	C	1		32768			1
260						2		16384	A		2
260						3		8191	A		3
260						4		4096	A		4
260						5		2048	A		5
260						6		1024	A		6
260						7		512	A		7
260						8			A		8
260						9			A		9
260						10			A		10
259		FTDT1F	FUEL TOTALIZER ENG NO 1	53	9	1		256			11
259						2		128	A		12
259						3		64	A		13
259						4		32	A		14
259						5		16	A		15
259						6		8	A		16
259						7		4	A		17
259						8		2	A		18
259						9		1	A		19
259						10			A		20
66		FTJT2C	FUEL TOTALIZER ENG NO 2	42	0	1		32768			21
66						2		16384	A		22
66						3		8191	A		23
66						4		4096	A		24
66						5		2048	A		25
66						6		1024	A		26
66						7		512	A		27
66						8			A		28
66						9			A		29
66						10			A		30
65		FTDT2F	FUEL TOTALIZER ENG NO 2	41	9	1		256			31
65						2		128	A		32
65						3		64	A		33
65						4		32	A		34
65						5		16	A		35
65						6		8	A		36
65						7		4	A		37
65						8		2	A		38
65						9		1	A		39
65						10			A		40
89		FTJT3C	FUEL TOTALIZER ENG NO 3	42	1	1		32768			41
89						2		16384	A		42
89						3		8191	A		43
89						4		4096	A		44
89						5		2048	A		45
89						6		1024	A		46
89						7		512	A		47
89						8			A		48

TODAY: 01/07/81 FLIGHT INSTRUMENTATION PARAMETER LIST PAGE 14 OF COPY 1

REV: D DATE: 7/24/79

VEHICLE: KC-135 WINGLET PROGRAM
FLT NO. 054
SCHED FLT DATE: 12/24/80
TM FREQ: MHZ S/N
PCM SYS/COM NO. 1-01 FORMAT NO. 1
PCM SYS MODEL: RMDU
PROJ INSTR ENGR: GENE KENNER

PCM BIT RATE: 125 KHZ
BITS/WORD: 10
WORDS/FRAME: 64
FR/DATA CY: 10
FBT=BIT1=MSB
MAIN FRAME SYNC WORDS: 00 , 01 , 02

ITEM NO. SYS	PARAMETER PARMID	PARMID NAME		DIGITAL WORD INFORMATION FRAME WORD	FRAME NO.	BIT NO.	BIT DESIGNATION 0	1	PARAMETERS AFFECTED REMARKS	ITEM NO. SEQ
A9						9		A		49
A9						10		A		50
A8	FTOT3F	FUEL TOTALIZER	ENG NO 3	41	1	1	256			51
A8						2	128	A		52
A8						3	64	A		53
A8						4	32	A		54
A8						5	16	A		55
A8						6	8	A		56
A8						7	4	A		57
A8						8	2	A		58
A8						9	1	A		59
A8						10		A		60
112	FTOT4C	FUEL TOTALIZER	ENG NO 4	42	2	1	32768			61
112						2	16384	A		62
112						3	8191	A		63
112						4	4096	A		64
112						5	2048	A		65
112						6	1024	A		66
112						7	512	A		67
112						8		A		68
112						9		A		69
112						10		A		70
111	FTOT4F	FUEL TOTALIZER	ENG NO 4	41	2	1	256			71
111						2	128	A		72
111						3	64	A		73
111						4	32	A		74
111						5	16	A		75
111						6	8	A		76
111						7	4	A		77
111						8	2	A		78
111						9	1	A		79
111						10		A		80
135	QPRO1C	PROP REF PRESS		42	3	1	2**19			81
135						2	2**18	A		82
135						3	2**17	A		83
135						4	2**16	A		84
135						5	2**15	A		85
135						6	2**14	A		86
135						7	2**13	A		87
135						8	2**12	A		88
135						9	2**11	A		89
135						10	2**10	A		90
134	QPRO1F	PROP REF PRESS		41	3	1	2**09			91
134						2	2**08	A		92
134						3	2**07	A		93
134						4	2**06	A		94
134						5	2**05	A		95
134						6	2**04	A		96

VEHICLE: KC-135 WINGLET PROGRAM
FLT NO. 054 PROJ INSTR ENGR: GENE KENNER
SCHED FLT DATE: 12/24/80
TM FREQ: MHZ S/N
PCM SYS/COM NO. 1-01 FORMAT NO. 1
PCM SYS MODEL: KMDU

PCM BIT RATE: 125 KHZ
BITS/WORD: 10
WORDS/FRAME: 64
FR/DATA CY: 10
FBT=BIT1=MSB
MAIN FRAME SYNC WORDS: 00 , 01 , 02

ITEM NO. SYS	PARAMETER PARMID1 PARMID2	NAME	SPECIAL WORD INFORMATION FRAME WORD POSN	FRAME NO.	BIT NO.	BIT DESIGNATION 0	1		PARAMETERS AFFECTED REMARKS	ITEM SEQ NO.
134					7		2**03	A		97
134					8		2**02	A		98
134					9		2**01	A		99
134					10		2**00			100
158	VT	AIRSPEED	42	4	1		4096			101
158					2		2048			102
158					3		1024			103
158					4		512			104
158					5					105
158					6					106
158					7					107
158					8					108
158					9					109
158					10					110
157	VIF	AIRSPEED	41	4	1		256			111
157					2		128			112
157					3		64			113
157					4		32			114
157					5		16			115
157					6		8			116
157					7		4			117
157					8		2			118
157					9		1			119
157					10					120
216	GROSSW	GROSS WEIGHT (ANALOG COARSE)	46	7	1		2**10			121
216					2		2**09	A		122
216					3		2**08	A		123
216					4		2**07	A		124
216					5		2**06	A		125
216					6		2**05	A		126
216					7		2**04	A		127
216					8		2**03	A		128
216					9		2**02	A		129
216					10		2**01	A		130
217	GROSSWF	GROSS WEIGHT (ANALOG FINE)	47	7	1		2**00			131
217					2		2**-01	A		132
217					3		2**-02	A		133
217					4		2**-03	A		134
217					5		2**-04	A		135
217					6		2**-05	A		136
217					7		2**-06	A		137
217					8		2**-07	A		138
217					9		2**-08	A		139
217					10		2**-09	A		140
218	WTDTG	GROSS WEIGHT (DIG COARSE)	48	7	1		2**10			141
218					2		2**09	A		142
218					3		2**08	A		143
218					4		2**07	A		144

TODAY: 01/07/81 FLIGHT INSTRUMENTATION PARAMETER LIST PAGE 16 OF COPY 1

REV: D DATE: 7/24/79

VEHICLE: KC-135 WINGLET PROGRAM
FLT NO. 054
SCHED FLT DATE: 12/24/80
TM FREQ: 4H7 S/N
PCM SYS/COM NO. A-01 FORMAT NO. 1
PCM SYS MODEL: RMDU

PROJ INSTR ENGR: GENE KENNER

PCM BIT RATE: 125 KHZ
BITS/WORD: 10
WORDS/FRAME: 64
FR/DATA CY: 10
FBT=BIT1=MSB
MAIN FRAME SYNC WORDS: 00 , 01 , 02

DIGITAL WORD INFORMATION

ITEM NO. SYS	PARAMETER PARMID1	PARMID	NAME	FRAME WORD	FRAME NO.	BIT NO.	BIT DESIGNATION 0	1		PARAMETERS AFFECTED REMARKS	ITEM NO. SEQ
218						5		2**15	A		145
218						6		2**14	A		146
218						7		2**13	A		147
218						8		2**12	A		148
218						9		2**11	A		149
218						10		2**10	A		150
219		WTDIGF	GROSS WEIGHT (FIG FINE)	49	7	1		2**09			151
219						2		2**08	A		152
219						3		2**07	A		153
219						4		2**06	A		154
219						5		2**05	A		155
219						6		2**04	A		156
219						7		2**03	A		157
219						8		2**02	A		158
219						9		2**01	A		159
219						10		2**00	A		160
267		HPI	ALTITUDE	62	9	1		4096			161
267						2		2048			162
267						3		1024			163
267						4		512			164
267						5					165
267						6					166
267						7					167
267						8					168
267						9					169
267						10					170
268		HPIF	ALTITUDE	61	9	1		256			171
268						2		128			172
268						3		64			173
268						4		32			174
268						5		16			175
268						6		8			176
268						7		4			177
268						8		2			178
268						9		1			179
268						10					180

END OF INFORMATION

```
*****   *IDENT FLT054
/////   *DELETE FLT053.1
        C L101 KC-135 WINGLET PROGRAM          125  053  GENE KENNER          12/23/80 10
/////   *DELETE FLT053.2
        C L102  64                        10 1  RMDU          00   01   02 01 K135053   00
```

MODIFICATIONS / CONTROL CARDS

```
WINGLET  C L101 KC-135 WINGLET PROGRAM          125  053  GENE KENNER          12/23/80 10 FLT053   1      D
WINGLET  C L101 KC-135 WINGLET PROGRAM          125  054  GENE KENNER          12/24/80 10 FLT054   1      I
WINGLET  C L102  64                        10 1  RMDU          00   01   02 01 K135053   00 FLT053   2      D
WINGLET  C L102  64                        10 1  RMDU          00   01   02 01 K135054   00 FLT054   2      I
```

CORRECTION IDENTS ARE LISTED IN CHRONOLOGICAL ORDER OF INSERTION

```
YANKSSS   WINGLET   FLT007   FLT013   THRUST   FLT014   FLT015   FLT016
FLT017    FLT018    FLT019   FLT020   FLT021   FLT022   FLT023   FLT024
FLT025    FLT026    FLT027   FLT028   FLT029   FLT030   FLT031   FLT032
FLT033    FLT034    FLT035   FLT036   FLT037   FLT038   FLT039   FLT040
FLT041    FLT042    FLT043   FLT044   FLT045   FLT046   FLT047   FLT048
FLT049    FLT050    FLT051   FLT052   FLT053   FLT054
```

17 PURGED IDENTS WERE FOUND

DECKS ARE LISTED IN THE ORDER OF THEIR OCCURRENCE ON A NEW PROGRAM LIBRARY IF ONE IS CREATED BY THIS UPDATE

```
YANKSSS   WINGLET   DIGITAL
```

KC-135 WING AND WINGLET FLIGHT PRESSURE DISTRIBUTIONS, LOADS, AND WING DEFLECTION RESULTS WITH SOME WIND TUNNEL COMPARISONS

Lawrence Montoya*, Peter Jacobs**,
Stuart Flechner**, and Robert Sims*

SUMMARY

A full-scale winglet flight test on a KC-135 airplane with an upper winglet was conducted in a joint NASA/USAF flight project. Data were taken at Mach numbers from 0.70 to 0.82 at altitudes from 34,000 feet to 39,000 feet at stabilized flight conditions for wing/winglet configurations of basic wing tip, 15°/-4°, 15°/-2°, and 0°/-4° winglet cant/incidence.

An analysis of selected pressure distribution and data showed that with the basic wing tip, the flight and wind tunnel wing pressure distribution data showed good agreement. With winglets installed, the effects on the wing pressure distribution were mainly near the tip. Also, the flight and wind tunnel winglet pressure distributions had some significant differences primarily due to the "oilcanning" in flight. However, in general, the agreement was good.

For the winglet cant and incidence configuration presented, the incidence had the largest effect on the winglet pressure distributions.

The incremental flight wing deflection data showed that the semispan wind tunnel model did a reasonable job of simulating the aeroelastic effects at the wing tip.

The flight loads data showed good agreement with predictions at the design point and also substantiated the predicted structural penalty (load increase) of the 15° cant/-2° incidence winglet configuration.

INTRODUCTION

The NASA Langley Research Center has conducted extensive experimental wind tunnel investigations on the effects of winglets on jet transports at various subsonic Mach numbers, references 1 through 8. Winglets, as described in reference 1, have shown significant performance improvements on the KC-135 airplane. To confirm these wind tunnel predictions, a joint NASA/USAF full-scale winglet flight evaluation on a KC-135 was conducted at the NASA Dryden Flight Research Center. The flight measurements consisted of total airplane lift and drag, loads, buffet, stability and control, range factor, and wing/winglet pressure distributions. These measurements were taken with the winglets on and off for various winglet cant and incident angles to determine the incremental effect of winglets on the airplane performance.

*NASA Dryden Flight Research Center
**NASA Langley Research Center

This paper presents selected wing and winglet pressure distributions, loads and wing deflection results with some wind tunnel comparisons. The data presented are for Mach numbers of 0.70, 0.78, 0.80 and 0.82 for altitudes between 34,000 feet to 39,000 feet. The configuration tested in flight consisted of the basic wingtip (winglets off) and wing/winglet with winglet variations of cant/incidence of 15°/-4°, 15°/-2°, and 0°/-4°. The design conditions for this study are the 15° cant/-4° incidence winglet configuration at a Mach number of 0.78 and lift coefficient of 0.42.

SYMBOLS

b'	Exposed Semispan of Wing with Basic Tip, 55.2 ft
c	Local Chord
$\bar{c}$	Mean Geometric Chord of Exposed Basic Wing, 18.73 ft
c_{av}	Average Chord of Exposed Basic Wing, s/b', 17.52 ft
c_L	Lift Coefficient
c_n	Section Normal-Force Coefficient, Integration of Pressure Measurements
c_{n_A}	Airplane Normal Force Coefficient
C_p	Pressure Coefficient, $(P_\ell, - P_\infty)/q_\infty$
g	Gravitational Acceleration, ft/sec^2
i	Incidence of Winglet Measured from Free-Stream Direction, Positive with Leading Edge Inward for Upper Winglet, deg (see figure 3).
M_∞	Free-Stream Mach Number
P_d	Differential Static Pressure, psi
P_ℓ	Local Static Pressure, psi
P_r	Reference Static Pressure, psi
P_∞	Free-Stream Static Pressure, psf
q_∞	Free-Stream Dynamic Pressure, psf
R	Reynolds Number per Unit Length, per ft
w/δ	Airplane Weight Divided by Ratio of Pressure at Test Altitude to Standard Sea Level Pressure

x	Chordwise Distance from Leading Edge, Positive Aft
y	Spanwise Distance from Wing-Fuselage Juncture, Positive Outboard
z	Vertical Coordinate of Airfoil
z'	Distance Along Winglet Span from Chord Plane of Wing, in.
α	Angle of Attack, deg
η	Exposed Wing Semispan Station (based on basic-wing panel), y/b'

SUBSCRIPT

basic	Reference Configuration, Basic Wing Tip

ABBREVIATION

L.S.	Lower Surface
U.S.	Upper Surface
G.W.	Gross Weight
B.M.	Bending Moment

AIRPLANE DESCRIPTION

A Boeing KC-135 airplane, figure 1, with modified outboard wing panels was used for this study. The modifications were primarily to the internal structure near the wing tips for installing the winglets with the capability to allow winglet cant/incidence changes on the ground. Provisions were also made so that a "basic" KC-135 wing tip configuration with the winglets removed could be installed.

The other major aerodynamic differences from a standard KC-135 was the addition of the nose boom for obtaining airspeed and flow direction, and the absence of the refueling boom.

Wing. The basic wing is a typical first generation transport configuration with a quarter-chord sweep of 35°, 7° dihedral and 2° of incidence at the root chord. The wing has no geometric twist and the thickness varies nonlinearly from 15 percent at the wing-fuselage juncture to 9 percent at the trailing edge break and then remains constant at 9 percent to the wing tip. A typical outboard wing airfoil section is shown in figure 2 with the coordinates presented in table I.

Winglets. The winglet configuration used in this investigation is presented in figure 3. The winglets employed an 8-percent-thick general aviation airfoil. Winglet airfoil coordinates are presented in table II.

The winglet has a span approximately equal to the wing tip chord, a root chord equal to about 65 percent of the wing tip chord, a leading-edge sweep of 38°, a taper ratio of 0.32, and an aspect ratio of 2.33. The planform area of the upper winglet is 3.8 percent of the exposed trapezoidal planform area of the basic wing. The upper winglet is canted outboard 15° from vertical (75° dihedral) and incidence (toed out) of 4° (leading edge outboard) relative to the fuselage center line. The upper winglet is untwisted and therefore has constant negative geometric incidence across its span. The "upper surface" of the upper winglet is the inboard surface. This geometry was derived from the wind-tunnel model coordinates with the exception of some slight wing/winglet juncture fairing differences which result from the method used to allow cant/incidence variations for the flight test.

TEST CONDITIONS

Flight data were obtained over a range of angles of attack at speeds from Mach 0.70 to Mach 0.82, for altitudes between 34,000 feet to 39,000 feet and dynamic pressures from about 129 psf to 240 psf. All the wing and winglet pressure data presented were taken at steady state trim conditions. The loads data are for cruise conditions and ±0.5g roller coaster maneuvers from trim conditions.

INSTRUMENTATION

Wing/Winglet Pressures. The flight wing/winglet pressure measurements were obtained on the right side from seven rows of orifices on the top and bottom surface at the span stations and locations shown in figure 4. Both the span and chordwise location of the orifices were essentially the same as the wind-tunnel model of reference 5.

All the wing orifices except the leading-edge orifices were externally mounted using the method similar to that found in reference 9. The external tubing size was 3/16 inch A.D. multibore (strip-a-tubing) tubing. All the winglet orifices were flush mounted with an inside diameter of 1/8 inch.

The wing/winglet pressures were transmitted to instrument bays, where the pressures were measured with scanivalves. The locations were chosen so that the pressure sensors could be as close as practical to the orifices.

Differential transducers were used on all scanivalves and referenced to a compartment source which was measured by precision absolute pressure transducer.

Wing Deflection Measurement. A medium format camera was mounted on the fuselage door looking out over the right wing upper surface toward the tip, figure 5. Two deflection targets were installed at the wing tip with reference

targets installed on the inboard portion of the wing to establish a plane from which the flight deflections were measured.

Wing/Winglet Load and Stress. The load and stress stations where strain gages were installed are shown in figure 6. The winglet, wing-winglet intersection, and outboard wing station gages were installed during the wing tip modification and after construction. These gages were calibrated for loads measurements during proof tests. The wing root station gages were installed chordwise on both the upper and lower surfaces strictly for stress measurements.

Air Data. Air data measurements were obtained from a standard NACA airspeed head mounted on the nose boom. The airspeed system was calibrated using the techniques described in reference 10. Flow direction was obtained from a flight path accelerometer (F.P.A.) system (reference 11), also mounted on the nose boom aft of the NACA head.

Accuracy. The pressure range for the scanivalve transducers was scaled on the basis of the wind tunnel pressure coefficients for flight conditions near the winglet design of Mach 0.78 and altitude of 35,000 feet. The scanivalve zero pressure differential was checked during each flight by connecting both sides of the differential transducer to the same pressure.

The average error in C_p based on the flight data was determined to be about 0.01, which is similar to that of the wind tunnel data.

The estimated error in each of the following measurements at M = 0.78 and at 35,000 feet altitude is as follows:

P_d, psi	±0.6
P_r, psi	±0.3
P_∞, psf	±0.02
M_∞	±0.01
α	±0.25°
q_∞, psf	±0.08

For the loads and stress measurements presented in this paper, the estimated accuracies are as follows:

Location	Type	Accuracy
Wing-Winglet Juncture	Bending	±6%
Outboard Wing	Bending	±2%
Wing Root	Stress	±250 psi

RESULTS AND DISCUSSION

The discussion presented herein will be limited to a few cases which are considered generally representative of the trends for the various configurations tested. Comparisons with wind tunnel results are also included for the 15°/-4° winglet cant/incidence configuration.

In figure 7, flight and wind tunnel pressure coefficient data are presented for the basic wing tip configuration. In general, the comparisons show good agreement at all four wing span stations, Mach numbers, and angles of attack. Some small differences do exist at some locations and test conditions which, in part, could be attributed to the airplane surface conditions and externally mounted orifices.

Figure 8 presents flight and wind tunnel wing and winglet pressure distributions comparisons for the 15° cant/-4° incidence winglet configuration. The wing pressure distributions comparisons, in general, show good agreement at all span stations and test conditions, while the winglet data have some significant differences. At semispan station 1.01 the main differences between flight and wind tunnel occur on the upper surface near the leading edge at all test conditions. These large differences at the leading edge are attributed to "oilcanning" (skin deflections) which occurred in flight. Observations of the "oilcanning" during flight showed that the existence of a large "oilcan" occurred in this region. A photograph of the "oilcanning" on the left winglet is shown in figure 9.

At semispan stations 1.03 and 1.05 the winglet flight and wind tunnel data in figure 8 generally show good agreement for the lower surface while the flight upper surface data tend to be more positive on the forward chord regions and more negative on the aft portion. These differences are in part attributed to the "oilcanning"; however, the trends and levels show good agreement.

In figure 10, flight wing pressure distributions for the basic wing tip and with the 15° cant/-4° incidence winglet configuration are presented. The data show that at all test conditions the effects of the winglet on the wing pressure distributions are mainly at the wing tip upper surface (semispan station 0.99). At this span station, the wing upper surface pressure distributions with the winglet tend to be more negative on the aft region with good trailing edge pressure recovery. The more negative pressure coefficients begin at about X/C = 0.4 which is where the winglet leading edge intersects the wing upper surface. These results are similar to those predicted by the wind tunnel data of reference 5. The other wing semispan stations (0.26, 0.77, and 0.92) along with the lower surface of semispan station 0.99 in general do not show significant effects due to the winglet.

Figure 11 presents wing tip and winglet pressure distribution comparisons for the 15°/-4°, 15°/-2°, and 0°/-4° winglet cant/incident configurations. The wing tip data (η - 0.99) in general show good agreement except for the 15° cant/-2° incidence data which have slightly more negative coefficients on the upper surface at the higher Mach numbers.

The winglet pressure distributions in figure 11 show that 15°/-4° and 0°/-4° data generally agree while the 15°/-2° data tend to be more negative on forward portion of the upper surface and more positive on the lower surface. This indicates that for the test conditions presented, the winglet incidence had a stronger effect on the pressure distribution than did cant.

Wing and winglet flight and wind tunnel span load distributions for the 15° cant/-4° incidence winglet configuration are presented in figure 12. Some differences exist at some of the test conditions presented. These differences are due to the airplane surface conditions; i.e., externally mounted pressure

tubing for the wing flight data and winglet "oilcanning," and the method used in the model construction to get the proper outboard wing deflections. With the above taken into account, agreement is considered good.

Figure 13 presents schematics of both the construction method used in the semispan model of reference 5, to get the predicted wing tip deflections along with the type of deflections which would be expected in actual flight and from the model. As is shown, the model deflections occur primarily outboard of the fill area while the actual flight deflections occur more uniformly throughout the span; although the total wing tip deflection may be similar. Therefore the wing span loads as shown in figure 12 may differ due to this effect.

Flight and wind tunnel measured deflections at the design cruise Mach number of 0.78 are compared in figure 14 for the winglets off and 15° cant/-4° incidence configurations. Because of the different reference planes, comparisons of absolute deflection cannot be made. However, comparing the incremental deflection from winglets off to 15° cant/-4° incidence at a given C_L, the wind tunnel and flight data are fairly close. The increment for the flight data appears to be slightly higher than the wind tunnel increment. From this and other data, the overall assessment is that the flexible wind tunnel model did a reasonable job of simulating the aeroelastic effects at the wing tip where it is important to get the winglet in the right environment.

The overall character of the winglet loading is shown in figure 15 where the center of pressure location outboard of the load station is plotted for the 15°/-2° and 15°/-4° configurations. The data were obtained from ±0.5g roller coaster maneuvers performed at the 0.78 design Mach number. Of particular note is the fairly aft chordwise locations, especially at the lower angle-of-attack points.

The effective center of pressure location for the total outboard wing loads is shown in figure 16 for the same maneuvers. The load penalty at this station for both winglet configurations is quite evident from the outboard shift in center of pressure. It is also interesting to note that for all three configurations the chordwise center of pressure remains virtually unchanged, with the data centering around the elastic (torque) axis.

In figure 17 the flight measured winglet intersection bending moment, as a function of airplane normal force coefficient, is compared with Boeing aeroelastic prediction data at the design test condition. The airload at 1g for the 15° cant/-2° incidence winglet configuration is about 34 percent higher than the 15°/-4° configuration, indicating the desirability of the 15°/-4° configuration. A comparison of the flight data with the predicted data shows good agreement at the 1g condition, but predictions are somewhat higher than flight data at the 1.5g condition.

The flight measured bending moment at the outboard wing station, as a function of airplane normal force coefficient, is shown in figure 18 for the design test condition. At 1g, the 15° cant/-4° incidence configuration shows a 32 percent increase in airload over the basic wing while the 15°/-2° configuration exceeds the basic wing by 50 percent. Comparison between the measured flight loads and the Boeing predicted data is considered quite good at both 1g and 1.5g.

The flight measured bending stress distribution at the wing root station is shown in figure 19 for the design cruise condition at 1g. As predicted from the flexible wind tunnel tests, the flight data for the 15° cant/-4° incidence winglet configuration show only a slight increase compared to the basic wing without winglets. The average stress increment is approximately 2.5 percent.

SUMMARY OF RESULTS

A full scale winglet flight program on a KC-135 airplane with an upper winglet was conducted. An analysis of selected wing and winglet pressure distribution data for the basic wing tip, 15°/-4°, 15°/-2°, and 0°/-4° winglet cant/incident configurations indicated the following:

1. The flight wing pressure distributions with the basic tip in general showed good agreement with the wind tunnel data.
2. Winglet configuration effects on the wing pressure distribution were mainly near the wing tip. The winglet made the aft upper surface pressure distributions more negative.
3. The flight and wind tunnel winglet pressure distributions had some significant differences primarily due to the "oilcanning" (skin deflections) in flight; however, in general the agreement was good.
4. For the winglet cant and incidence configurations presented the incidence had the largest effect on the winglet pressure distributions.

Also, the loads and deflection data showed the following:

5. The incremental flight wing deflection data showed that the semispan wind tunnel model did a reasonable job of simulating the aeroelastic effects at the wing tip.
6. At the design conditions the flight loads agreed with predictions.
7. The flight loads substantiated the predicted structural penalty (load increase) of the 15° cant/-2° incidence winglet configuration.

REFERENCES

1. Whitcomb, Richard T.: A Design Approach and Selected Wind-Tunnel Results at High Subsonic Speeds for Wing-Tip Mounted Winglets. NASA TN D-8260, 1976.
2. Flechner, Stuart G.; Jacobs, Peter F.; and Whitcomb, Richard T.: A High Subsonic Speed Wind-Tunnel Investigation of Winglets on a Representative Second-Generation Jet Transport Wing. NASA TN D-8264, 1976.
3. Jacobs, Peter F.; and Flechner, Stuart G.: The Effect of Winglets on the Static Aerodynamic Stability Characteristics of a Representative Second Generation Jet Transport Model. NASA TN D-8267, 1976.

4. Jacobs, Peter F.; Flechner, Stuart G.; and Montoya, Lawrence C.: Effect of Winglets on a First-Generation Jet Transport Wing. I - Longitudinal Aerodynamic Characteristics of a Semispan Model at Subsonic Speeds. NASA TN D-8473, 1977.

5. Montoya, Lawrence C.; Flechner, Stuart G.; and Jacobs, Peter F.: Effect of Winglets on a First-Generation Jet Transport Wing. II - Pressure and Spanwise Load Distributions for a Semispan Model at High Subsonic Speeds. NASA TN D-8474, 1977.

6. Montoya, Lawrence C.; Jacobs, Peter F.; and Flechner, Stuart G.: Effect of Winglets on a First-Generation Jet Transport Wing. III - Pressure and Spanwise Load Distributions for a Semispan Model at Mach 0.30. NASA TN D-8478, 1977.

7. Meyer, Robert R., Jr.: Effect of Winglets on a First-Generation Jet Transport Wing. IV - Stability Characteristics for a Full-Span Model at Mach 0.30. NASA TP-1119, 1978.

8. Jacobs, Peter F.: Effect of Winglets on a First-Generation Jet Transport Wing. V - Stability Characteristics of a Full-Span Wing With a Generalized Fuselage at High Subsonic Speeds. NASA TP-1163, 1978.

9. Montoya, Lawrence C.; and Lux, David P.: Comparison of Wing Pressure Distribution from Flight Tests of Flush and External Orifices for Mach Numbers from 0.50 to 0.97. NASA TM X-56032, April 1975.

10. Larson, Terry J.; and Ehernberger, L. J.: Techniques Used for Determination of Static Source Position Error of a High Altitude Supersonic Airplane. NASA TM X-3152, 1975.

11. Final Report Flight Path Accelerometer System AFFTC Report FTC-TR-68-28, December 1968.

TABLE I. - COORDINATES OF TYPICAL OUTBOARD WING SECTION

Wing Section at 2° Incidence			
Upper Surface		Lower Surface	
x/c	z/c	x/c	z/c
0	0	0	0
.0011	.0042	.0020	-.0054
.0022	.0056	.0035	-.0063
.0034	.0071	.0061	-.0073
.0058	.0090	.0092	-.0081
.0095	.0116	.0201	-.0097
.0132	.0136	.0391	-.0116
.0180	.0161	.0631	-.0139
.0234	.0186	.0950	-.0168
.0324	.0221	.1016	-.0174
.0415	.0253	.1445	-.0212
.0536	.0291	.1826	-.0245
.0716	.0338	.2235	-.0284
.0897	.0377	.2597	-.0314
.0990	.0394	.2950	-.0341
.1132	.0417	.3326	-.0366
.1408	.0454	.3726	-.0391
.1589	.0471	.4276	-.0418
.1740	.0483	.4690	-.0429
.1861	.0492	.5110	-.0433
.2011	.0501	.5560	-.0430
.2192	.0510	.5967	-.0424
.2342	.0516	.6386	-.0414
.2584	.0522	.6818	-.0406
.3432	.0522	.7243	-.0397
.3729	.0524	.7620	-.0389
.4090	.0513	.7951	-.0381
.4572	.0489	.8308	-.0377
.5054	.0454	.8662	-.0371
.5416	.0420	.9029	-.0363
.6379	.0304	.9790	-.0348
.6862	.0226	.9999	-.0350
.7343	.0513		
.7582	.0108		
.7823	.0065		
.8040	.0027		
.8344	-.0023		
.8642	-.0076		
.8874	-.0119		
.9223	-.0810		
.9492	-.0229		
.9718	-.0269		
.9920	-.0308		
1.0001	-.0347		

TABLE II. - AIRFOIL COORDINATES FOR WINGLETS

x/c	z/c for -	
	Upper Surface	Lower Surface
0	0	0
.0020	.0077	-.0032
.0050	.0119	-.0041
.0125	.0179	-.0060
.0250	.0249	-.0077
.0375	.0296	-.0090
.0500	.0333	-.0100
.0750	.0389	-.0118
.1000	.0433	-.0132
.1250	.0469	-.0144
.1500	.0499	-.0154
.1750	.0525	-.0161
.2000	.0547	-.0167
.2500	.0581	-.0175
.3000	.0605	-.0175
.3500	.0621	-.0174
.4000	.0628	-.0168
.4500	.0627	-.0158
.5000	.0618	-.0144
.5500	.0599	-.0122
.5750	.0587	-.0106
.6000	.0572	-.0090
.6250	.0554	-.0071
.6500	.0533	-.0053
.6750	.0508	-.0033
.7000	.0481	-.0015
.7250	.0451	.0004
.7500	.0419	.0020
.7750	.0384	.0036
.8000	.0349	.0049
.8250	.0311	.0060
.8500	.0270	.0065
.8750	.0228	.0064
.9000	.0184	.0059
.9250	.0138	.0045
.9500	.0089	.0021
.9750	.0038	-.0013
1.0000	-.0020	-.0067

Figure 1. - Inflight photograph of KC-135 with winglets

Figure 2. - Typical outboard wing airfoil section

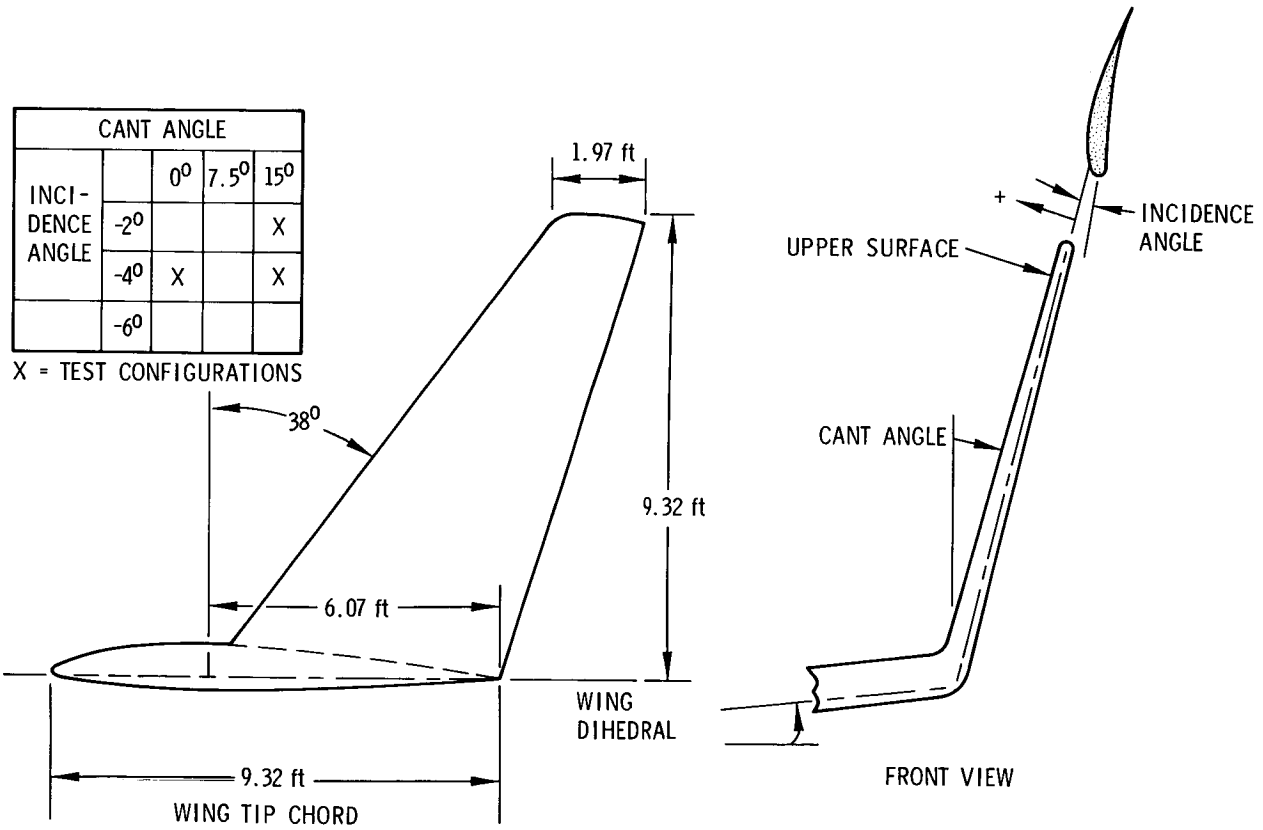

Figure 3. - KC-135 winglet geometry

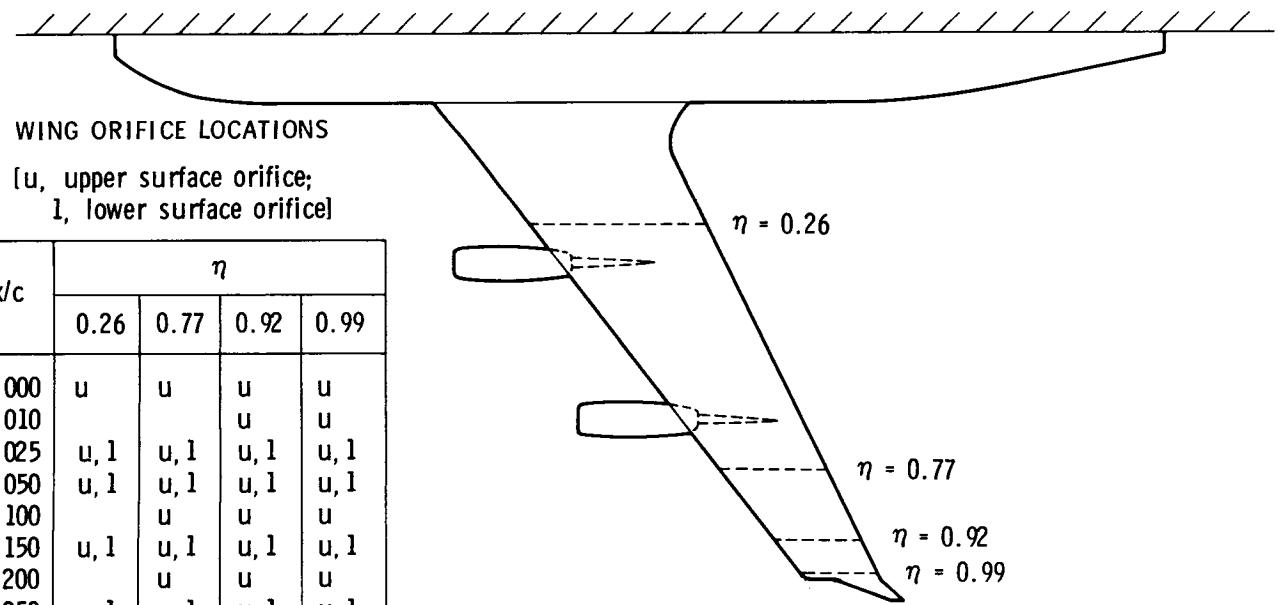

WING ORIFICE LOCATIONS

[u, upper surface orifice;
l, lower surface orifice]

x/c	η			
	0.26	0.77	0.92	0.99
0.000	u	u	u	u
.010			u	u
.025	u, l	u, l	u, l	u, l
.050	u, l	u, l	u, l	u, l
.100		u	u	u
.150	u, l	u, l	u, l	u, l
.200		u	u	u
.250	u, l	u, l	u, l	u, l
.300		u	u	u
.350	u, l	u, l	u, l	u, l
.400		u	u	u
.450	u, l	u, l	u, l	u, l
.500		u	u	u
.550	u, l	u, l	u, l	u, l
.600		u	u	u
.650	u, l	u, l	u, l	u, l
.700		u	u	u
.750	u, l	u, l	u, l	u, l
.800		u	u	
.850	u	u, l	u, l	u, l
.900		u	u	u
.950	u, l	u, l	u, l	u, l

(a) ON WING.

Figure 4. - Wing and winglet static-pressure orifice locations

WINGLET ORIFICE LOCATIONS

[u, upper surface orifice;
l, lower surface orifice]

x/c	η		
	UPPER WINGLET		
	1.01	1.03	1.05
0.000	u	u	u
.020	u, l	u, l	u, l
.050	u, l	l	u, l
.150	u, l	u, l	u, l
.250	u, l	u, l	u, l
.350	u, l	u	u, l
.450	u, l	u, l	u, l
.550	u, l	u, l	u, l
.650	u, l	u, l	u, l
.750	u, l	u, l	u, l
.850	u, l	u, l	u, l
.950	u, l	u, l	u, l

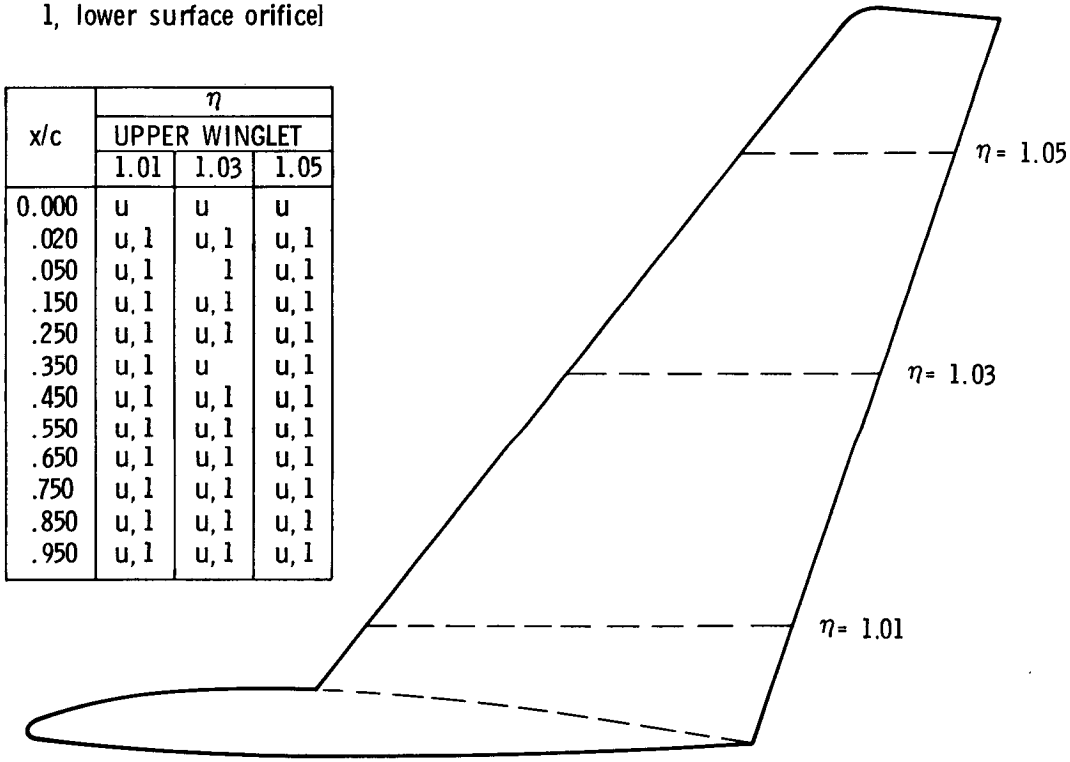

(b) ON WINGLETS.

Figure 4. - Concluded

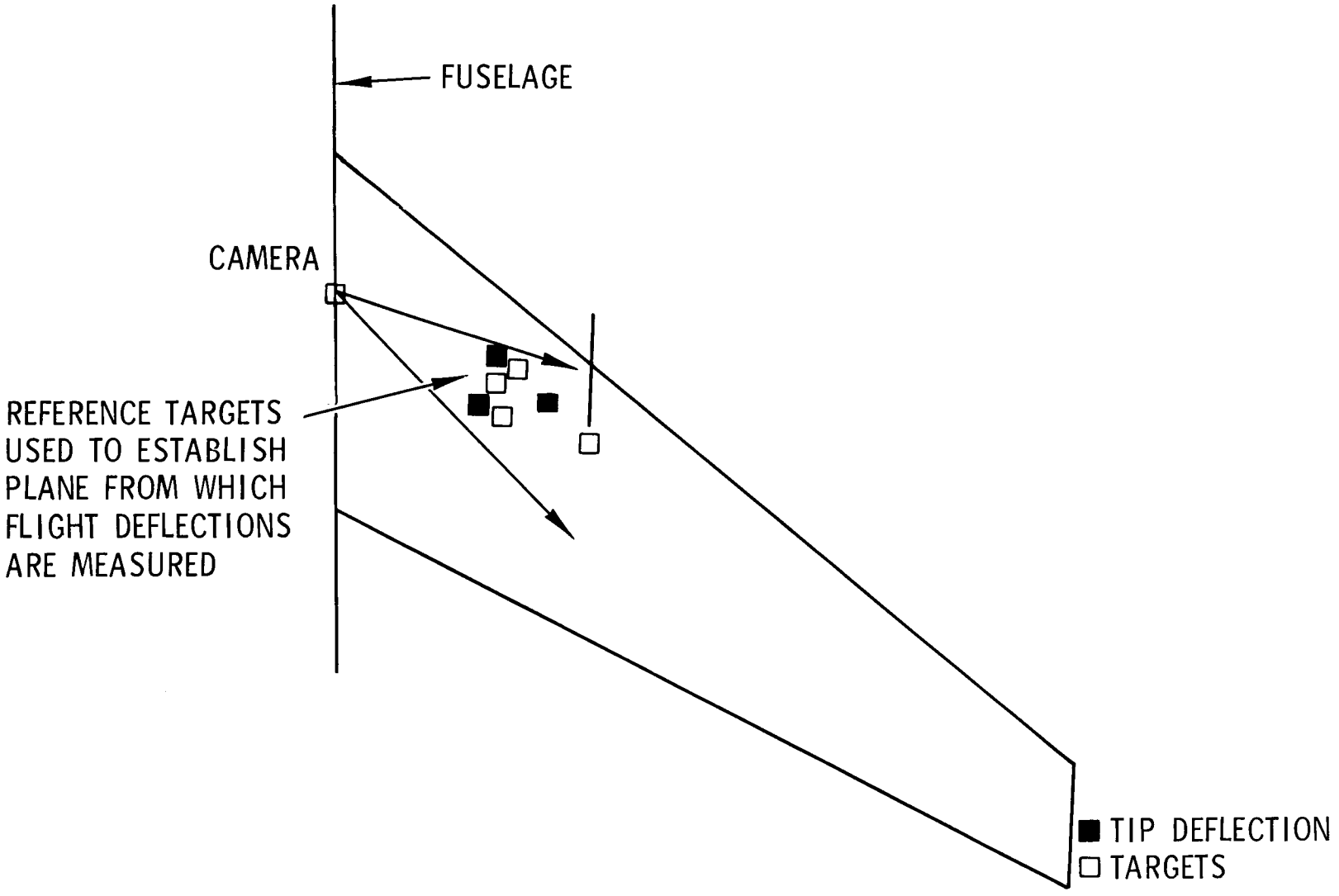

Figure 5. - Schematic of flight wing deflection camera and wing targets

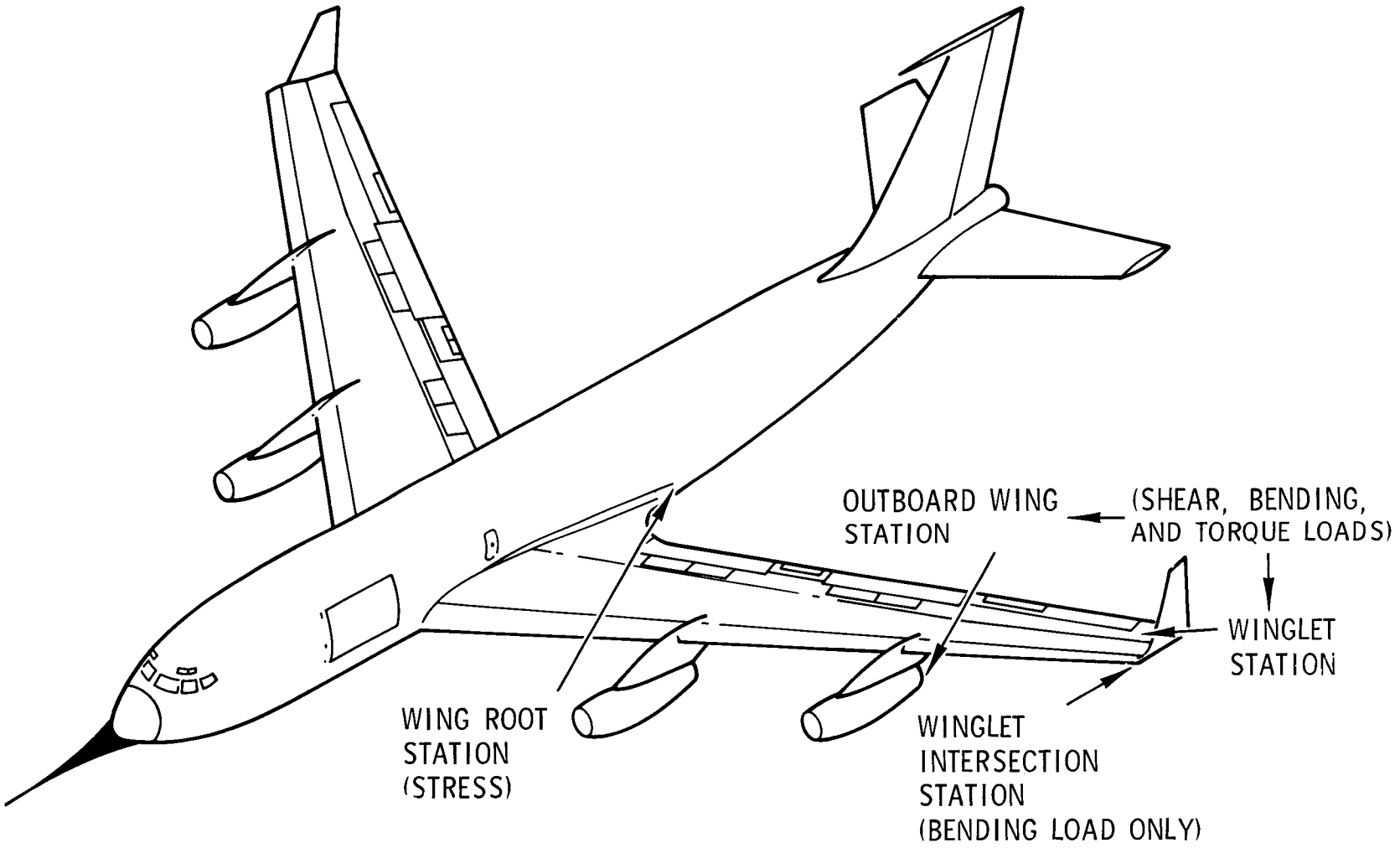

Figure 6. - KC-135 strain gage stations

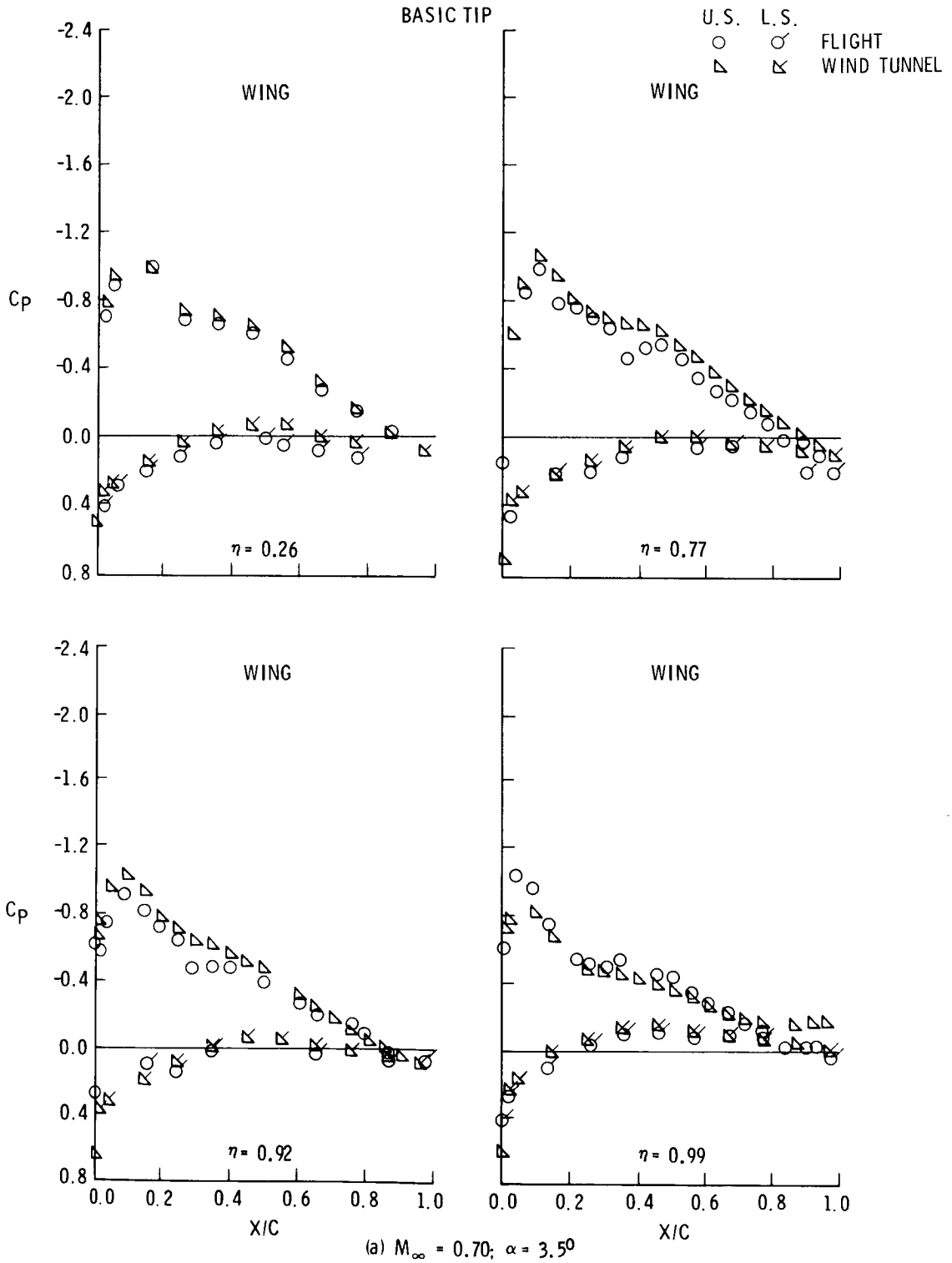

Figure 7. - Flight and wind tunnel wing pressure distribution comparisons

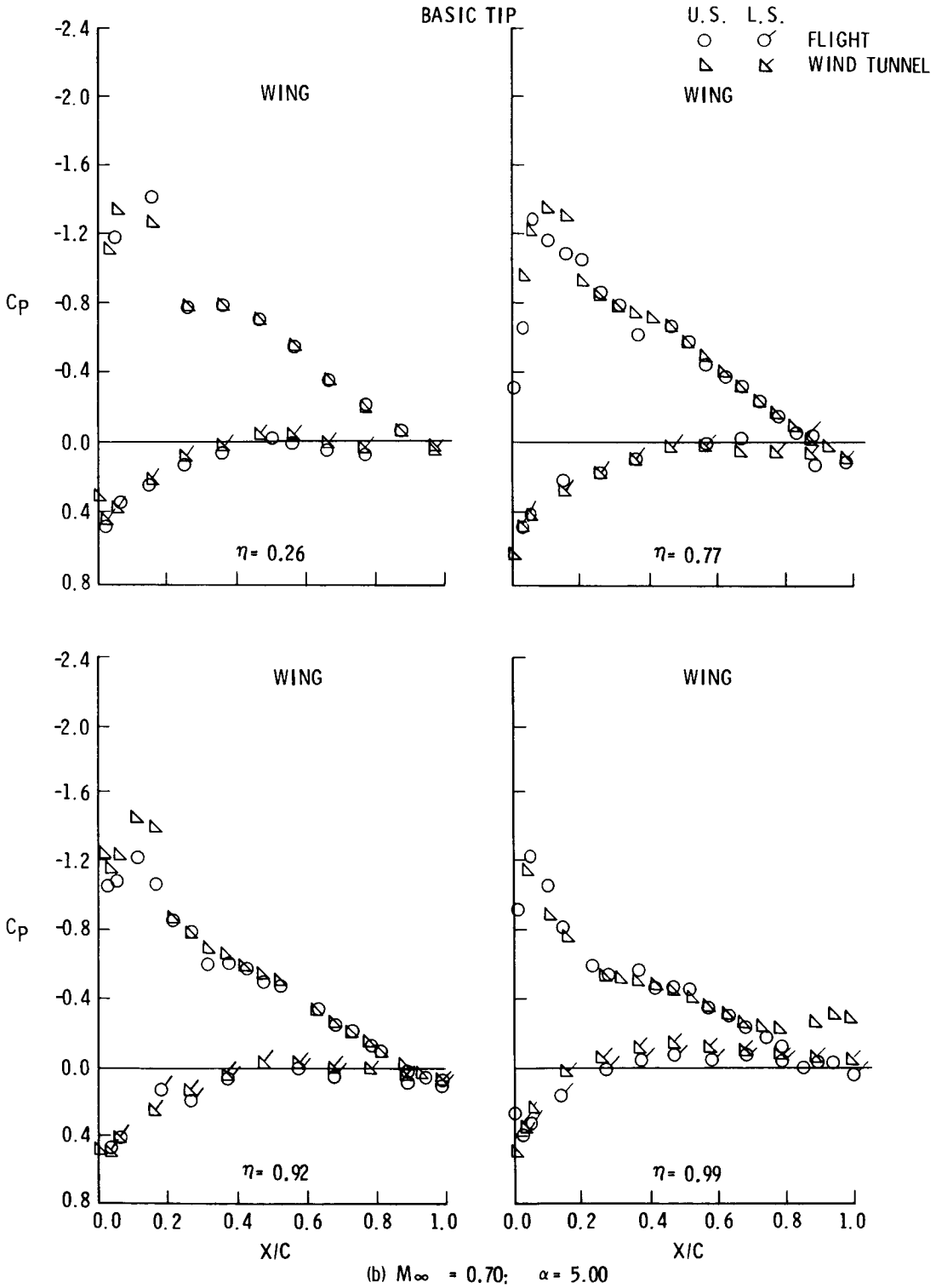

(b) $M_\infty = 0.70$; $\alpha = 5.00$

Figure 7. - Continued

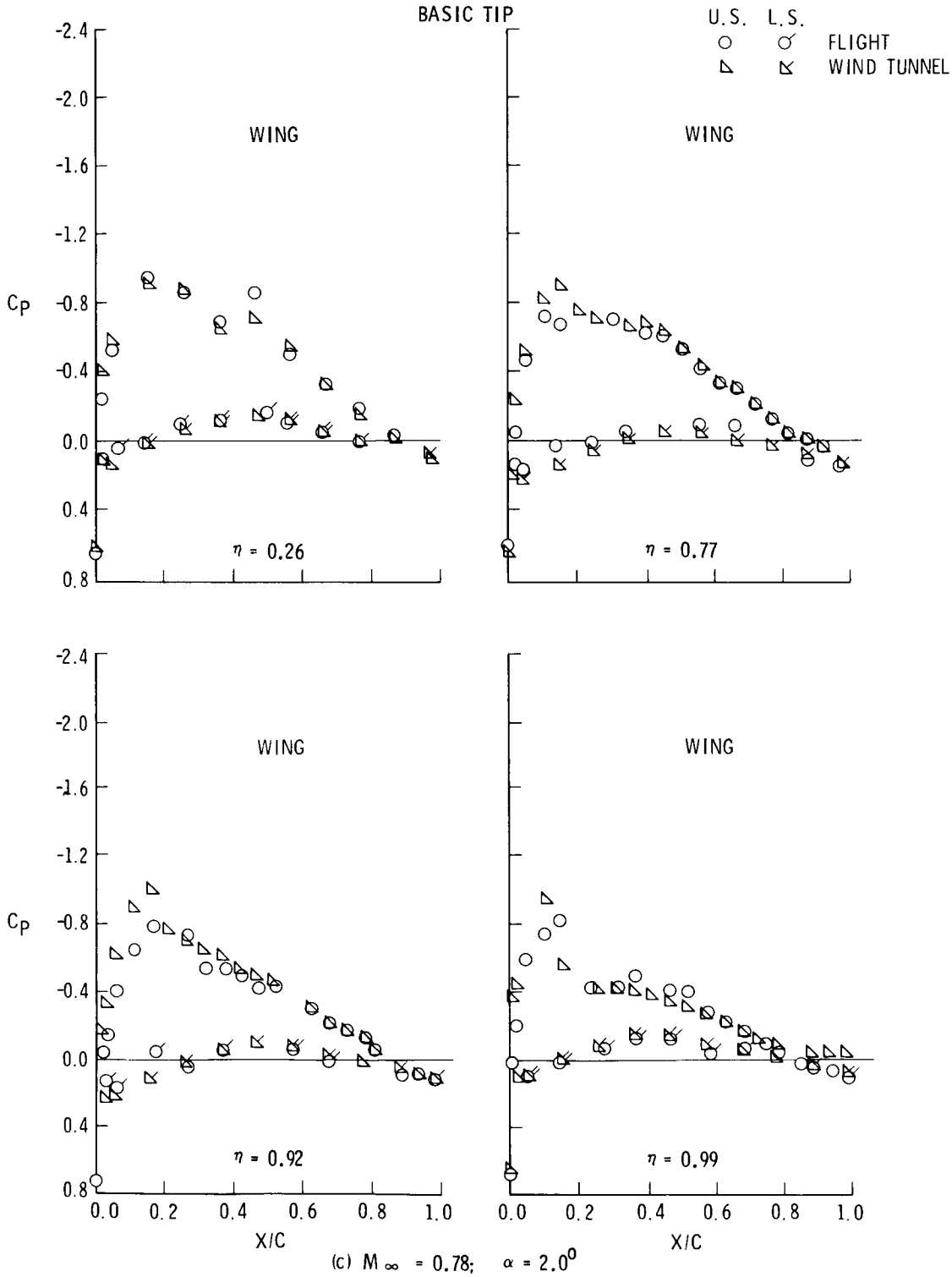

(c) $M_\infty = 0.78$; $\alpha = 2.0^0$

Figure 7. - Continued

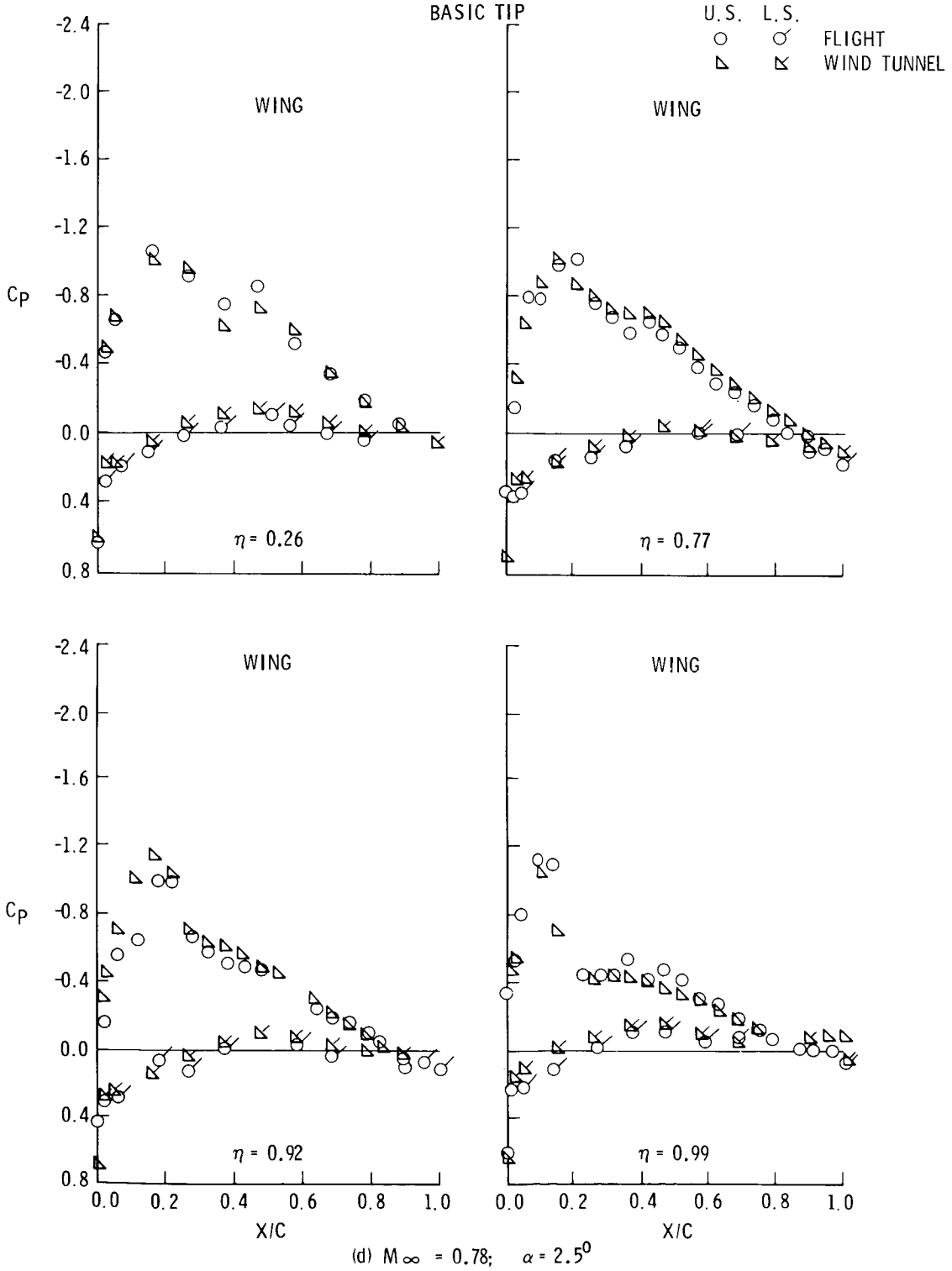

(d) $M_\infty = 0.78$; $\alpha = 2.5^0$

Figure 7. - Continued

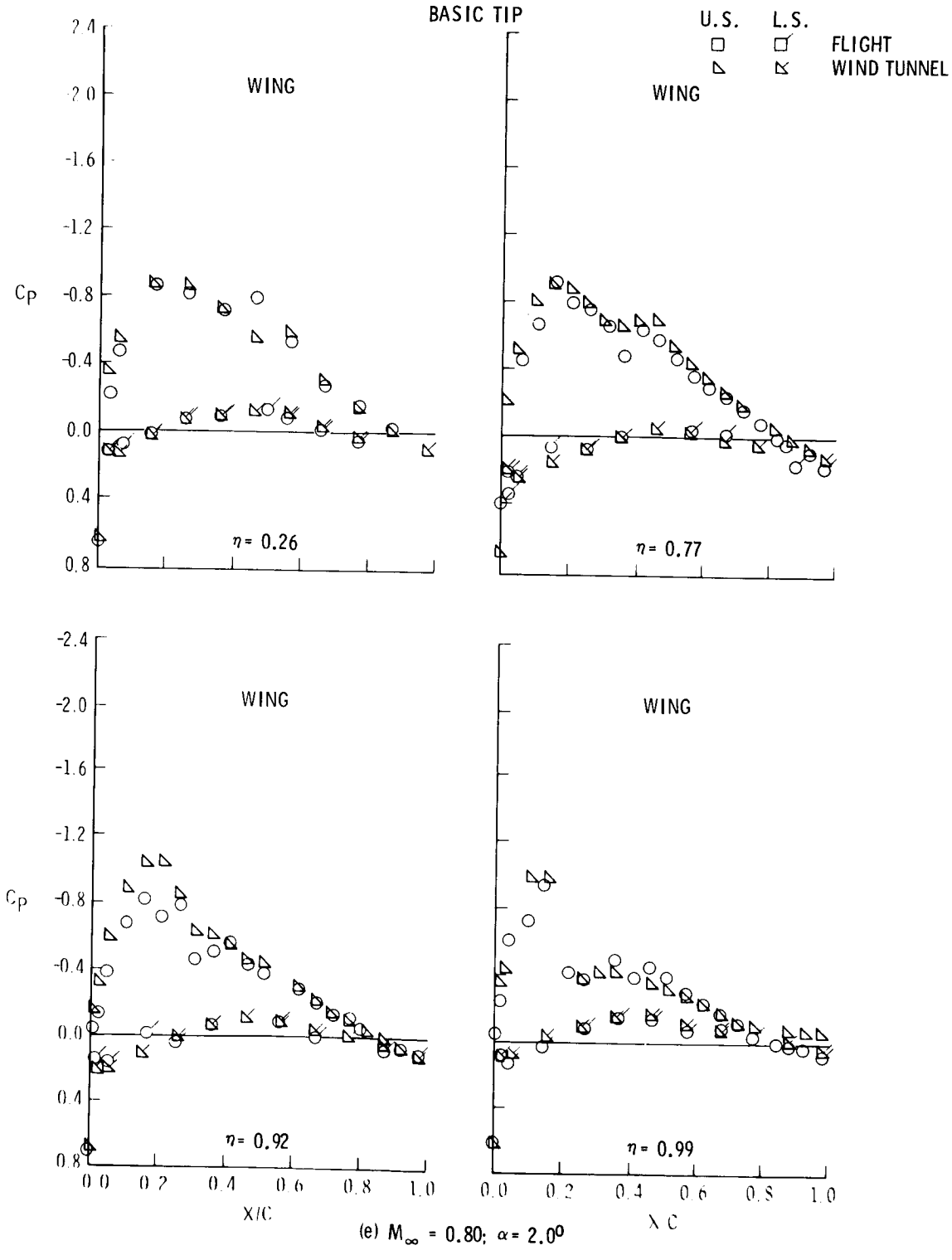

Figure 7. - Continued

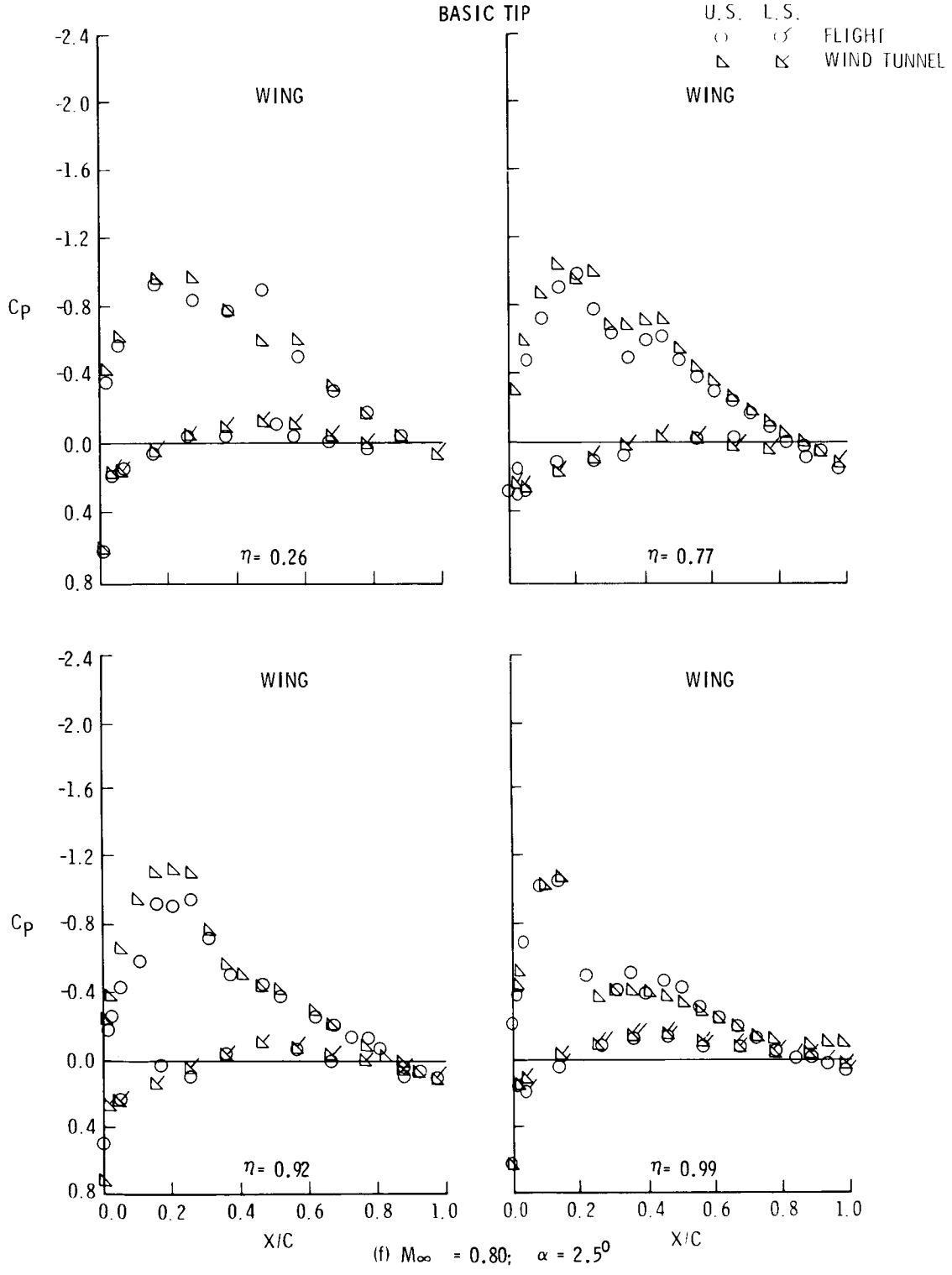

Figure 7. - Concluded

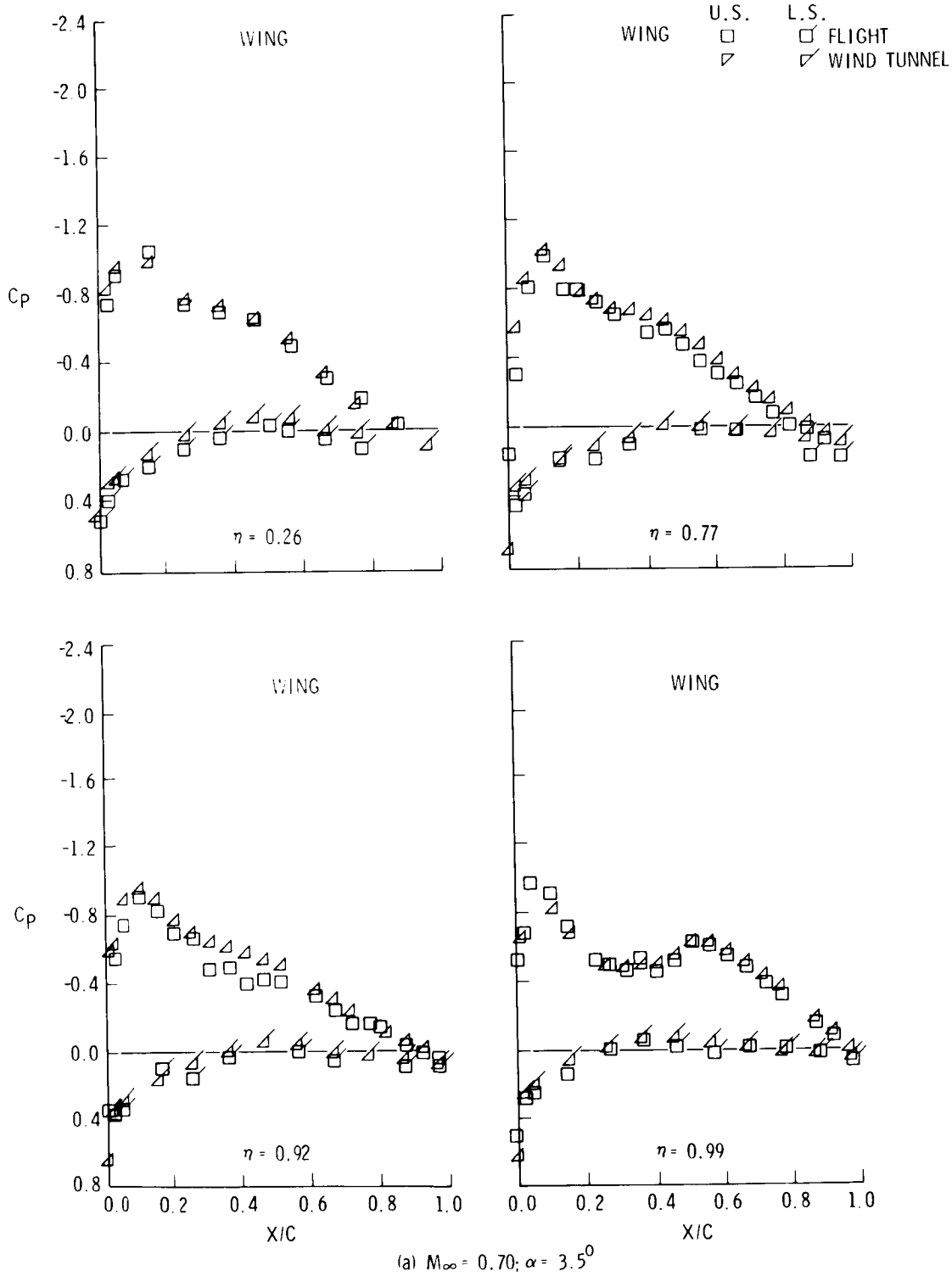

(a) $M_\infty = 0.70; \alpha = 3.5^0$

Figure 8. - Comparison of flight and windtunnel wing and winglet pressure distribution for the 15°/-4° winglet configuration

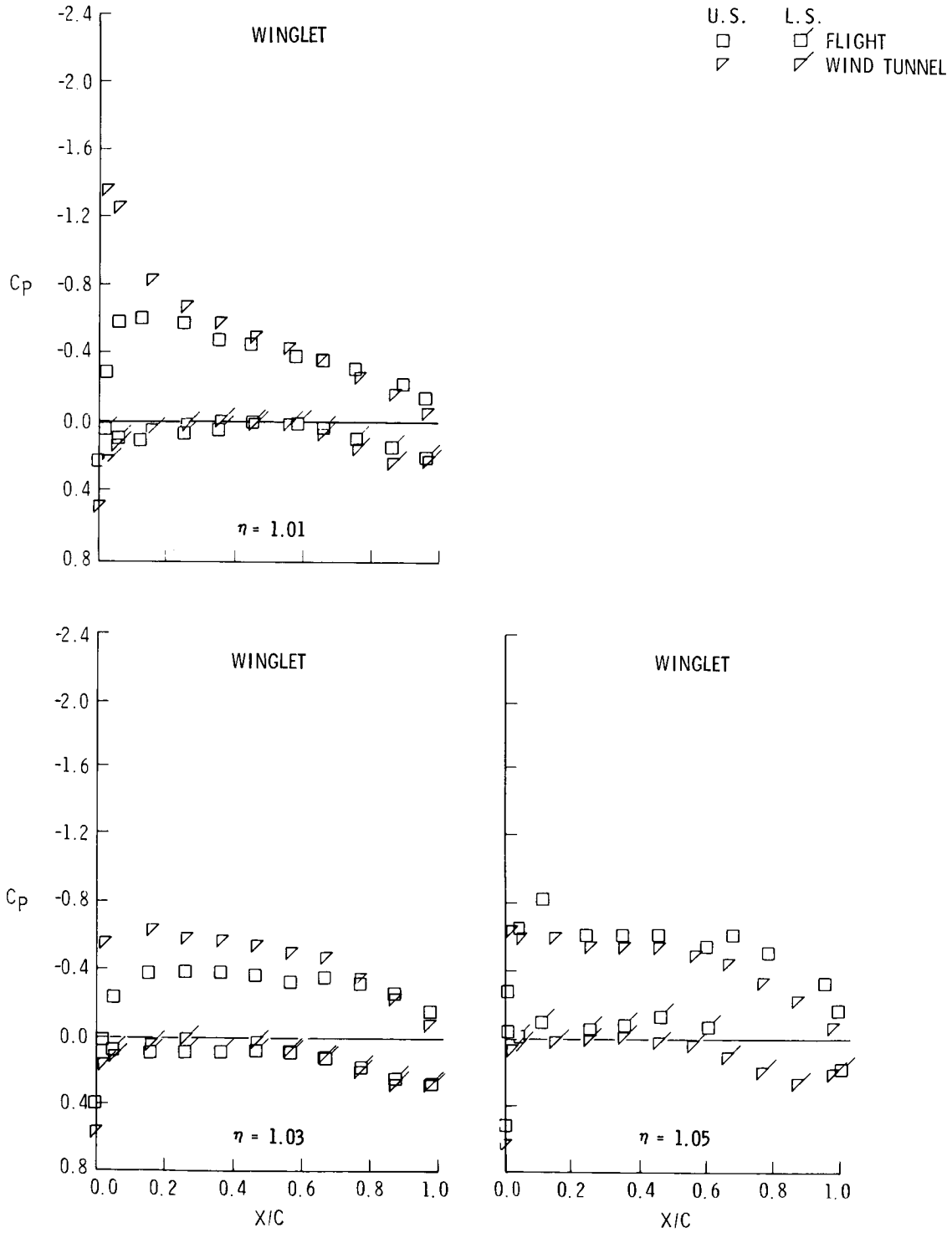

(a) $M_\infty = 0.70$; $\alpha = 3.5^0$ CONCLUDED

Figure 8. - Continued

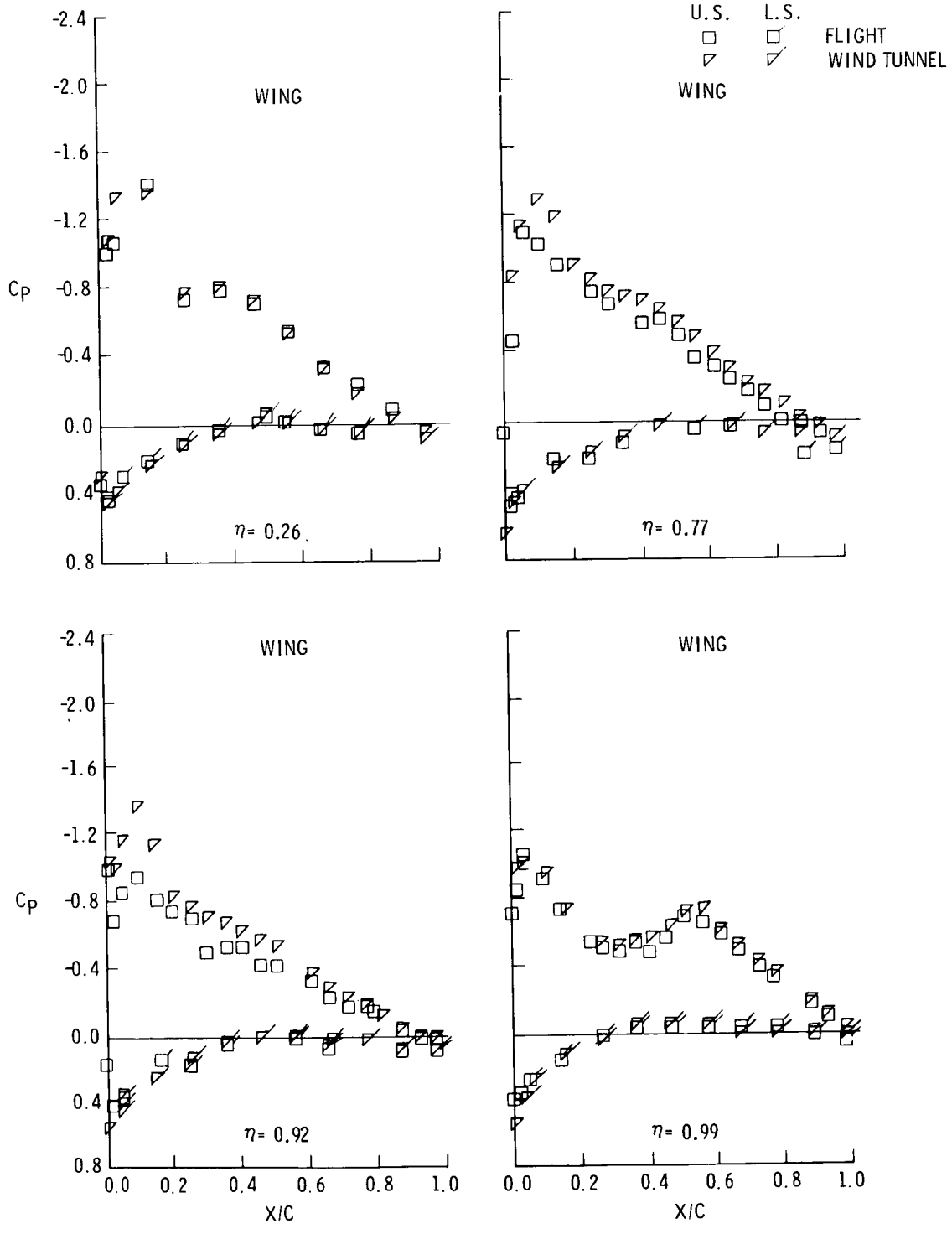

(b) M_∞ = 0.70; α = 5.0°

Figure 8. - Continued

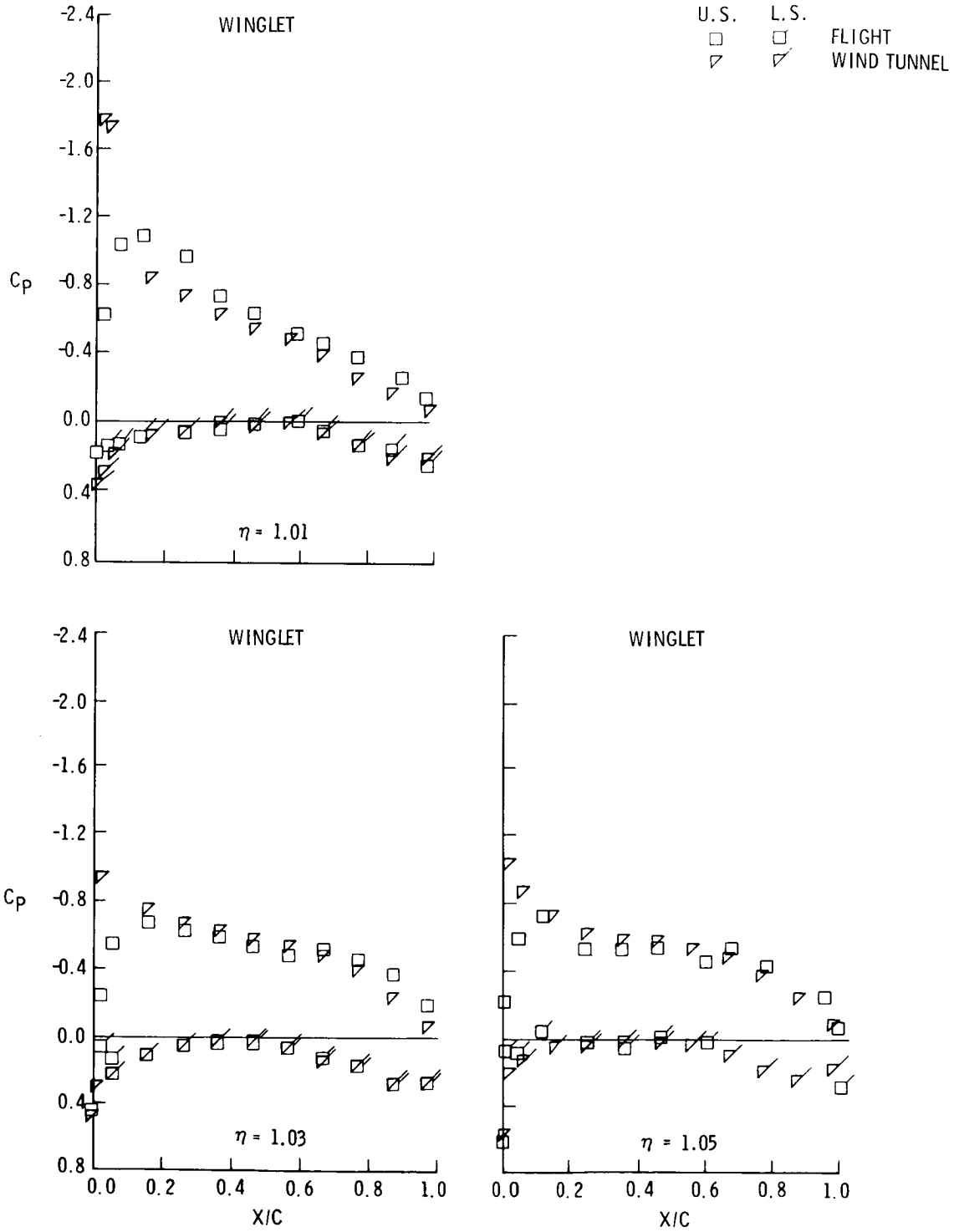

(b) $M_\infty = 0.70$; $\alpha = 5.0^0$ CONCLUDED

Figure 8. - Continued

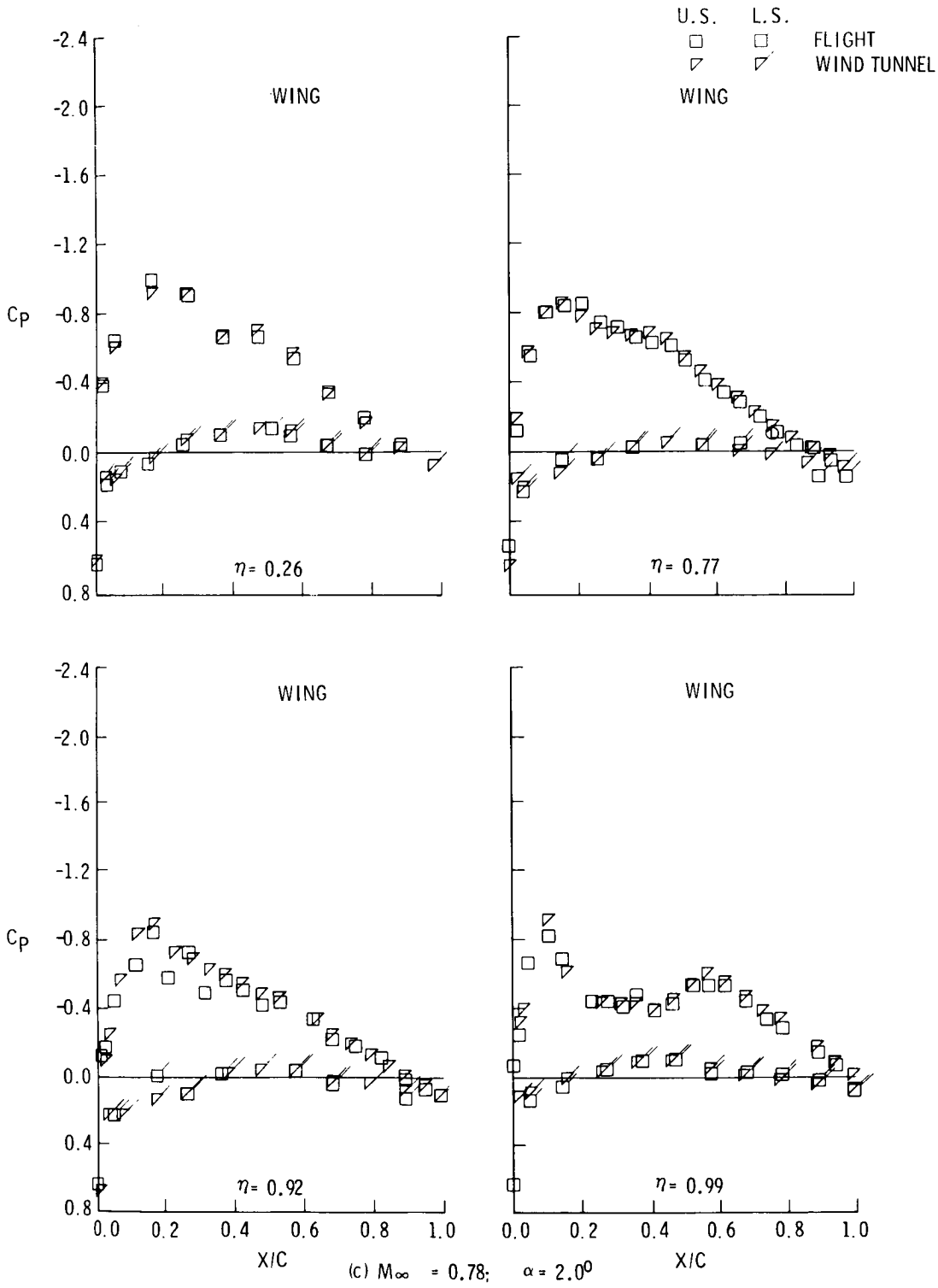

Figure 8. - Continued

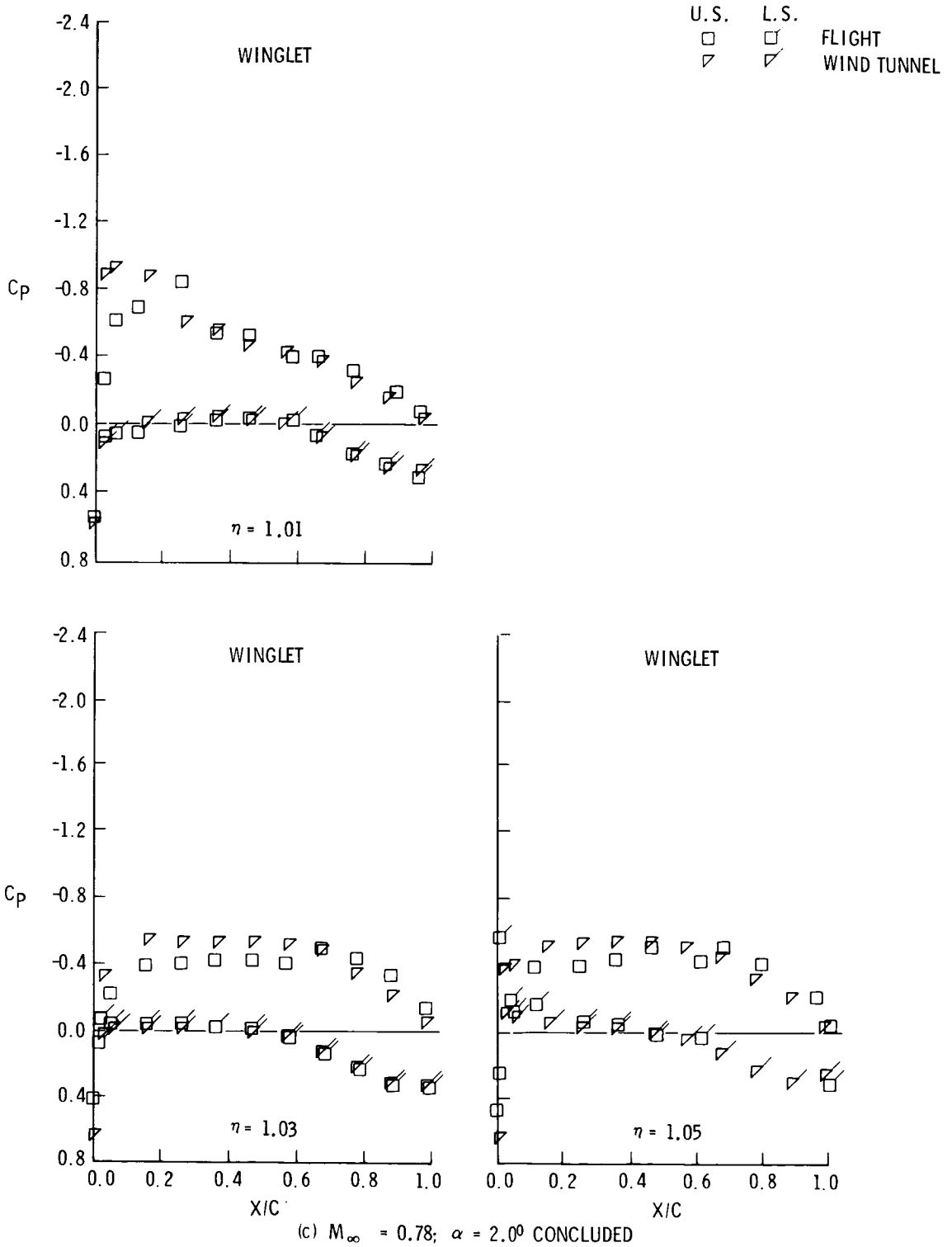

(c) M_∞ = 0.78; α = 2.0° CONCLUDED

Figure 8. - Continued

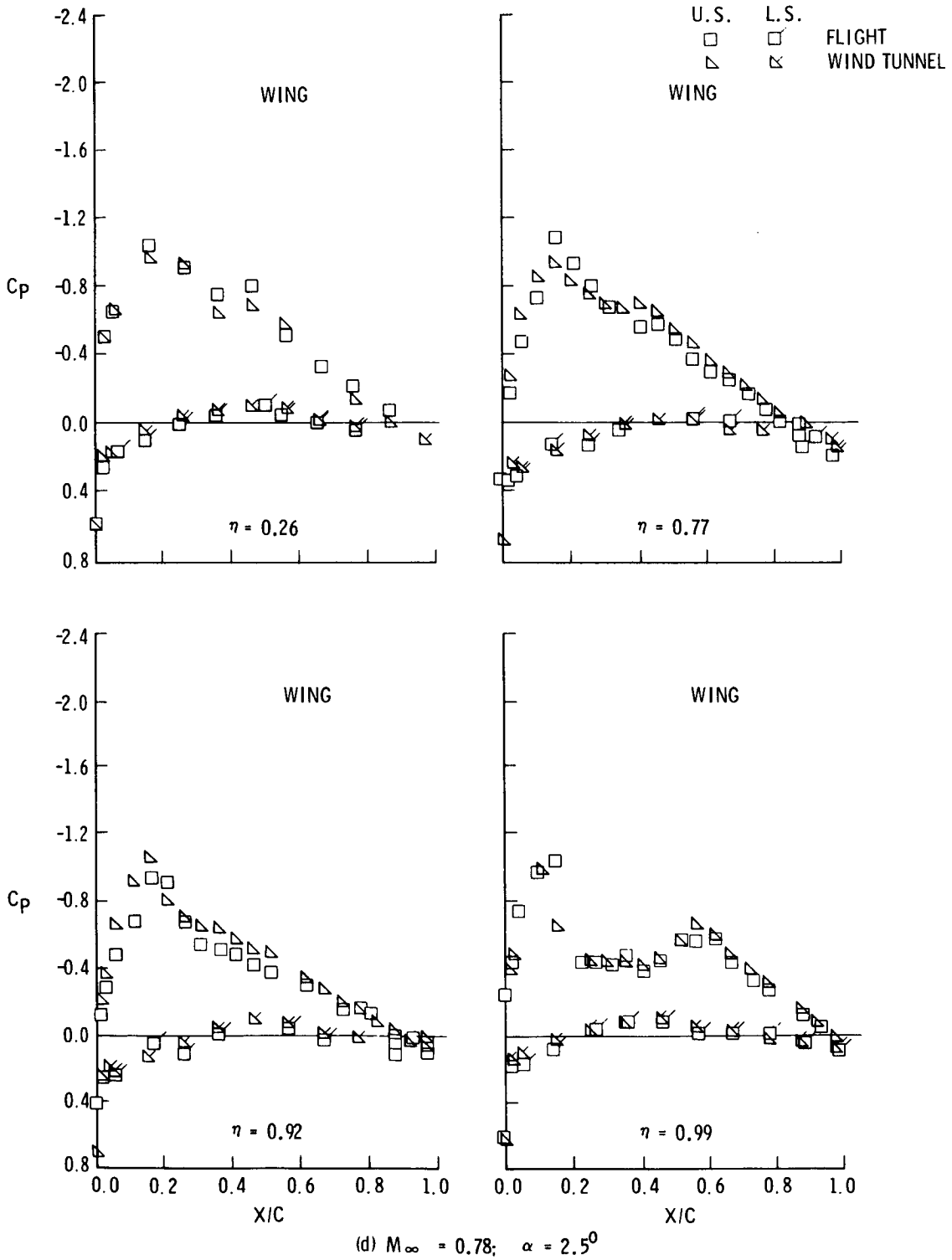

(d) $M_\infty = 0.78$; $\alpha = 2.5^0$

Figure 8. - Continued

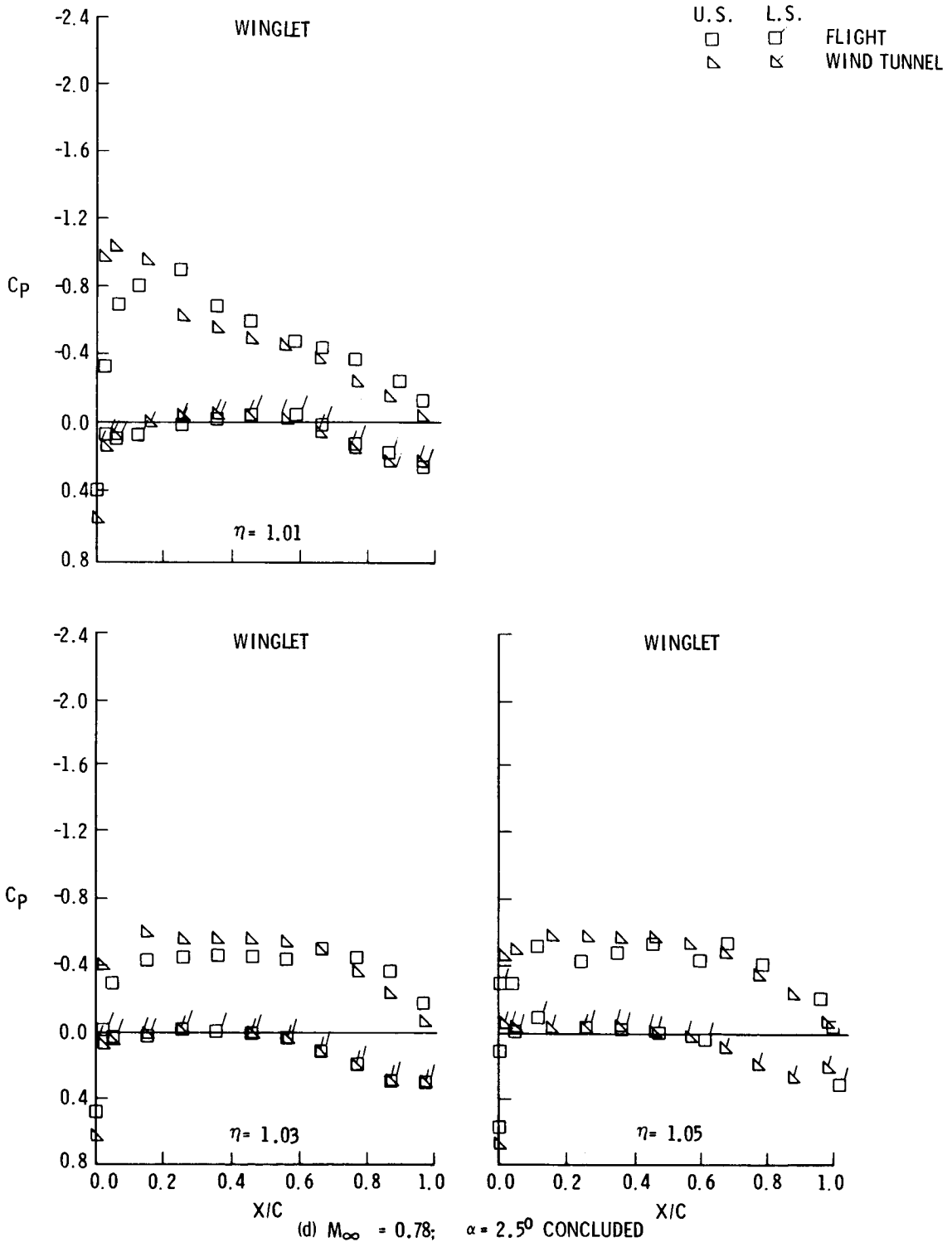

(d) M_∞ = 0.78; α = 2.5° CONCLUDED

Figure 8. - Continued

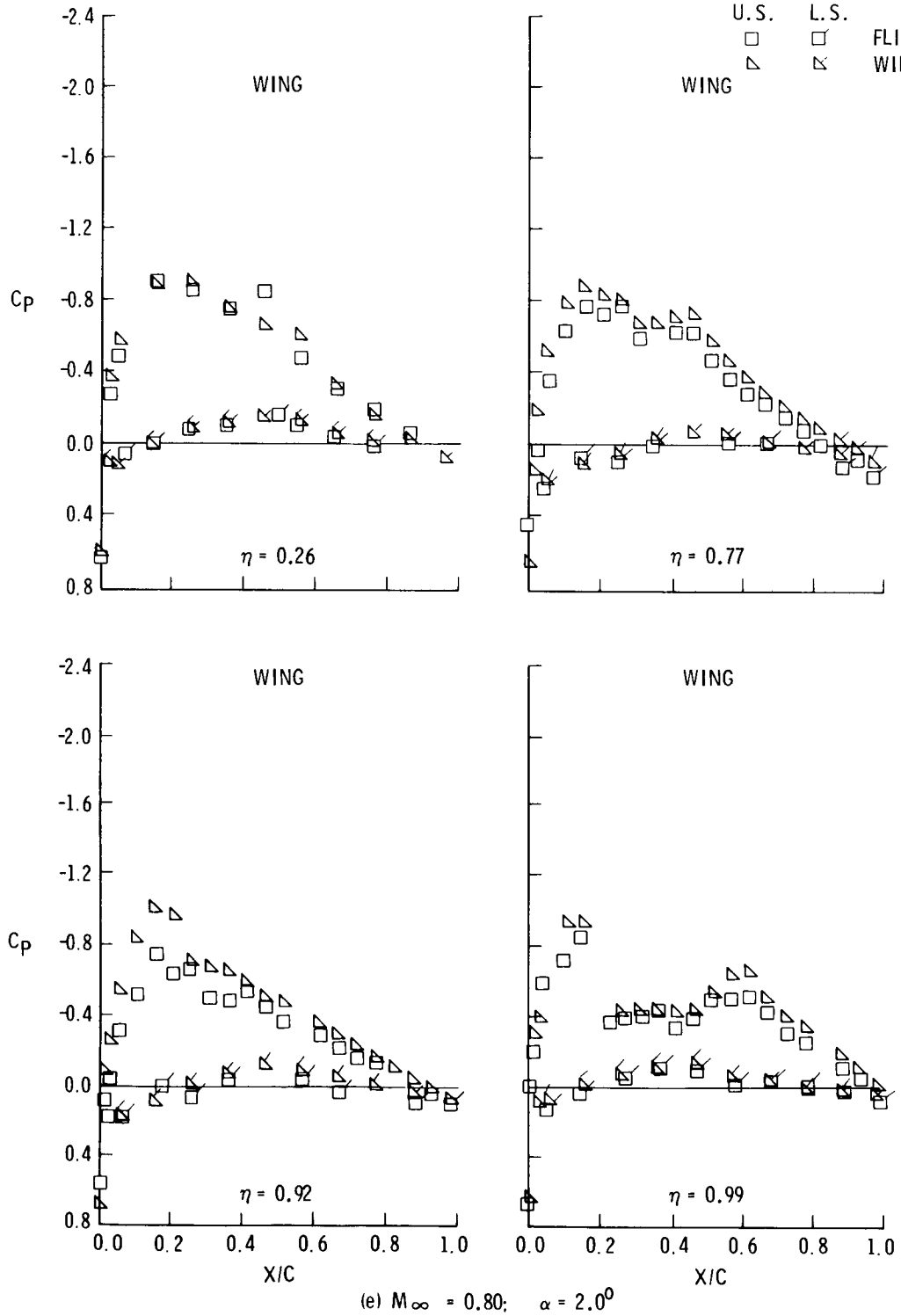

(e) $M_\infty = 0.80$; $\alpha = 2.0^0$

Figure 8. - Continued

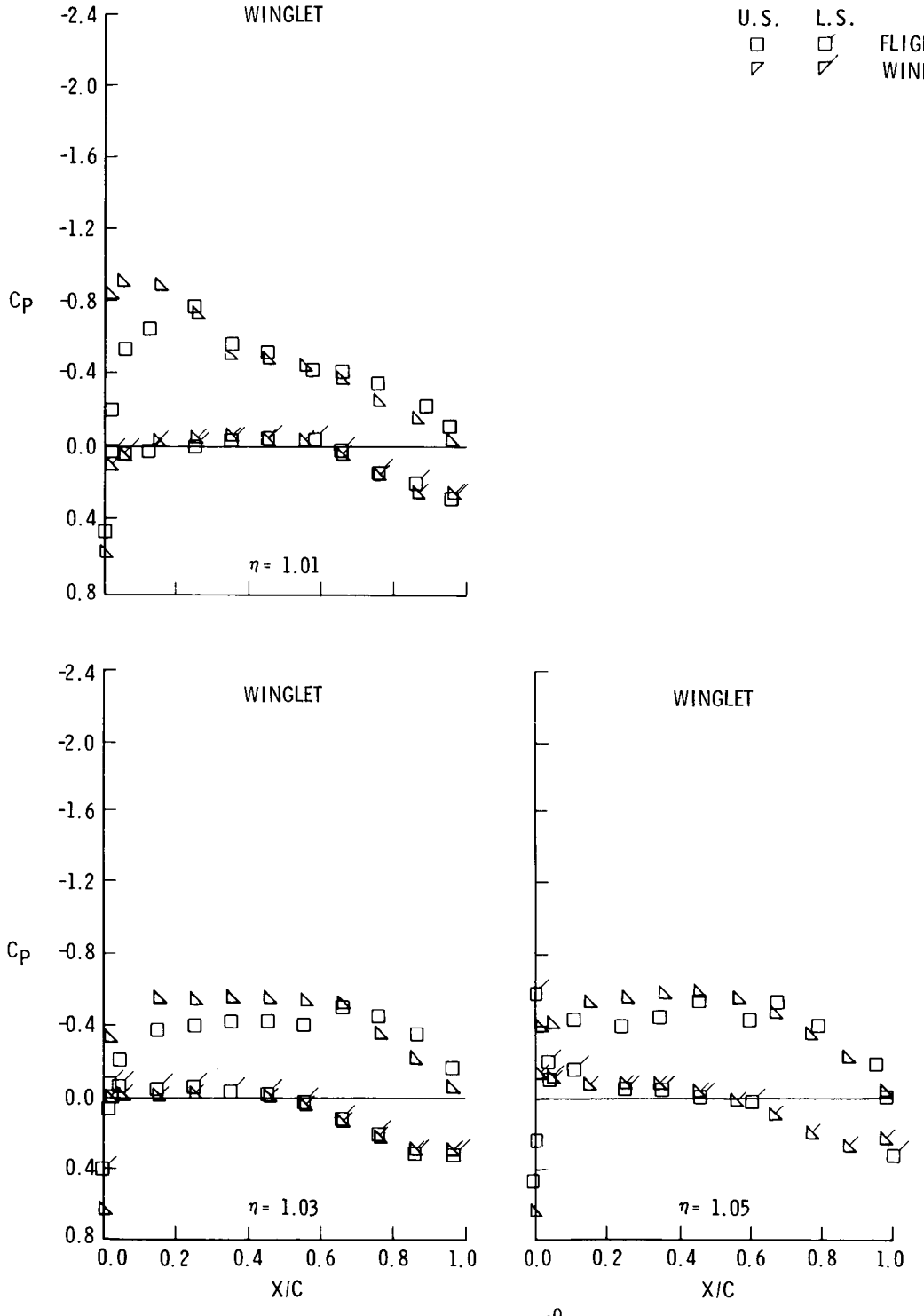

(e) $M_\infty = 0.80$; $\alpha = 2.0^0$ CONCLUDED

Figure 8. - Continued

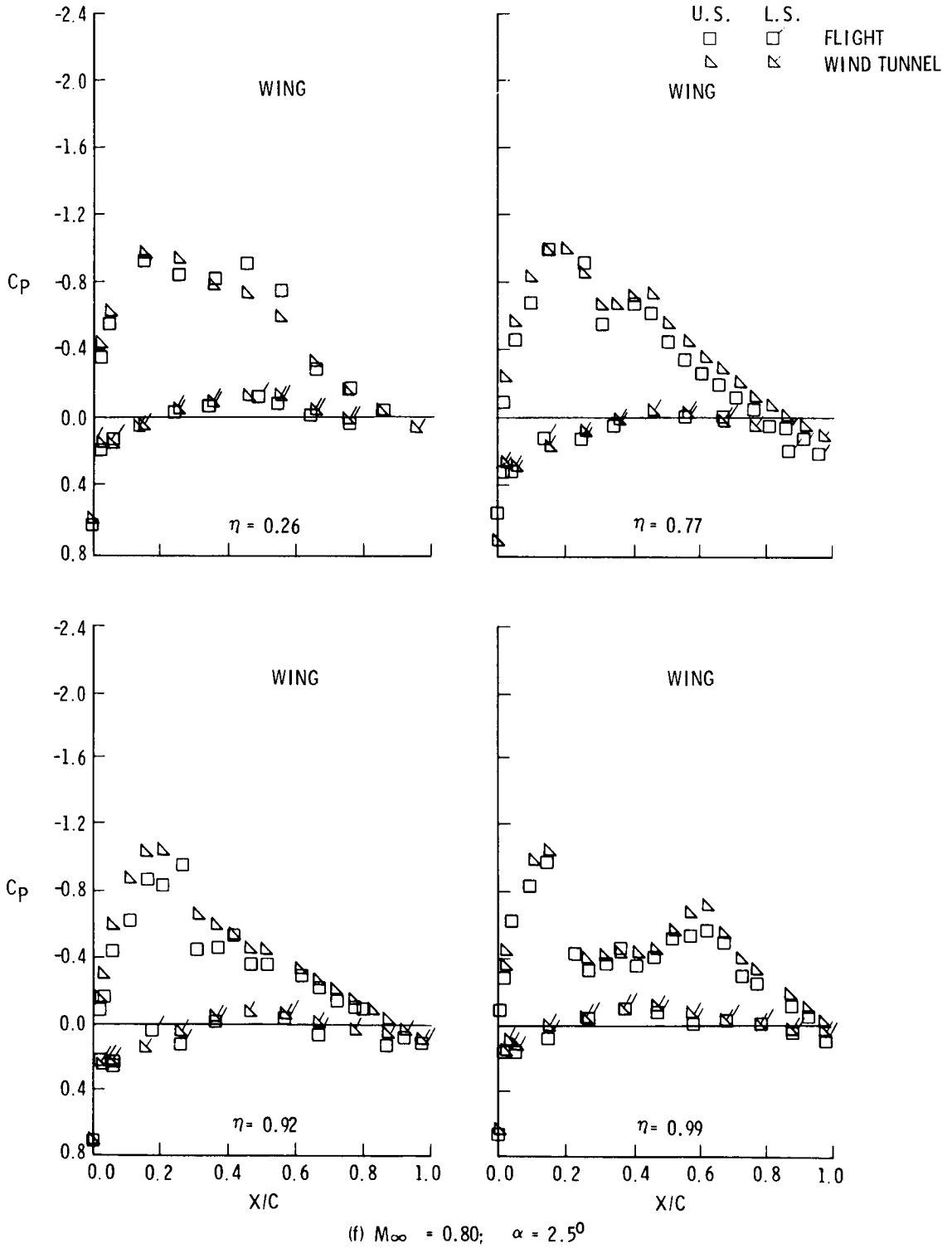

(f) $M_\infty = 0.80$; $\alpha = 2.5^0$

Figure 8. - Continued

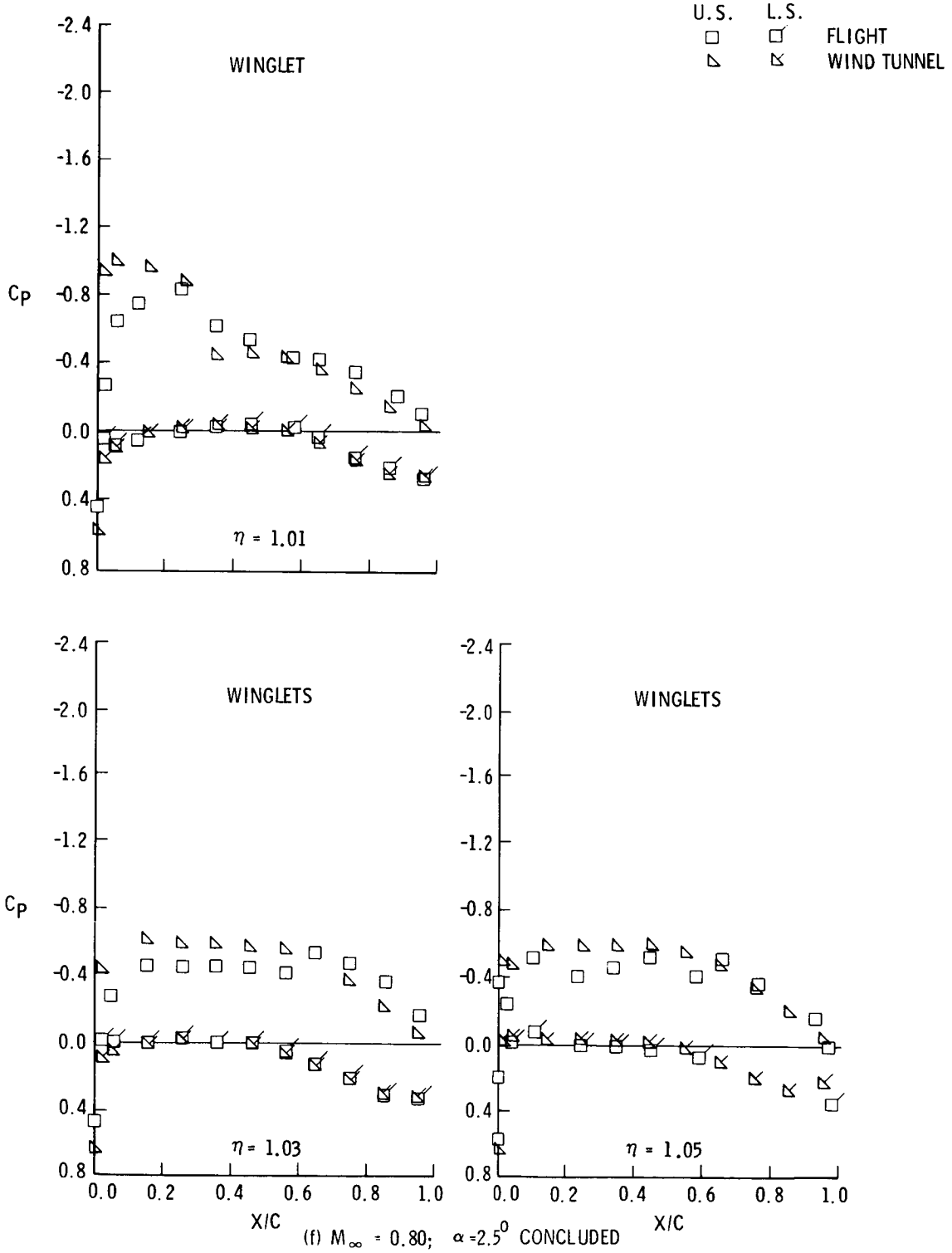

(f) $M_\infty = 0.80$; $\alpha = 2.5^0$ CONCLUDED

Figure 8. - Concluded

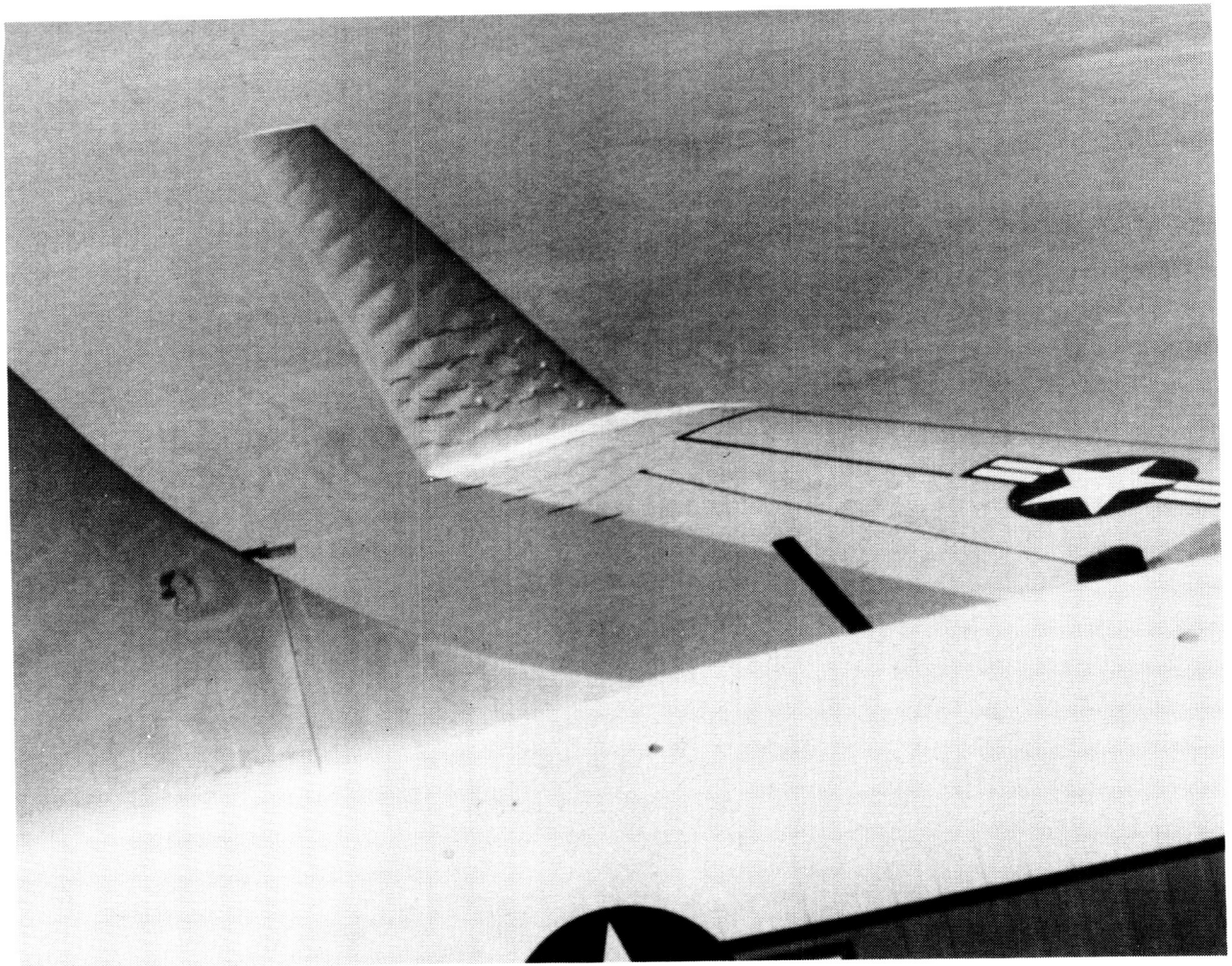

Figure 9. - Inflight photo of winglet "oilcanning"

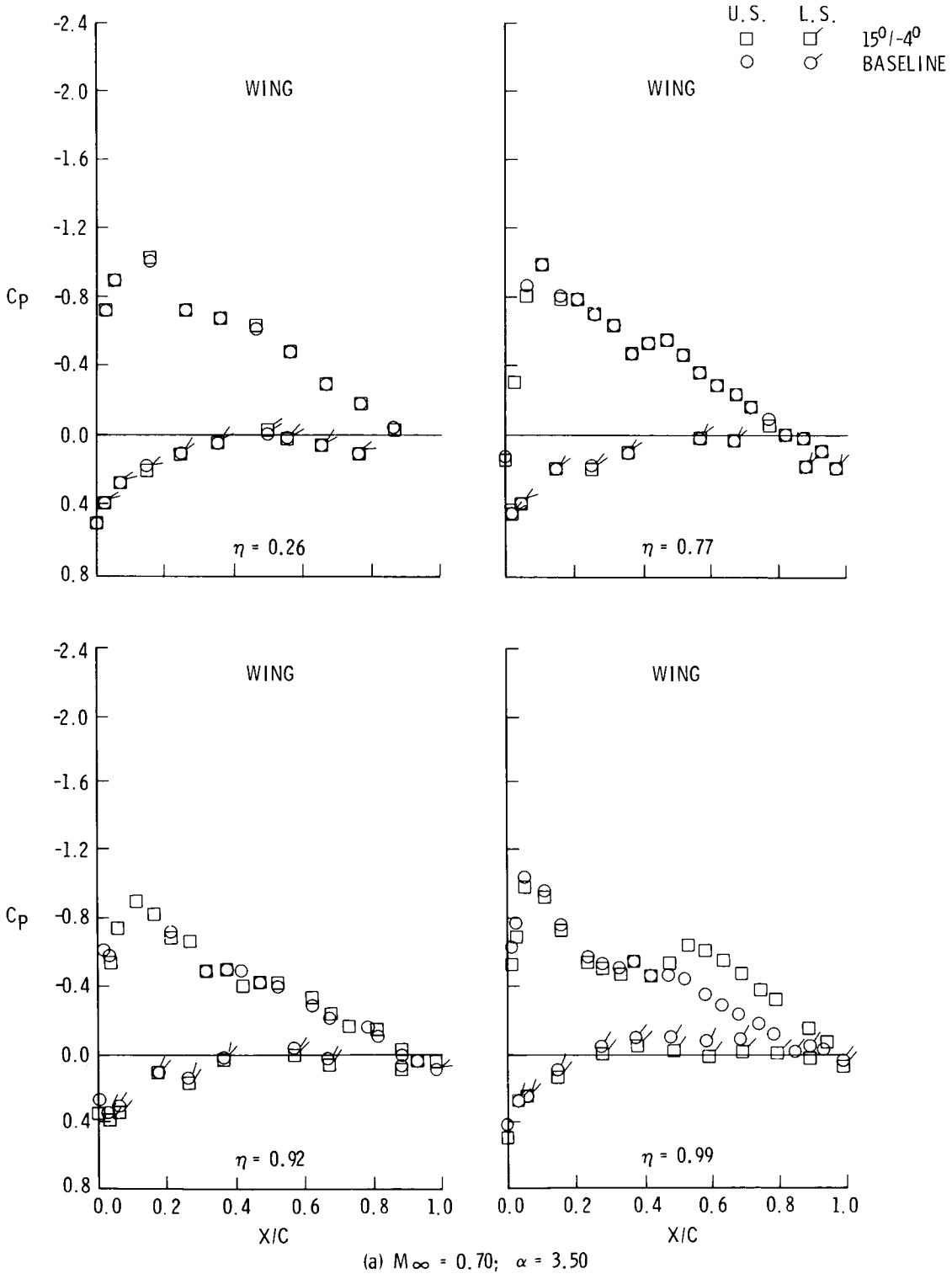

(a) $M_\infty = 0.70$; $\alpha = 3.50$

Figure 10. - Flight wing pressure distribution comparisons with the basic wing tip and 15°/-4° winglet configuration

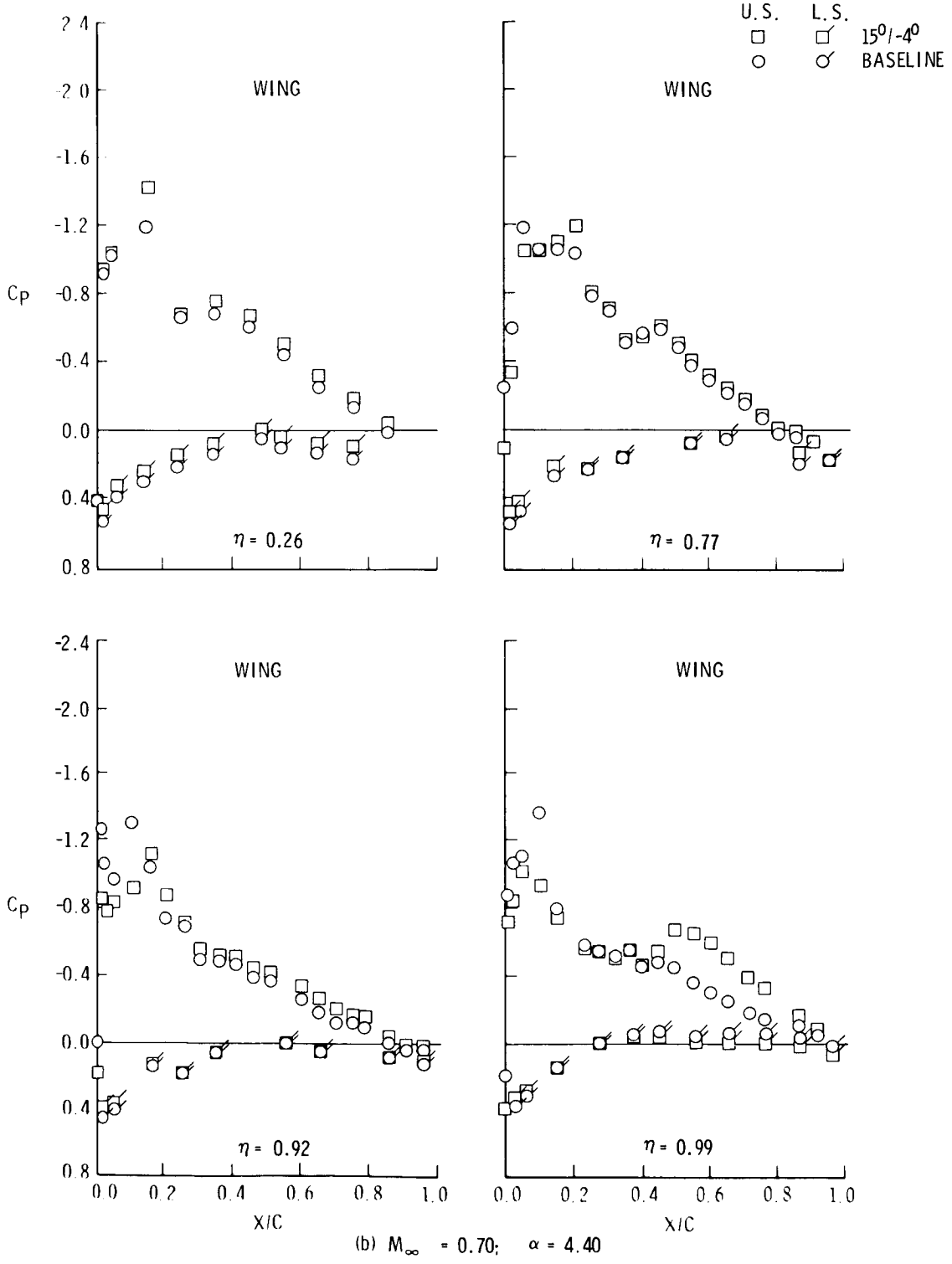

(b) M_∞ = 0.70; α = 4.40

Figure 10. - Continued

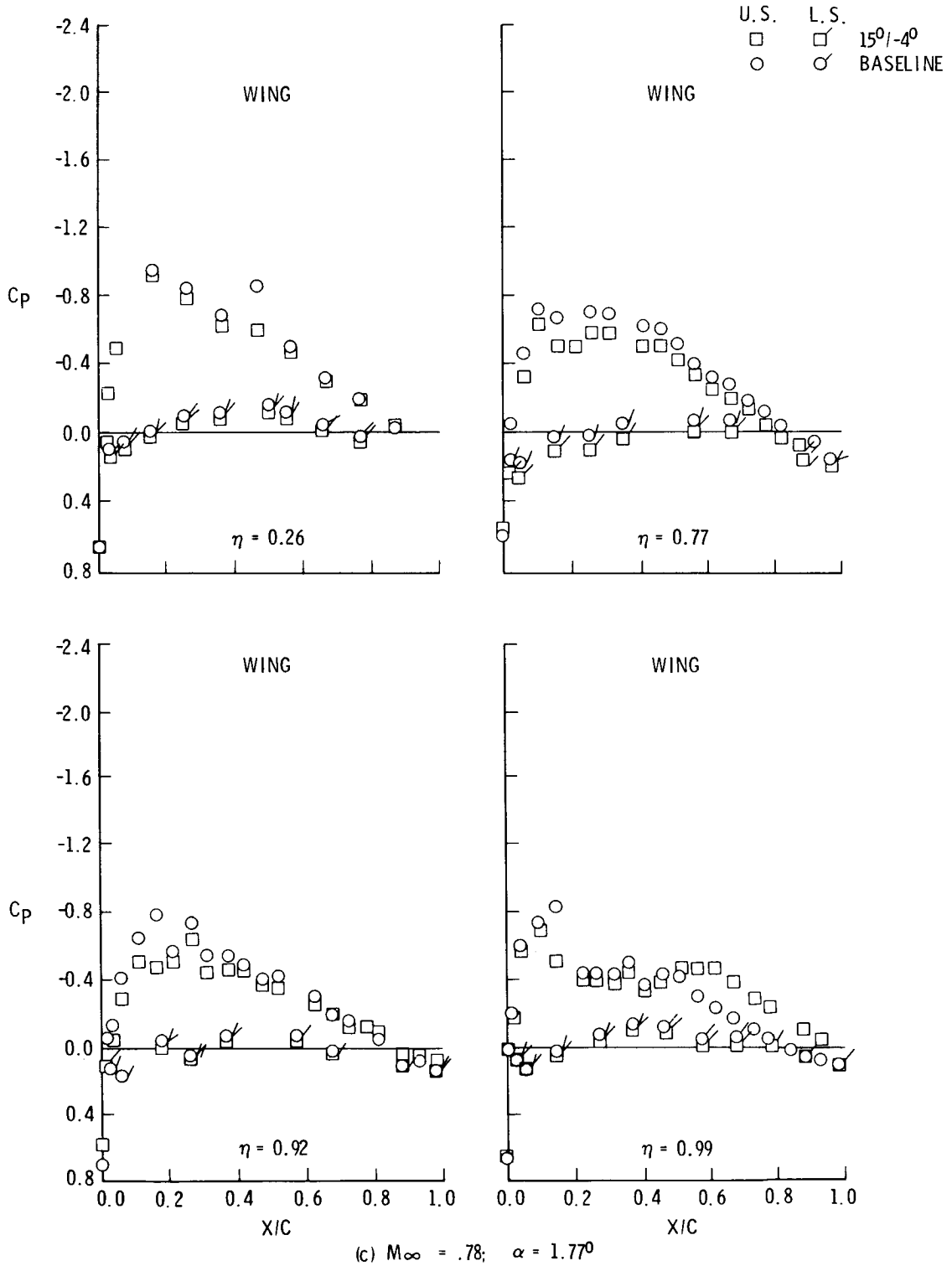

(c) M_∞ = .78; α = 1.77°

Figure 10. - Continued

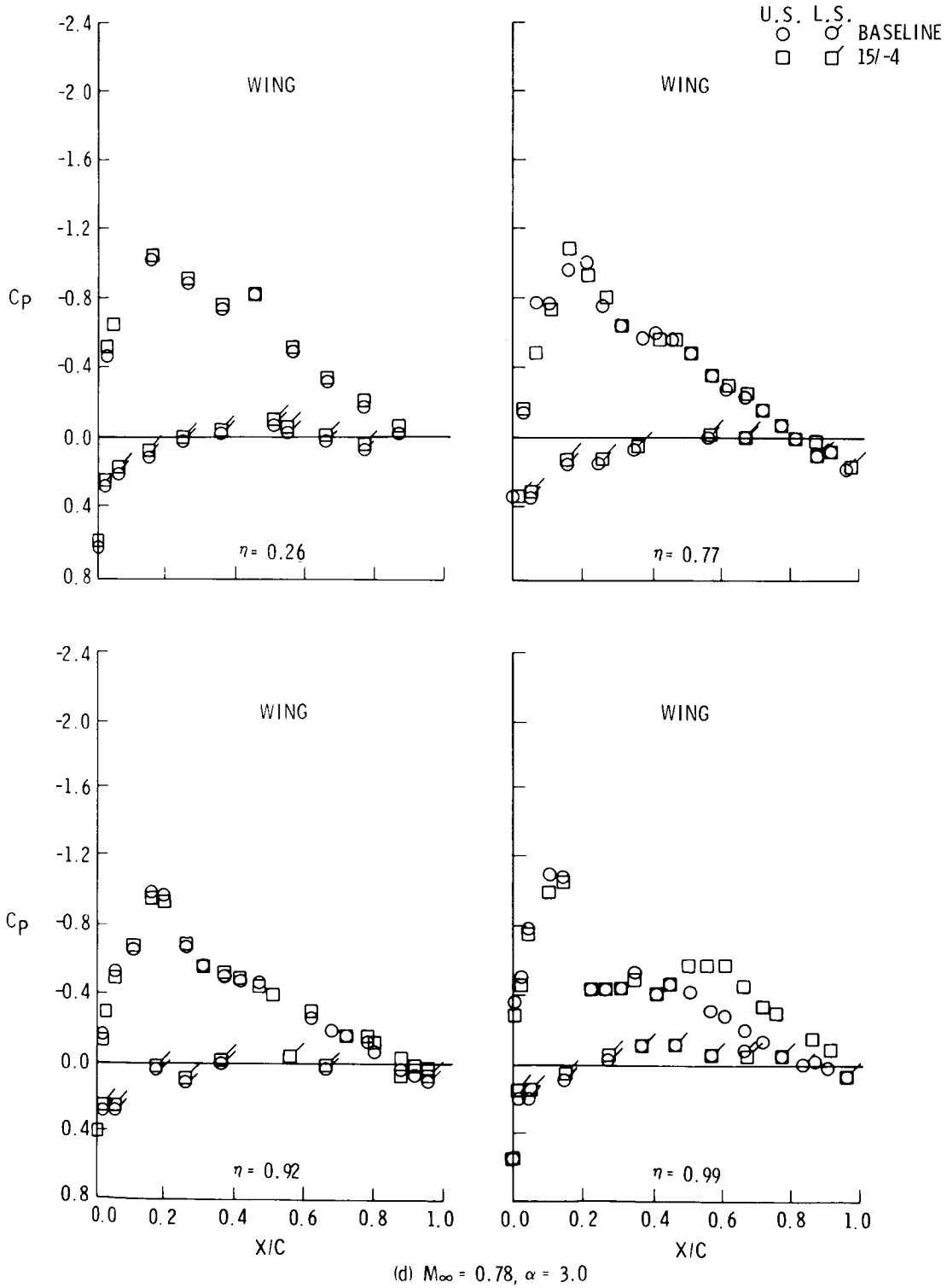

(d) $M_\infty = 0.78$, $\alpha = 3.0$

Figure 10. - Continued

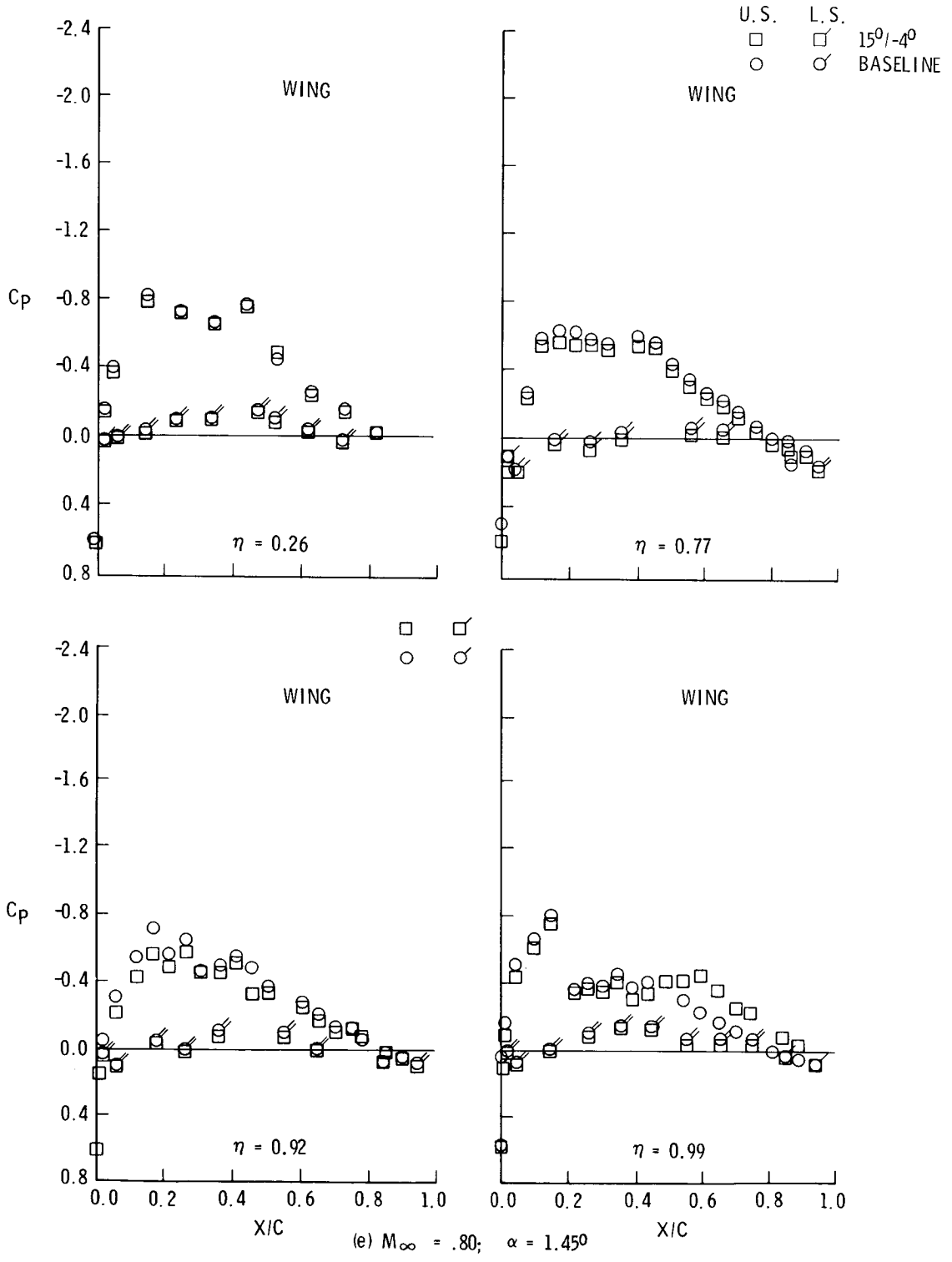

(e) $M_\infty = .80$; $\alpha = 1.45^0$

Figure 10. - Continued

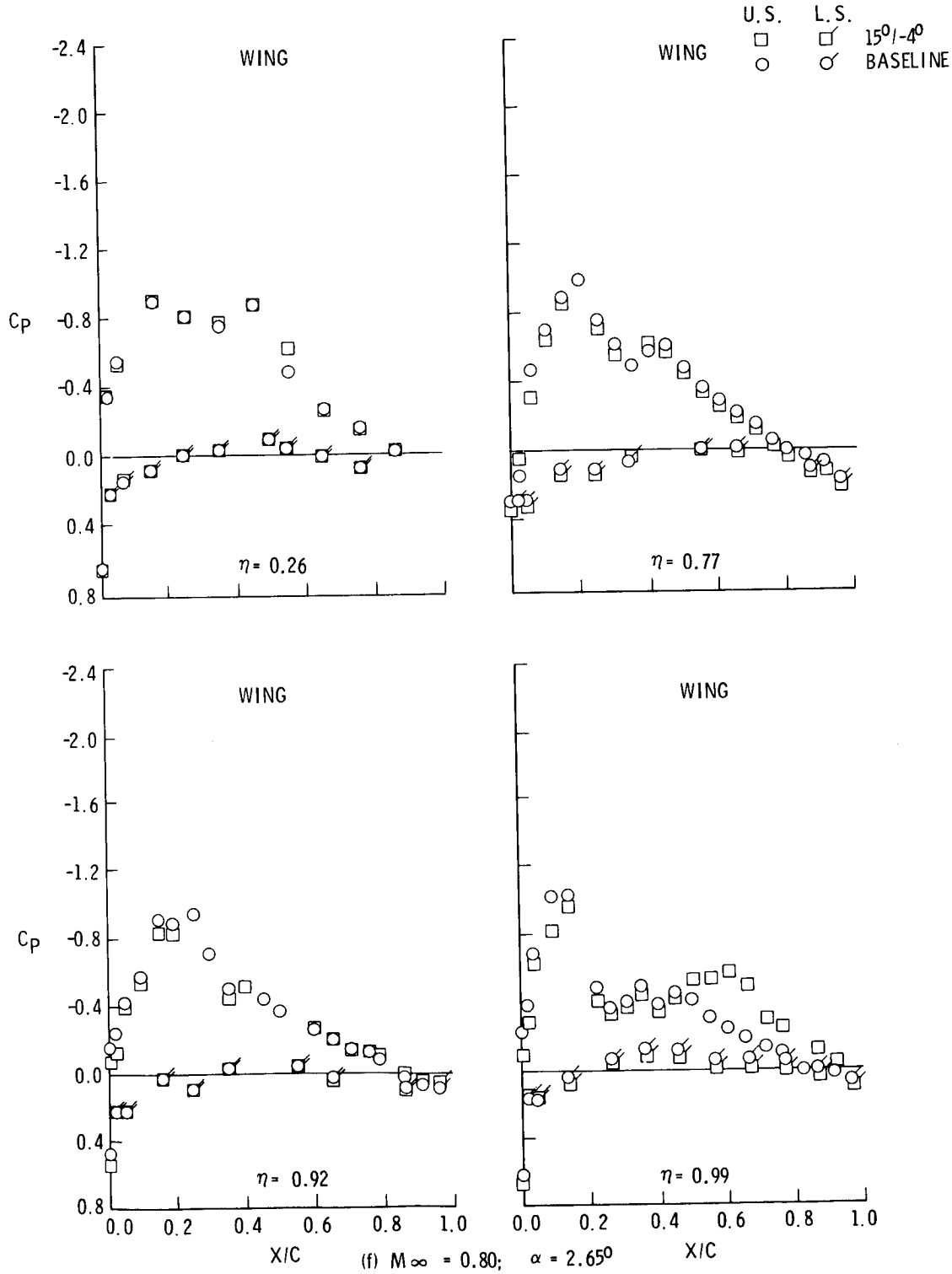

Figure 10. - Continued

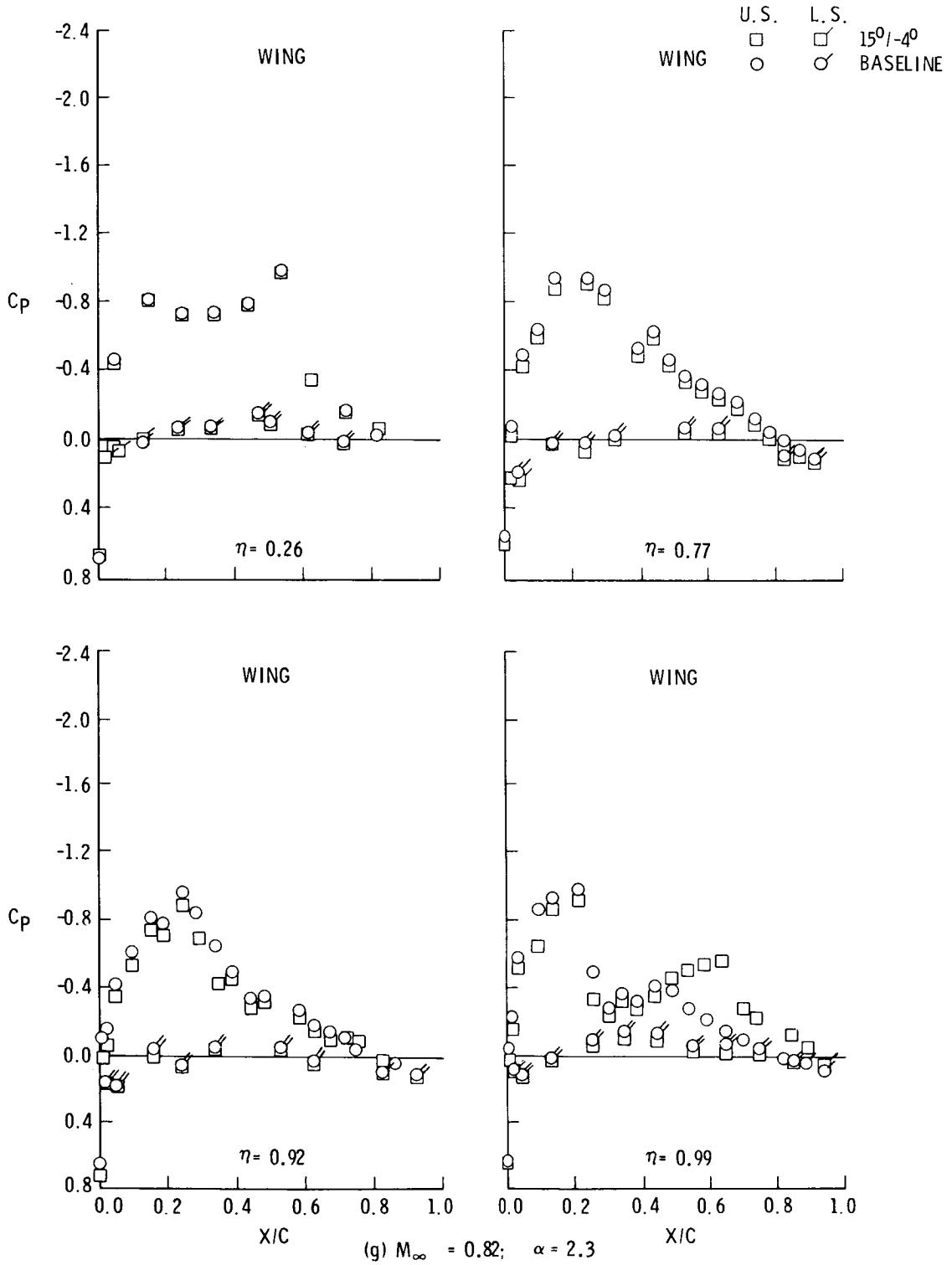

Figure 10. - Concluded

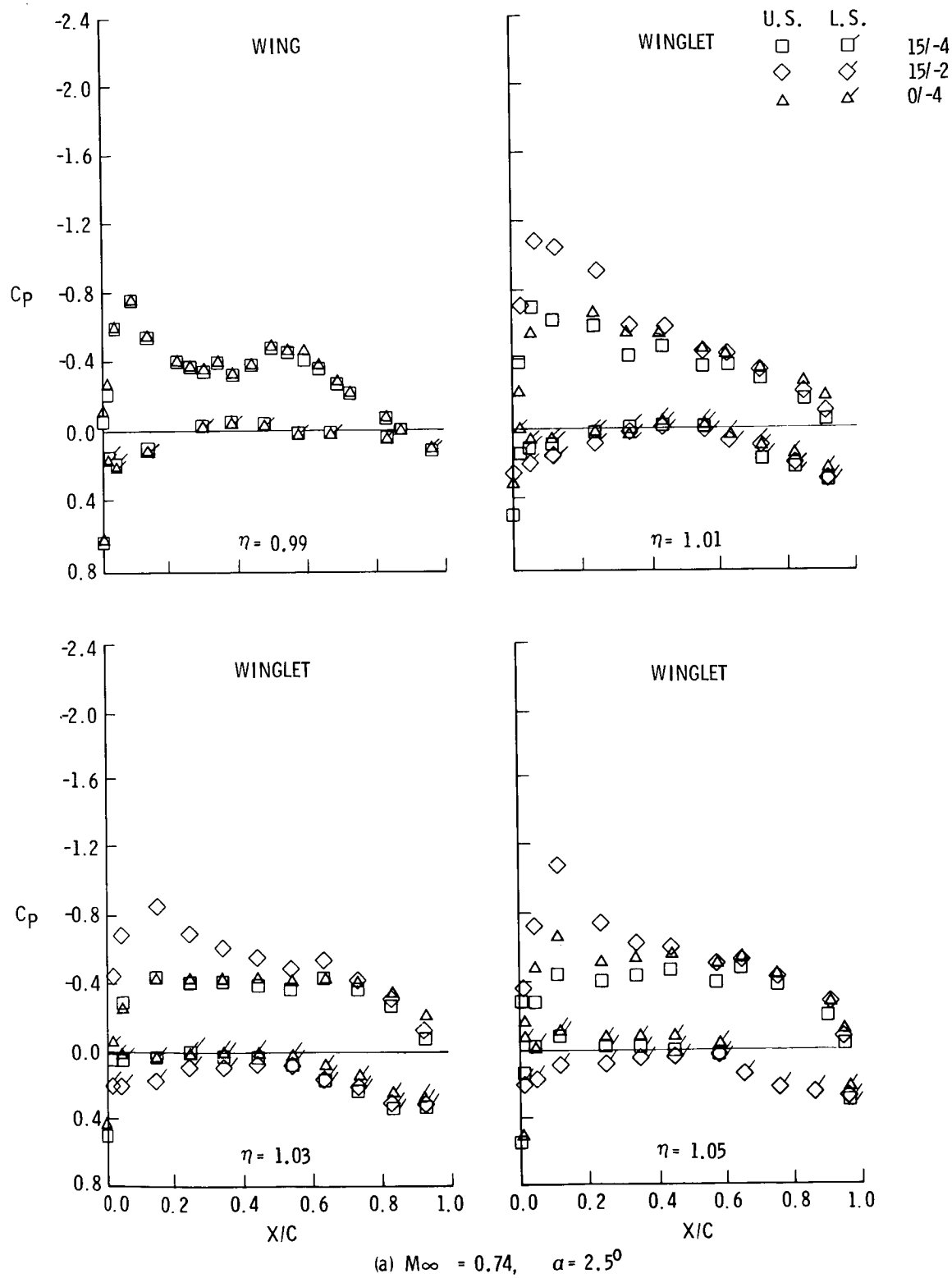

(a) $M_\infty = 0.74$, $\alpha = 2.5^0$

Figure 11. - Flight wing tip and winglet pressure distributions for the 15°/-4°, 15°/-2°, and 0°/-4° winglet cant/incidence configurations

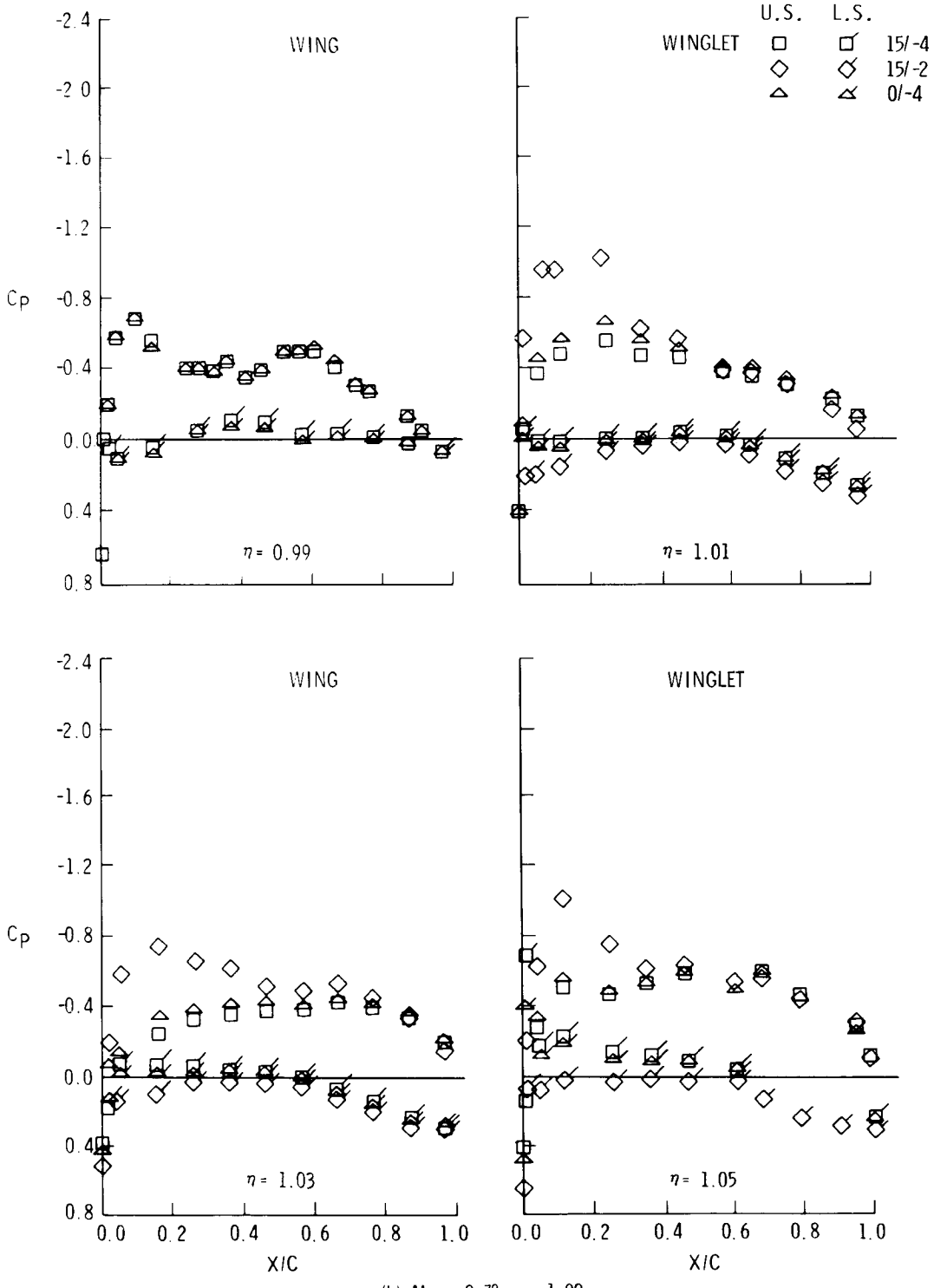

(b) $M_\infty = 0.78$, $\alpha = 1.90$

Figure 11. - Continued

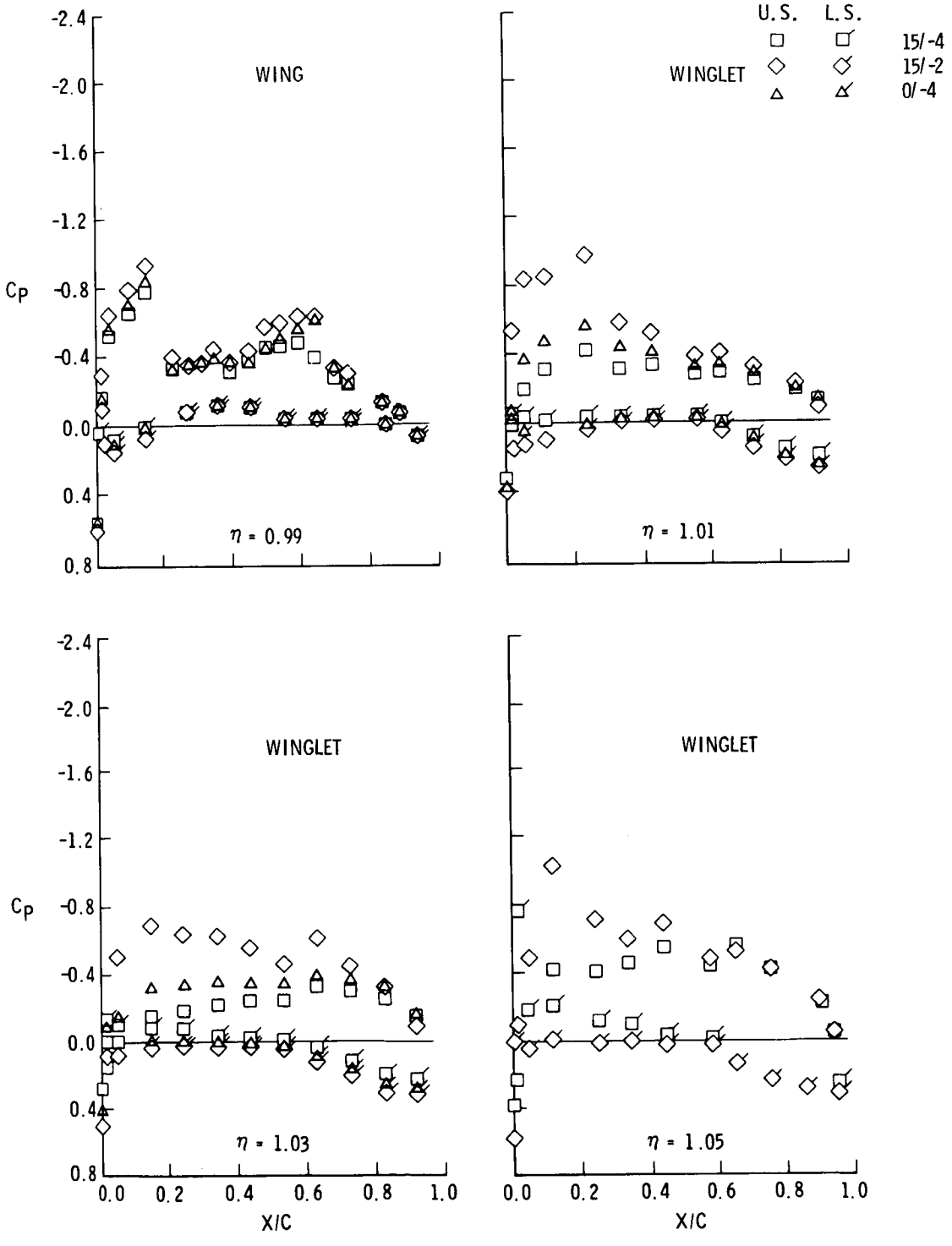

(c) $M_\infty = 0.80$, $\alpha = 1.80$

Figure 11. - Continued

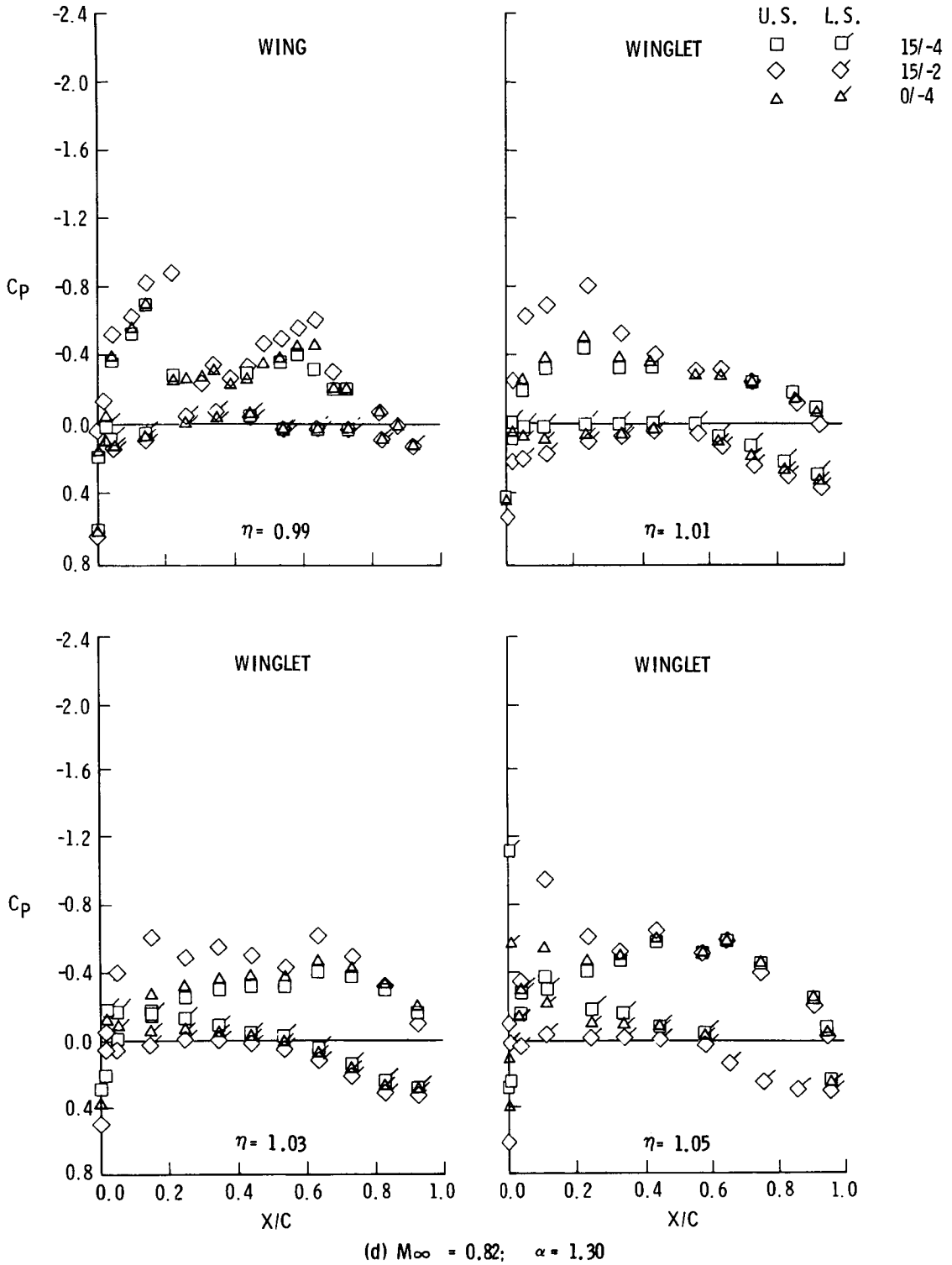

(d) $M_\infty = 0.82$; $\alpha = 1.30$

Figure 11. - Concluded

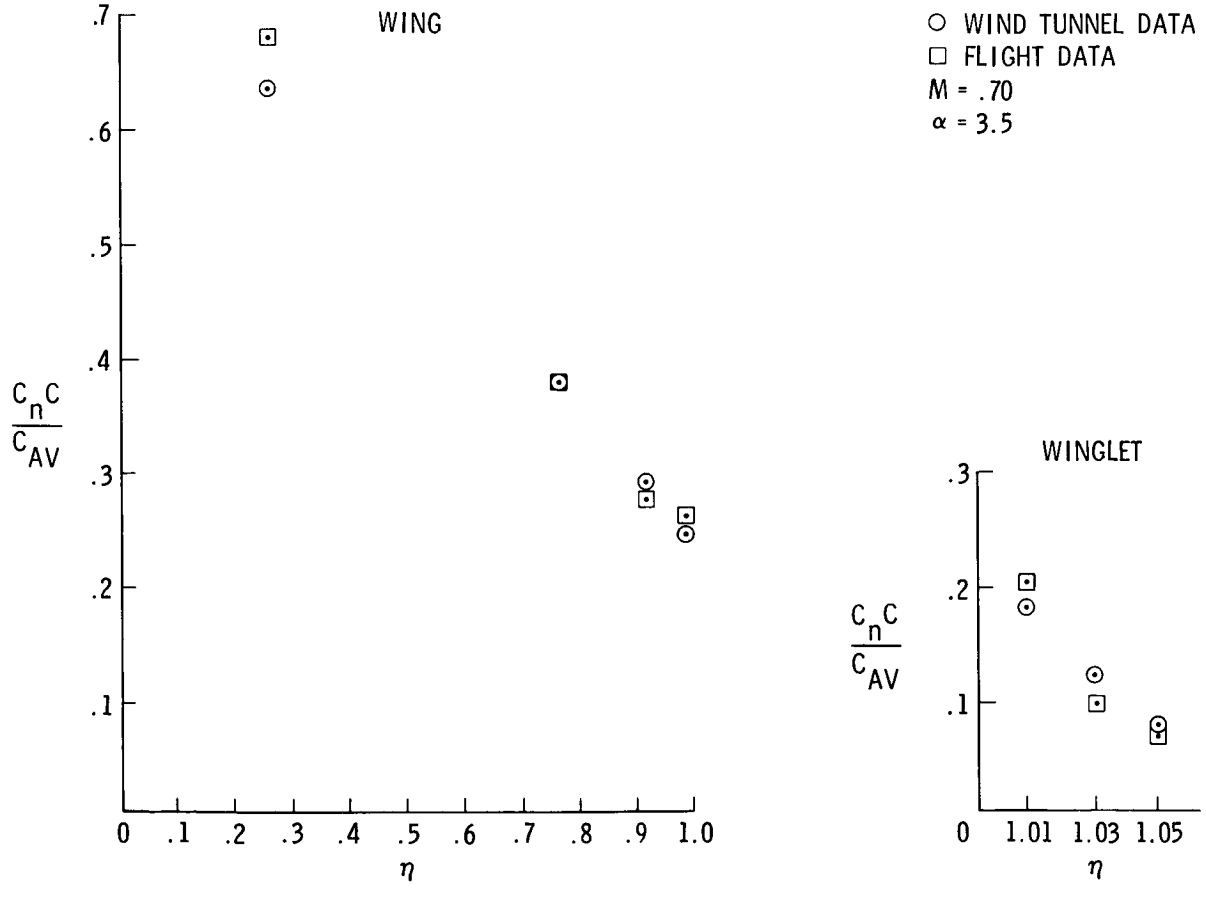

Figure 12. - Comparison of flight and windtunnel wing and winglet span load

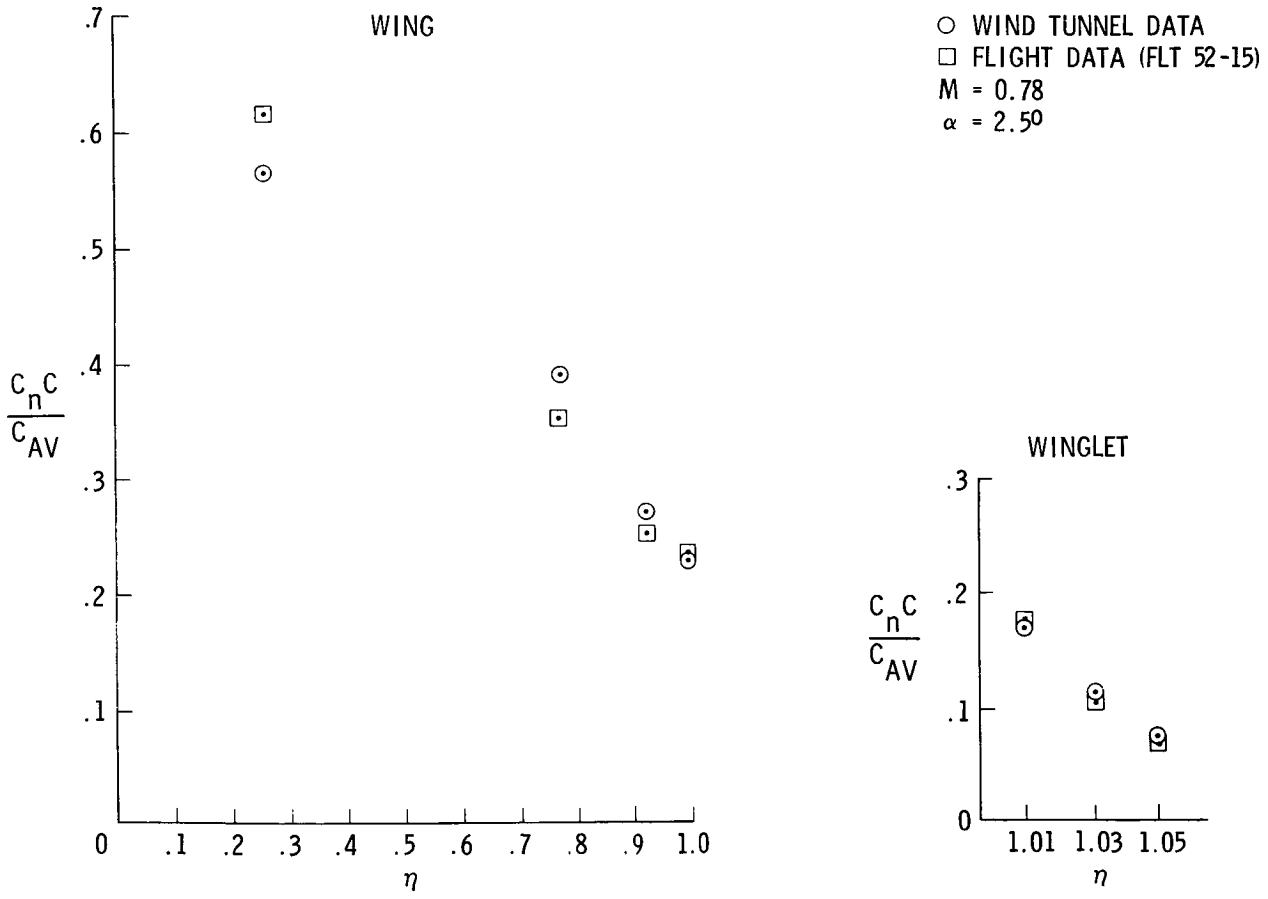

Figure 12. - Continued

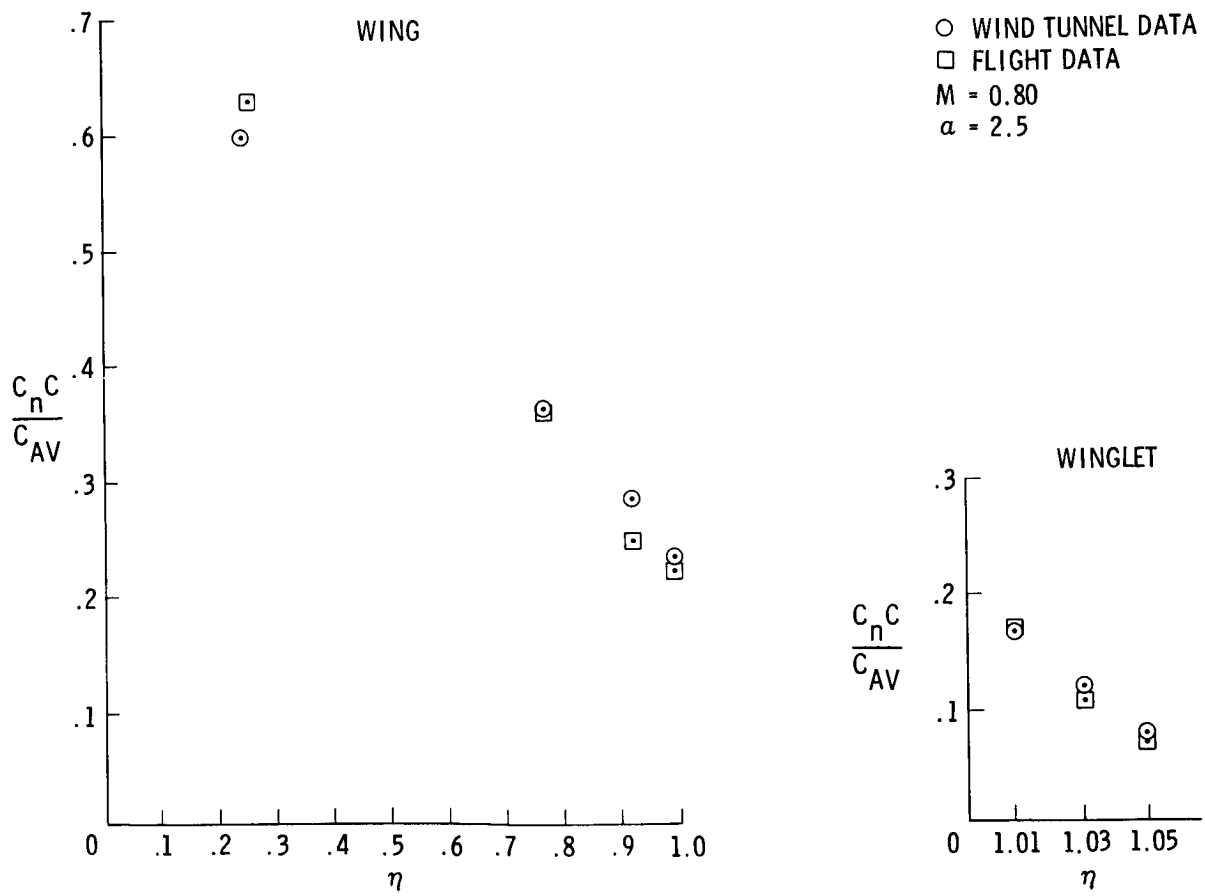

Figure 12. - Concluded

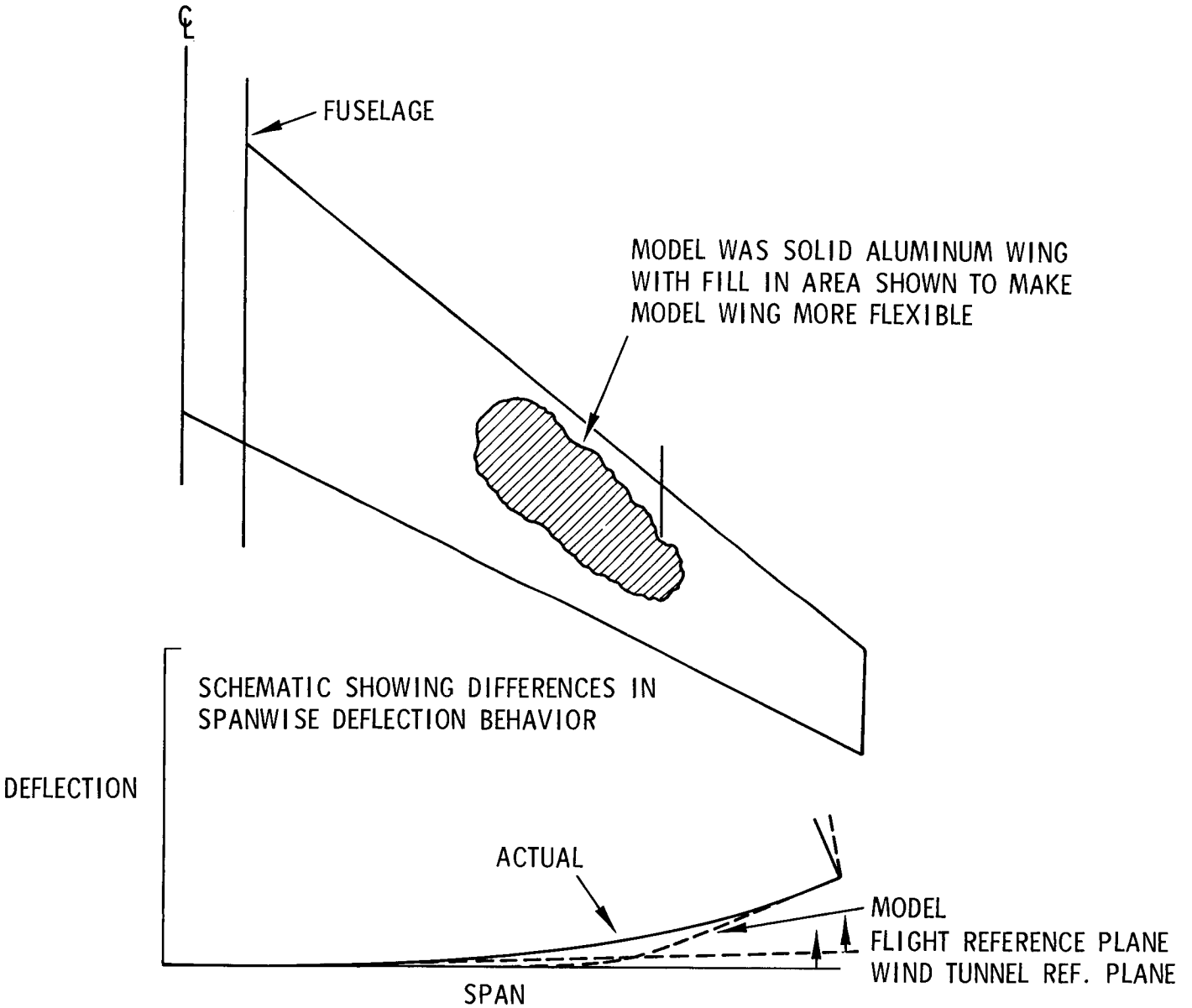

Figure 13. - Schematics of the semispan model wing construction flight versus wind tunnel model deflection measurements

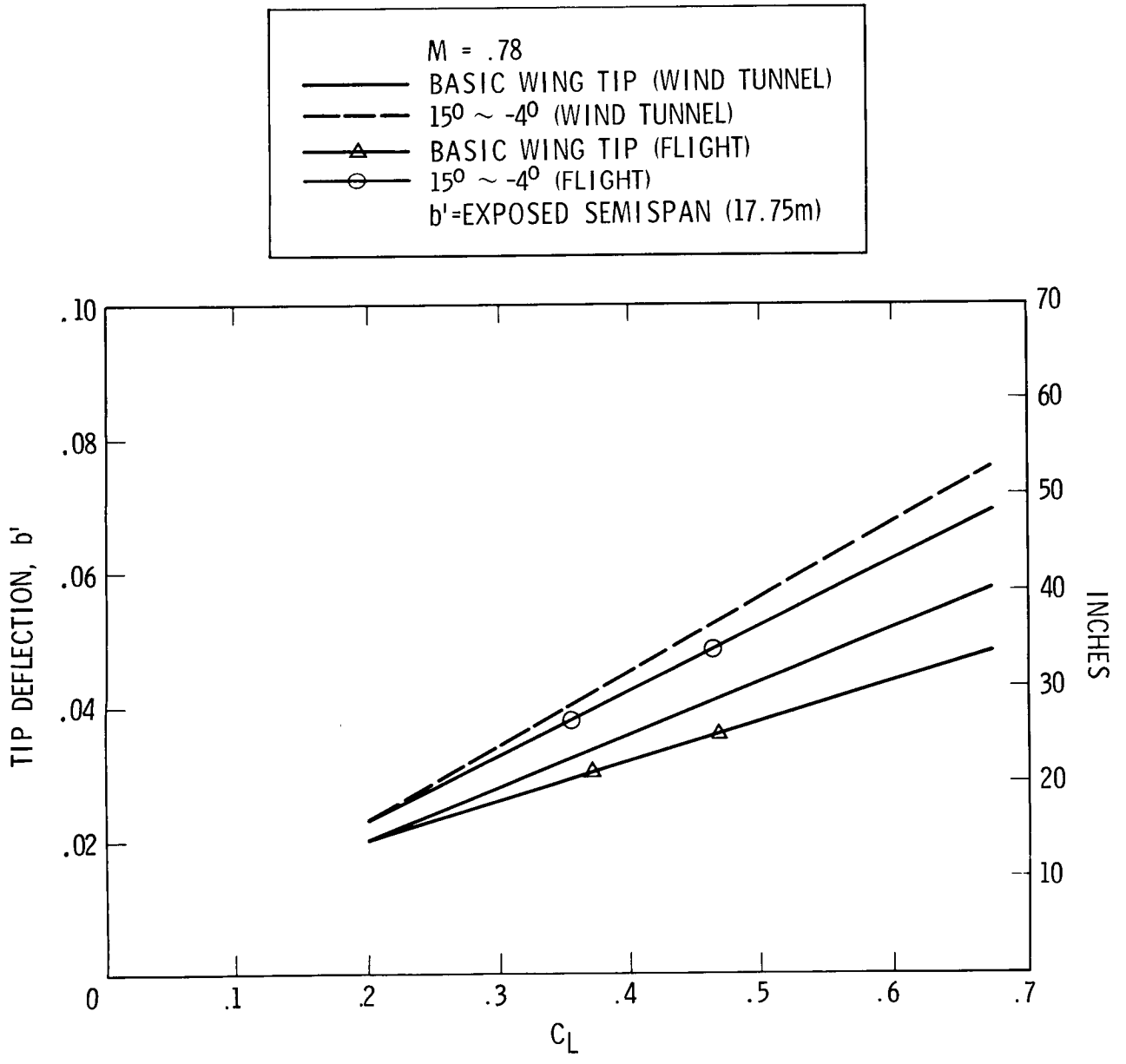

Figure 14. - Flight versus wind tunnel deflections at the design cruise condition

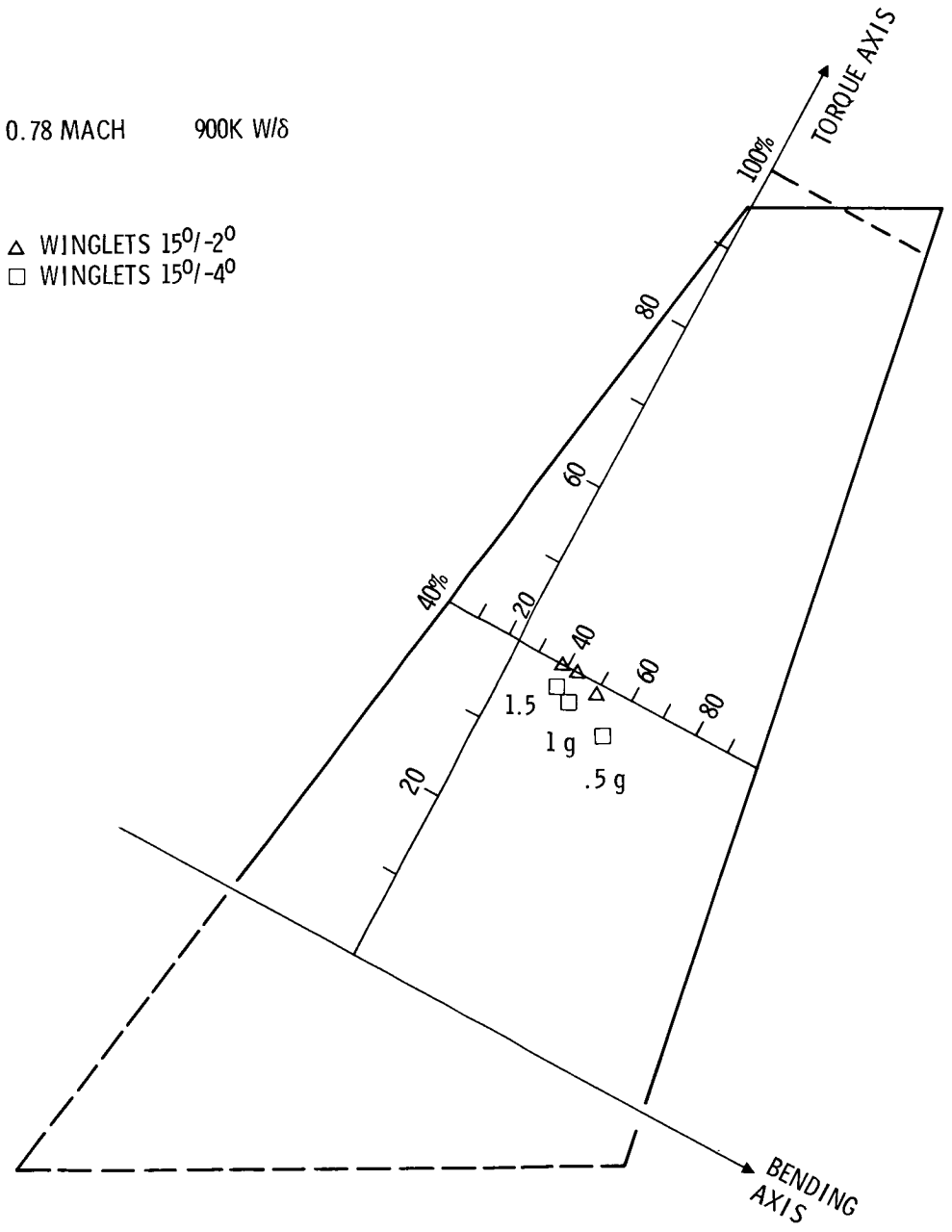

Figure 15. - Winglet center of pressure location

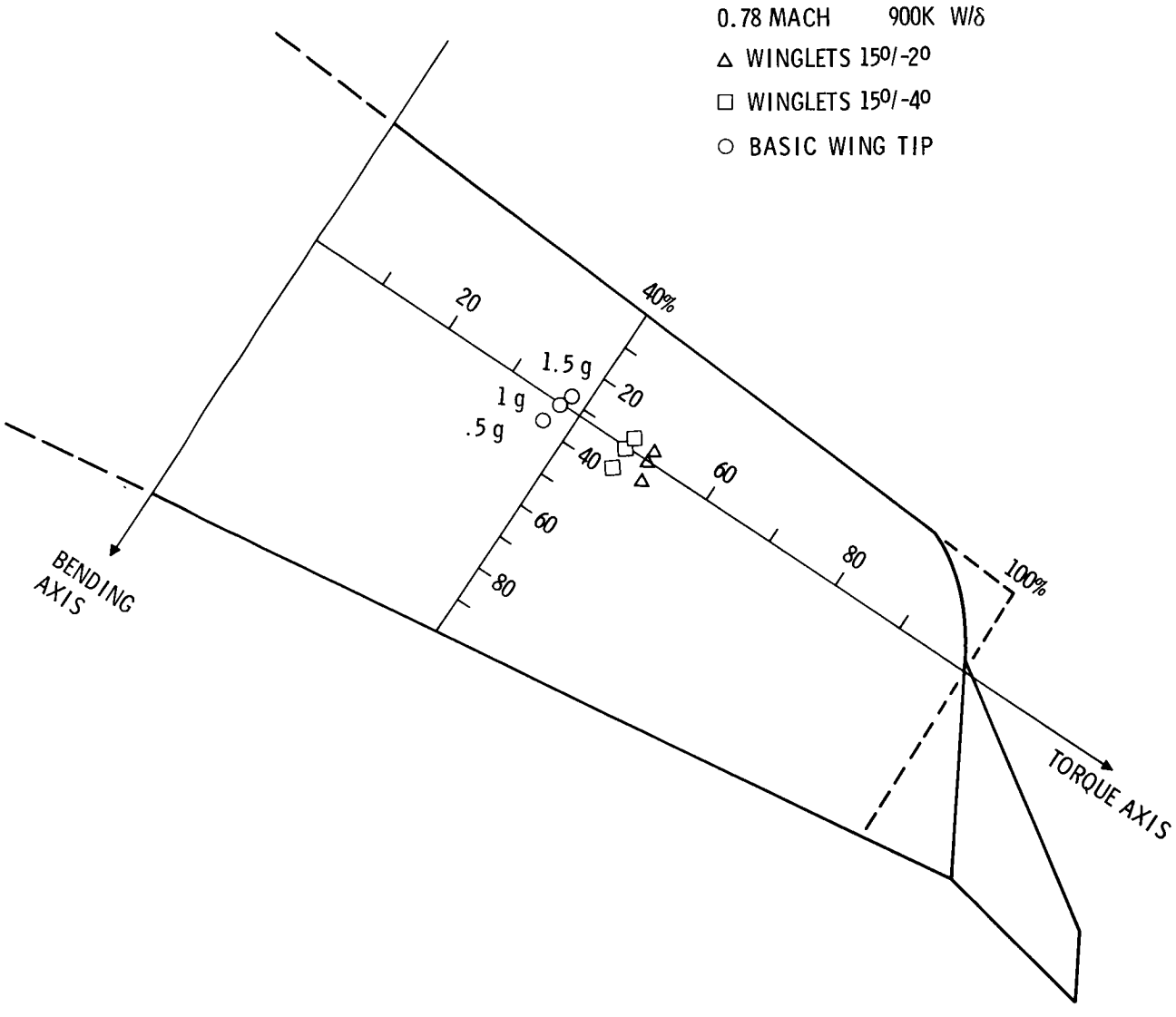

Figure 16. - Outboard wing center of pressure location

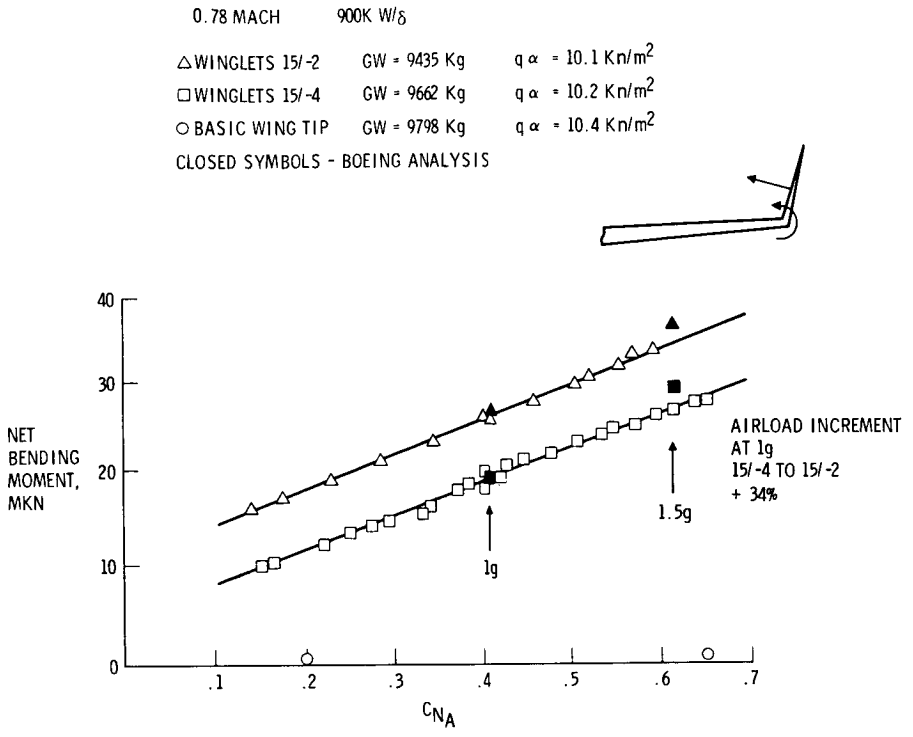

Figure 17. - Winglet intersection bending moment loads

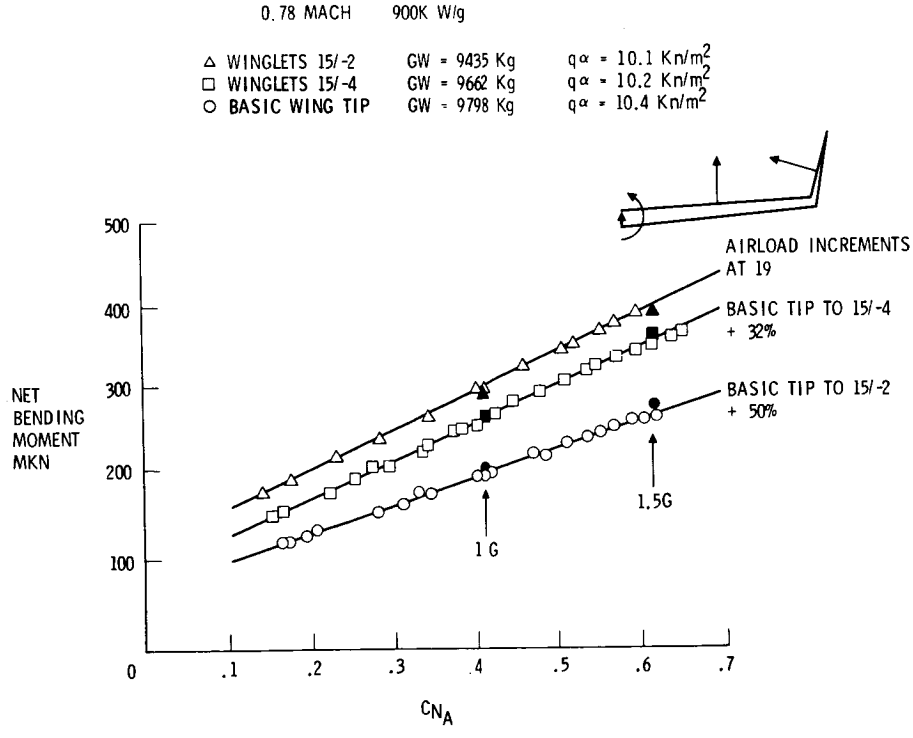

Figure 18. - Outboard wing bending moment loads

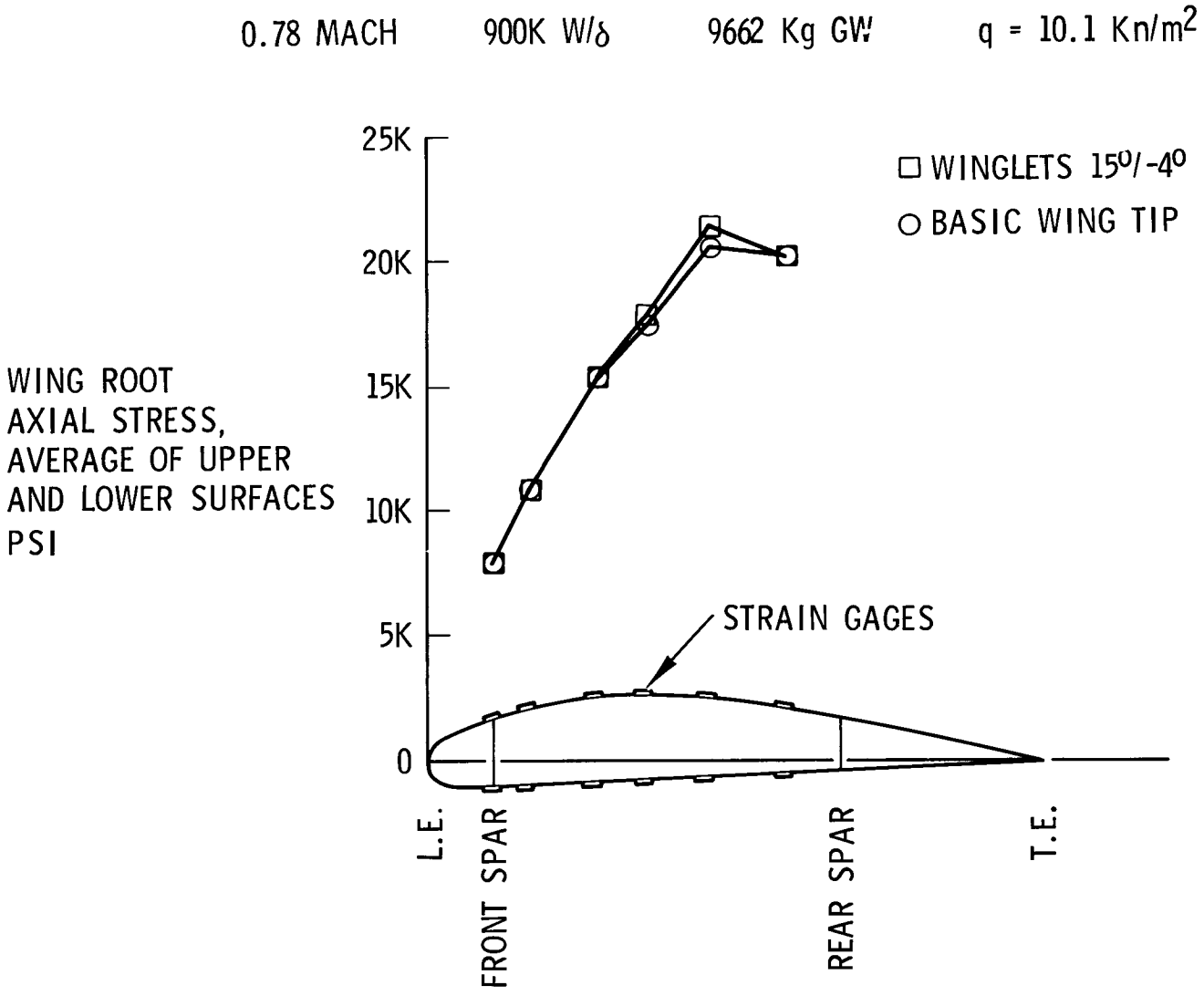

Figure 19. - Wing root bending stress distribution

IN-FLIGHT LIFT AND DRAG MEASUREMENTS ON A FIRST GENERATION JET TRANSPORT EQUIPPED WITH WINGLETS

David P. Lux
NASA Dryden Flight Research Center

SUMMARY

NASA in a joint project with the USAF flight tested a KC-135A aircraft equipped with wing tip winglets to demonstrate and validate the potential performance gain of the winglet concept as predicted from analytical and wind tunnel data. Flight data were obtained at cruise conditions for Mach numbers of 0.70, 0.75, and 0.80 at a nominal altitude of 36,000 ft. and winglet configurations of 15° cant/-4° incidence, 0° cant/-4° incidence, and baseline.

For the Mach numbers tested the data show that the addition of winglets did not affect the lifting characteristics of the wing. However, both winglet configurations showed a drag reduction over the baseline configuration, with the best winglet configuration being the 15° cant/-4° incidence configuration. This drag reduction due to winglets also increased with increasing lift coefficient.

It was also shown that a small difference (ΔC_D = 0.00045) exists between the 15° cant/-4° incidence flight and wind tunnel predicted data. This difference was attributed to the pillowing of the winglet skins in flight which would decrease the winglet performance.

INTRODUCTION

With the advent of the 1973 fuel crisis, the fuel efficiency of transport type aircraft has become of paramount importance to all operators of this type of aircraft, including the Federal Government. To improve the fuel efficiency of these aircraft, Dr. Richard T. Whitcomb developed wing tip mounted winglets which reduce the drag of the wing lifting system. Many analytical studies and wind tunnel tests have been conducted (references 1, 2, 3), to show the decreased drag of the wing/winglet system and it was determined that a flight evaluation of this concept was in order. Therefore, the USAF, in a joint project with NASA, contracted for the design and fabrication of winglets to be attached to a KC-135A aircraft as shown in figure 1.

The objective of the NASA/USAF flight project was to demonstrate the incremental performance gains, predicted from analytical and wind tunnel studies, by installing winglets on an aircraft without degrading aircraft stability. This was accomplished by making measurements to obtain lift, drag and pressure distributions on both right wing and winglet, and to obtain fuel mileage data.

This report presents the lift and drag data for a Mach number range of 0.70 to 0.80 for the cruise flight condition at one altitude (36,000 feet nominal). Angle of attack and lift coefficient were varied by varying weight (fuel burn). The aircraft center of gravity was maintained at 25% mean

aerodynamic chord. Flights were made with winglets off (baseline) and winglets on for several cant and incidence conditions. The data presented in this report are for the baseline, 0° cant/-4° incidence, and 15° cant/-4° incidence.

SYMBOLS

A_d	Area of Engine Inlet Duct, ft^2
A_e	Area of Engine Nozzle, ft^2
A_x	Longitudinal Acceleration, g
A_z	Normal Acceleration, g
$\bar{c}$	Mean Aerodynamic Chord
C_d	Drag Coefficient, $\frac{Drag}{qs}$
C_f	Nozzle Efficiency Coefficient
C_L	Lift Coefficient, $\frac{Lift}{qs}$
F_g	Gross Thrust, lbs
F_r	Ram Drag, lbs
M_∞	Freestream Mach Number
M_d	Inlet Duct Mach Number
P_t	Total Pressure, psi
P_s	Static Pressure, psi
P_∞	Free Stream Static Pressure, psi
q	Dynamic Pressure, $0.7M_\infty^2 P_\infty$, psf
s	Wing Reference Area, ft^2
w	Aircraft Gross Weight, lb
α_i	Indicated Angle of Attack, deg
α_t	True Angle of Attack, deg
δ	Ambient Pressure Ratio
γ	Ratio of Specific Heats

DESCRIPTION OF TEST AIRCRAFT

The test aircraft used for this study was a KC-135A aerial refueling tanker modified to allow the installation of wing tip mounted winglets. Also, an air data boom was added with provisions for measuring free stream impact pressure, static pressure, angle of attack, and angle of sideslip. Incorporated into the angle of attack and sideslip vanes were flight path accelerometers; however, these were not used in this study.

The configuration of the winglets, as tested in this study, is shown in figure 2. The winglets, as manufactured by the Boeing Military Aircraft Company (BMAC), were constructed to accommodate changing the angle of cant and incidence on the ground. This allowed flight testing to determine the optimum winglet configuration.

FLIGHT TEST INSTRUMENTATION

In order to obtain the necessary parameters to allow calculation of lift and drag, the KC-135 aircraft had to be instrumented to accurately obtain aircraft weight, thrust, angle of attack, freestream impact and static pressures, and normal and longitudinal accelerations.

Each of the four engines' inlet ducts was instrumented to measure total pressure (P_{t_2}) and static pressure (P_{s_2}) for determining inlet momentum and with total pressure probes after the turbine (P_{t_7}) to obtain gross thrust. As can be seen from figure 3, engine 1 and 2 used inlet rakes to obtain P_{t_2} while engines 3 and 4 used two P_{t_2} probes. All of the engine pressures were measured using differential pressure transducers located in the aircraft cabin. These transducers were all referenced to a single reference pressure taken from a P_{t_2} probe of engine 2. This reference pressure was measured by a very accurate absolute pressure transducer also located in the aircraft cabin.

Other instrumentation pertinent to the engines were fuel flow meters located in the fuel supply lines of all the engines to enable aircraft weight to be determined and instrumentation of the engine bleed doors. For all test points the engine bleed doors were closed.

As previously mentioned, an air data noseboom was installed on the flight test aircraft. The angle of attack that was used in this study was taken from the angle-of-attack vanes mounted on the noseboom. Freestream impact and static pressures were obtained from the noseboom pitot-static system. This system is described in detail in reference 4.

Normal and longitudinal accelerations were obtained from accelerometers mounted at the aircraft center of gravity. Alignment of this accelerometer package was checked periodically throughout the flight test program to ensure that the accelerometer mount plate was not shifting from flight to flight.

Other parameters that were measured which concern this study were ambient air temperature, engine rotor speeds, and all control surface deflections.

All data parameters were recorded through a pulse code modulation (PCM) system onto magnetic tape. In postflight processing the magnetic flight tape was formatted and processed to allow follow-on data programs to access the data and perform all pertinent calculations.

FLIGHT TEST PROCEDURE

Of all the tasks that were to be flown during the flight test, by far the most difficult task was to obtain good fuel mileage data. Since these data were of primary concern to the USAF, the requirements for this task dictated the manner in which the lift and drag task were to be performed. A discussion of how the data points were obtained and the manner in which the data was reduced follows.

Data were obtained at Mach numbers of 0.70, 0.75, 0.78, and 0.80 at three W/δ conditions for each winglet configuration. By varying W/δ it was possible to obtain a C_L range that was representative of the aircraft envelope. For each data point the aircraft was flown to the desired Mach number and altitude to obtain the proper W/δ. This condition would be held for a minimum of three minutes. An onboard flight test engineer would determine if the aircraft/airmass was stable enough during the data run for the run to be acceptable. If not, the data run would be repeated. It was found that in most cases where the data runs were deemed unacceptable for fuel mileage data, the data was most adequate for lift and drag data.

One of the critical aspects of the flight program was the stability of the airmass required for data acquisition. Many times this required that the mission be flown at extreme distances from Base precluding real time ground monitoring of flight parameters. As a result a real time onboard computation capability was provided to allow both monitoring of instrumentation and computation of aircraft weight.

Throughout any given flight, a crew member would monitor the fuel status of the aircraft. Fuel would be transferred either forward or aft to maintain the aircraft's center of gravity at 25% $\bar{c}$. The accuracy to which this could be maintained is about ±1%.

LIFT/DRAG DATA REDUCTION

The following are the equations for C_L and C_D used in this investigation:

$$C_L = \frac{1}{qs}\left[w(A_z \cos \alpha_t + A_x \sin \alpha_t) - F_g \sin \alpha_t\right]$$

and

$$C_D = \frac{1}{qs}\left[w(A_z \sin \alpha_t - A_x \cos \alpha_t) + F_g \cos \alpha_t - F_r\right]$$

These equations and their derivations can be found in reference 5. From these equations it can be seen that the important parameters are weight,

dynamic pressure, gross thrust and ram drag, longitudinal and normal accelerations, and true angle of attack. Each of these will be briefly discussed below.

Aircraft weight was determined by fueling and weighing the aircraft and crew prior to flight. From engine start to engine shutdown fuel flow meters on each engine supplied the information necessary to allow the integration of the fuel weight burned, which determined the weight of the aircraft at any given time. This calculation was checked after each flight by a postflight weighing of the aircraft.

Thrust and ram drag of the aircraft were determined from total and static pressures in the inlet duct and total pressures after the engine turbine. A very simple method of calculating thrust and ram drag was used for this investigation since the real interest was the incremental performance of winglets over a baseline configuration. For this investigation the following equations were used to determine gross thrust and ram drag per engine.

$$F_g = A_e C_f \left[\left(\frac{2}{\gamma+1} \right)^{\left(\frac{\gamma}{\gamma-1} \right)} (\gamma+1) \, P_{t_7} - P_\infty \right] = C_f A_e \left(1.259 P_{t_7} - P_\infty \right)$$

where γ is taken to be 1.33. C_f is the nozzle efficiency coefficient and is obtained from thrust stand runs. C_f for this investigation is shown in figure 4.

$$F_r = 1.4 \, A_d M_\infty M_d P_{s_2} \left(\frac{1 + 0.2 \, M_d^2}{1 + 0.2 \, M_\infty^2} \right)$$

where

$$M_d = 2.236 \left[\left(\frac{P_{s_2}}{P_{t_2}} \right)^{\frac{-2}{7}} - 1 \right]^{1/2}$$

For a more indepth discussion of this technique of determining F_g and F_r see reference 6.

Longitudinal and normal accelerations were obtained from the center of gravity accelerometer package. The accelerometer package consisted of a -1.0/+3g normal accelerometer, -1.0/+1.0g longitudinal accelerometer, and a ±0.25g sensitive longitudinal accelerometer. When longitudinal accelerations were small the sensitive longitudinal accelerometer was used in the lift, drag calculations. All accelerometers were filtered at 3 hertz.

True angle of attack proved the most difficult parameter to determine. The KC-135 is a large, flexible aircraft and the angle of attack as measured

from the noseboom vanes and the c.g. accelerometers changes with changing flight conditions. Since all data points during this study were to be taken at 1g cruise conditions it was felt that the best method of determining true angle of attack was to calibrate α in flight by relating true α to the longitudinal accelerometer by the expression

$$\alpha_t = \sin^{-1} A_x$$

Indicated angle of attack was plotted against α_t for each flight and a polynormal regression curve fit was made of this data (figure 5). This curve then became the calibration of angle of attack. It should be noted that this curve takes into account upwash effects, noseboom misalignment, and fuselage deflection effects. This is true only because the data was flown at cruise conditions, i.e. 1g stabilized flight.

RESULTS AND DISCUSSION

The effect of the addition of winglets on the KC-135 aircraft aerodynamic parameters can be seen in figure 6 as lift coefficient versus angle of attack and lift coefficient versus drag coefficient.

The addition of winglets had little or no effect upon the C_L vs α curve for either the 15/-4 or 0/-4 configuration. This was anticipated since the wind tunnel data of reference 1 also predicted little or no effect on C_{L_α} with the addition of winglets.

The addition of winglets, however, did affect the drag data as seen in figure 6. For every Mach number and lift coefficient tested, the addition of winglets to the aircraft reduced the total aircraft drag. Also the 15/-4 configuration is seen to be more effective at reducing the drag than the 0/-4 configuration for all Mach numbers and lift coefficients. This also was anticipated as a result of the wind tunnel tests which showed the 15/-4 configuration to be the optimum winglet configuration for the KC-135 aircraft.

Figure 7 shows the drag increment, ΔC_D, plotted versus lift coefficient for each of the test Mach numbers. These data were obtained by computing the difference in C_D at a given C_L between the baseline data fairing and the fairing of the 15/-4 and 0/-4 data. These data show that the C_D reduction due to winglets increases with increasing lift coefficient for both winglet configurations. Also, the 15/-4 configuration is increasingly more effective in reducing drag than is the 0/-4 configuration, as C_L is increased. The data also show that, for the most part, the effect of the winglets is independent of Mach number for the small range of Mach numbers tested. (M = 0.70 to 0.80.)

Also shown in figure 7 as the dashed line is the wind tunnel predicted decrease in drag due to winglets for the 15/-4 configuration at a Mach number of 0.78. These data were taken from Langley test 754 and do not incorporate corrections for Reynolds number and trim drag which were considered to be small. The wind tunnel data show a decrease of approximately 0.00045 C_D more than the flight data over the entire C_L range. There are several factors that could contribute to the miscomparison of the two sets of data, such as model

aeroelasticity, as compared to the flight vehicle, or angle of attack definition. However, the single most probable cause would be the existence of winglet skin pillowing as shown in figure 8. This pillowing, caused by a structural deficiency of the skin, would increase the drag of the winglet and not allow it to perform as predicted in the wind tunnel data. Further discussion of the effect of the winglet skin pillowing on the winglet performance can be found in reference 7.

CONCLUDING REMARKS

NASA in a joint project with the USAF flight tested a KC-135A aircraft equipped with wing tip winglets to demonstrate and validate the potential performance gain of the winglet concept as predicted from analytical and wind tunnel data. Flight data were obtained at cruise conditions for Mach numbers of 0.70, 0.75, 0.78, and 0.80 at a nominal altitude of 36,000 ft and winglet configurations of 15/-4, 0/-4 and baseline. The data show the following:

- No change was observed in the lift curve slope between the baseline (winglets off) configuration and winglets on configuration at any Mach number tested.
- Both the 15/-4 and 0/-4 winglet configuration reduced the airplane drag as compared with the baseline configuration for all Mach numbers and lift coefficients tested. The 15/-4 configuration had the highest drag reduction.
- The drag reduction due to winglets increased with increasing C_L and appeared to be independent of Mach number for the Mach number range tested.

Also observed was that the 15/-4 flight data and wind tunnel predicted C_D reduction disagreed by a small amount ($\Delta C_D = 0.00045$). This difference was attributed to pillowing of the winglet skins in flight which would decrease winglet performance.

REFERENCES

1. Jacobs, Peter F.; Flechner, Stuart G.: Effect of Winglets on a First-Generation Jet Transport Wing, I-Longitudinal Aerodynamic Characteristics of a Semispan Model at Subsonic Speeds. NASA TN D-8473, 1977.
2. Whitcomb, Richard T.: A Design Approach and Selected Wind-Tunnel Results at High Subsonic Speeds for Wing-Tip Mounted Winglets. NASA TN D-8260, 1976.
3. Flechner, Stuart G.; Jacobs, Peter F.; and Whitcomb, Richard T.: A High Subsonic Speed Wind-Tunnel Investigation of Winglets on a Representative Second-Generation Jet Transport Wing. NASA TN D-8264, 1976.
4. Sakamoto, Glenn M.: Aerodynamic Characteristics of a Vane Flow Angularity Sensor System Capable of Measuring Flightpath Accelerations for the Mach Number Range from 0.40 to 2.54. NASA TN D-8242, 1976.

5. Arnaiz, Henry H.: Flight-Measured Lift and Drag Characteristics of a Large, Flexible, High Supersonic Cruise Airplane. NASA TM X-3532, 1977.

6. Beeler, De B.; Bellman, Donald R.; and Saltzman, Edwin J.: Flight Techniques for Determining Airplane Drag at High Mach Numbers. NACA TN 3821, 1956.

7. Dodson, Robert O.: Comparison of Flight Measured, Predicted and Wind Tunnel Measured Winglet Characteristics on a KC-135 Aircraft.

Figure 1. - KC-135A aircraft modified with winglets

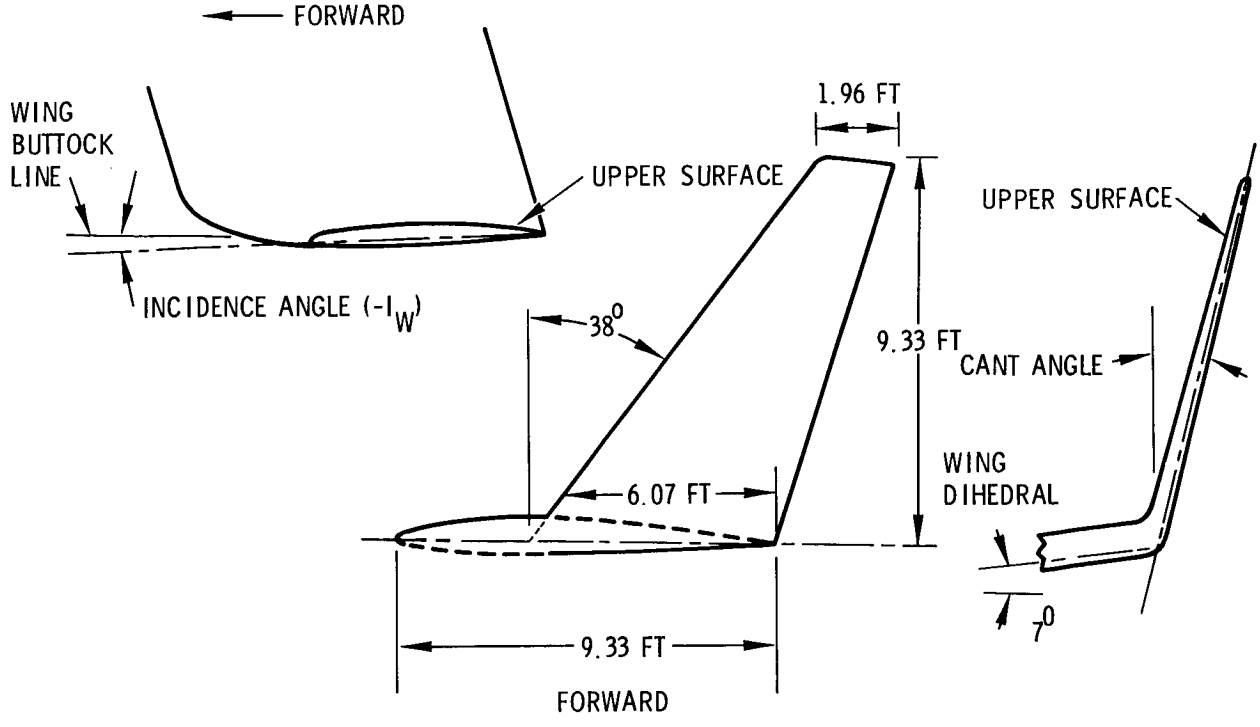

Figure 2. - Definition of winglet cant and incidence angles

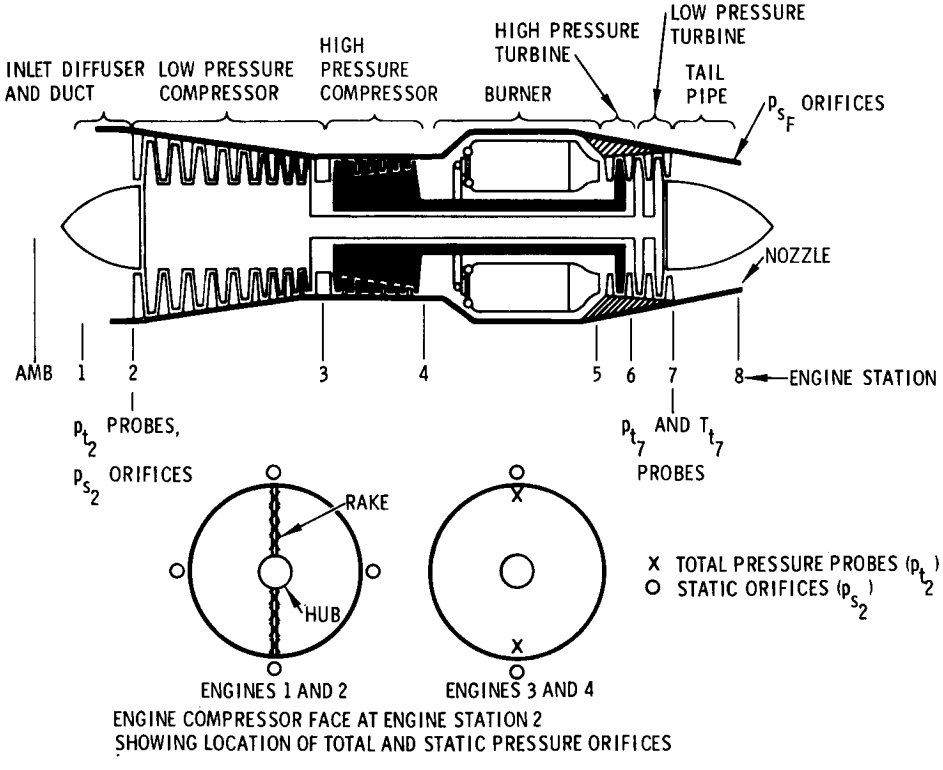

Figure 3. - J57-P-43W turbofan engine with station designations and measured parameter locations

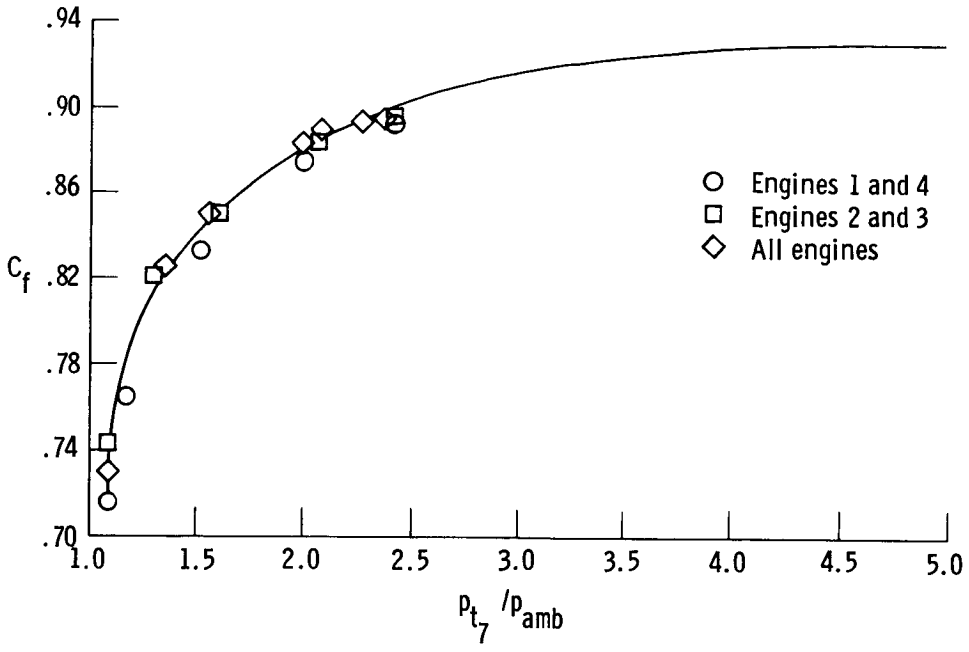

Figure 4. - Nozzle coefficient determined by ground thrust calibration

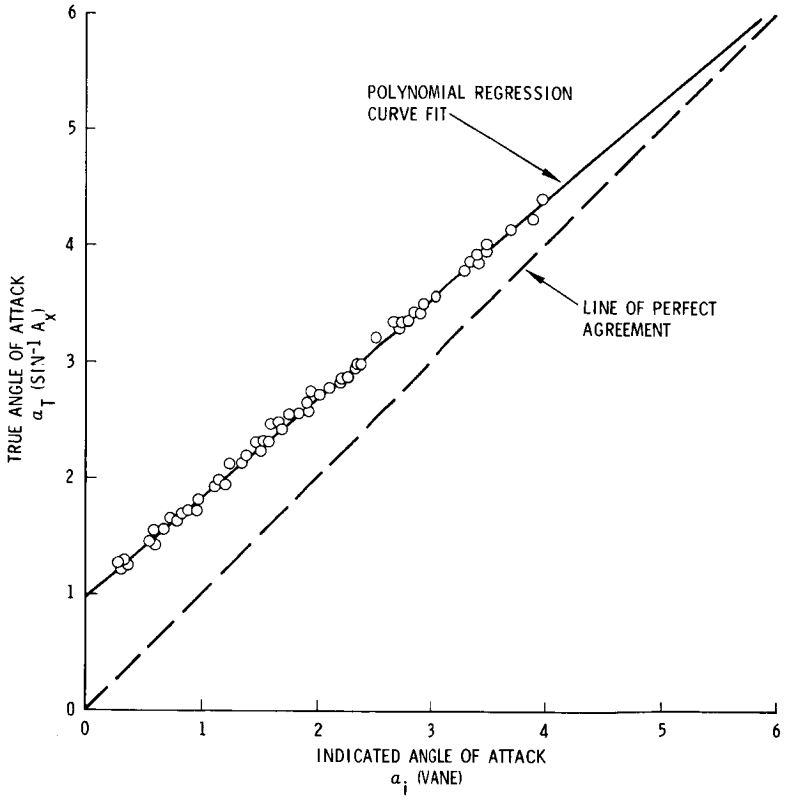

Figure 5. - Angle of attack calibration

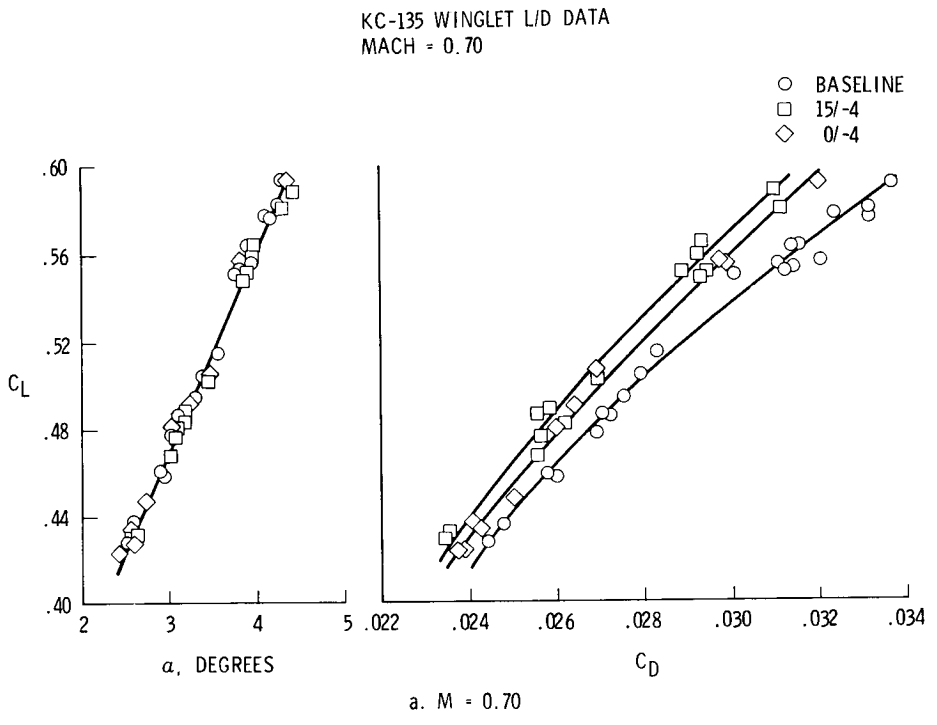

a. M = 0.70

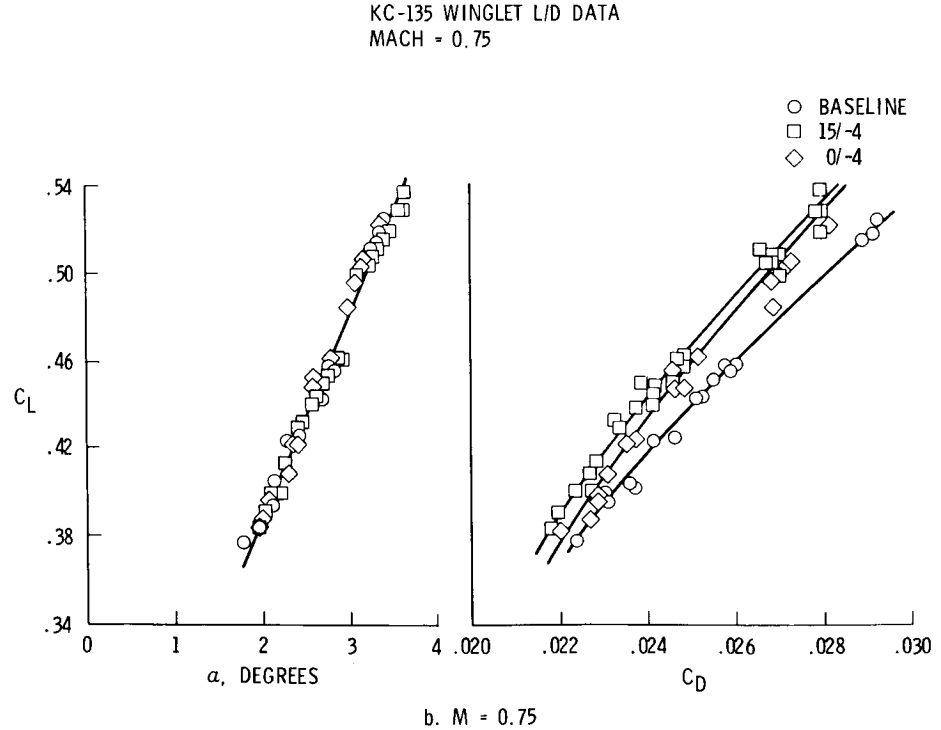

b. M = 0.75

Figure 6. - C_L vs. α and C_L vs. C_D for baseline, 15/-4, and 0/-4 configurations for KC-135 airplane

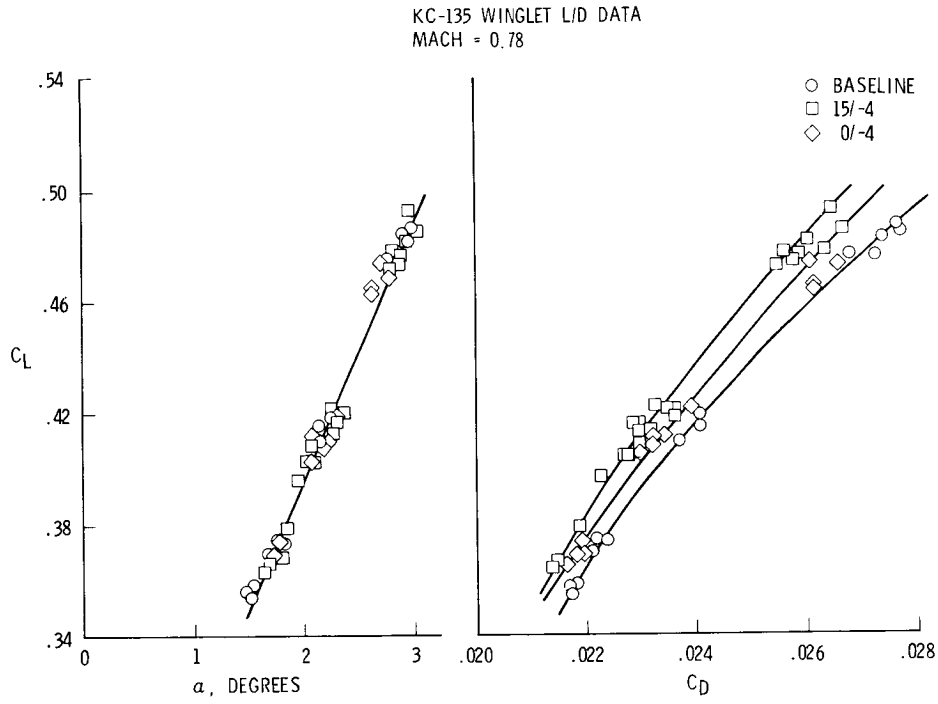

c. M = 0.78

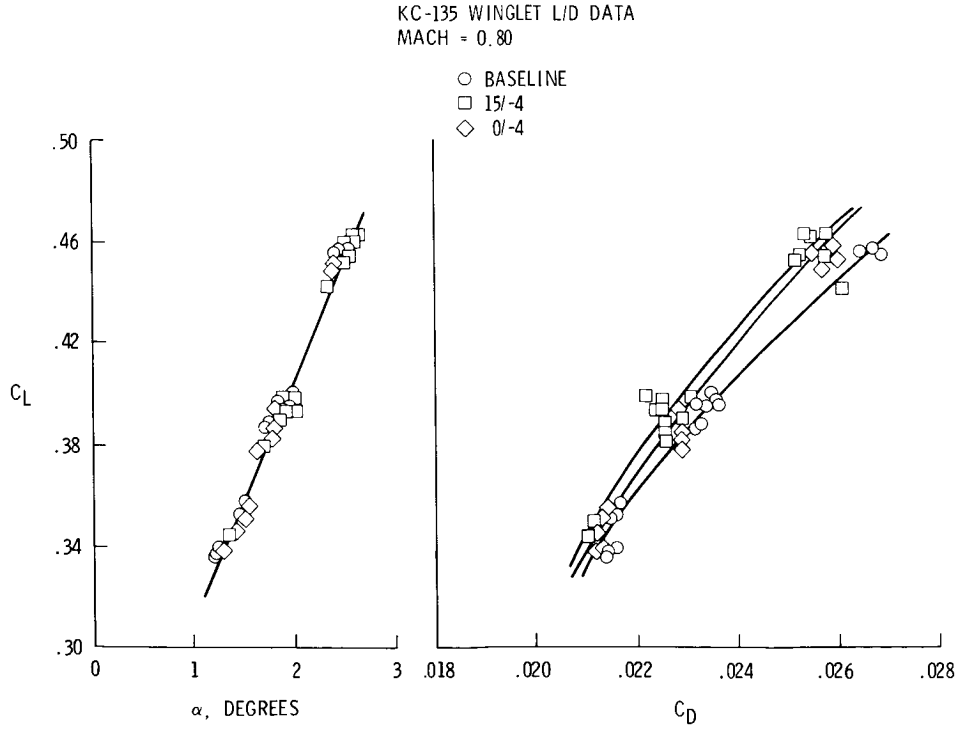

Figure 6. - concluded

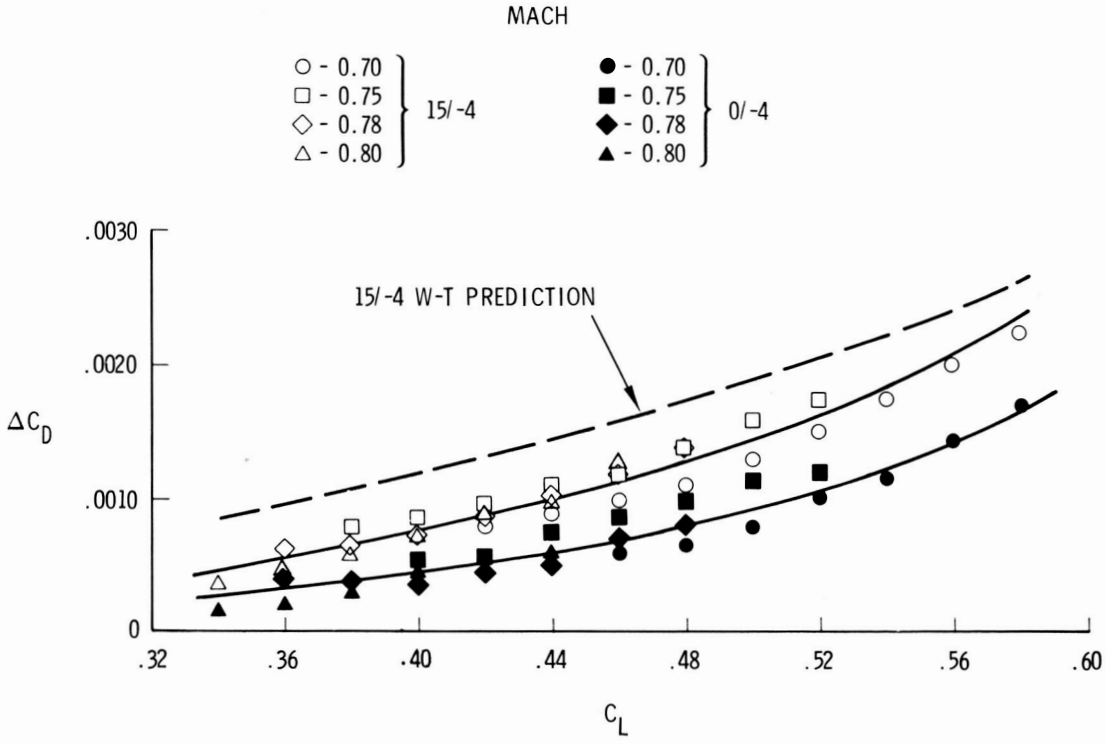

Figure 7. - Summary of drag results

Figure 8. - Winglet in flight with skin "pillowing"

MEASUREMENTS OF THE FUEL MILEAGE OF A KC-135 AIRCRAFT WITH AND WITHOUT WINGLETS

Gary E. Temanson
Boeing Military Airplane Company

SUMMARY

The KC-135A Winglet Flight Research and Demonstration Program was a joint effort of the Air Force, NASA and the Boeing Military Airplane Company to flight test winglets on the KC-135A. The primary objective of the program was to verify the cruise performance improvements predicted by analysis and wind tunnel tests. Flight test data were obtained for winglets positioned at 15° cant/-2° incidence, 0° cant/-4° incidence, 15° cant/-4° incidence and for winglets off (baseline). Both fuel mileage and drag measurements were obtained.

The 15° cant/-4° incidence winglet configuration provided the greatest performance improvement. The flight test measured fuel mileage improvement for a 0.78 Mach number was 3.1 percent at 8×10^5 pounds W/δ and 5.5 percent at 1.05×10^6 pounds W/δ. Correcting the flight measured data for surface pressure differences between wind tunnel and flight resulted in a fuel mileage improvement of 4.4 percent at 8×10^5 pounds W/δ and 7.2 percent at 1.05×10^6 pounds W/δ. The agreement between the fuel mileage and drag data was excellent.

INTRODUCTION

Analytical and experimental investigation indicated that a significant drag reduction could be realized on large transport aircraft through the incorporation of winglets. Winglets were projected to reduce the KC-135's cruise drag between 6 and 8 percent, which translates into a significant fuel savings for the KC-135 fleet. As a result the KC-135 Winglet Flight Research and Demonstration Program was developed to design, fabricate and flight test a set of winglets to verify the cruise performance improvement predicted by analysis and by wind tunnel tests (references 1 through 6). Three specific areas of performance were investigated:

- Fuel mileage performance obtained from fuel flow and airspeed measurements.
- Drag determined from engine thrust measurements.
- Pressure distributions on the wing and winglet.

This paper discusses the cruise performance testing and results obtained from the first two areas of investigation. The pressure distributions are discussed in reference 7. A detailed analysis of the final results of the overall program is presented in reference 8.

SYMBOLS

A_D	Inlet Duct Area
A_j	Jet Nozzle Area
Alt	Altitude
A_X	Longitudinal Acceleration in g's
A_Z	Normal Acceleration in g's
C_D	Drag Coefficient
C_L	Lift Coefficient
C_f	Jet Nozzle Coefficient
CF	Correction Factor
D	Drag
F_g	Gross Thrust
FM	Fuel Mileage
F_R	Ram Drag
H_e	Energy Altitude
H_p	Pressure Altitude
INS	Inertial Navigation System
KCAS	Knots Calibrated Airspeed
K_1	Constant
K_2	Constant
L	Lift
LHV	Lower Heating Value
M	Mach Number
M_D	Duct Mach Number
NAM	Nautical Air Miles
P_{Amb}	Ambient Pressure at Tailpipe Exit

P_{S_2}	Static Pressure at the Compressor Face
P_{t_7}	Total Pressure at Tailpipe Exit
q	Dynamic Pressure
S	Wing Area
SFC	Specific Fuel Consumption
t	Time
TSFC	Thrust Specific Fuel Consumption
V_g	Ground Speed
V_T	True Airspeed
W	Gross Weight
$\dot{W}_f$	Fuel Flow
α	Angle of Attack
δ	Ambient Pressure Ratio
Δ	Increment
θ	Ambient Temperature Ratio

FLIGHT TEST PROGRAM OVERVIEW

The test airplane was a KC-135 S/N 55-3129, on loan to NASA Dryden Flight Research Center from the 4950th Air Force Test Wing (figure 1). The external aerodynamic configuration of the basic airplane was that of a standard KC-135A, except that the refueling boom had been removed and an airspeed nose boom with angle of attack and angle of sideslip vanes had been installed. Since the goal of the testing was to determine the incremental benefit of winglets, the data reduction methods did not attempt to correct the data to a standard airplane configuration.

The flight test winglets were designed to provide for variation of winglet cant and incidence as well as for removal of the winglet to obtain baseline data. Figure 2 presents the general winglet geometry.

The performance testing was conducted at Edwards Air Force Base, Edwards, California. The testing occurred in two time segments beginning in August 1979 and July 1980, respectively.

The first series of tests were flown in the proximity of the Edwards Air Force Base complex in order that the test data could be telemetered to NASA's ground station for real time monitoring. Data were obtained for three configurations:

- Winglets on, 15° cant/-2° incidence
- Winglets on, 15° cant/-4° incidence
- Winglets off, baseline

Several attempts were made to obtain data with the winglets set at 0° cant/-4° incidence. However, the persistent fuel leaks and the discovery of the cracked wing spar chord aborted these attempts during the preliminary testing.

Data scatter and instrumentation problems were prevalent during the preliminary testing. The scatter in the fuel mileage data masked the performance increment. A review of the fuel flow data used in determining fuel mileage indicated that scanivalve operation created electrical noise and bias in the fuel flow instrumentation which resulted in erroneous fuel flow indications. Isolating the fuel flow instrumentation on separate power supplies eliminated the scanivalve interference. The fuel flow instrumentation was also modified to provide better ranging over the cruise fuel flows. During airplane downtime between the two time segments it was decided that the criteria for determining stabilized flight should be clearly specified and more strictly adhered to when flying resumed. The following criteria were decided on:

Parameter	Maximum Allowable Change During Three-Minute Run
Altitude	±80 ft
Ambient Air Temperature	±0.5°C
Mach Number (Airspeed)	±0.004 (±1.5 KCAS)
True Airspeed	±2 kts
$W/_{\delta}$	±5,000 lb from Nominal

Testing was accomplished for three nominal $W/_{\delta}$'s (8×10^5, 9×10^5 and 1.05×10^6 lb) throughout the range of Mach numbers from 0.70 to 0.82. Data were obtained during three minute stabilized runs at altitudes between 34,000 and 40,000 ft.

In order to find and test in stable air masses, the airplane was equipped with an onboard real time data monitoring computer. This eliminated the need for the ground station real time monitoring and allowed the airplane to leave the Edwards Air Force Base area in search of smooth stable air. The final testing was flown over the ocean, off the coast of southern California.

An inertial navigation system (INS) was installed on the airplane during the final tests and was operational from flight 31-42 to the completion of testing. The INS facilitated navigation and also furnished information on ground speed through a digital cockpit display.

Final performance data were acquired for the following configurations:

- Winglets on, 0° cant/-4° incidence
- Winglets on, 15° cant/-4° incidence
- Baseline

Table 1 lists the successful data flights and the type of performance data obtained for each flight test segment.

RESULTS AND DISCUSSION

Fuel Mileage

The basic parameters required to determine the cruise performance of an airplane at a given Mach number and gross weight are true airspeed (V_T), fuel flow ($\dot{W}_f$) and ambient pressure ratio (δ). Normalized fuel mileage (FM) is obtained by combining these parameters in the following equation:

$$FM_{Test} = \frac{V_T \times \delta \times 1000}{\dot{W}_f}$$

The FM test value for a given condition was based on the average value of these parameters over the stabilized condition time. Each parameter was sampled every second over a nominal three minute time period.

The test fuel mileage was then corrected to standard conditions so that a valid comparison could be made among configurations. Differences in drag (off W/δ and changing energy state), fuel lower heating values and altitudes were normalized by means of correction factors applied to the test FM:

$$FM_{Corr} = FM_{Test} \times CF_{Drag} \times CF_{LHV} \times CF_{Alt}$$

The drag correction factor had two components: off, W/δ and changing energy state.

The off W/δ correction occurs when the data are not obtained at exactly the targeted W/δ. This results in the airplane operating at a different C_L than desired and thus a different C_D as illustrated in figure 3. The increment of drag associated with returning to the nominal W/δ is:

$$\left(\frac{\Delta Drag}{\delta}\right)_{W/\delta} = 1481.4 \; S \; M^2 \left(\Delta C_D\right)_{W/\delta}$$

The basic KC-135A drag polars (reference 9) were used to determine the W/δ correction for all test configurations.

The changing energy state correction occurs when the airplane is in accelerated, climbing or descending flight during the test condition. At any given point in time the airplane's energy state is described by its energy altitude (H_e) which is the sum of the airplane's geopotential altitude and its speed

converted to an equivalent geopotential altitude. An increase in H_e over the condition time indicates that the airplane is accelerating and that the engines are producing more thrust than is required to balance the drag force. A decrease in H_e indicates less thrust is being produced than that required to balance drag. Since level unaccelerated flight performance where thrust equals drag is desired, a correction for any energy state change must be applied. The time rate of change of H_e is related to drag by the following equation:

$$\left(\frac{\Delta Drag}{\delta}\right)_{H_e} = -0.592484 \times W/_{\delta} \times \frac{1}{V_T} \times \frac{dH_e}{dt}$$

When determining H_e, the reference for the airplane speed and for the geopotential altitude should be the earth. Therefore, airplane ground speed (V_g) is the relevant speed. However, ground speed measurements were not available until late in the program (Flight No. 31-42 and on) when an inertial navigation system was installed in the airplane. In a stable air mass with no wind or horizontal temperature gradients, changes in true airspeed are the same as changes in ground speed. Therefore, true airspeed was used in determining H_e.

On those flights where the INS was installed, an energy correction was also determined using the hand-recorded ground speed from the digital cockpit display. The energy correction was determined based on the following relationship.

$$\left(\frac{\Delta Drag}{\delta}\right)_{INS} = -0.052459 \times W/_{\delta} \times \frac{dV_g}{dt}$$

The altitude change during a test run was minimized by the use of the altitude hold function on the autopilot. The altitude excursions experienced during the testing were negligible, and no corrections were applied in the calculation of the INS drag correction.

The relationship between the airplane drag at the nominal $W/_{\delta}$ in level unaccelerated flight and the drag of the airplane under the test conditions is given by the following equation:

$$\left(\frac{Drag}{\delta}\right)_{Nominal} = \left(\frac{Drag}{\delta}\right)_{Test} + \left(\frac{\Delta Drag}{\delta}\right)_{W/_{\delta}} + \left(\frac{\Delta Drag}{\delta}\right)_{\substack{Energy \\ Changes}}$$

where

$$\left(\frac{\Delta Drag}{\delta}\right)_{\substack{Energy \\ Changes}} = \left(\frac{\Delta Drag}{\delta}\right)_{INS} \text{ or } \left(\frac{\Delta Drag}{\delta}\right)_{H_e}$$

Differences between drag for the nominal and test conditions result in different thrust requirements which may cause a change in the specific fuel consumption ($TSFC/\sqrt{\theta}$). The drag correction factors applied to the test fuel mileage accounts for both the difference in thrust levels and specific fuel consumption in the following manner:

$$CF_{Drag} = \frac{\left(\frac{Drag}{\delta}\right)_{Test}}{\left(\frac{Drag}{\delta}\right)_{Nominal}} \times \frac{\left(\frac{TSFC}{\sqrt{\theta}}\right)_{Test}}{\left(\frac{TSFC}{\sqrt{\theta}}\right)_{Nominal}}$$

The variation of specific fuel consumption with thrust was obtained from the basic engine data contained in reference 10.

The energy content of JP-4 fuel, as measured by the lower heating value, can vary from flight to flight because of differences in such items as sources, shipments, contaminates and seasonal additives. Therefore, a fuel sample was obtained from the airplane fuel tanks before each flight. The samples were analyzed to determine the lower heating value. The test fuel mileage data were then corrected to a standard fuel energy level of 18,400 BTU/lb by applying the following correction factor:

$$CF_{LHV} = \frac{18,400}{LHV_{Test}}$$

Cruise performance testing was conducted between 34,000 ft and 40,000 ft pressure altitude. The specific fuel consumption for a given F_n/δ varies with altitude in this altitude test range. For comparison purposes the cruise data were corrected to a standard altitude of 36,000 ft by applying the following correction factor:

$$CF_{Alt} = \frac{\left(\frac{TSFC}{\sqrt{\theta}}\right)_{Test\ Altitude}}{\left(\frac{TSFC}{\sqrt{\theta}}\right)_{36,000\ ft}}$$

The specific fuel consumption variation with altitude was obtained from the KC-135A engine data presented in reference 10.

The corrected fuel mileage was obtained by applying the three preceding correction factors to the fuel mileage measured under the test conditions:

$$FM_{Corr} = FM_{Test} \times CF_{Drag} \times CF_{LHV} \times CF_{Alt}$$

Normalized fuel mileage obtained using the airspeed/altitude method for the baseline configuration, the winglets on 15° cant/-4° incidence configuration and the winglets on 0° cant/-4° incidence configuration, are presented in figures 4, 5 and 6, respectively. These data were all obtained during the second segment of the flight test program. The cruise mileage data obtained during the preliminary testing were discarded because of extreme data scatter caused by instrumentation problems and relaxed stability criteria as previously discussed.

Figure 7 compares the faired cruise mileage performance associated with each winglet configuration. This improvement is a function of W/δ and Mach number. Figure 8 compares the percentage improvement of both winglet configurations at 0.78 Mach number. As predicted, the 15° cant/-4° incidence winglet configuration resulted in the better performance gain.

The baseline and 0°/-4° winglet data exhibit good repeatability between flights and minimal data scatter. However, the 15°/-4° winglet data exhibits almost twice the scatter, particularly at 9×10^5 lb W/δ. All of these data were corrected using the airspeed/altitude energy methods discussed previously. A comparison of these energy corrections to the INS energy corrections for the same test run revealed numerous discrepancies. These discrepancies are indicative of an unstable air mass which would invalidate the assumption made in the airspeed/altitude energy method, that changes in ground speed are reflected in changes in the true airspeed. The INS energy corrected data for the baseline and 15°/-4° winglets on configurations are shown in figures 9 and 10, respectively. The scatter in the winglets on data was greatly reduced while the scatter in the baseline data was not significantly affected. Since the INS provides a more accurate measure of the energy of the airplane, these data were used in determining the 15°/-4° winglets on performance increments.

The percentage improvement in cruise mileage attributable to the flight test 15°/-4° winglet configuration is presented as a function of W/δ and Mach number in figure 11.

Drag

NASA-Dryden was responsible for the drag measurements. The NASA basic approach is presented in reference 11 and is only outlined in this report for the convenience of the reader. The lift and drag measurements dealt with two primary areas:

- The thrust developed by the engines.
- The acceleration experienced by the airplane.

Gross thrust was determined from engine pressures measured during the test condition, using the following relationship:

$$F_g = C_f A_j (1.259 P_{t_7} - P_{Amb})$$

Ram drag was subtracted from the gross thrust to arrive at the net thrust used in the drag calculation. The gross thrust was resolved into the flight path to be consistent with the drag direction. The relationship for ram drag is:

$$F_R = 1.4\ A_D\ MM_D\ P_{S2} \sqrt{\frac{1 + 0.2\ M_D^2}{1 + 0.2\ M^2}}$$

An accelerometer package was located at approximately the airplane center of gravity to measure longitudinal and normal accelerations along the body axis. These accelerations were resolved into the flight path axis system by rotation through the angle of attack. The lift and drag were determined from these measurements as follows:

$$C_L = \frac{1}{qS} = \frac{1}{qS} \left[W\ (A_Z\ \cos\alpha + A_X\ \sin\alpha) - F_g\ \sin\alpha\right]$$

$$C_D = \frac{D}{qS} = \frac{1}{qS} \left[W\ (A_Z\ \sin\alpha - A_X\ \cos\alpha) + F_g\ \cos\alpha - F_R\right]$$

The drag data were then corrected to the nominal $W/_\delta$ as follows:

$$C_{D_{Corr}} = C_{D_{Test}} + \left(\Delta C_D\right)_{W/_\delta}$$

This is the same drag correction discussed previously in the Fuel Mileage section which results from the test C_L being different than the desired C_L at the test Mach number. The corrected drag is presented as a function of Mach number in figures 12, 13, 14 and 15 for the baseline, 15° cant/-4° incidence, 15°/-2° incidence and 0° cant/-4° incidence configurations, respectively.

Both preliminary (solid triangles) and final (open symbols) drag data are presented in figures 12 and 13 for the baseline and 15°/-4° configurations. The preliminary data tends to exhibit higher drag levels as well as a slight counterclockwise rotation of the drag polar. Contributing factors to these differences include the limited amount of preliminary data, differing stability criteria and varying angle of attack calibrations.

The quantity of data obtained for each configuration was very limited during the preliminary tests. Only five data points per $W/_\delta$ were obtained and only one flight each was flown for the baseline and 15°/-4° configurations.

Due to excessive scatter in the preliminary fuel mileage data, the criteria for determining when the airplane was stabilized were tightened as previously noted. This minimized the size of corrections applied to the final data.

Although C_L is not sensitive to small angle of attack changes, C_D is highly sensitive to such changes. This requires that the angle of attack instrumentation provide a repeatable nonshifting calibration with a high degree of

resolution. Variations as small as 0.03 degree are significant since they result in approximately a 1 percent change in airplane drag in the cruise range. NASA's method of calibrating the angle of attack vane consisted of applying the steady state relationship:

$$\alpha_{cal} = \sin^{-1} A_X = K_1 \alpha_I + K_2$$

A random scattering of energy corrections (accelerations/decelerations) were assumed during the preliminary flight tests to determine K_1 and K_2. Therefore, all of the data points were utilized in defining the linear relationship between indicated angle of attack (α_I) and α_{cal}. During the final flight tests the data were screened to eliminate all points having accelerations or decelerations resulting in over a 1 percent change in airplane drag. A linear calibration was determined for each airplane configuration. Variations in calibrated angle of attack and indicated angle of attack of 0.10 degree between configurations were common as shown in figure 16. Similar variations were noted when the data were compared from flight to flight for the same configuration. Analytical studies of the influence of winglets on the flow upwash at the angle of attack vane indicated a negligible effect. No instrumentation changes were made to the angle of attack measurement system between flights. Therefore, no change was expected in the α calibration. Apparently these variations are the result of limitations in instrumentation accuracies. As a result, the data from all of the final data flights were combined to arrive at a single calibration which was used to reduce the final drag data.

No reason for the shift in the α calibration between the preliminary and final testing was found. Since C_D is so sensitive to changes in α, the preliminary data were corrected using the final α calibration to eliminate any bias. These data were also shown in figures 12, 13 and 14, (solid circles). A 2 to 3 percent drag reduction results from the α calibration change. The preliminary data now tends to exhibit lower drag levels than the final data. The sensitivity of C_D to α changes is obvious.

Because of the uncertainties associated with the changing stability criteria and the varying α calibration, as well as the limited data, the preliminary data were not utilized in the final data analysis.

Fuel mileage improvements were determined using the drag data and engine specific fuel consumption data for each winglet configuration at 0.78 Mach number. Figure 17 compares this improvement to the measured fuel mileage benefit. The airspeed/altitude energy corrected fuel mileage data was used for both winglet configurations in this comparison since INS corrected data was not available for the 0° cant/-4° incidence data. The drag and fuel mileage data exhibited excellent agreement for the 15° cant/-4° incidence winglet configuration. The drag based benefit for the 0° cant/-4° incidence configuration showed a greater benefit than was measured by fuel mileage data. The agreement was good at 1.05×10^6 lb $W/_{\delta}$ but varied by 1.3 percent at 8×10^5 lb $W/_{\delta}$.

Figure 18 compares the 15° cant/-4° incidence data to the INS corrected fuel mileage data. Again the agreement is excellent.

The INS offers an alternative data correction method to the accelerometers. The INS correction is not dependent on α, which eliminates the α sensitivity problem. Using the INS, the drag equation becomes:

$$C_D = \frac{1}{qS}\left[F_g \cos\alpha - F_R + \left(\frac{\Delta Drag}{\delta}\right)_{INS} \times \delta\right]$$

The $(\Delta Drag/_\delta)_{INS}$ was obtained from the INS ground speed changes recorded during the test run as discussed in the Fuel Mileage section. INS data are available for only four of the five baseline flights and the 15° cant/-4° incidence configuration flights. The INS corrected drag is presented in figures 19 and 20.

Fuel mileage improvements were calculated based on the drag improvements obtained from the INS corrected data and SFC improvements obtained from reference 10. A comparison of this drag improvement to the directly measured fuel mileage improvement is presented in figure 21. The drag based improvement is 0.1 percent to 0.5 percent higher than that shown by the measured fuel mileage data. This is considered excellent agreement.

Flight Test - Wind Tunnel Data Comparison

The drag improvement determined from the flight tests was compared to wind tunnel data obtained by NASA at their Langley facilities. The flight test demonstrated benefit for winglets at 15° cant/-4° incidence was not as great as the wind tunnel data indicated. Figure 22 presents the comparison for a Mach number of 0.78 over the range of test $W/_\delta$'s. The excellent agreement between the drag and fuel mileage test data gave confidence to the accuracy of flight test data. As a result, a careful comparison of wind tunnel and flight test pressure data was made to ensure that the winglets were developing comparable loadings in flight. Differences in winglet loading were discovered as shown in figure 23. A detailed analysis of these differences is presented in reference 7.

The winglet pressure data were affected by the "pillowing" of the winglet skin between the ribs which caused some distortions in the airfoil contour. There was also a leading edge pressure loss on the lower inboard portion of the winglet at test Mach numbers between 0.70 and 0.82 during flight testing that was not observed during wind tunnel testing. The pressure loss only occurred when the local flow in this area became supersonic. Two-dimensional transonic flow analyses were used to verify that the leading edge pressure loss was not caused by the "pillowing" of the winglet's skin. The difference is attributed to the five percent chord trip strip used on the wind tunnel model. Integration of the pressure drag differences on the winglet between wind tunnel and flight test resulted in a significant drag difference (approximately 1.5 to 2.0%) as shown in figure 24. Note that the drag data are shown plotted against the section normal force at the outboard wing station instead of the usual total airplane lift coefficient. This was done to compensate for any differences in aeroelastic twist at the wing tip between the wind-tunnel model and the flight test airplane. The relationship between airplane lift coefficient and wing tip normal force coefficient for the flight test airplane is shown

figure 25. Accounting for this difference resulted in the final flight test fuel mileage improvements shown in figure 26. The corrected flight test fuel mileage improvement is in good agreement with fuel mileage estimates obtained from the wind tunnel test data as shown in figure 27.

CONCLUSIONS

The results of the cruise performance testing reveal a significant improvement in fuel mileage associated with the installation of winglets on the KC-135A. The 15° cant/-4 incidence winglet provided the greatest performance improvement of the three test configurations. For a 0.78 Mach number the benefit was approximately 4.4% at 8 x 10^5 lb W/δ and 7.2% at 1.05 x 10^6 lb W/δ.

REFERENCES

1. Whitcomb, R. T., "A Design Approach and Selected Wind-Tunnel Results at High Subsonic Speeds for Wing-Tip Mounted Winglets", NASA TN D-8260, dated July 1976.
2. Jacobs, P. F., Flechner, S. G., Montoya, L. C., "Effect of Winglets On a First-Generation Jet Transport Wing, I - Longitudinal Aerodynamic Characteristics of a Semispan Model at Subsonic Speeds", NASA TN D-8473, dated June 1977.
3. Montoya, L. C., Flechner, S. G., Jacobs, P. F., "Effect of Winglets On a First-Generation Jet Transport Wing, II - Pressure and Spanwise Load Distributions For a Semispan Model at High Subsonic Speeds", NASA TN D-8474, dated July 1977.
4. Meyer, R. R., "Effect of Winglets On First-Generation Jet Transport Wing, V - Stability Characteristics For a Full-Span Model at Mach 0.30", NASA Technical Paper 1119, dated February 1978.
5. Flechner, S. G., "Effect of Winglets on a First-Generation Jet Transport Wing, VI - Stability Characteristics For a Full-Span Model at Subsonic Speeds", NASA Technical Paper 1330, dated October 1979.
6. Ishimitsu, K. K., VanDevender, N., Dodson, R. O., et al, "Design and Analysis of Winglets for Military Aircraft", AFFDL-TR-76-6, dated February 1976.
7. Dodson, R. O., "Comparison of Flight Measured, Predicted and Wind Tunnel Measured Winglet Characteristics on a KC-135 Aircraft", to be published in a NASA CP.
8. Dodson, R. O., Ayala, J., Shurtz, R. M., and Temanson, G., "KC-135 Winglet Flight Research and Demonstration Program", Boeing document D453-10087, to be published as an AFWAL-TR.
9. Boeing document D6-5599, "Substantiating Data Report For the KC-135A Flight Manual", dated 7 May 1964.

10. Boeing document D-16906, "Specification Engine Performance For Use in Airplane Performance Determination", dated 9 May 1955.

11. Beeler, D., Bellman, D. and Saltzman, E., "Flight Techniques for Determining Airplane Drag at High Mach Numbers", NASA TN 3821.

TABLE 1. - PERFORMANCE DATA FLIGHT TESTS

Flight No.*	Configuration	Date	Data Obtained
		Preliminary Data	
10-21	15° cant/-2° incidence	8-24-79	Drag, pressure
11-22	15° cant/-2° incidence	9-19-79	Drag, pressure
12-23	15° cant/-2° incidence	9-21-79	Drag, pressure
14-25	15° cant/-4° incidence	11-02-79	Drag, pressure
16-27	Baseline	11-16-79	Drag, pressure
		Final Data	
24-35	0° cant/-4° incidence	7-29-80	Fuel mileage, drag
27-38	0° cant/-4° incidence	8-08-80	Fuel mileage, drag
28-39	0° cant/-4° incidence	8-14-80	Fuel mileage, drag
30-41	Baseline	8-25-80	Fuel mileage, drag
31-42	Baseline	8-28-80	Fuel mileage, drag
32-43	Baseline	9-05-80	Fuel mileage
33-44	Baseline	9-09-80	Fuel mileage, drag
34-45	Baseline	9-11-80	Fuel mileage, drag
35-46	15° cant/-4° incidence	9-17-80	Fuel mileage, drag
36-47	15° cant/-4° incidence	9-23-80	Fuel mileage, drag
37-48	15° cant/-4° incidence	9-25-80	Fuel mileage
38-49	15° cant/-4° incidence	10-03-80	Fuel mileage, drag
40-51	15° cant/-4° incidence	12-17-80	Fuel mileage, drag, pressure
41-52	15° cant/-4° incidence	12-19-80	Fuel mileage, drag, pressure
42-53	15° cant/-4° incidence	12-23-80	Fuel mileage, drag, pressure
44-55	15° cant/-4° incidence	1-08-81	Fuel mileage, drag, pressure

*The first two digits of the flight number refer to the number of data flights and the last two digits refer to the cumulative number of flights.

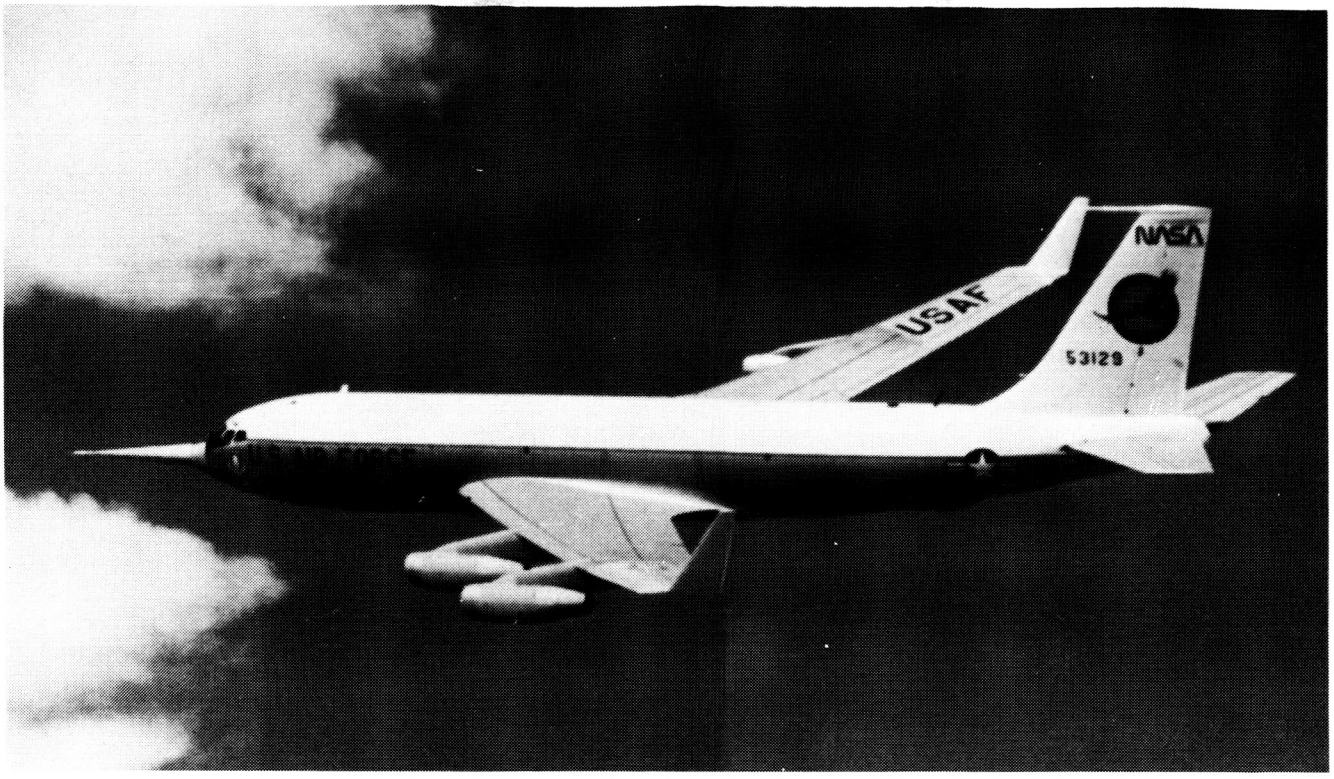

Figure 1. - Test KC-135A with winglets

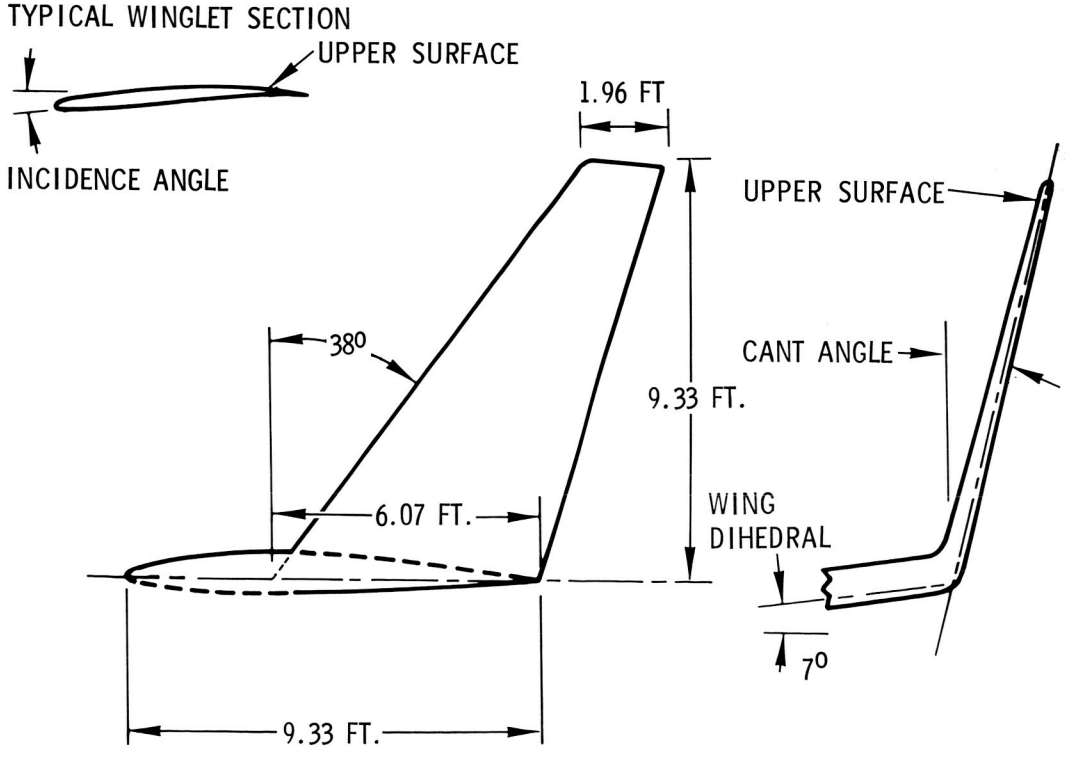

Figure 2. - Winglet geometry

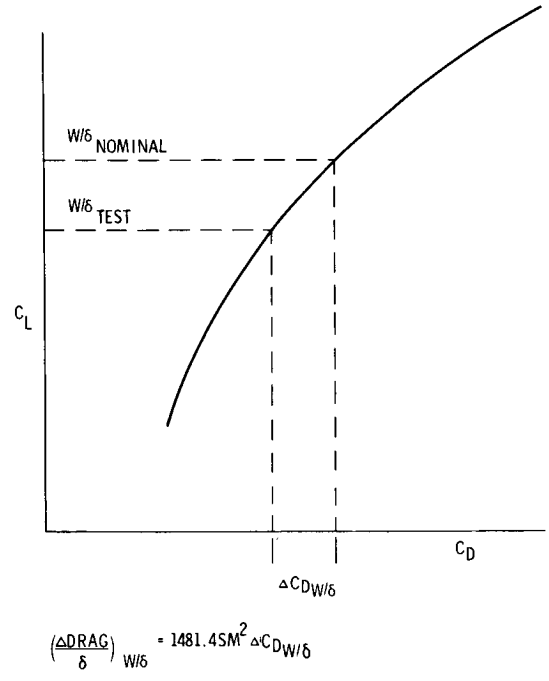

Figure 3. - Off W/δ drag correction

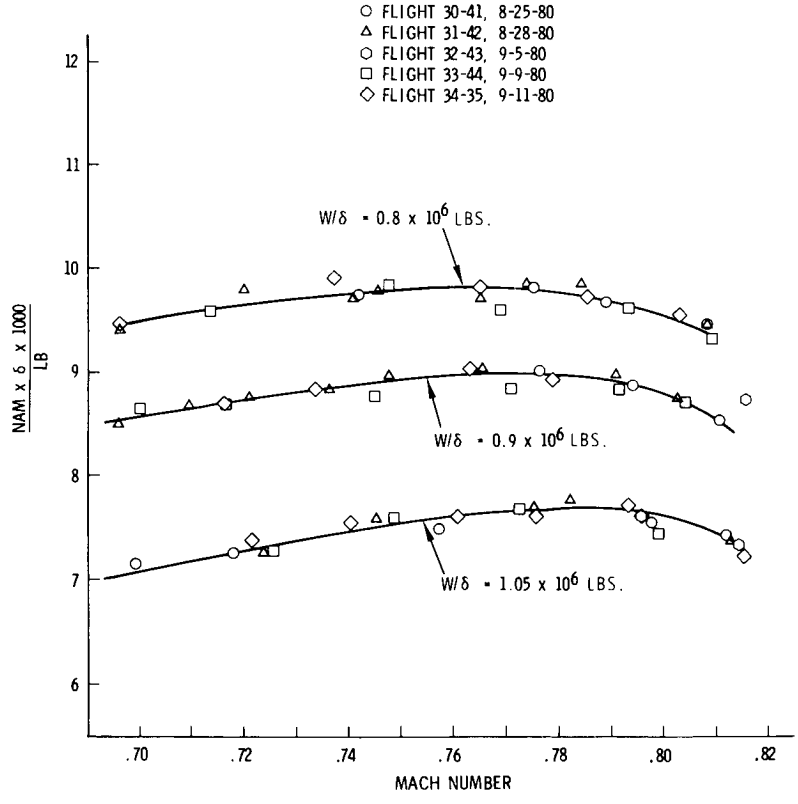

Figure 4. - KC-135 winglet flight test, baseline, Hp = 36,000 feet airspeed/altitude energy correction

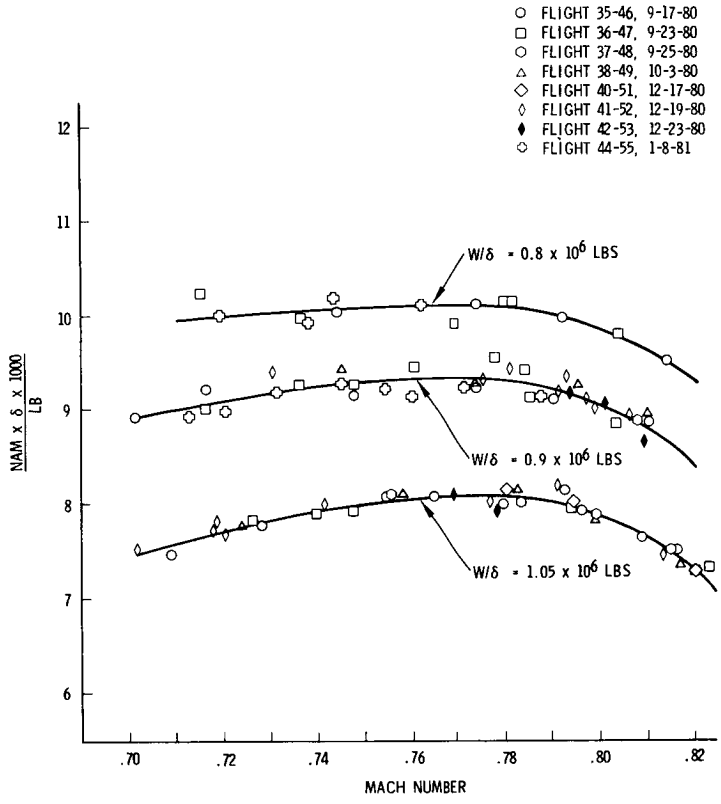

Figure 5. - KC-135 winglet flight test, 15° cant/-4° incidence, Hp = 36,000 feet airspeed/altitude energy correction

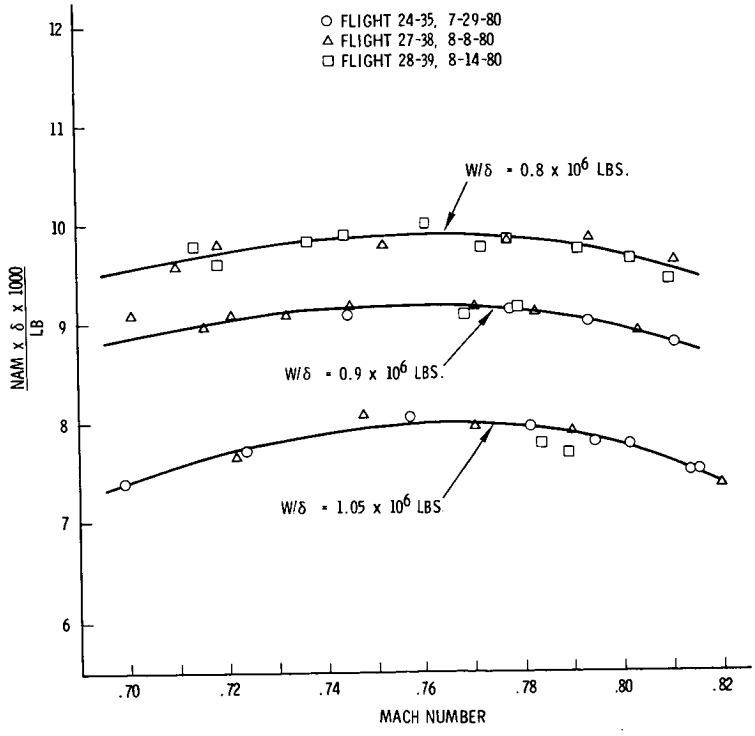

Figure 6. - KC-135 winglet flight test, 0° cant/-4° incidence, Hp = 36,000 feet airspeed/altitude energy correction

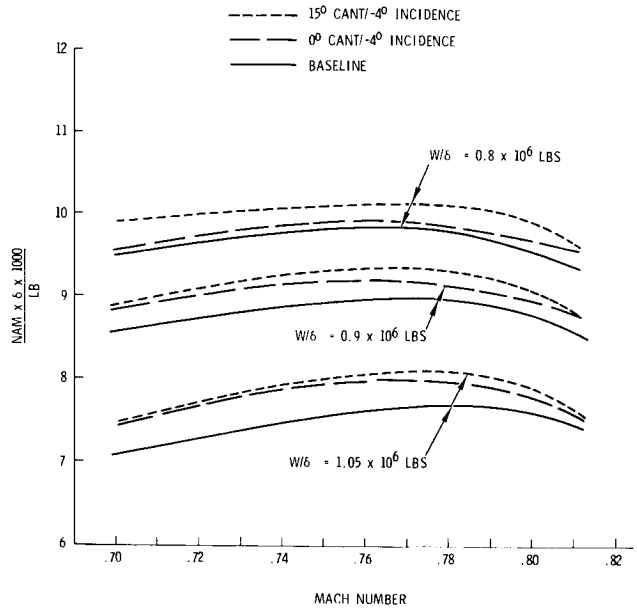

Figure 7. - KC-135 flight test data, Hp = 36,000 feet airspeed/altitude energy correction

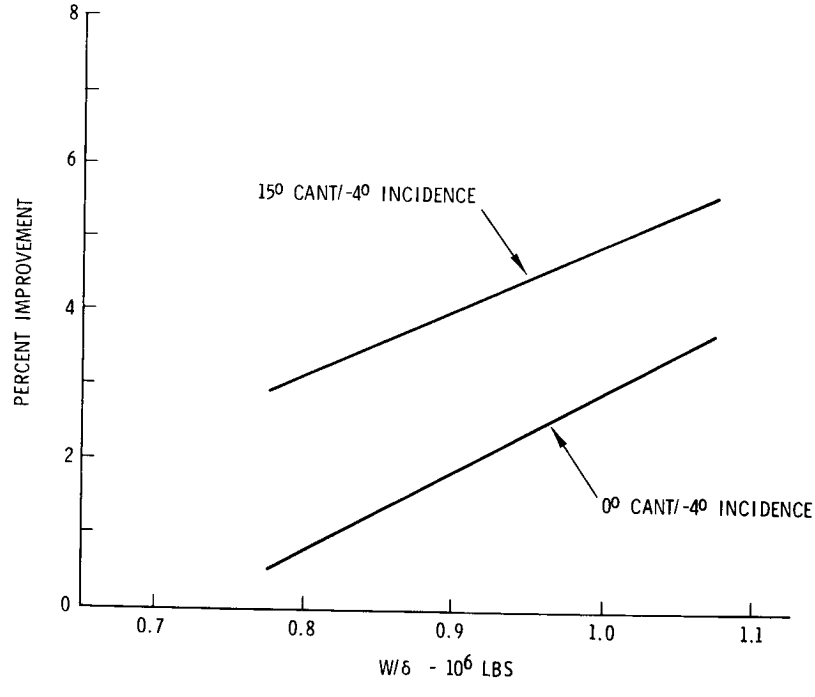

Figure 8. - KC-135A winglet flight test, cruise mileage improvement, airspeed/altitude energy correction mach = 0.78

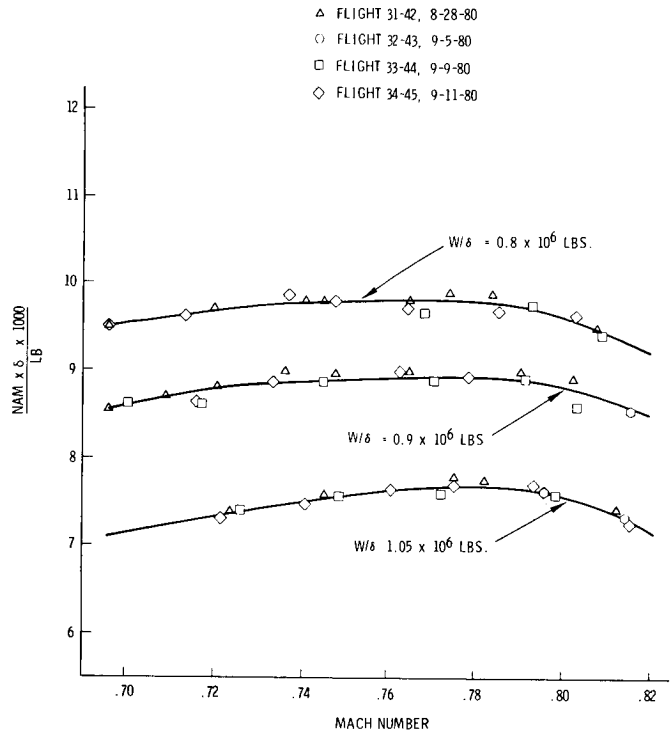

Figure 9. - KC-135A winglet flight test, baseline, Hp = 36,000 ft., INS energy correction

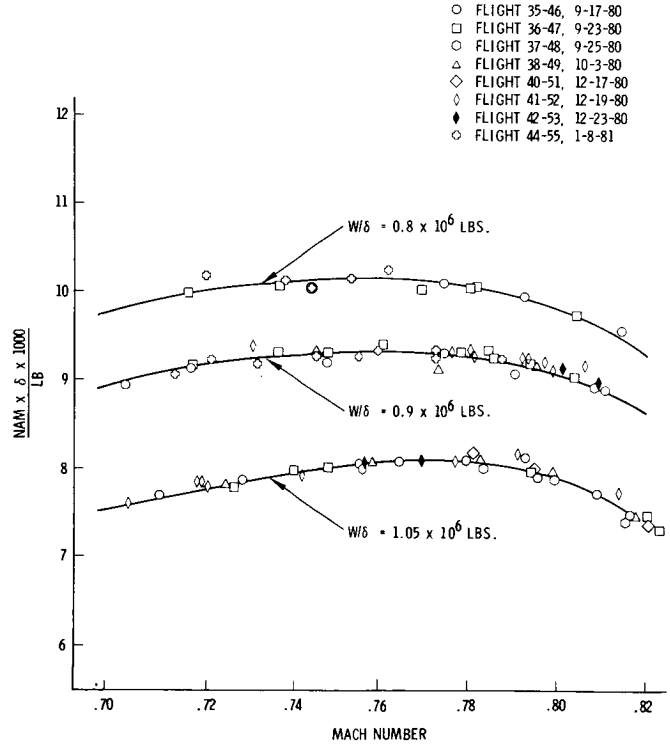

Figure 10. - KC-135A winglet flight test, 15° cant/-4° incidence, Hp = 36,000 ft., INS energy correction

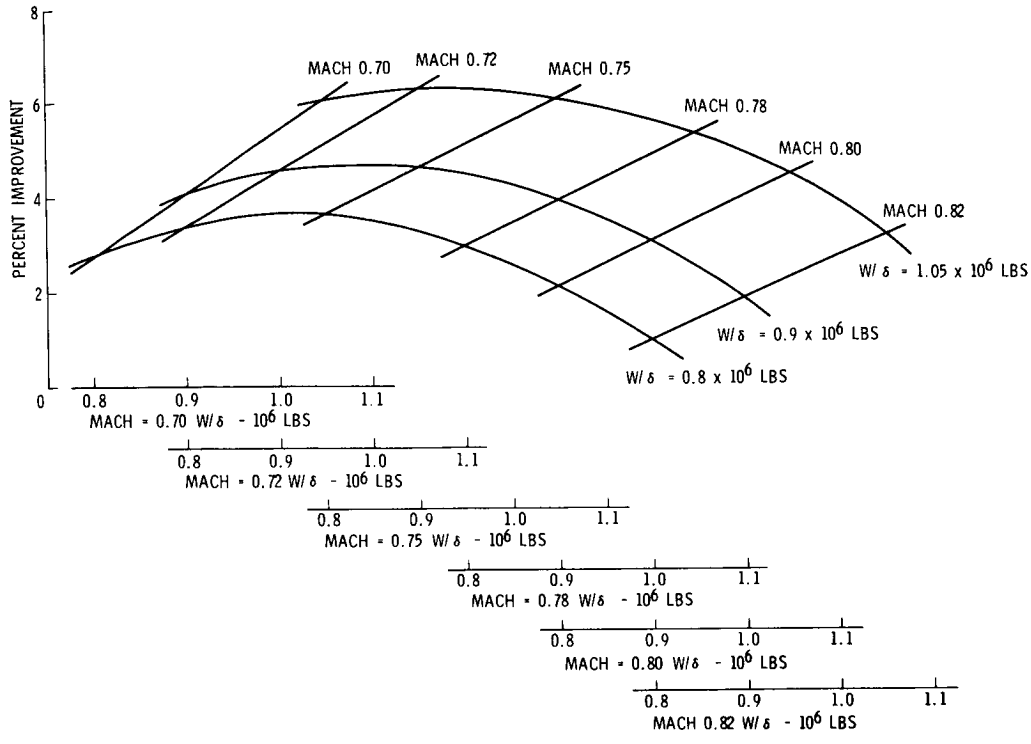

Figure 11. - KC-135A winglet flight test, cruise mileage improvement, winglet 15° cant/-4° incidence, INS energy correction

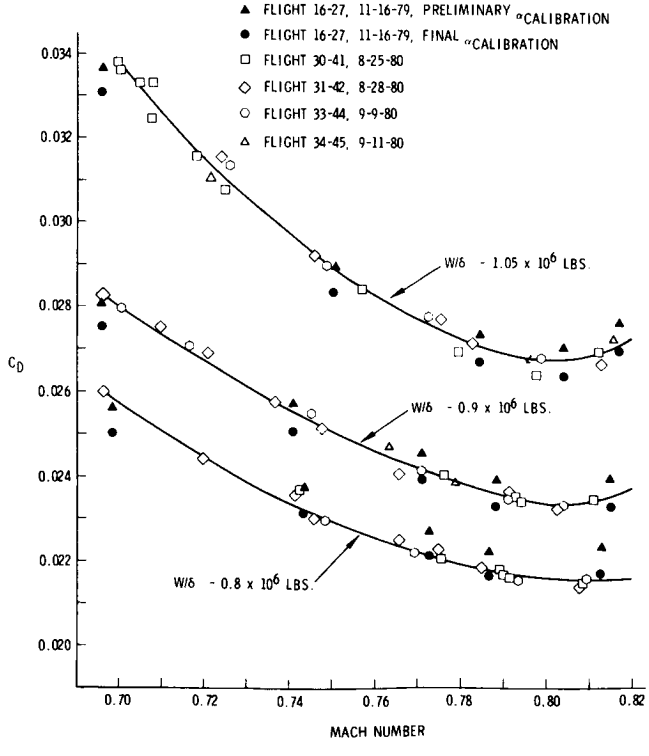

Figure 12. - KC-135A winglet flight test - baseline

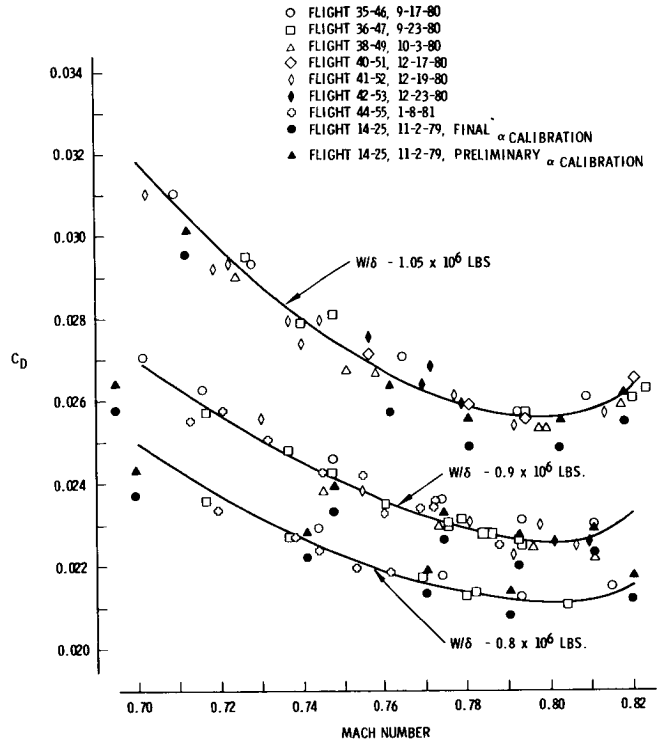

Figure 13. - KC-135A winglet flight test, 15° cant/-4° incidence

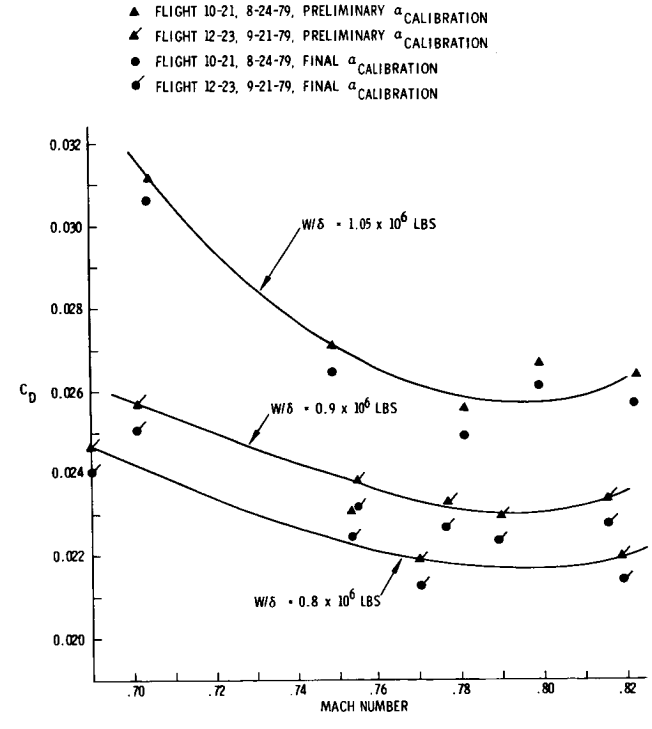

Figure 14. - KC-135A winglet flight test, 15° cant/-2° incidence

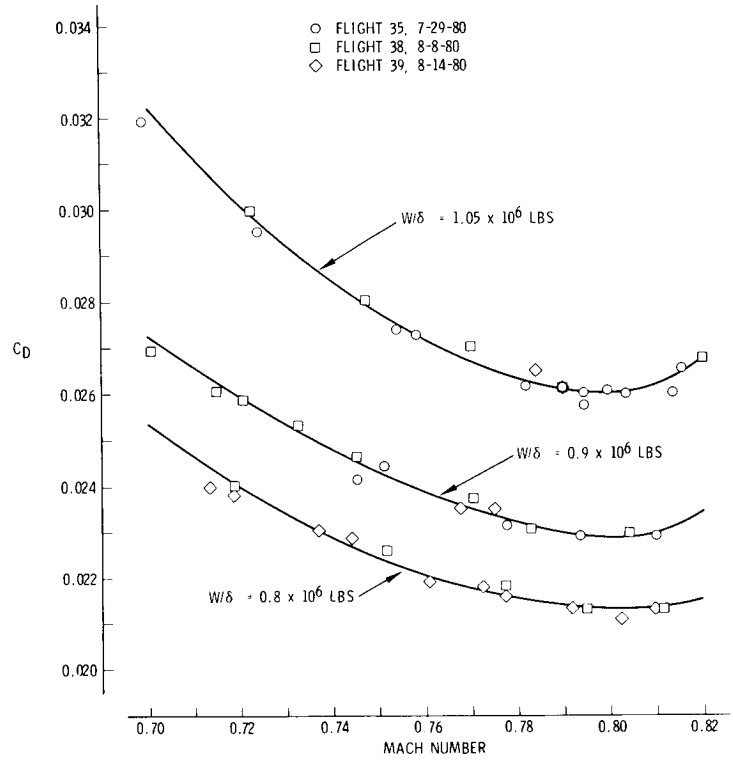

Figure 15. - KC-135A winglet flight test, 0° cant, -4° incidence

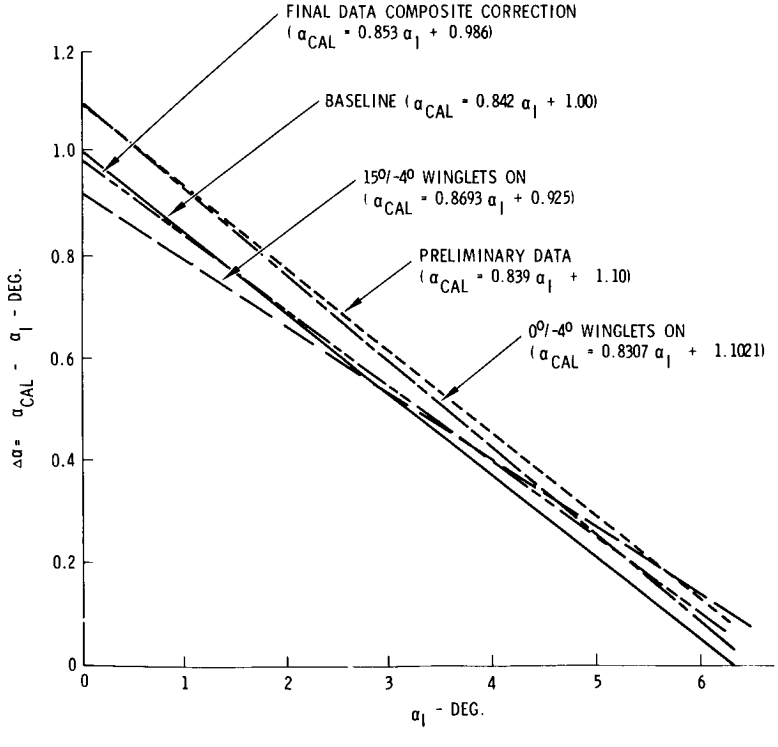

Figure 16. - Angle of attack comparison

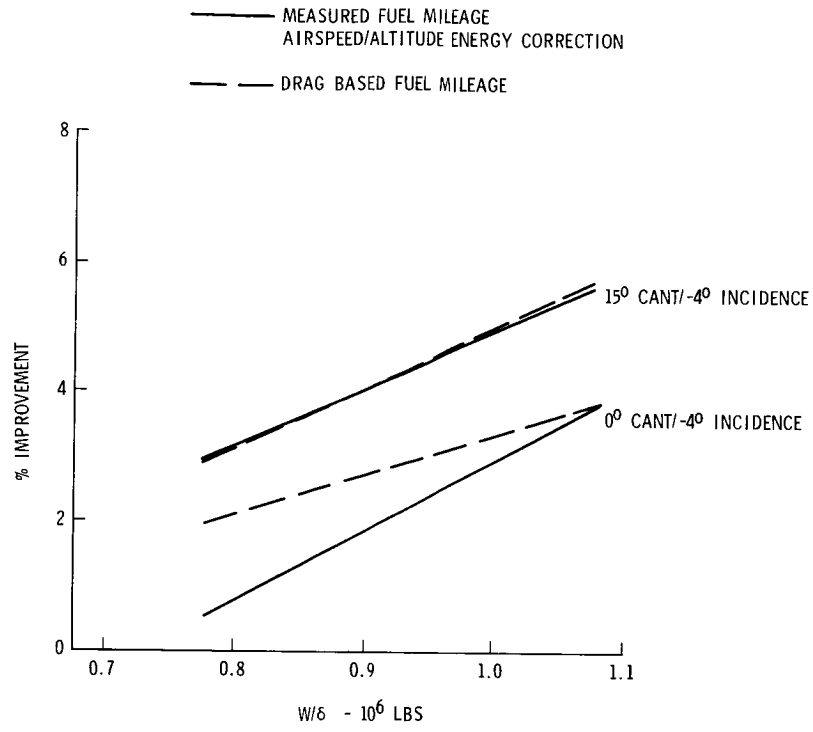

Figure 17. - KC-135A winglet flight test cruise cruise mileage improvement, mach = 0.78

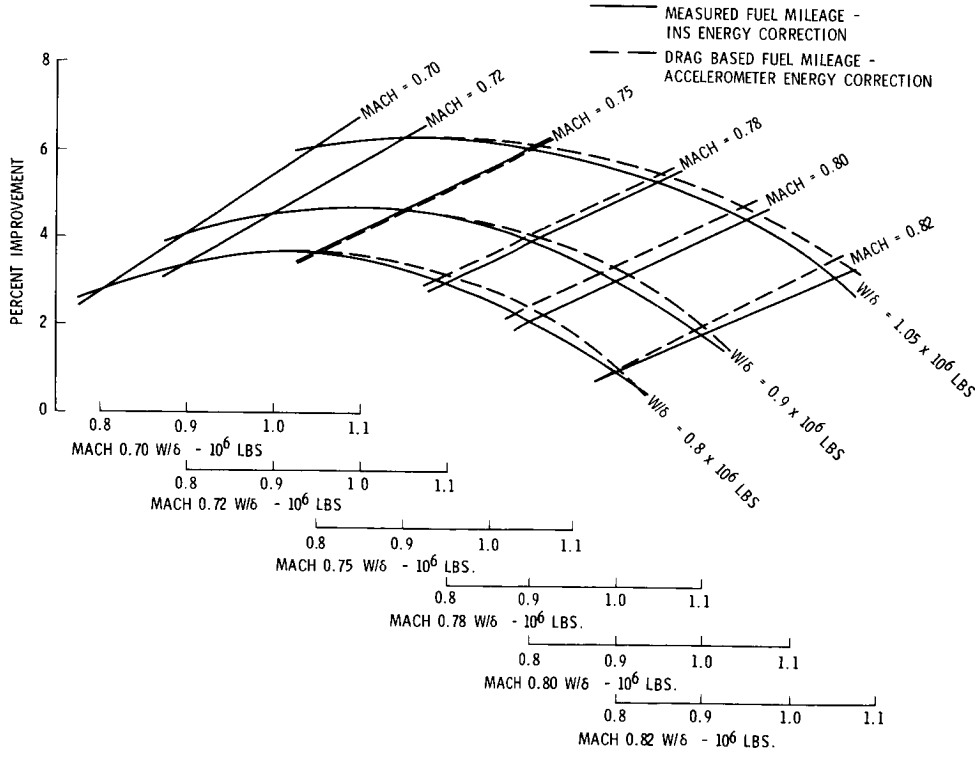

Figure 18. - KC-135A winglet flight test cruise mileage improvement, winglets 15° cant/-4° incidence

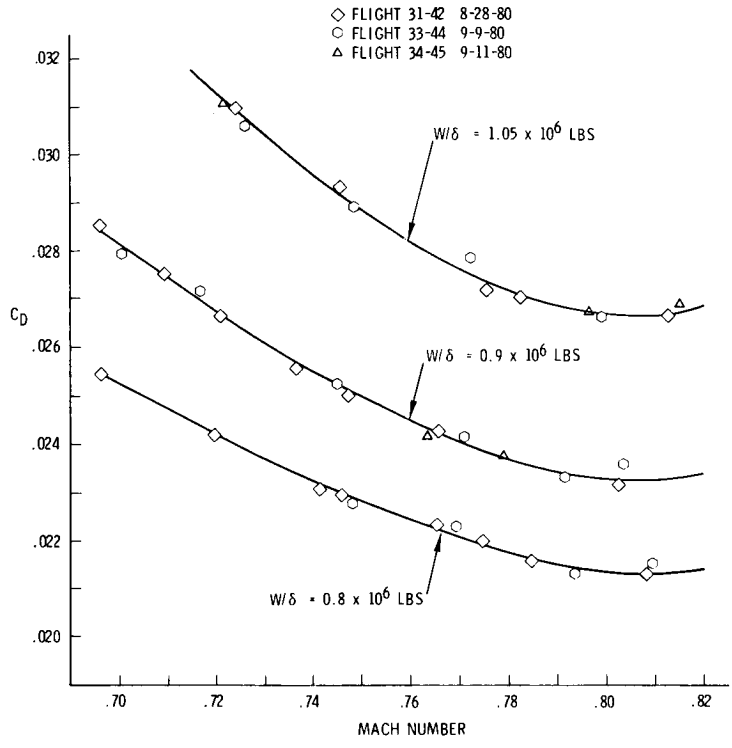

Figure 19. - KC-135A winglet flight test, baseline, INS energy correction

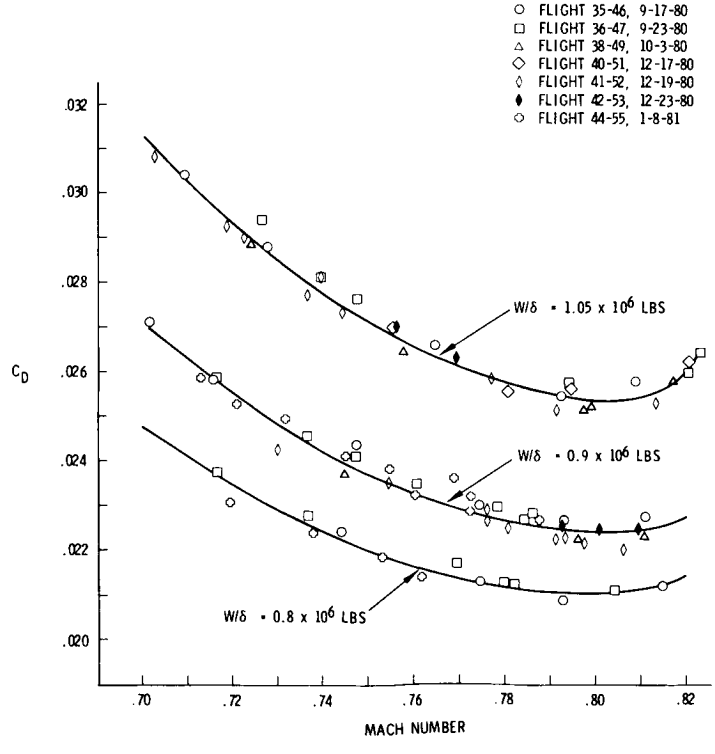

Figure 20. - KC-135A winglet flight test, 15° cant/-4° incidence, INS energy correction

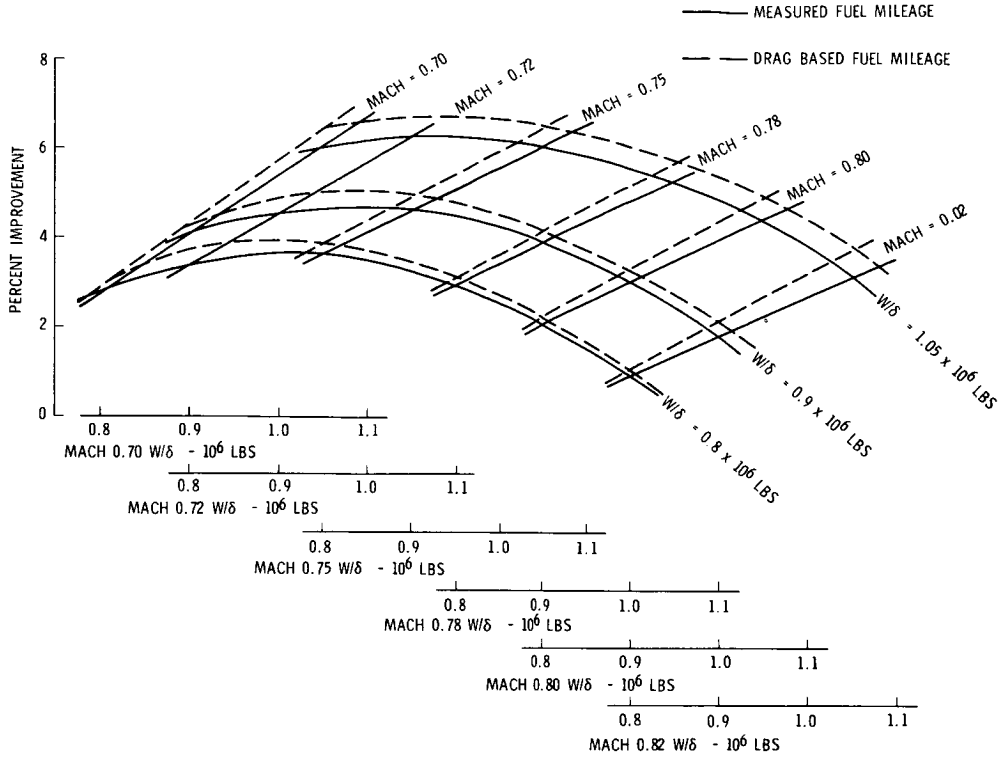

Figure 21. - KC-135A winglet flight test, cruise mileage improvement, winglet 15° cant/-4° incidence, INS energy correction

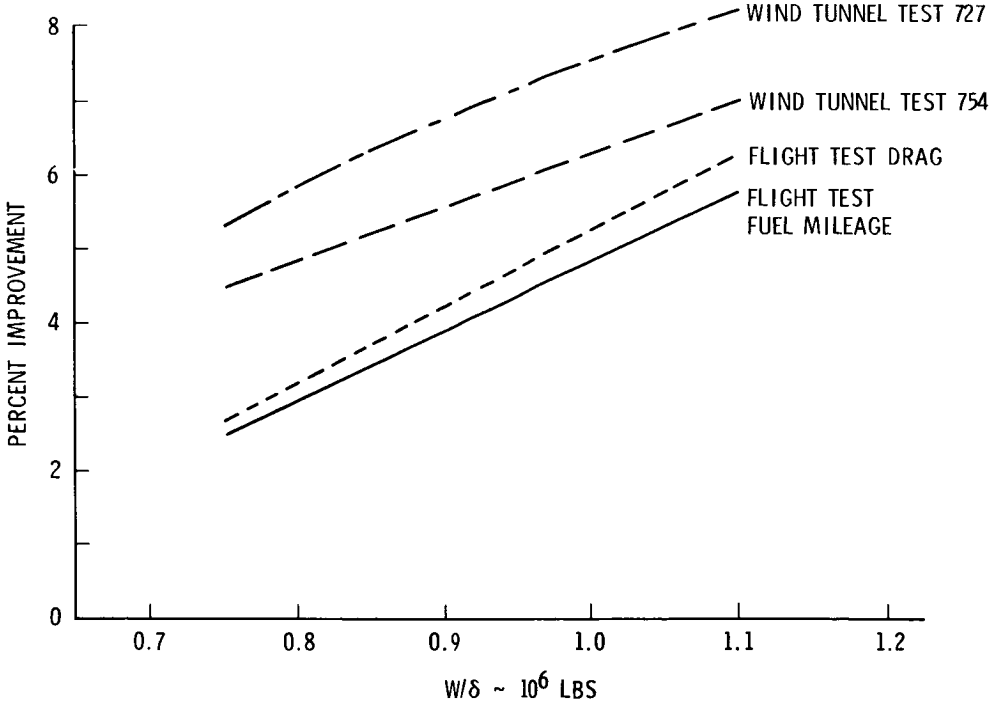

Figure 22. - KC-135A winglet flight test, cruise improvement mach = 0.78

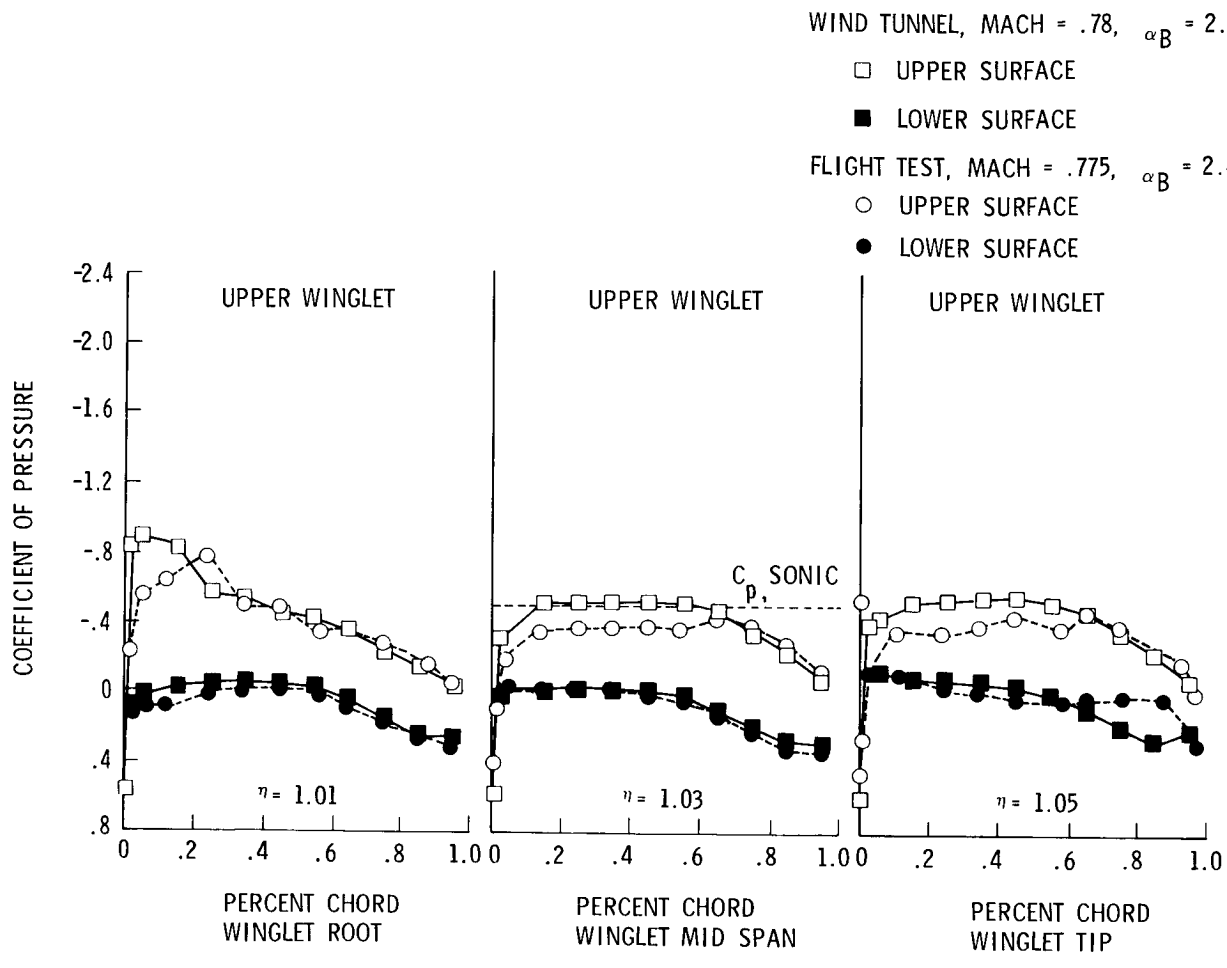

Figure 23. - KC-135 winglet program flight test and wind tunnel test winglet pressure comparison

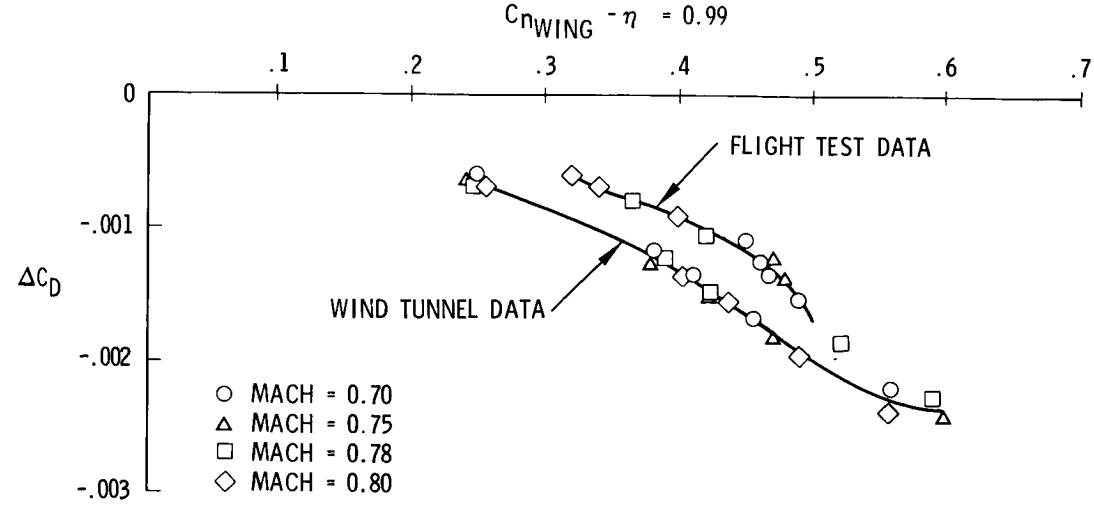

Figure 24. - Comparison of winglet flight test and wind tunnel pressure drag

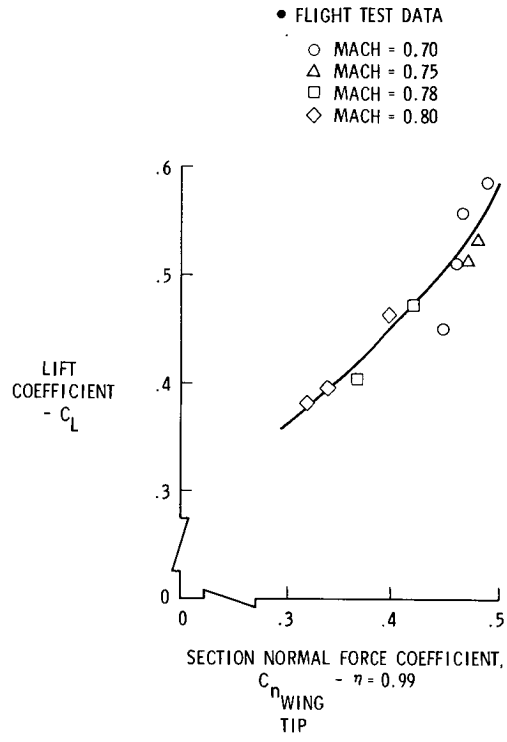

Figure 25 - Airplane lift and wing tip section normal force relationship

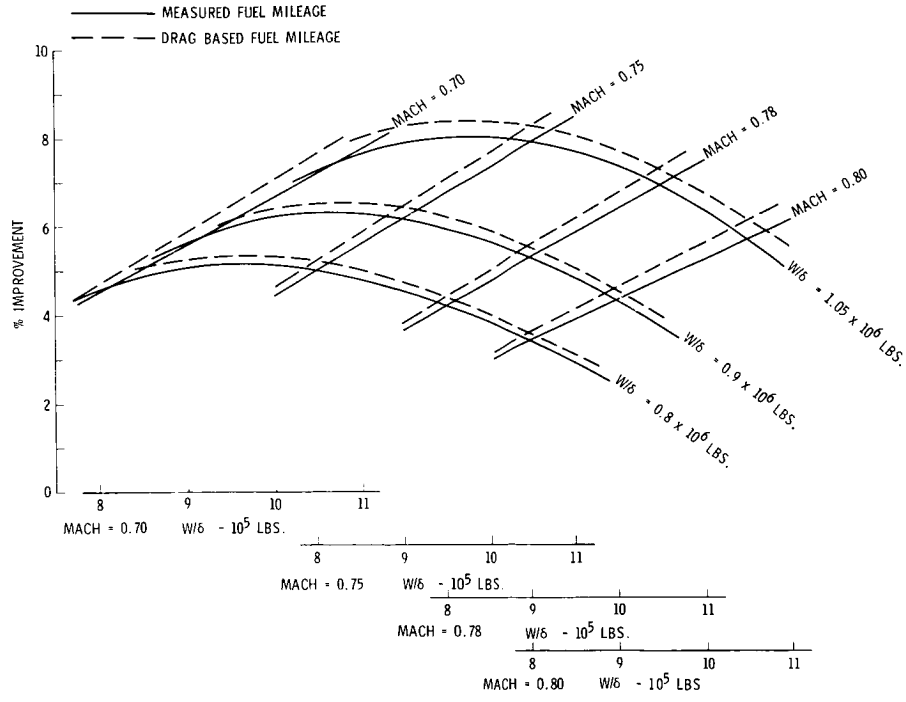

Figure 26. - KC-135A cruise mileage improvement, winglets 15° cant/-4° incidence, includes correction for pressure differences

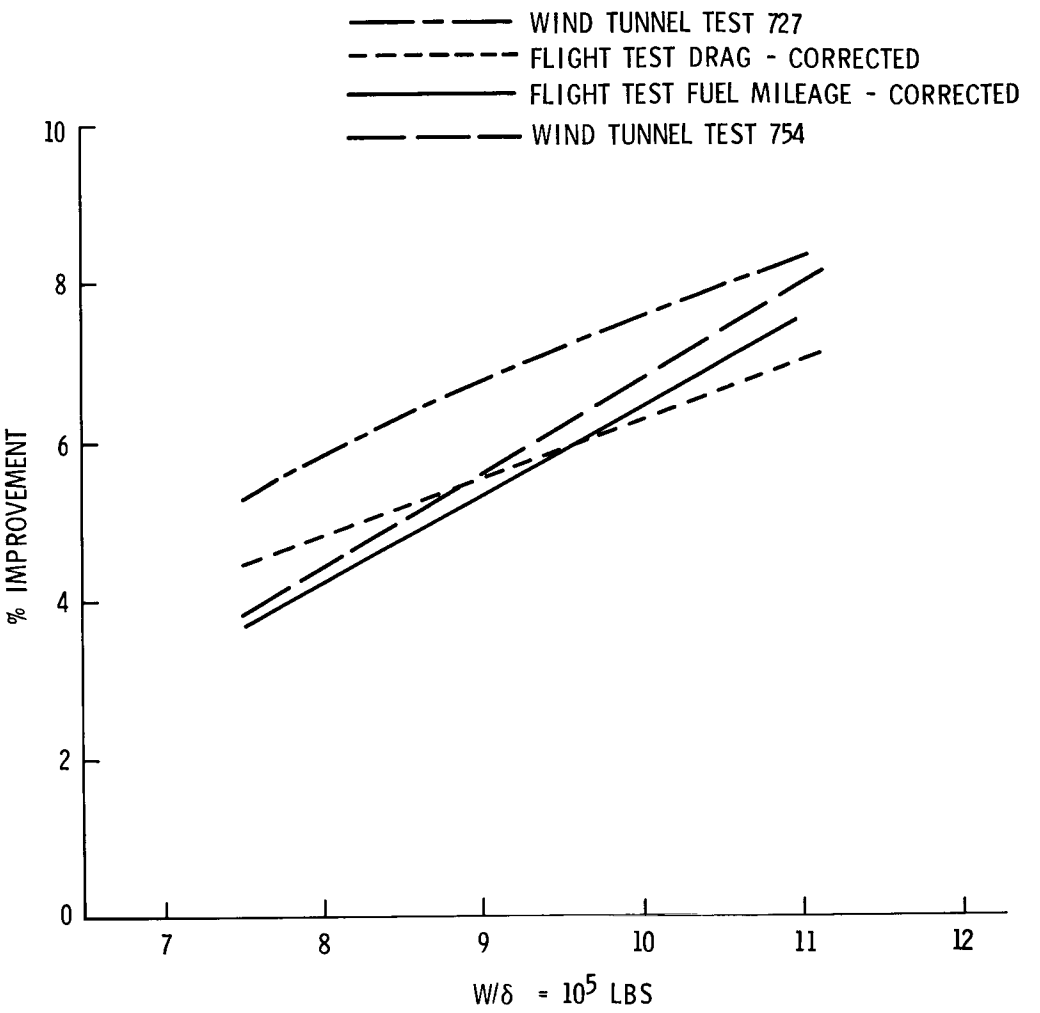

Figure 27. - KC-135A winglet flight test cruise mileage improvement, mach = 0.78

COMPARISON OF FLIGHT MEASURED, PREDICTED AND WIND TUNNEL MEASURED WINGLET CHARACTERISTICS ON A KC-135 AIRCRAFT

Robert O. Dodson, Jr.
Boeing Military Airplane Company

SUMMARY

One of the objectives of the KC-135 Winglet Flight Research and Demonstration Program was to obtain experimental flight test data to verify the theoretical and wind tunnel winglet aerodynamic performance prediction methods. Good agreement between analytic, wind tunnel and flight test performance was obtained when the known differences between the tests and analyses were accounted for. The flight test measured fuel mileage improvements for a 0.78 Mach number was 3.1 percent at 8×10^5 pounds W/δ and 5.5 percent at 1.05×10^6 pounds W/δ. Correcting the flight measured data for surface pressure differences between wind tunnel and flight resulted in a fuel mileage improvement of 4.4 percent at 8×10^5 pounds W/δ and 7.2 percent at 1.05×10^6 pounds W/δ. The performance improvement obtained was within the wind tunnel test data obtained from two different wind tunnel models.

The buffet boundary data obtained for the baseline configuration was in good agreement with previously established data. Buffet data for the 15° cant/-4° incidence configuration showed a slight improvement, while the 15° cant/-2° incidence and 0° cant/-4° incidence data showed a slight deterioration.

INTRODUCTION

Analytical and experimental investigations from the references 1 through 6 studies indicated that a significant drag reduction could be realized on large transport aircraft through the incorporation of winglets. Winglets were projected to reduce the KC-135 cruise drag between 6 and 8 percent, which translates into a significant fuel savings for the KC-135 fleet. This projected cruise performance improvement resulted in the KC-135 Winglet Flight Research and Demonstration Program. The primary objective of the program was to design, fabricate and flight test a set of winglets to prove the fuel conserving attributes of the winglet concept. A secondary objective was to obtain experimental flight test data to verify the theoretical and wind tunnel winglet aerodynamic performance prediction methods.

The Flight Research and Demonstration Program was a joint effort between the Boeing Military Airplane Company (BMAC), the U.S. Air Force and NASA.

BMAC, under contract to the Flight Dynamics Laboratory (FDL), designed, fabricated, ground tested and delivered a set of outboard wings and winglets, which were flight tested by NASA-Dryden. The wind tunnel performance data and the winglet external configuration description were provided by NASA-Langley. The BMAC role throughout the flight test program was to provide engineering

support and to promote understanding and confidence in the data being generated. A detailed discussion of the final results of the program can be found in references 7 and 8. Results presented in reference 9 discuss the analysis of flight test fuel mileage and drag measurements. This report summarizes the results of the comparisons between flight-measured, predicted and wind tunnel-measured winglet characteristics on the KC-135 aircraft.

SYMBOLS

ALT	Altitude
b	Wingspan
c, C	Chord Length
C_D	Drag Coefficient
C_{D_i}	Induced Drag Coefficient
C_L	Lift Coefficient
C_ℓ	Sectional Lift Coefficient
C_{N_A}	Normal Force Coefficient
C_n	Yawing Moment Coefficient, Section Normal Force Coefficient
C_p	Pressure Coefficient
D	Drag
FM	Fuel Mileage
i_w	Winglet Incidence Angle
L	Lift
ℓ	Winglet Height
M	Mach Number
M_ℓ	Local Mach Number
MAC	Mean Aerodynamic Chord
q	Dynamic Pressure
R_N, RE NO	Reynolds Number
TSFC	Thrust Specific Fuel Consumption

W, G.W.	Gross Weight
Y	Spanwise Distance Along Wing from B.L. = 0
Z	Spanwise Distance from Winglet Root Measured in Winglet Chord Plane, or Vertical Displacement
α	Angle of Attack
α_B	Body Angle of Attack
β	Angle of Sideslip
δ	Ambient Pressure Ratio
Δ	Increment
η	Nondimensional Wing Semispan
θ	Ambient Temperature Ratio
ϕ	Winglet Cant Angle

WIND TUNNEL TESTS AND DATA CORRECTIONS

The airplane performance wind tunnel tests were accomplished by NASA at their Langley facilities. All tests were conducted in the NASA-Langley 8-foot Transonic Pressure Tunnel except for a limited amount of low-speed flaps-down testing in the NASA-Langley 7-foot x 10-foot High Speed Tunnel to obtain high angles of sideslip. Three different wind tunnel models were used during the NASA-Langley tests. Figure 1 pictures the 0.035 scale rigid full wing span model. The wing for this model was built in a jig position. A photograph of the 0.035 scale model used for the flaps-down wind tunnel tests is shown in figure 2. The model is a rigid full wing span model with brackets for flap deflections of 30 degrees and 50 degrees and outboard aileron deflections. Figure 3 presents the 0.07 scale half model. This particular photograph shows the early upper and lower winglet configuration. The wing of this model had internal structural material removed so that the wing tip would deflect to an approximate full scale cruise position in the wind tunnel. Figure 4 shows the 0.07 scale wind tunnel model static pressure port span locations. On the 0.035 scale models the wing pressures were at the same locations and the winglet static pressure port span locations were at winglet stations 1.01 and 1.05. A summary of the KC-135A winglet wind tunnel test conducted at NASA-Langley is shown in table 1. The test number, model configuration, conditions and type of data recorded are presented.

The "flexible" wing wind tunnel half model used during the NASA-Langley test 727 had a clipped wing tip, the fuselage was not connected to the balance and the wing was built to deflect to a cruise flight position. The data from this test were based on the exposed trapezoidal wing area of the model. The

winglet on and off test data with the clipped wing, based on the exposed trapezoidal area, were corrected to the KC-135 wing area of 2,433 square feet. The incremental drag, due to the winglets, was obtained by taking the difference between the wing area-corrected clipped wing drag polars (winglet on and off) and then adjusting the drag increment to the correct lift by accounting for the fuselage lift carryover. To determine the fuselage lift contribution, the rigid and elastic effects for the KC-135A lift curves were used (reference 10) with the wind tunnel flexible model lift data. The drag increment was then corrected for trim drag and Reynolds number. The corrected incremental drag versus lift coefficient is shown in figure 5 for M = 0.78. The data points are the incremental drag from the wind tunnel corrected for wing area. The body lift correction was then applied and the combined trim drag and Reynolds number corrections were added. The resulting final corrections to the NASA test 727 data is shown by the dashed line. At M = 0.78 and C_L = 0.45 the drag increment was -17.5 drag counts.

The full span model used during the NASA-Langley test 754 had a rigid wing in the jig position and the winglet was at 12 degrees cant angle. A potential flow analysis was accomplished using wing and winglet geometry corrected for aeroelastic effects to determine the effect of wing aeroelastic effects on the winglet drag increment. The correction was for the cruise condition and amounted to 2.9 degrees additional wing dihedral and -2.9 degrees additional wing twist. The "flexible" wing solution reduced the winglet drag benefit compared to the rigid wing in the jig position. At a lift coefficient of 0.45 the winglet drag benefit was about 2.2 drag counts less for the "flexible" wing than the jig position wing.

From the test 727 cant angle variation there was no discernible difference in winglet drag increment between 12 and 15 degrees cant angles. The corrections for trim drag and Reynolds number were made in the same manner outlined for test 727. The winglet drag increment at M = 0.78 for the NASA test 754 data is shown in figure 6. Again, the test points are noted by the symbols and the dashed line has the combined trim drag and Reynolds number correction noted on the plot.

The KC-135A winglet performance improvements predicted from the wind tunnel data are summarized in table 2. The corrected winglet drag increments obtained from both NASA wind tunnel tests 727 and 754 were added to the basic KC-135A drag polar and the cruise conditions were reoptimized for both sets of data. The performance data shown are an average from both data sets. The values shown are for a flight speed at 99 percent maximum range and the noted corrections.

SURFACE PRESSURE COMPARISONS AND ANALYSIS

During the winglet flight tests, chordwise static pressures were measured at four wing and three winglet span locations, as shown in figure 4. These were the same locations where pressures were obtained during the 0.07 scale half model wind tunnel tests.

Comparisons of the flight test and wind tunnel measured pressures for a typical cruise condition are shown in figures 7 and 8 for the wing and winglet, respectively. As can be seen in figure 7 the wing pressure comparison shows good agreement. On the flight test airplane the three inboard rows of wing pressures were measured using pressure belts. The outboard row of wing pressures were especially installed flush static ports. At the 0.92 wing semispan station the flight test pressures indicate some irregularities in the pressure belt contour. At the outboard wing station the flight test-measured pressure, at about 82 percent chord, indicates an ambient pressure. This was attributed to a bad pressure tap and was consistent throughout the flight test for all the flight test-measured pressures.

Figure 8 is a comparison of the flight test and wind tunnel measured pressures on the winglet for the same typical cruise condition. The overall agreement is good. However, a close look at the comparison reveals some subtle differences. First, the three flight test-measured pressures at the winglet tip on the outboard winglet surface at chord stations of about 0.65, 0.75 and 0.87 are bad pressure taps. Next, note the slight local velocity increase measured in flight, beginning at about 60 percent chord for the winglet midspan and tip locations. This effect on the flight test winglet pressures was due to the winglet pillowing causing an irregular contour change in the winglet airfoil shape at these locations. The effect of the winglet pillowing on the flight measured pressures actually begins at about 25 percent chord and a close look indicates an effect at all three span locations.

An inflight photograph of the inboard winglet surface is shown in figure 9, showing the surface contour pillowing when the winglet experiences inflight loads. The surface contour bulges inboard between the winglet ribs and spars due to the compressive stresses in the skin and the inboard suction of the local negative pressures.

The forward winglet spar is located at 15 percent chord and no pillowing effect on surface contour was noticed in flight along the leading edge. However, the inboard winglet root pressure comparison in figure 8 indicates a substantial difference between the flight test and wind tunnel measured pressures at the leading edge. At this Mach number both sets of data show a weak shock at about 25 or 30 percent chord. However, the flight test pressures do not peak to the same levels as the wind tunnel data. A close look at the flight test-measured pressures in this area at other Mach numbers revealed that as soon as the local flow went supersonic the leading edge pressure peak was affected.

The lowest Mach number that pressure data was obtained was 0.468 for the 15°/-2° winglet position. During the flight test program the first winglet position tested was the 15°/-2° position in order to clear the airplane in this configuration first for flutter. During these flights a limited amount of pressure data was taken to check out the pressure instrumentation which included a condition at a Mach number of 0.468 and an angle of attack of 2.0 degrees. To aid in determining if the winglet root leading pressure peak loss was associated with a local sonic flow condition, these flight test pressures were compared to the wind tunnel pressures. The lowest Mach number at which pressure data was recorded in the wind tunnel was 0.70, and only for the 15°/-4° winglet position. A comparison of these pressures is shown in figure 10. Since the winglet positions do not have the same incidence angle, data

at three angles of attack are shown for the wind tunnel data in order to compare the general shape of the leading edge pressures. This comparison showed that at subcritical Mach numbers the winglet root leading edge was loading the way it should. This indicated that the flight test winglet root leading edge pressure peak loss was not associated with any difference in airfoil contour between flight and wind tunnel test, but rather with a local supersonic flow condition.

In an attempt to understand the differences in the leading edge pressures and to further substantiate the effect of the winglet pillowing, a comprehensive two-dimensional transonic analysis was conducted on the winglet streamwise root airfoil section. The primary tool in the analysis was the Bauer-Garabedian-Korn-Jameson 2-D transonic viscid/inviscid analysis code (references 11 and 12). The first step in the analysis was to analyze the basic airfoil, figure 11. This figure shows that the airfoil has good characteristics that are typical of supercritical airfoils. The leading edge pressures, in general, also match the winglet root, low Mach number wind tunnel pressures in figure 8. Since the airfoil ordinates used in the analysis were the same as the ordinates used in lofting, no lofting problem was suspected. However, photographs of the winglets in flight (figure 9) reveal that there was a pillowing effect on the winglets. The rib and spar construction of the flight test article allow bulging out of the unsupported skin panels. This pillowing extends from the forward spar to the aft spar and from the aft spar to the trailing edge winglet structure between the ribs.

The skin pillowing was estimated to bulge approximately one-quarter inch on the 65 inch chord, or 0.38 percent chord at the winglet root station. The model airfoil geometry was modified to simulate the presence of this pillowing. The modified airfoil geometry was again analyzed and the results are shown in figure 12. It should be pointed out that because of the sweep of the winglet, $M_{normal} = 0.64$ is approximately equal to $M_{freestream} = 0.78$. Comparing the aft 50 percent of these pressures to the aft 50 percent of the flight test pressures in figure 8 shows a very close resemblance in shapes. One cannot expect the magnitudes to match because of the three-dimensional losses from the analysis; however, the shapes of the curves should be similar.

The comparisons of the aft portions of the pressures are very similar, but the leading edge pressures do not indicate a leading edge pressure peak loss due to the skin pillowing. A close examination of the flight test photographs and conferences with the structural engineers indicated that the pillowing between the spars may not have been modeled correctly. The way the skin panel is mounted to the ribs and spar would not allow the pillowing to extend over as large a portion of the chord as originally assumed. Remodeling the airfoil, as shown at the bottom of figure 13, yielded the corresponding changes in the pressures. At slightly higher Mach numbers, the pressures seem to hold a peak at about 33 percent chord similar to the flight test pressures. However, the leading edge pressure peak was not appreciably affected.

Since the leading edge pressures were experiencing higher peaks in the analysis than in the flight test at cruise Mach numbers and the flight test pressures match wind tunnel pressures at low subcritical Mach numbers, it was concluded that a small region of separation exists on the winglet leading edge and grows with Mach number on the flight test article. The reason the separation did not show in the wind tunnel data may have been because the wind tunnel

model had a trip strip at 5 percent chord. Although the grit size was small, No. 22, it was still 3 to 4 times greater than the displacement thickness of a laminar boundary layer at this point. The grit in this case may have been doing more than forcing a transition from laminar to turbulent flow in the boundary layer. The grit may have been acting like a row of very small vortex generators which were injecting energy into the boundary layer, preventing separation.

The next step in the investigation was to define what effect the differences between flight test and wind tunnel measured winglet pressures had on winglet pressure drag. To do this, the winglet flight test and wind tunnel pressure data were transformed to suction and drag loops along the winglet span using the winglet incidence angle. This was accomplished for all Mach numbers and angles of attack for which wind tunnel and flight test pressure data existed. A typical comparison between flight test and wind tunnel data at cruise conditions is shown in figures 14 through 16 for the three winglet stations. Note the relatively large difference in the suction loop area at the winglet root station due to the flight test leading edge pressure peak loss.

A chordwise and spanwise integration on the winglet of these data yielded the incremental winglet pressure drag data shown in figure 17. Note that the drag data are shown plotted against the section normal force at the outboard wing station instead of the usual total airplane lift coefficient. This was done to compensate for any differences in aeroelastic twist at the wing tip between the wind tunnel model and the flight test airplane. The relationship between airplane lift coefficient and wing tip normal force coefficient for the flight test airplane is shown in figure 18.

Referring back to the incremental pressure drag plot in figure 17 indicates that at typical cruise conditions the difference between the flight test and wind tunnel measured drag data would be about 4 drag counts, which is about 1.5 to 2 percent when transformed to a cruise fuel mileage benefit. This difference reveals the importance of the aerodynamic pressure loading on the winglet in order to obtain the expected winglet performance benefit.

In order to obtain a feel for the amount of the drag difference obtained between flight test and wind tunnel data that can be attributed to the winglet root leading edge suction loss and the winglet pillowing effect, the winglet root suction/drag loop for the flight test was assumed to be exactly equal to the wind tunnel data. Performing a similar integration over the winglet revealed the drag differences shown in figure 19. The drag differences shown here between the flight test and wind tunnel data are approximately the differences that can be attributed to the winglet pillowing effect. About one-third of the total difference shown in figure 17 can be attributed to winglet pillowing and two-thirds to the winglet root leading edge suction loss obtained in flight.

COMPARISONS OF WIND TUNNEL AND THEORETICAL PREDICTION TO FLIGHT TEST DATA

One of the objectives of the KC-135 Winglet Flight Research and Demonstration Program was to obtain experimental flight test data to verify the theoretical and wind tunnel winglet performance prediction methods.

Theoretical surface pressures and drag increments due to the winglets were compared to wind tunnel and flight test data for selected conditions. The following discussion presents the results of these comparisons.

A comparison of theoretical potential flow, wind tunnel and flight test pressure distributions on the wing tip and winglet are presented in figure 20. The comparison is at a Mach number of 0.70. The overall comparison is good. The potential flow wing geometry had an aeroelastic twist distribution representative of typical 1g cruise conditions. Also note in figure 20 the loss of the leading edge pressure peak at the winglet root obtained from the flight test data.

Integrating the wind tunnel and flight test pressure data to obtain the section normal force results in the typical comparison shown in figure 21. The 15° cant/-4° incidence angle data compared well. At the winglet midspan and tip positions the flight test data may be slightly lower compared to the wind tunnel data. The 15° cant/-2° incidence data show the winglet carrying more load as expected.

Flight test incremental drag results are compared to wind tunnel and theoretical predicted drag increments in figures 22 through 24. The flight test data shown in the figures have the pressure drag increment correction included. The wind tunnel drag increments have been corrected for Reynolds number and trim drag.

The data shown in figure 20 compares the test data to a predicted theoretical drag increment at a Mach number of 0.70. The theoretical drag increment was obtained using the same potential flow geometry model with aeroelastic twist that was discussed before. The wing and winglet potential flow span loading solution was again used as input to a Trefftz plane analysis computer program to compute the induced drag. The induced drag was then corrected for skin friction and trim drag. As can be seen in figure 22, the comparison was good between theory, wind tunnel and flight test. Since the theoretical potential flow method was a subcritical flow method, only a comparison at a Mach number of 0.70 is shown. At the higher Mach numbers shock waves begin to appear on the surface and the method is no longer valid.

Wind tunnel predicted and flight test incremental drag comparisons at higher Mach numbers are shown in figures 23 and 24. In each case the comparison was good except at a Mach number of 0.82. The flight test drag increment shows less improvement than predicted from wind tunnel data at this Mach number. This was attributed to the winglet root leading edge pressure peak loss in flight and the surface pillowing problems becoming more aggravated at this higher Mach number, as previously discussed.

The KC-135A performance improvements based on these incremental drag data are shown in table 3. The winglet drag increment was added to the basic KC-135A Flight Manual drag polar and cruise conditions were reoptimized. The wind tunnel-predicted fuel mileage improvement value previous to the flight test was 6.3 percent (table 2) and, using the flight test obtained drag increment, the fuel mileage improvement was 6.5 percent. These percentages were obtained by ratioing the winglet on and off fuel mileage at the optimum W/δ of each configuration.

Figure 25 presents the performance benefit for winglets obtained from flight test fuel mileage and drag data compared to the wind tunnel predicted improvement at M = 0.78. The percent improvement shown has been corrected to account for the winglet surface pressure discrepancies. Good agreement was obtained between the corrected flight test data and the corrected full model wind tunnel data.

Buffet boundaries were established during the flight test program using wing tip mounted accelerometer data. Data were obtained for the winglets on configurations as well as for the baseline configuration, as shown in figure 26. The buffet boundary data obtained for the baseline configuration was in good agreement with the previously established data. The buffet data for the 15° cant/-4° incidence configuration shows a slight improvement over the baseline. The 15° cant/-2° incidence configuration showed a slight deterioration to the baseline configuration again indicating that the additional winglet loading was causing an earlier flow separation. The 0° cant/-4° incidence configuration exhibited buffet characteristics similar to the 15° cant/-2° incidence configuration. The decrease in buffet boundary for the 0° cant/-4° incidence configuration is in agreement with the performance data that showed a lower than predicted performance increase, possibly due to flow separation between the wing tip and winglet root.

CONCLUSIONS

Results of the KC-135 winglet flight test have verified that the performance improvement can be predicted using conventional analytic and wind tunnel testing techniques. The data show that winglet retrofit would provide a six percent performance improvement for the KC-135 at the optimum cruise condition.

Particular attention should be paid to the design of the wing tip and winglet intersection. Since the drag differences obtained between flight test and wind tunnel data were significant, the implications for a production winglet design are important. First a production winglet should be constructed so that no winglet pillowing could occur, possibly by using composite material or reinforced honeycomb techniques. Second, a production winglet should be designed so that the highly sensitive winglet root leading edge area does not experience a peak pressure loss during flight conditions that result in locally supersonic flow in this area. A row of vortex generators to prevent a separation bubble or a winglet root leading edge fairing to prevent local supersonic flow conditions are two possible solutions.

REFERENCES

1. Whitcomb, R. T., "A Design Approach and Selected Wing-Tunnel Results at High Subsonic Speeds for Wing-Tip Mounted Winglets," NASA TN D-8260, dated July 1976.

2. Jacobs, P. F., Flechner, S. G., Montoya, L. C., "Effect of Winglets on a First-Generation Jet Transport Wing, I - Longitudinal Aerodynamic Characteristics of a Semispan Model at Subsonic Speeds," NASA TN D-8473, dated June 1977.

3. Montoya, L. C., Flechner, S. G., Jacobs, P. F., "Effects of Winglets on a First-Generation Jet Transport Wing, II - Pressure and Spanwise Load Distributions For a Semispan Model at HIgh Subsonic Speeds," NASA TN D-8474, dated July 1977.

4. Meyer, R. R., "Effect of Winglets on a First-Generation Jet Transport Wing, IV - Stability Characteristics For a Full-Span Model at Mach 0.30," NASA Technical Paper 1119, dated February 1978.

5. Flechner, S. G., "Effect of Winglets on a First-Generation Jet Transport Wing, VI - Stability Characteristics For a Full-Span Model at Subsonic Speeds," NASA Technical Paper 1330, dated October 1979.

6. Ishimitsu, K. K., VanDevender, N., Dodson, R. O., et al., "Design and Analysis of Winglets For Military Aircraft," AFFDL-TR-76-6, dated February 1976.

7. Dodson, R. O., Ayala, J., Shurtz, R. M., et al., "KC-135 Winglet Flight Research and Demonstration Program - Trade Study Results," AFWAL-TR-81-3031, dated May 1981.

8. Dodson, R. O., Ayala, J., Shurtz, R. M. and Temanson, G., "KC-135 Winglet Flight Research and Demonstration Program," Boeing document D453-10087, to be published as an AFWAL-TR.

9. Temanson, G., "Measurements of the Fuel Mileage of a KC-135 Aircraft With and Without Winglets," to be published in a NASA CP.

10. Boeing document D3-9090, "Summary of the Stability, Control and Flying Qualities Information for All the -135 Series Airplanes," dated October 1973.

11. Bauer, F., Garabedian, P., Korn, D., "Supercritical Wing Sections," Lecture Notes in Economics and Mathematical System 66, 1972.

12. Bauer, F., Garabedian, P., Korn, D., Jameson, A., "Supercritical Wing Sections II," Lecture Notes in Economics and Mathematical Systems 108, 1975.

TABLE 1. — KC-135A WINGLET WIND TUNNEL TESTS

Test		Fuselage	Wing	Winglet	Tail		α Range (deg)	β (deg)	Mach										Data		
					Hor.	Vert.			0.30	0.50	0.70	0.75	0.78	0.80	0.82	0.85	0.90	0.95	Force & moment	Pressure	
																				Wing	Winglet
8 FT TPT	727	A	D	OFF/ON	OFF	OFF	-1/7	0			X	X	X	X					X	X	X
							4/12	0	X										X	X	X
	754	B	E	OFF/ON	OFF	OFF	-2/5	0, ±5		X	X	X	X	X	X	X	X	X	X	X	
	755	C	F	OFF/ON	G	ON	-6/14	0, ±5	X										X		
	766	B	E	OFF/ON	OFF	OFF	-8/14	0, ±5			X		X				X	X	X	X	X
	767	C	F	ON	-10°	ON	-8/16	0, ±5	X										X		X
	772	C	E	OFF/ON	G	ON	-6/16	0, ±5	X	X	X		X		X				X	X	X
7 x 10 HST	20	C	F	ON	-10°	ON	-6/16	0, ±5 ±8, ±12	X										X		X

Fuselage codes: A - Semispan 0.070 scale KC-135A
B - Full span cylindrical body of revolution
C - Full span 0.035 scale KC-135A

Wing codes: D - Semispan 0.07 scale KC-135A
E - Full span 0.035 scale KC-135A; right hand panel has orifice rows
F - Full span 0.035 scale KC-135A; provisions for flaps and ailerons

Hor. tail code: G - OFF, 0°, -4°, -10°

TABLE 2. — KC-135A WINGLET PERFORMANCE BENEFITS PREDICTED FROM WIND TUNNEL DATA

- Flight speed for 99% maximum range
- Climb cruise corrected
- 5% service tolerance (fuel flow increase per MIL-C-5011B)
- Bleed and power extraction included (1.25%)

	W/δ** (lbs)	Mach	L/D*	M(L/D)*	TSFC*/$\sqrt{\theta}$ (lb/hr-lb)	Fuel* Mileage (nm/lb)	Range** Factor (nm)
KC-135A (basic)	882,300	0.79	17.4	13.8	1.1151	0.0407	8084
KC-135A with winglets	933,000	0.79	18.4	14.6	1.1106	0.0433	8597
Percent change relative to KC-135A			5.7%	5.8%	0.4%	6.3%	6.3%

*200,000 lbs gross weight
**Average over gross weight range (includes owe change for winglets)

TABLE 3. — KC-135A WINGLET PERFORMANCE BENEFITS PREDICTED

FROM FLIGHT TEST DATA

- Flight speed for 99% maximum range
- Climb cruise corrected
- 5% service tolerance (fuel flow increase per MIL-C-5011B)
- Bleed and power extraction included (1.25%)

	W/δ** (lbs)	Mach	L/D*	M(L/D)*	TSFC*/$\sqrt{\theta}$ (lb/hr-lb)	Fuel* Mileage (nm/lb)	Range** Factor (nm)
KC-135A (basic)	882,300	0.79	17.4	13.8	1.1151	0.0407	8084
KC-135A with winglets	942,000	0.79	18.43	14.63	1.1114	0.04335	8611
Percent change relative to KC-135A			5.9%	6.0%	0.33%	6.5%	6.5%

*200,000 lbs gross weight
**Average over gross weight range (includes owe change for winglets)

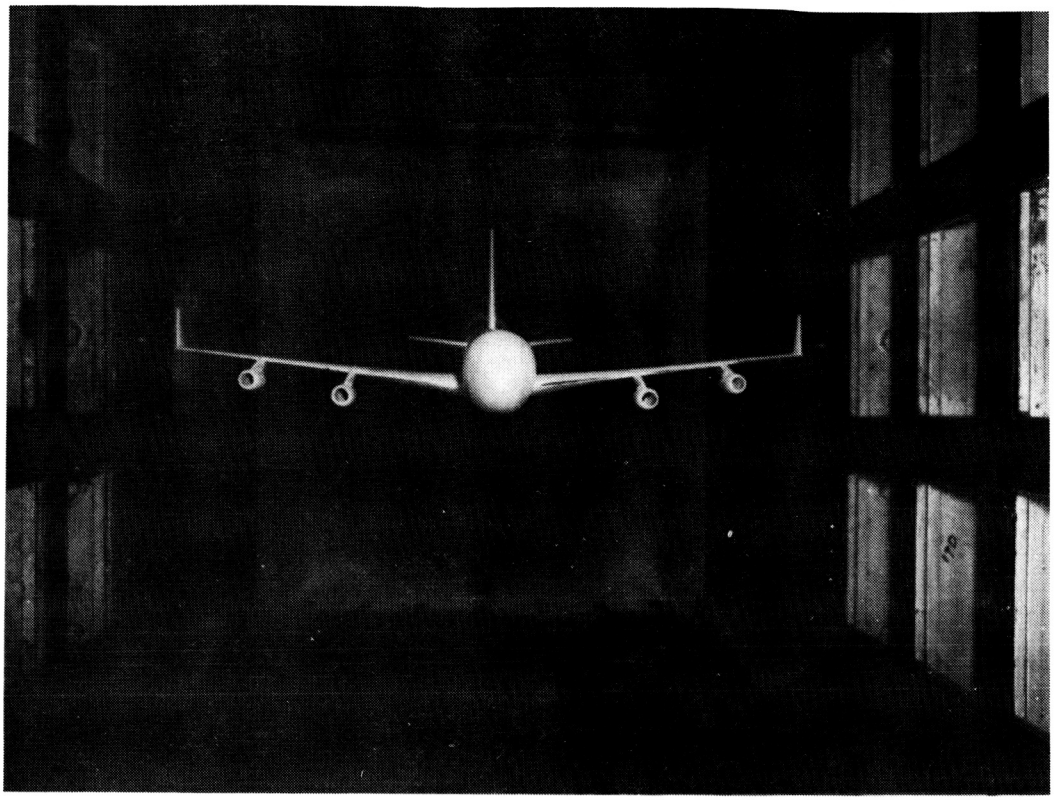

Figure 1. - Rigid wind tunnel model - 0.035 scale

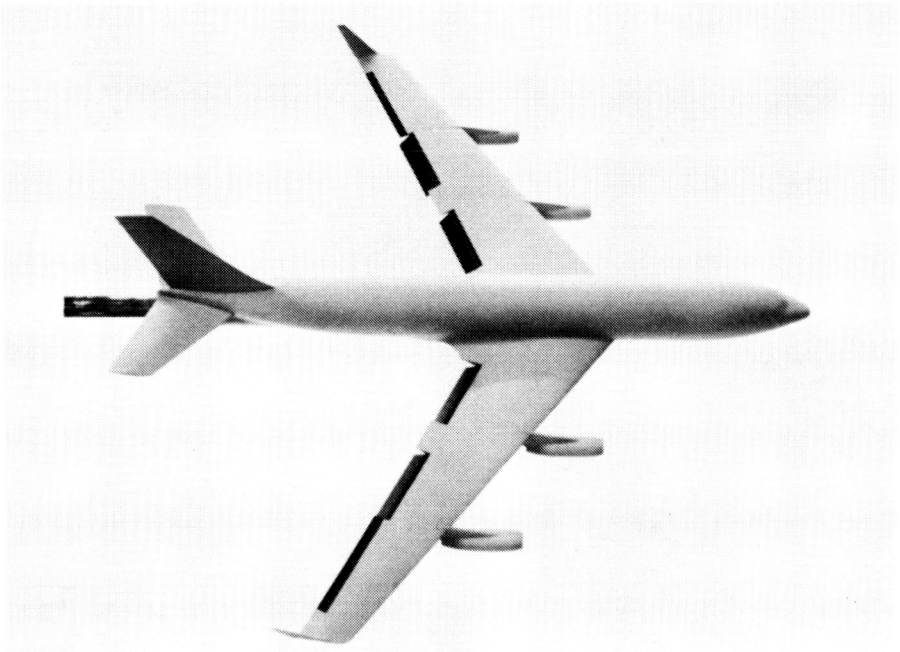

Figure 2. - Flaps down wind tunnel model - 0.035 scale

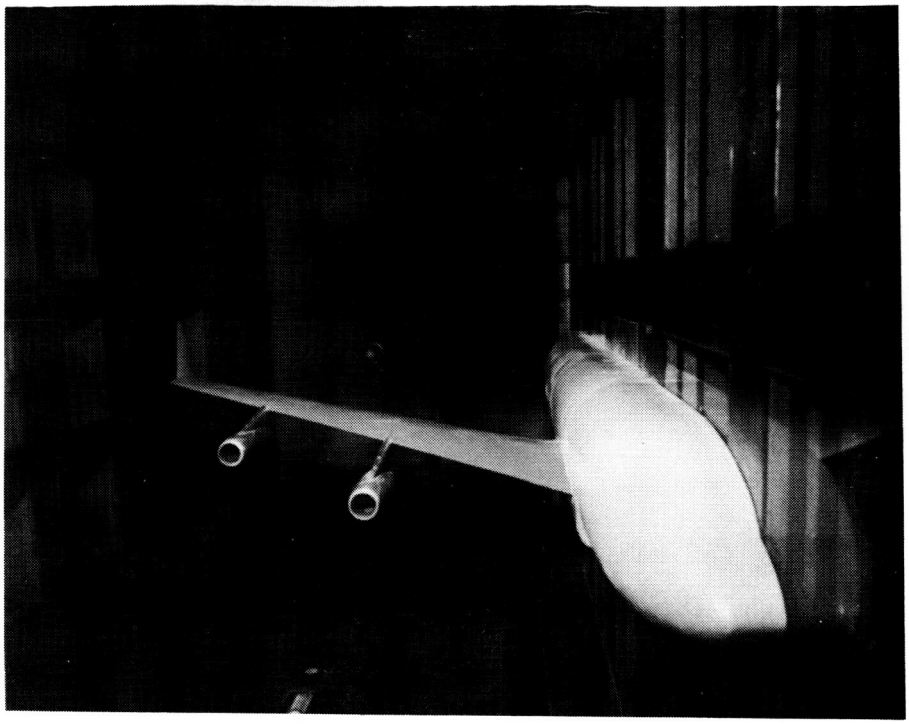

Figure 3. - Wind tunnel half-model - 0.07 scale

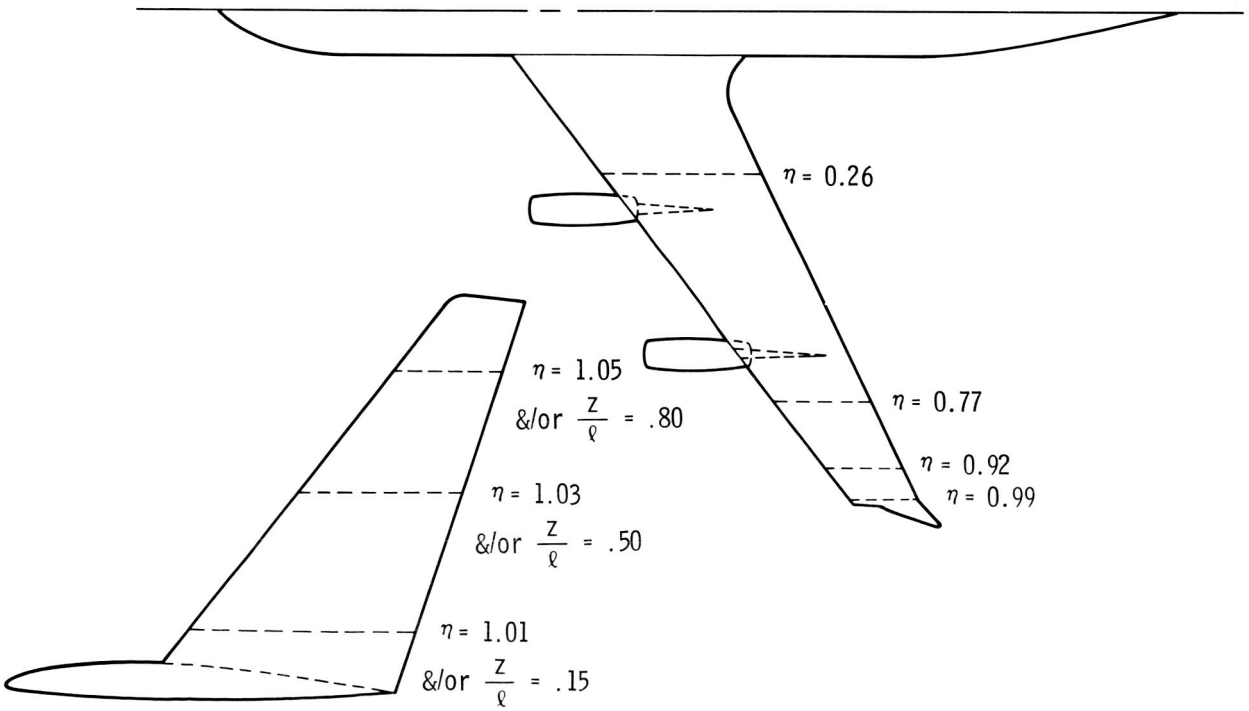

Figure 4. - Wing and winglet static pressure span locations

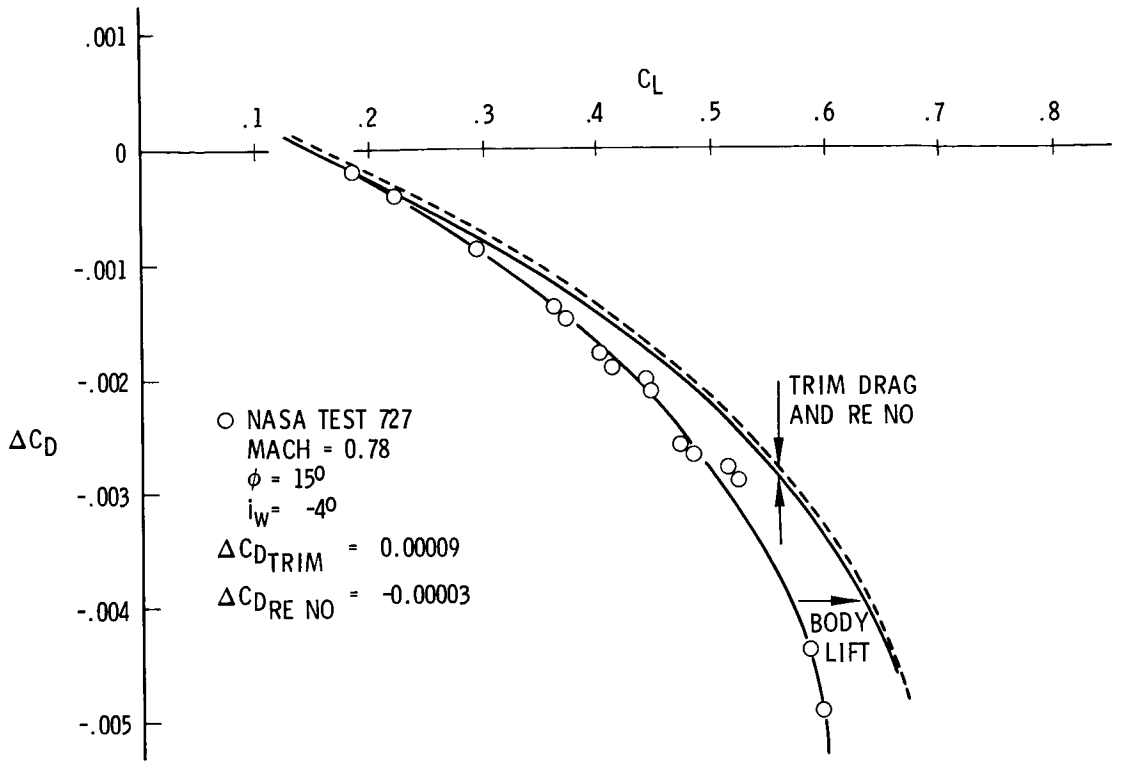

Figure 5. - Winglet drag increment wind tunnel data corrections, 0.07 scale flexible wing half model

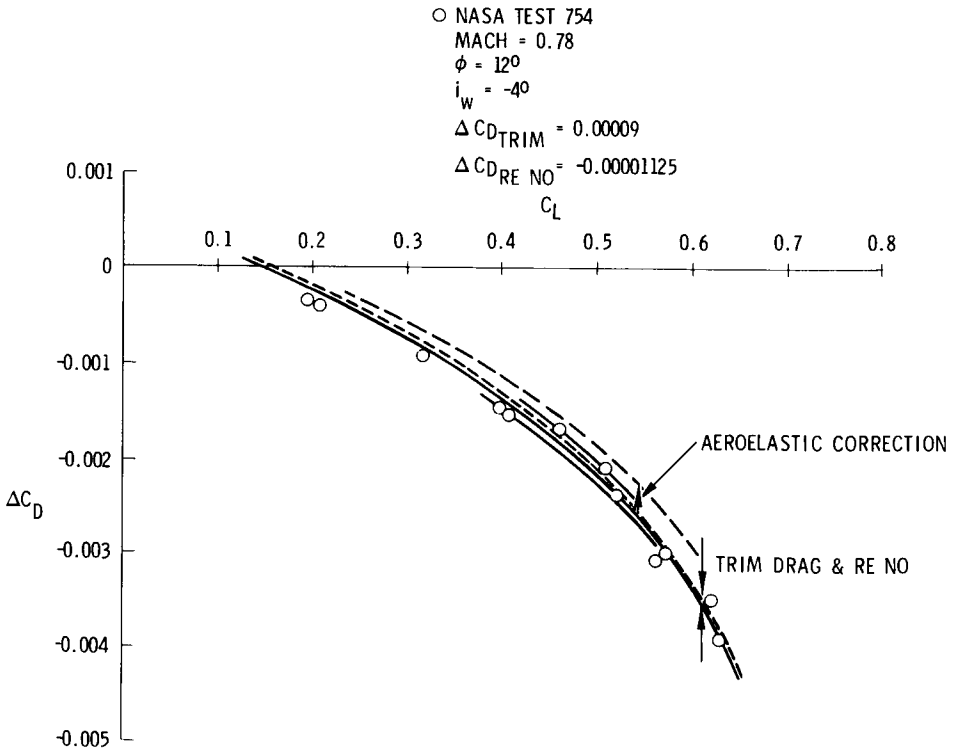

Figure 6. - KC-135 winglet drag increment - wind tunnel data corrections, 0.035 scale rigid full model

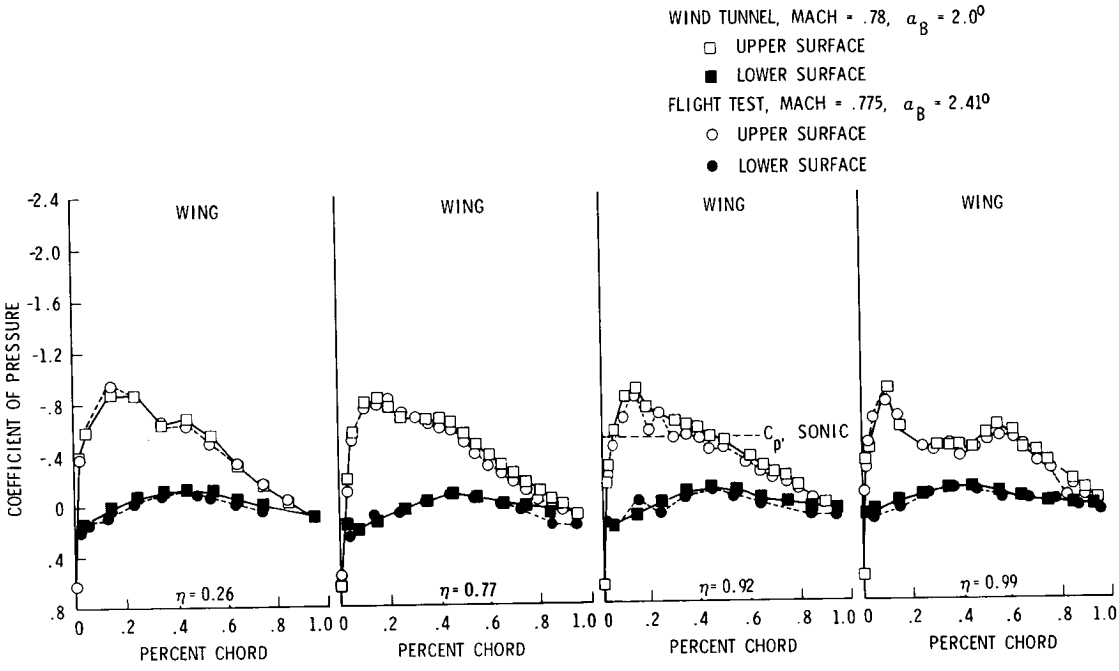

Figure 7. - KC-135 winglet program - flight test and wind tunnel test wing pressure comparison

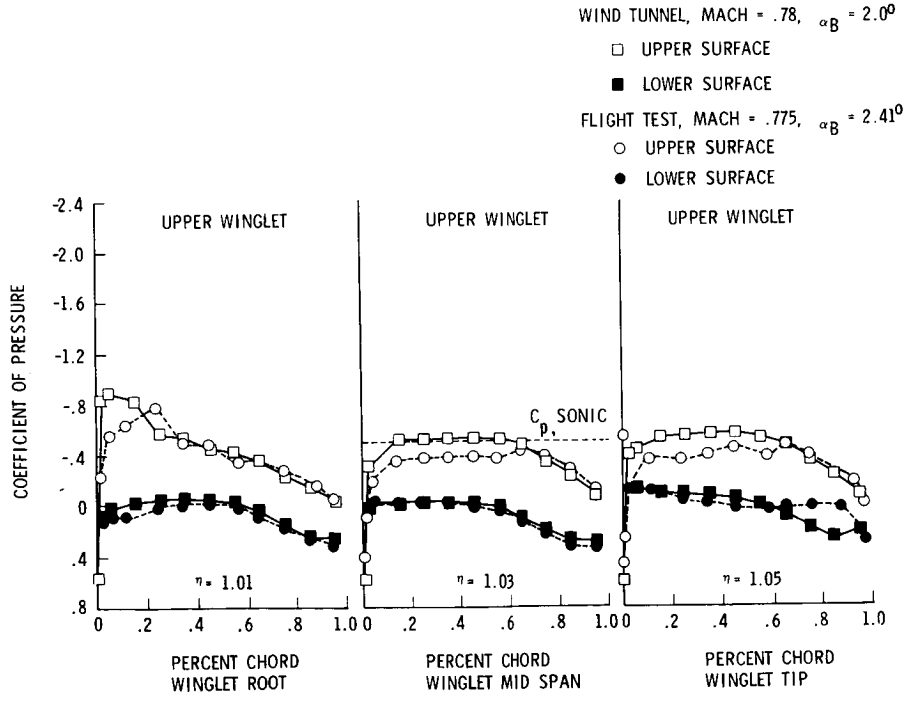

Figure 8. - KC-135 winglet program - flight test and wind tunnel test winglet pressure comparison

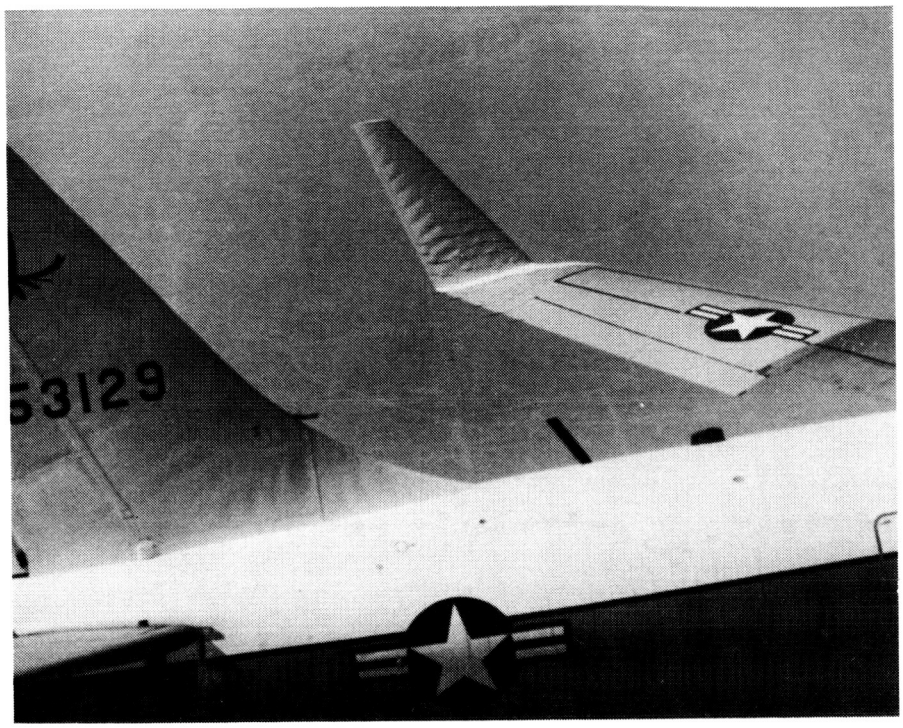

Figure 9. - Winglet in flight with skin "pillowing"

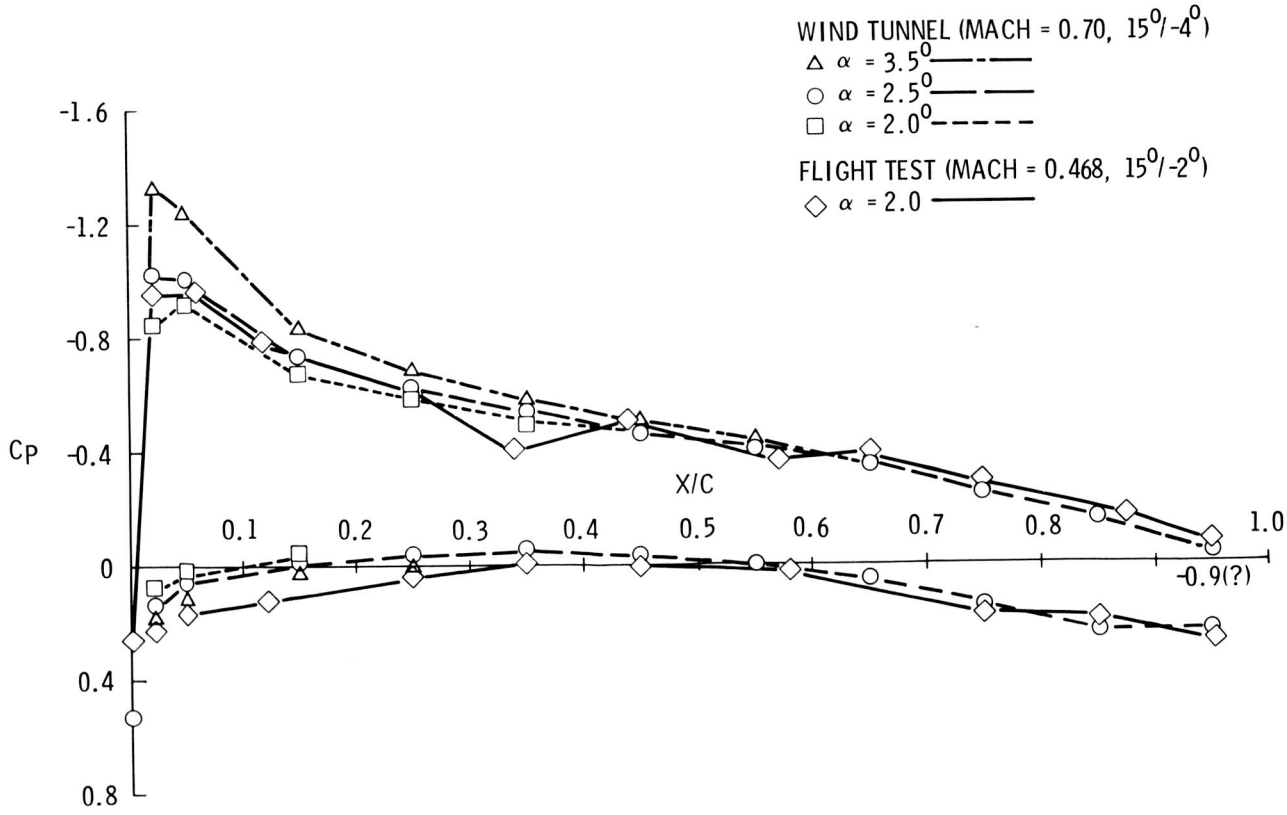

Figure 10. - Pressure comparisons near winglet root, η = 1.01 and/or Z/ℓ = 0.15

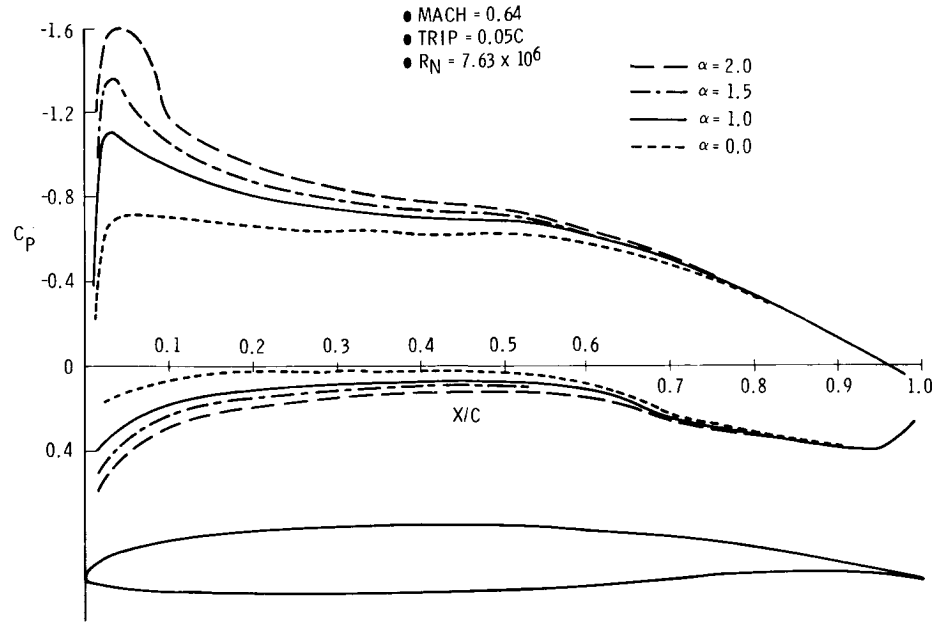

Figure 11. - Bauer-Garabedian-Korn-Jameson 2-D transonic airfoil analysis (smooth airfoil)

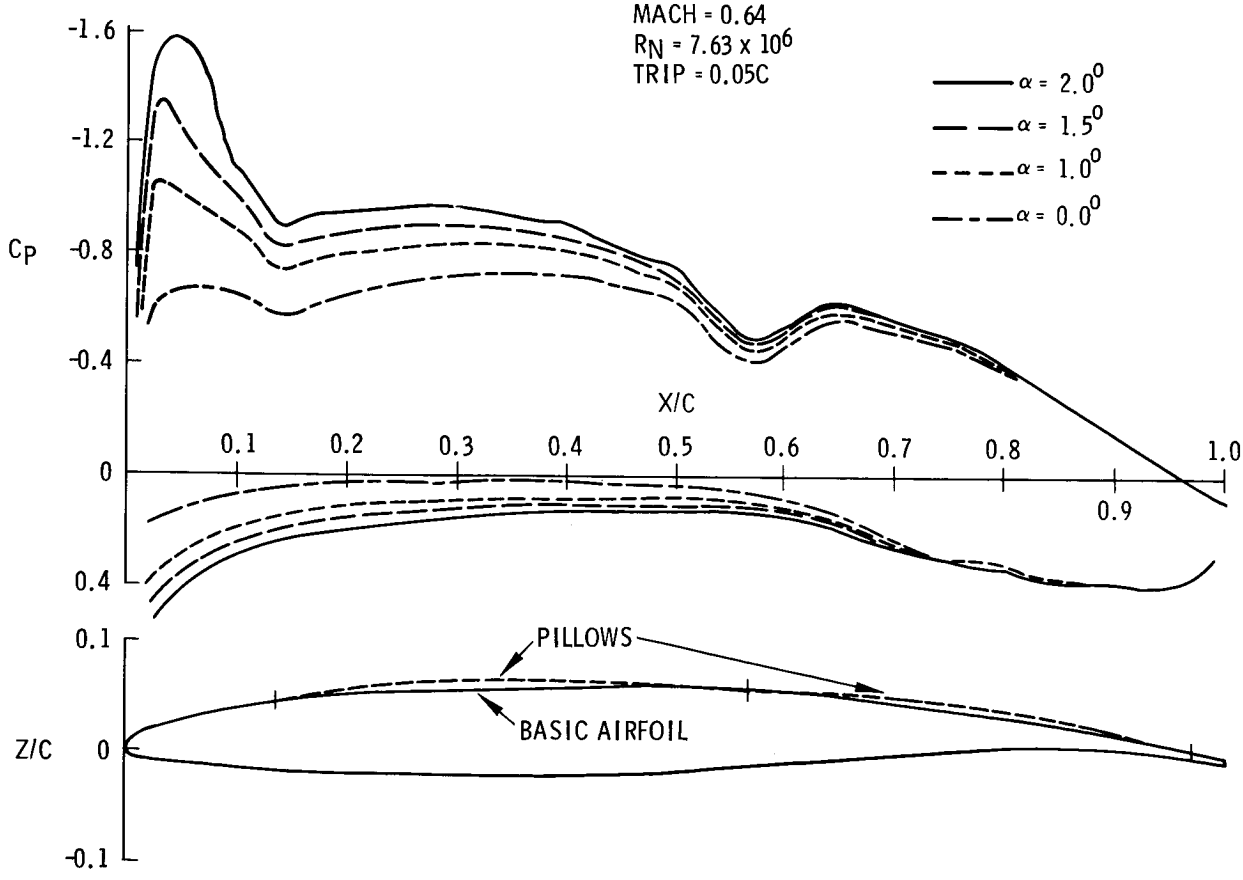

Figure 12. - Bauer-Garabedian-Korn-Jameson 2-D transonic airfoil analysis with 0.004C pillows

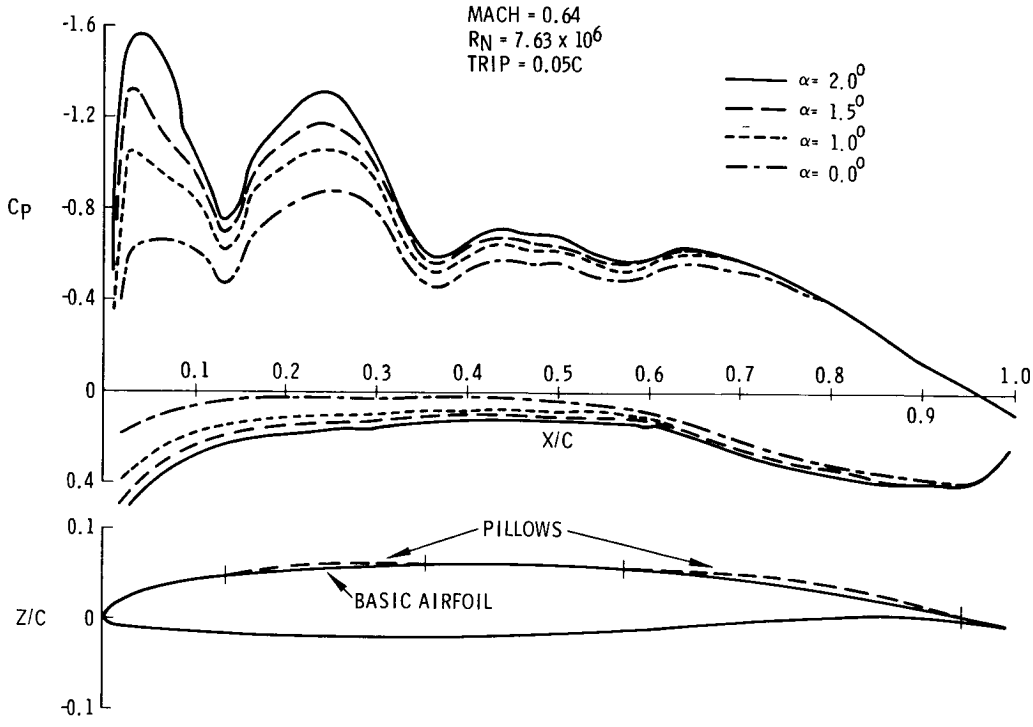

Figure 13. - Bauer-Garabedian-Korn-Jameson 2-D transonic airfoil analysis with 0.004C pillows

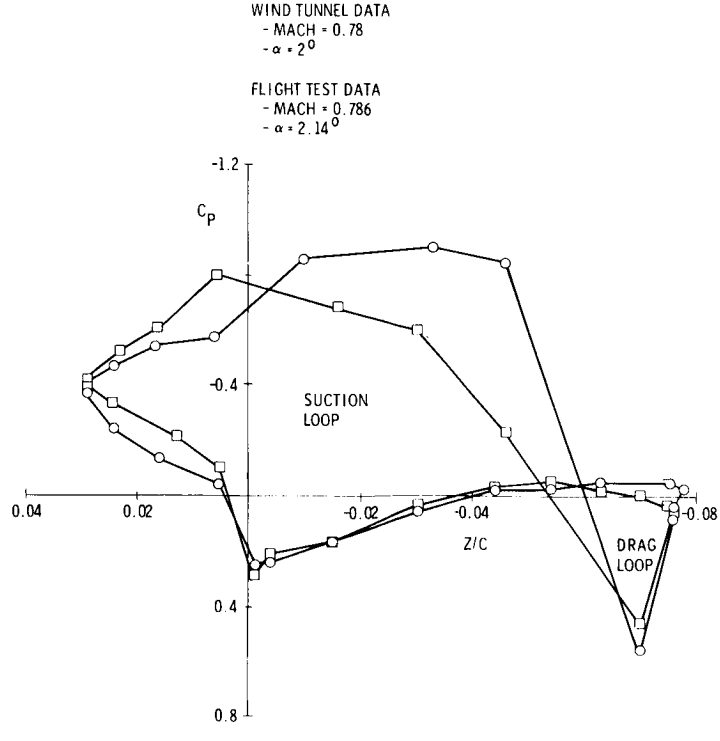

Figure 14. - Sectional drag comparison, η = 1.01

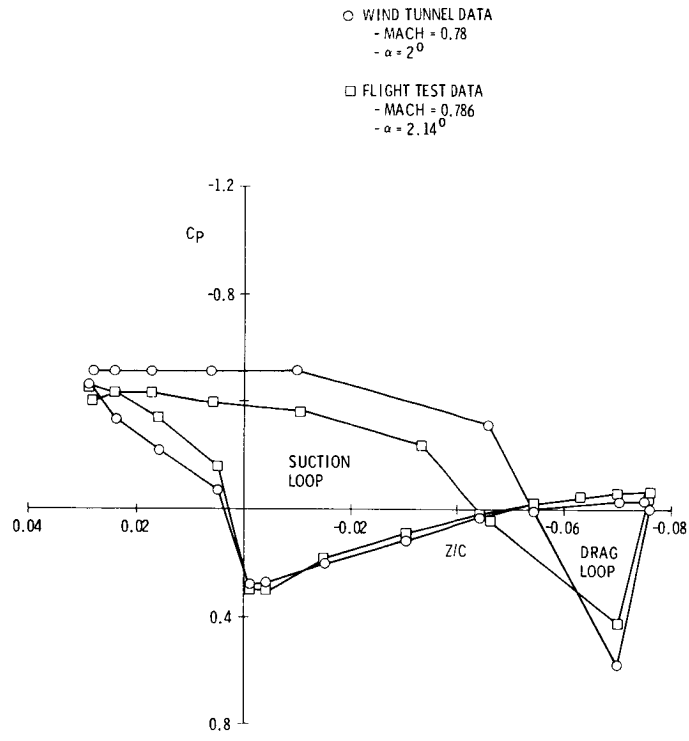

Figure 15. - Sectional drag comparison, $\eta = 1.03$

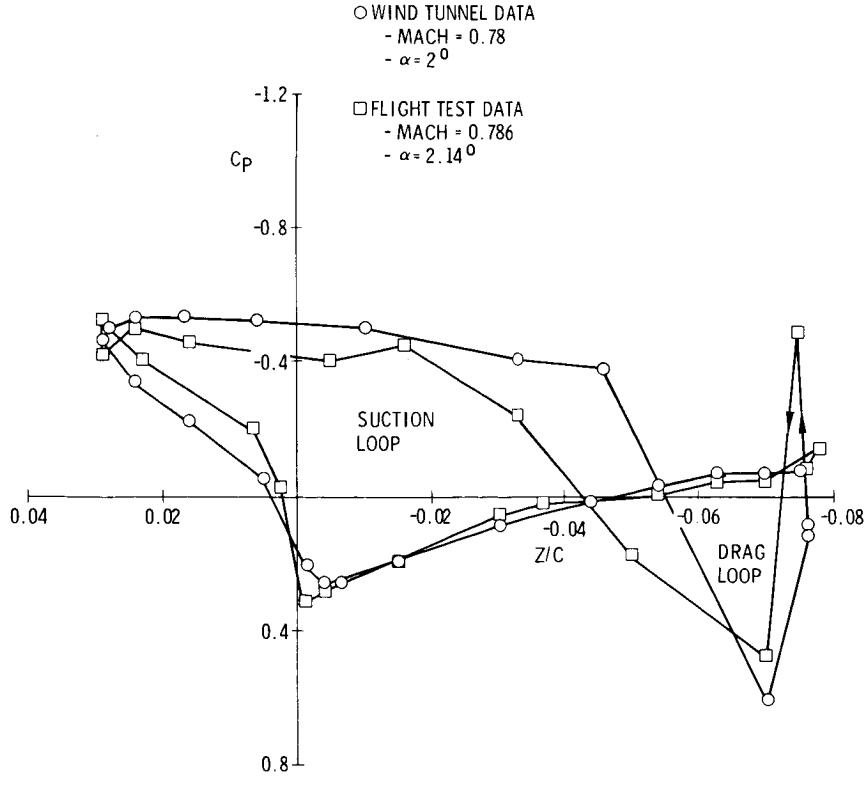

Figure 16. - Sectional drag comparison, $\eta = 1.05$

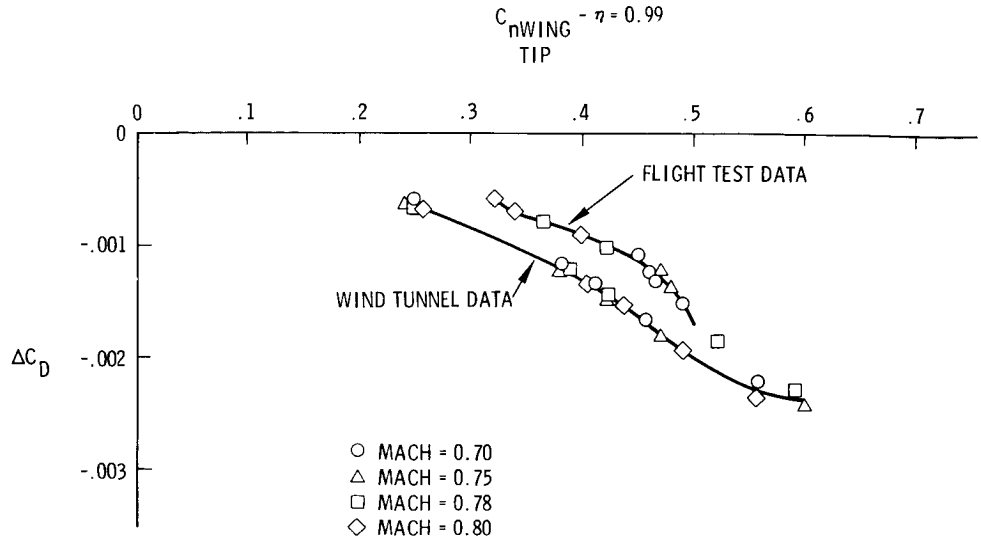

Figure 17. - Comparison of winglet flight test and wind tunnel pressure drag

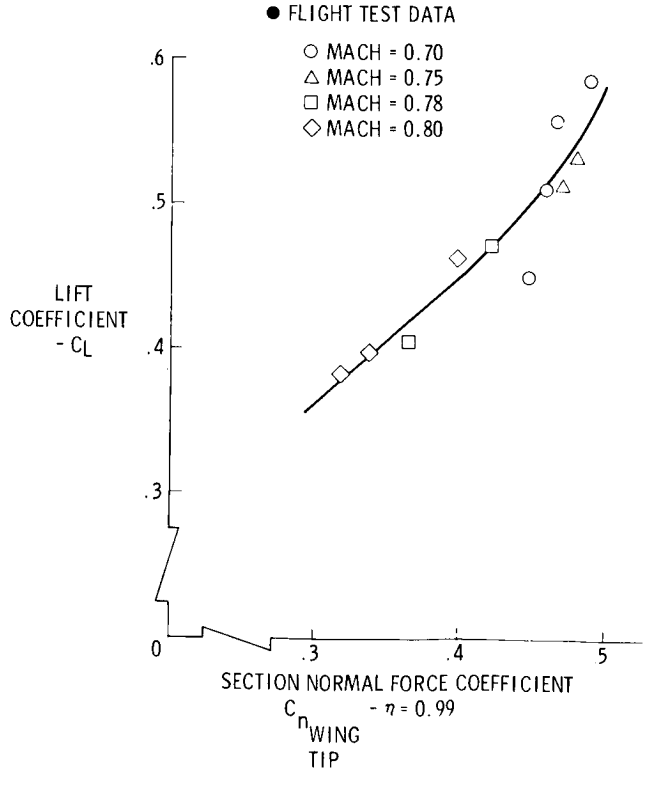

Figure 18. - Airplane lift and wing tip section normal force relationship

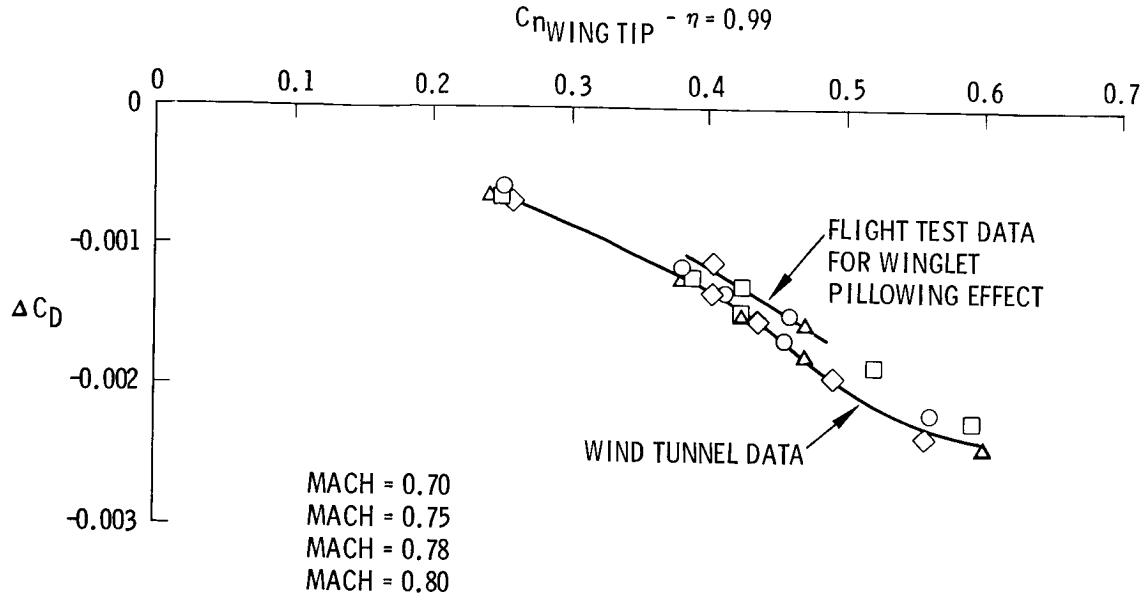

Figure 19. - Comparison of winglet flight test and wind tunnel pressure drag

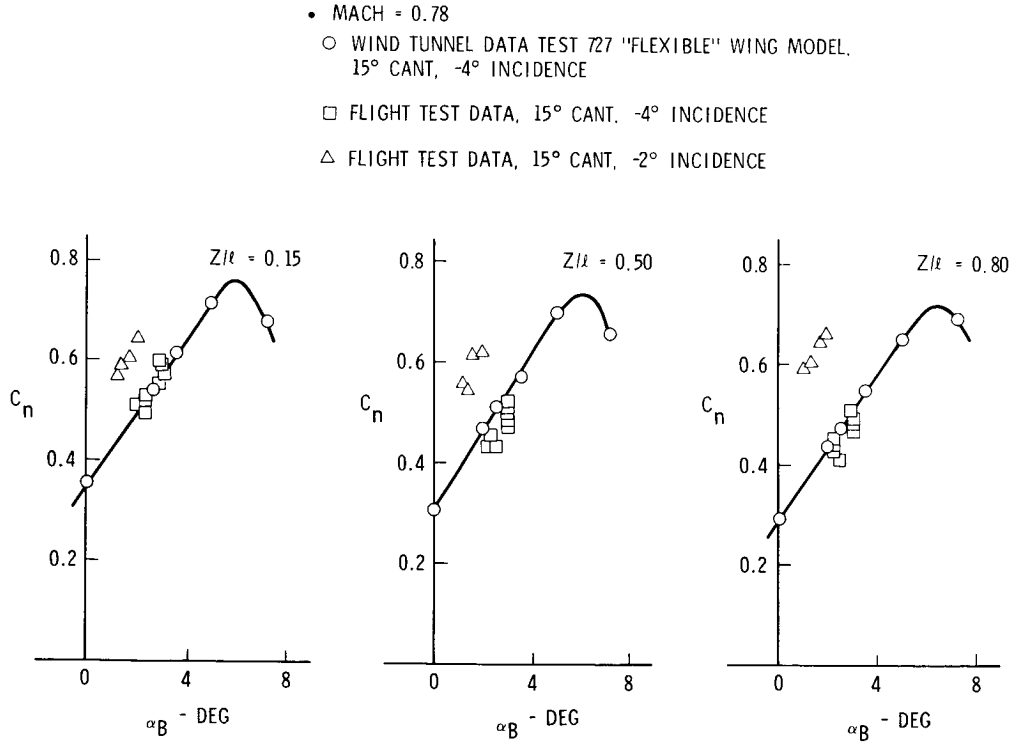

Figure 20. - Comparison of theory, wind tunnel and flight test KC-135 winglets and wing tip pressures, mach = 0.70, ϕ = 15°, i_w = -4°

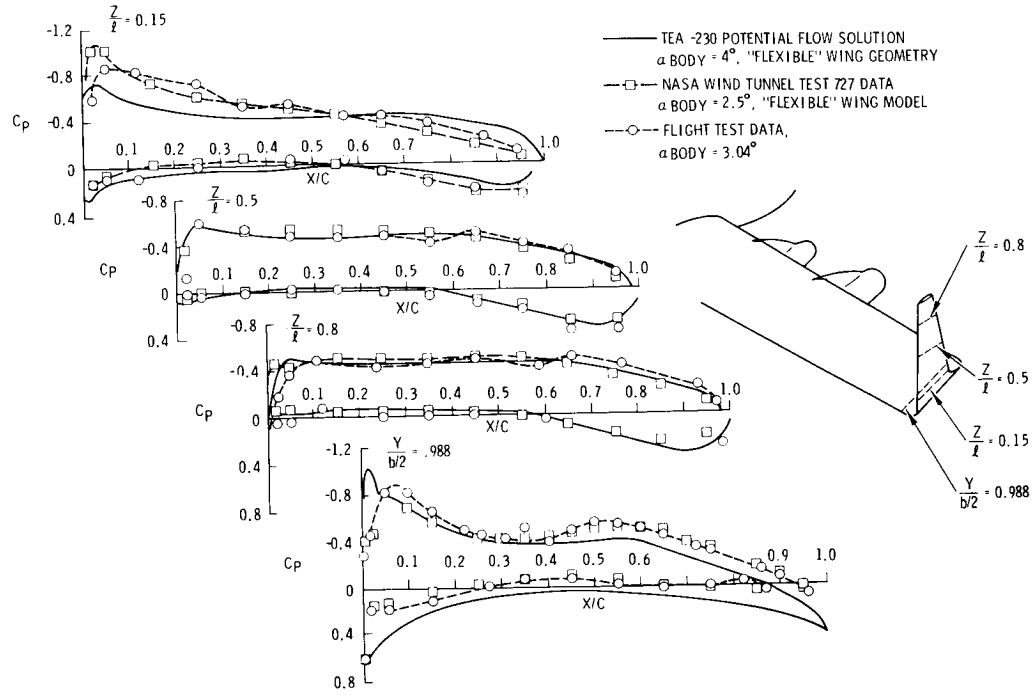

Figure 21. - KC-135 winglet section normal force comparison of wind tunnel to flight test data

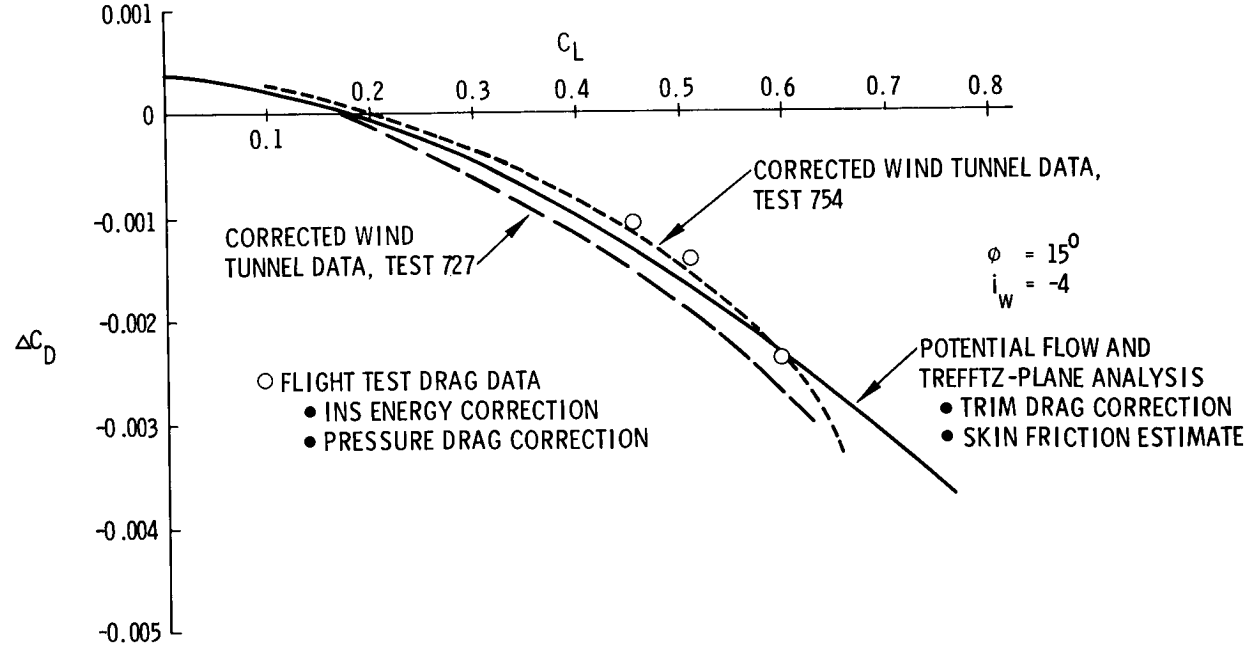

Figure 22. - Comparison of flight measured, theoretical and wind tunnel predicted incremental drag due to winglets, mach = 0.70

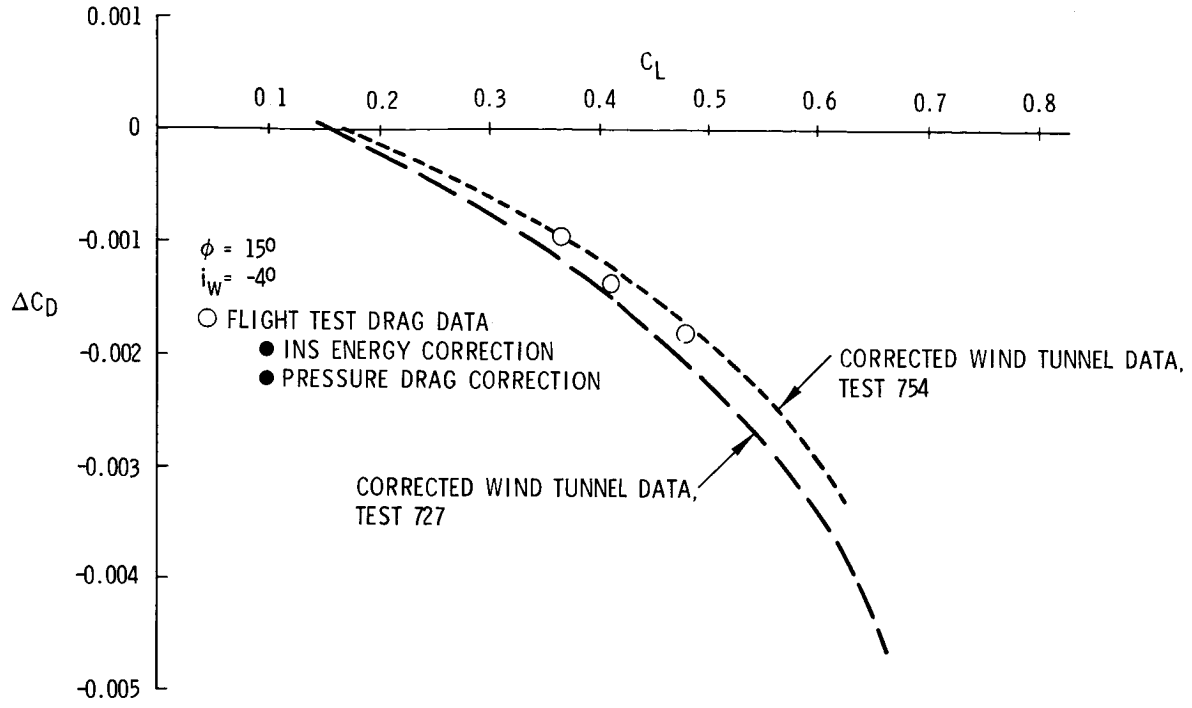

Figure 23. - Comparison of flight measured and wind tunnel predicted incremental drag due to winglets, mach = 0.78

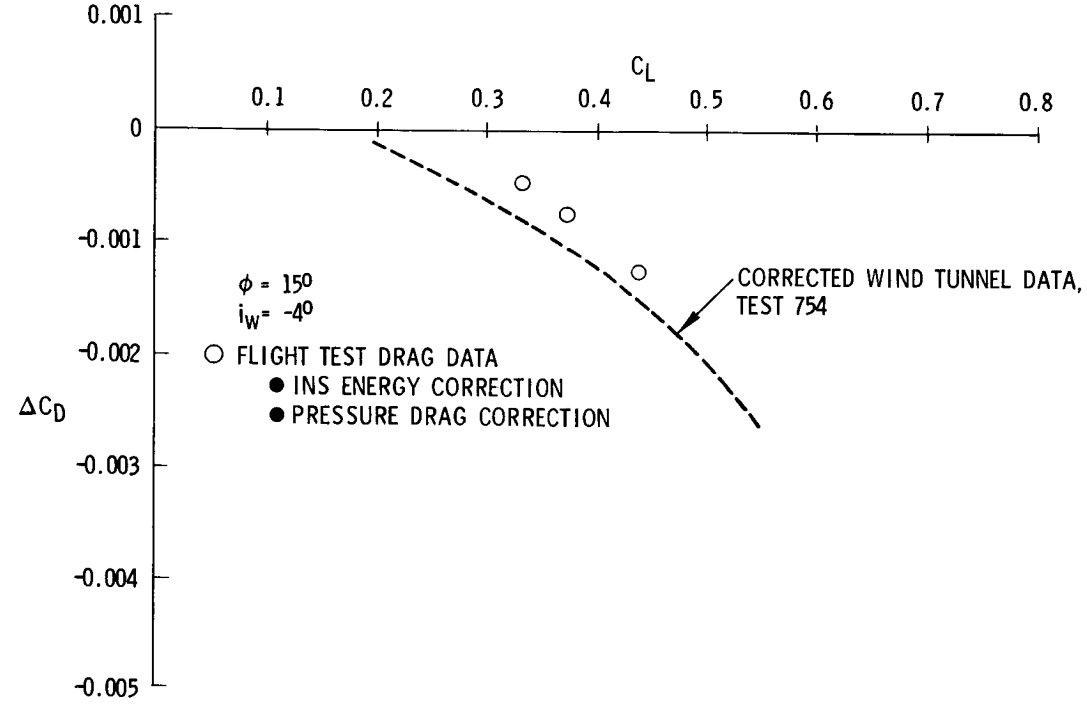

Figure 24. - Comparison of flight measured and wind tunnel predicted incremental drag due to winglets, mach = 0.82

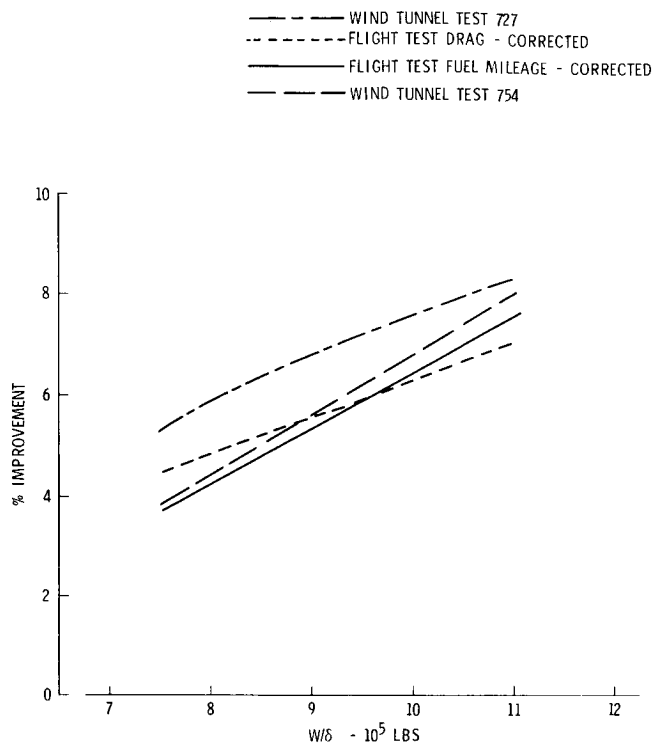

Figure 25. - KC-135A winglet flight test cruise mileage improvement, mach = 0.78

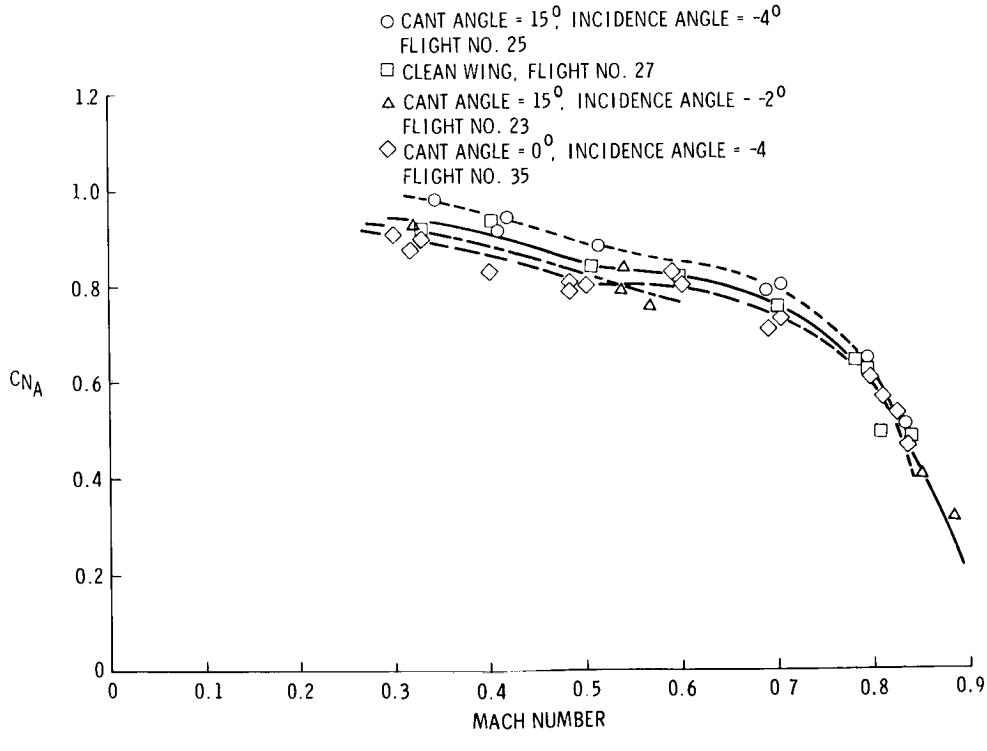

Figure 26. - KC-135 buffet boundaries

KC-135A WINGLET FLIGHT FLUTTER PROGRAM

Michael W. Kehoe
NASA Dryden Flight Research Center

SUMMARY

This paper discusses the evaluation techniques, results and conclusions for the flight flutter testing conducted on a KC-135A airplane configured with and without winglets. Test results are presented for the critical symmetric and antisymmetric modes for a fuel distribution that consisted of 10,000 pounds in each wing main tank and empty reserve tanks. The results indicated that a lightly damped oscillation was experienced for a winglet configuration of 0° cant and -4° incidence. The effects of cant and incidence angle variation on the critical modes are also discussed. Lightly damped oscillations were not encountered for any other winglet cant and incidence angles tested.

INTRODUCTION

A KC-135A aircraft was modified with winglets for use in a flight research and demonstration program to evaluate the effects of winglets on the performance of the airplane. Due to the addition of the winglet and the structural modifications necessary for the attachment to the wing, flight flutter testing of the airplane was required. The methods used to clear the KC-135A with winglets for flutter were:

1. A low speed wind tunnel flutter model test (reference 1).
2. A ground vibration test (GVT) of a cantilevered outer wing panel with the winglet attached (reference 2).
3. A predictive flutter analysis (reference 3).
4. A flight flutter test (reference 4).

The concept used for this program was to compare flight test data for the airplane with winglets off (baseline) versus winglets on to determine the effects of winglets on the basic airplane. The winglets on data were comprised of data for different winglet cant and incident angle configurations.

The objectives of the program were:

1. To provide a flutter clearance for the KC-135A winglet airplane to allow performance and loads testing on the baseline and selected winglet configurations.
2. To obtain frequency and damping information for critical structural modes of vibration.

ABBREVIATIONS

ALT	Altitude
CONF	Configuration
F	Frequency
$\bar{g}$	Damping Coefficient
G	Modal Damping same as $\bar{g}$
GVT	Ground Vibration Test
KCAS	Knots Calibrated Airspeed
KEAS	Knots Equivalent Airspeed
LE	Leading Edge
L/H	Left Hand
R/H	Right Hand
S/N	Serial Number
TE	Trailing Edge
V_D	Limit Dive Speed

WINGLET AND FUEL CONFIGURATIONS TESTED

Flutter testing of the KC-135A winglet airplane was originally planned to be accomplished at an altitude of 21,500 feet for the winglet off (baseline) configuration and for the following winglet cant and incidence configurations:

- 15° cant/-2° incidence.
- 15° cant/-6° incidence.
- 0° cant/-2° incidence.
- 0° cant/-6° incidence.
- USAF selected optimum (later determined to be 15° cant/-4° incidence).

The USAF selected optimum winglet configuration was also to be tested at an altitude of 35,000 feet. Flight testing these configurations would clear all other winglet configurations for flutter.

The flutter speed was dependent on the airplane fuel distribution. The lowest flutter speed for the critical symmetric mode was predicted by analysis and exhibited in the wind tunnel to occur when the wing fuel tanks were nearly empty (light wing fuel loading). The critical antisymmetric mode was predicted to yield the lowest flutter speed with the wing tanks full (heavy wing fuel loading). In order to verify wind tunnel test data and the predictive flutter

analysis, the first winglet configuration (15° cant/-2° incidence) was to be tested with the first five different fuel configurations presented in table 1.

Due to program constraints fuel configuration 2 was eliminated. The locations of the fuel tanks in the airplane are illustrated in figure 1. The winglet off and all other winglet on configurations were to be flight tested in the heavy and light wing fuel configurations. For the flight test program, fuel configurations 5 and 6 were the light and heavy wing loading, respectively.

The test data for the 15° cant/-2° incidence winglet configuration indicated that the lowest damping exhibited for the antisymmetric mode was with fuel configuration 4. The lowest damped symmetric mode was exhibited with fuel configuration 5 but there was not a significant change in damping trend or level between configurations 4 and 5. The antisymmetric mode appeared to be the most critical so it was decided to test all other winglet configurations with fuel configurations 4 and 6 instead of 5 and 6.

During the first flutter flight, significant skin wrinkling was noticed on the winglets. Due to uncertainty of the effect of the wrinkling on the performance of the winglets, program engineers chose to deviate from the flight test plan and to test the 15° cant/-4° incidence winglet configuration next. It was at this configuration that the majority of wind tunnel pressure distribution data had been acquired. Subsequently, a decision was made not to test all four corners of the winglet configuration matrix (figure 2) for flutter, but to limit the remaining configurations to those specifically needed to be cleared for performance testing.

ENVELOPE EXPANSION

Flutter testing was accomplished at an altitude of 21,500 feet. A maximum Mach number of 0.91 and airspeed of 395 knots equivalent airspeed (KEAS) were attainable at this altitude. Each flutter flight consisted of a constant altitude, incremental airspeed flight envelope expansion. Aircraft dives were required for test points above 390 knots calibrated airspeed (KCAS). The incremental airspeed test points are illustrated in figure 3. The yaw damper was off and the rudder boost power was on for all these test points.

Test points at 300, 350 and 390 KCAS were repeated with the autopilot turned on to evaluate the effect of the autopilot on the flutter characteristics of the airplane.

INSTRUMENTATION

Flutter instrumentation onboard the airplane consisted of accelerometers and control surface position indicators as listed in table 2. Locations of the instrumentation on the airplane are shown in figure 4. The airspeed and altitude were measured from a nose boom installed on the test airplane.

EXCITATION

The structure was excited at each test point by pilot induced control surface pulses. The excitation consisted of nose-up and nose-down elevator pulses, left and right rudder pulses and left and right aileron pulses for all straight and level test points. For test points that required dives, only a nose-up elevator pulse, a left rudder pulse and left aileron pulse were accomplished.

Random atmospheric turbulence was used to excite the structural modes of vibration which were not excited by control surface pulses. Typically, two minutes of random data were collected at the test points of interest.

TEST RESULTS

Eight symmetric and five antisymmetric modes were tracked during the program for each winglet configuration tested. The velocity/frequency and velocity/damping plots for each winglet configuration tested are contained in reference 4.

Significant skin wrinkling was present on the winglets during all flights. The depth of the wrinkles appeared to increase with an increase in dynamic pressure. A review of pressure distributions and modal frequency data indicated that the winglet skin wrinkling did not have a significant effect on the flutter characteristics of the winglet.

The damping values calculated for autopilot-on test points were similar to data calculated for autopilot-off test points. The autopilot-on data did not reveal any significant changes in structural damping for all winglet configurations tested.

The winglet structural modes were monitored during data analysis. The pilot induced pulses did not excite the winglet modes because of the low frequency content of the pulses. Random data were acquired at selected test points to analyze the winglets modes. The damping levels of the winglet were satisfactory from a flutter standpoint.

SUMMARY OF TEST RESULTS FOR ELEVATOR EXCITATION

The critical mode excited by elevator pulses was approximately 4.5 Hz. The flight test data indicated the 4.5 Hz mode consistently exhibited a flat damping trend with damping values generally lower than other modes excited by elevator pulses. Flight test results also indicated the damping to be the lowest for this mode in fuel configuration 5 (2,500 pounds in each wing main tank, reserve tanks empty). The response of this mode was most clearly indicated by the wing tip longitudinal accelerometer.

Predictive flutter analysis indicated that a 4.6 Hz symmetric mode exhibited the lowest flutter speed for a fuel configuration which included empty body and center wing tanks, empty outboard main and reserve tanks, and inboard main tanks 46 percent full. The analysis predicted a 35 percent

margin of safety. Wind tunnel testing indicated the frequency of the critical symmetric mode to be 4.5 to 4.8 Hz for the same fuel configuration.

A comparison of the frequency and damping trends between the baseline and winglets on configurations is presented in figures 5 and 6 for the 4.5 Hz mode. The fuel loading was configuration 4. The data points were faired so that the general data trends can be followed. The baseline frequency (4.9 Hz) was greater than the frequencies for the winglets on configurations ($\cong$4.5 Hz).

The comparison of the cant angle variation results (figure 5) yielded:

1. The baseline configuration exhibited the highest damping values.
2. As the cant angle was decreased from 15° to 0°, the damping increased.
3. The damping trends were fairly flat.
4. The winglets on frequency trends exhibited a small increase in frequency as airspeed was increased.

The comparison of the incidence angle variation (figure 6) results yielded:

1. The baseline configuration exhibited the highest damping values.
2. As the incidence angle was increased from -2° to -4°, the damping decreased.
3. The damping trends were fairly flat.
4. The winglets on frequency trends revealed a small increase in frequency as airspeed was increased.

SUMMARY OF TEST RESULTS FOR AILERON AND RUDDER EXCITATION

The critical mode excited by aileron and rudder pulses was a 3.0 Hz antisymmetric mode. A damping of $\bar{g}$ = 0.015 was obtained for this mode at 370 KEAS with fuel configuration 4 (10,000 pounds in each wing main tank, empty reserves) for the 0° cant/-4° incidence winglet configuration. Wind tunnel test data indicated that a 2.8 Hz mode was the critical antisymmetric mode. However, the critical wind tunnel fuel configuration was with wing main and reserve fuel tanks full.

A 4.3 Hz antisymmetric mode was analytically predicted to have the lowest flutter speed. The fuel configuration in the analysis was:

Tank	Percent Full
Forward Body	90.2
Center Wing	47.3
Aft Body	100
Upper Deck	42.8
Wing Inboard Main	100
Wing Outboard Main	100
Reserve	100

The predicted flutter speed margin of safety for this antisymmetric mode was greater than the margin for the critical symmetric mode (4.6 Hz).

A comparison of the frequency and damping trends between the baseline and winglets on configurations is presented in figures 7 and 8 for the 3.0 Hz mode. The fuel loading was configuration 4. The frequency of the baseline configuration was lower than the frequency of the winglets on configurations in spite of the increased wing tip mass. The difference is most likely due to the aerodynamic effects of the winglets on the wing structure.

A comparison of the cant angle variation results (figure 7) yielded:

1. At airspeeds below 330 KEAS, the damping level was about equal for the baseline and winglets on configurations.
2. At airspeeds above 330 KEAS, the baseline configuration had the highest level of damping.
3. At airspeeds above 360 KEAS, the damping decreased as the cant angle decreased from 15° to 0°. Testing was terminated at 370 KEAS for the 0° cant configuration.
4. The baseline and the 15° cant configuration frequency trends exhibited an increase in frequency as the airspeed was increased above 340 KEAS.
5. The 0° cant configuration exhibited a fairly flat frequency trend.

A comparison of the incidence angle variation (figure 8) revealed:

1. At airspeeds above 360 KEAS, the baseline configuration exhibited the highest damping.
2. The -2° and -4° incidence angle data exhibited similar damping trends.
3. At airspeeds above 340 KEAS, the frequency trends for the baseline and winglets on configurations increased in frequency as airspeed was increased.

Testing was terminated at 370 KEAS with fuel configuration 4 due to a lightly damped 3.0 Hz antisymmetric oscillation in the 0° cant/-4° incidence winglet configuration. The damping exhibited at termination was $\bar{g} = 0.015$. The 3.0 Hz mode was best excited by aileron pulses. The time history traces of several accelerometers responding to an aileron pulse at 370 KEAS are presented in figure 9. The inflight mode shape of this 3.0 Hz oscillation is presented in table 3. The frequency and damping trends for a 2.6 Hz mode and 3.0 Hz mode are presented in figure 10. The data exhibited a constant increase in frequency for the 2.6 Hz mode while the 3.0 Hz mode frequency trend remained flat. Both modes exhibited wing bending and wing torsion at all airspeeds. It appeared that the coalescence of these two modes was the cause of the oscillation for this flight configuration. The coalescence of the 2.6 Hz and 3.0 Hz modes did not occur in other winglet configurations that were flight flutter tested. The damping trends for both modes exhibit a constant decrease in damping starting at 330 KEAS. The modes could no longer be separated at airspeeds above 355 KEAS. There were no adverse damping trends exhibited for the 0° cant/-4° incidence winglet configuration with fuel configuration 6. Testing was terminated at 382 KEAS due to the onset of Mach buffet. It was thought that keeping the airplane out of buffet would help reduce the number of fuel leaks

that were occurring in the airplane. There was no indication from the flutter data obtained that the testing could not have continued to 395 KEAS.

CORRELATION WITH ANALYSIS

A comparison of flight test data with analysis for the 3.0 Hz antisymmetric mode is presented in figure 11. The winglet configuration was 0° cant/ -4° incidence. The fuel loading was fuel configuration 4. This analysis (figure 11) was accomplished after the flight test data was obtained. The exact fuel distribution was incorporated in the analysis. The flight test damping exhibited a steep slope toward zero damping around 500 knots true airspeed (KTAS). The analysis does not predict a flutter speed with either 0.85 or 0.95 Mach number aerodynamics. There is no explanation at this time for the lack of correlation between the flight test data and the analysis.

CONCLUDING REMARKS

Flight flutter testing was accomplished for the KC-135A winglet airplane in the baseline (modified wing tips - no winglets) configuration to a maximum airspeed of 397 KEAS at an altitude of 21,500 feet with the wing main and reserve tanks full of fuel. The aircraft was also tested to a maximum airspeed of 395 KEAS at an altitude of 21,500 feet with 10,000 pounds of fuel in each wing main tank and reserve tanks empty. The results showed satisfactory damping and damping trends for all structural modes.

Flutter testing was also accomplished for the KC-135A winglet airplane configured in the following conditions:

Cant (degrees)	Incidence (degrees)	Maximum Airspeed (KEAS) Tested	Fuel
15	-2	393	Wing Main Tanks Full, Reserve Tanks Full, Minimum Body Fuel
15	-2	399	10,000 lbs in Main Tanks 1,300 lbs in Reserve Tanks
15	-2	392	10,000 lbs in Main Tanks Empty Reserve Tanks
15	-2	399	2,500 lbs in Main Tanks Empty Reserve Tanks
15	-4	398	Wing Main Tanks Full Reserve Tanks Full
15	-4	395	10,000 lbs in Main Tanks Empty Reserve Tanks
0	-4	370	10,000 lbs in Main Tanks Empty Reserve Tanks
0	-4	382	Wing Main Tanks Full Reserve Tanks Full

The results revealed satisfactory damping for all winglet configurations tested except the 0° cant/-4° incidence configuration. Testing was terminated in this winglet configuration at 370 KEAS at an altitude of 21,500 feet due to a lightly damped ($\bar{g}$ = 0.015), 3.0 Hz antisymmetric oscillation. The fuel distribution at this condition was 10,000 pounds in each wing main tank and empty wing reserve tanks.

As the cant angle was decreased from 15° to 0°, the damping of the critical symmetric mode increased. As the incidence angle was increased from -2° to -4°, the damping decreased. The critical symmetric mode exhibited the highest damping in the baseline configuration.

The critical antisymmetric mode exhibited the highest damping in the baseline configuration. At airspeeds above 330 KEAS, the damping level decreased with winglets installed on the airplane regardless of cant or incidence angle configuration. The -2° and -4° incidence angle data exhibited similar damping trends. At airspeeds above 360 KEAS, the damping decreased as the cant angle decreased from 15° to 0°.

REFERENCES

1. Schneider, F. C., and Shoup, G. S.: "KC-135A Winglet Flutter Model Test," Boeing Document D3-11353-1, Boeing Wichita Company, Wichita, Kansas, May 5, 1978.

2. Shoup, G. S.: "KC-135 Winglet Ground Vibration Test Report," Boeing Document D3-11591-1, Boeing Wichita Company, Wichita, Kansas, June 12, 1979.

3. French, H. S., and Shoup, G. S.: "KC-135 Winglet Flutter Analysis and Test," Boeing Document D3-11437-1, Boeing Wichita Company, Wichita, Kansas, January 5, 1979.

4. Kehoe, M. W.: "KC-135A Winglet Flight Flutter Test Program," AFFTC-TR-81-4, Air Force Flight Test Center, Edwards Air Force Base, California, June 1981.

TABLE 1. - PLANNED TEST FUEL CONFIGURATIONS

Fuel Configuration Number	Center Wing and Body Fuel	Wing Fuel - Pounds Per Tank	
		Main Tanks	Reserves
1	Note 1	Full	Full
2	Note 3	Full	Full
3	Note 2	10,000	1,300
4	Note 2	10,000	0
5	Note 2	2,500	0
6	Note 2	Full	Full

Notes

1. As required to complete condition with minimum body fuel.
2. As required to accomplish testing.
3. As required to maintain a gross weight above 230,000 pounds at end of test condition.

TABLE 2. - AIRCRAFT FLUTTER INSTRUMENTATION

Item No.	Parameter Identification
1	R/H Wing Tip LE Normal Acceleration
2	R/H Wing Tip TE Normal Acceleration
3	R/H Wing Tip LE Longitudinal Acceleration
4	R/H Winglet LE Normal Acceleration
5	R/H Winglet TE Normal Acceleration
6	R/H Winglet LE Longitudinal Acceleration
7	L/H Wing Tip LE Normal Acceleration
8	L/H Winglet LE Normal Acceleration
9	L/H Winglet LE Longitudinal Acceleration
10	R/H Otbd Nacelle Normal Acceleration
11	R/H Otbd Nacelle Lateral Acceleration
12	Aft Body Normal Acceleration
13	Aft Body Lateral Acceleration
14	R/H Horizontal Stabilizer Acceleration
15	Vertical Fin Lateral Acceleration
16	L/H Inbd Aileron Position
17	R/H Inbd Aileron Position
18	L/H Otbd Aileron Position
19	R/H Otbd Aileron Position
20	L/H Elevator Position
21	R/H Elevator Position
22	Rudder Position
23	Lower Wing Skin Panel Acceleration

See Figure 4 for locations

TABLE 3. - 3.0 Hz LIGHTLY DAMPED OSCILLATION MODE SHAPE
Reference: R/H Fwd Wing Tip Normal Accelerometer
Flight Conditions: 370 KEAS, 21,500 ft.,
Fuel Configuration 4

Accelerometer	Phase (Degrees)	Direction of Motion	Normalized Amplitude
R/H Fwd Wingtip Normal	---	Up	1.0
R/H Rear Wingtip Normal	0	Up	1.16
R/H Wingtip Longitudinal	180	Rear	0.29
R/H Fwd Winglet Normal	0	Inboard	0.29
R/H Winglet Longitudinal	0	Fwd (R/H Wing LE Down)	1.19
L/H Fwd Wingtip Normal	180	Outboard	0.19
Aft Body Lateral	0	Right	0.16
Vertical Fin Lateral	0	Right	0.48
R/H Horizontal Stabilizer	180	Down	0.5

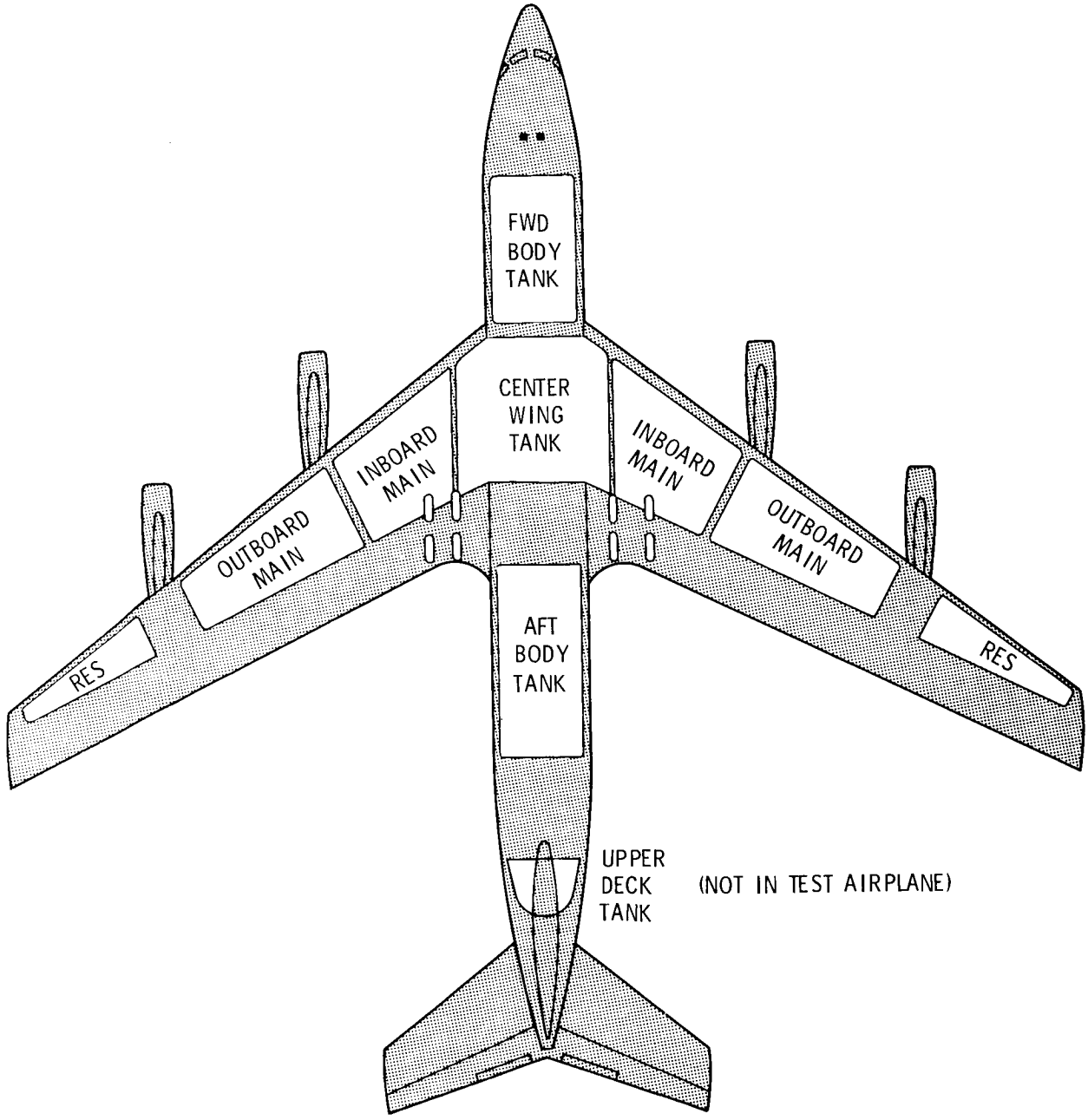

Figure 1. - Airplane fuel tank locations

ORIGINAL PLAN

WINGLET INCIDENCE	WINGLET CANT ANGLE 0	7.5	15
-2	FUEL CONF. 5 FUEL CONF. 6		FUEL CONF. 1 FUEL CONF. 2 FUEL CONF. 3 FUEL CONF. 4 FUEL CONF. 5
-4			
-6	FUEL CONF. 5 FUEL CONF. 6		FUEL CONF. 5 FUEL CONF. 6

FLIGHT TESTED

WINGLET INCIDENCE	WINGLET CANT ANGLE 0	7.5	15
-2			FUEL CONF. 1 FUEL CONF. 3 FUEL CONF. 4 FUEL CONF. 5
-4	FUEL CONF. 4 FUEL CONF. 6		FUEL CONF. 4 FUEL CONF. 6
-6			

Figure 2. - Winglet configuration matrix

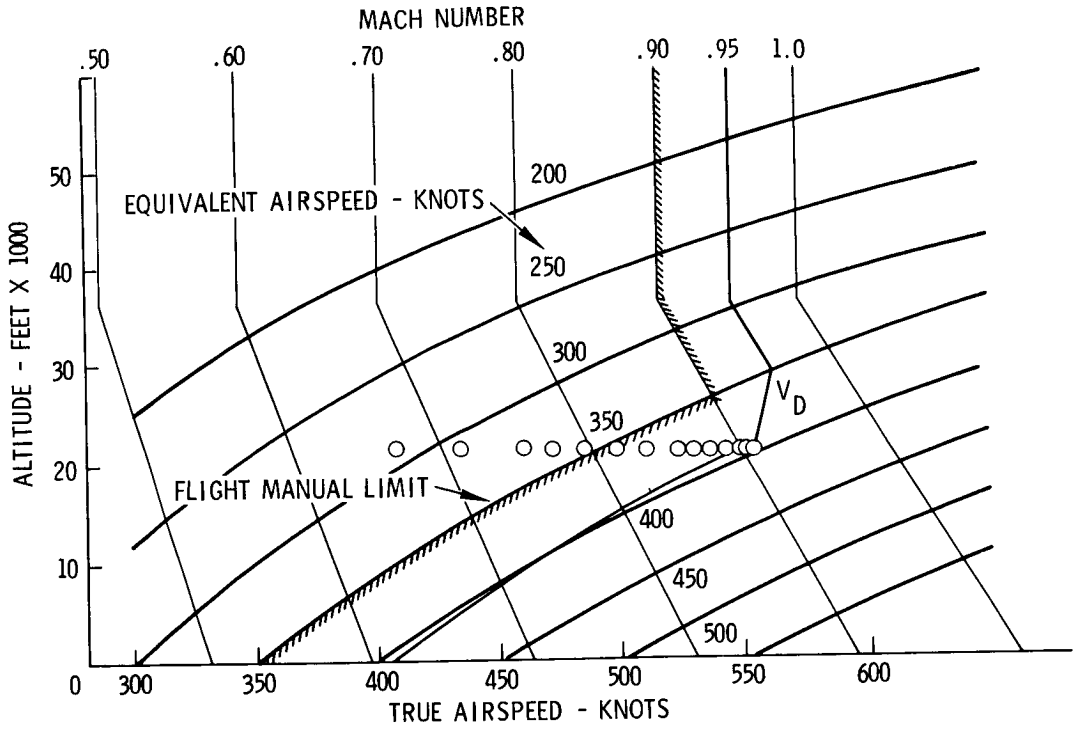

Figure 3. - Flight test envelope

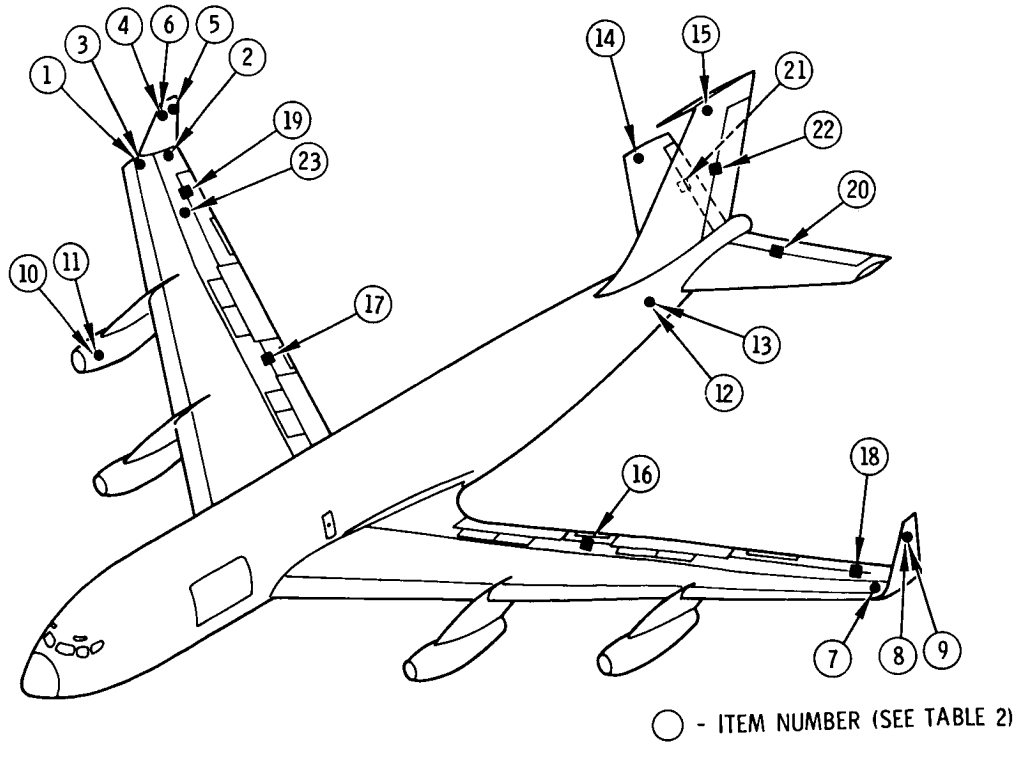

Figure 4. - Airplane instrumentation locations

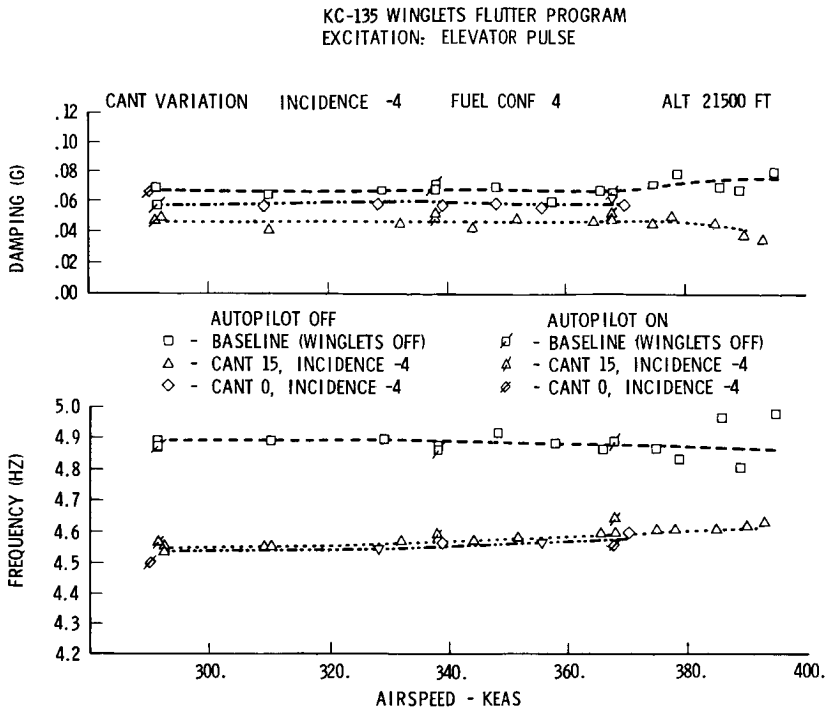

Figure 5. - Cant angle variation for elevator excitation

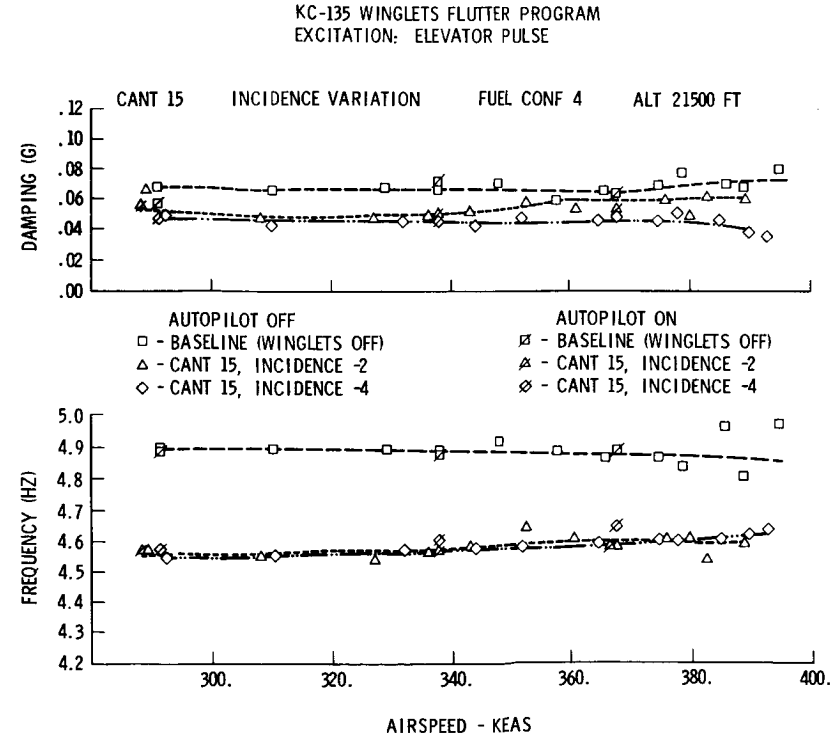

Figure 5. - Incidence angle variation for elevator excitation

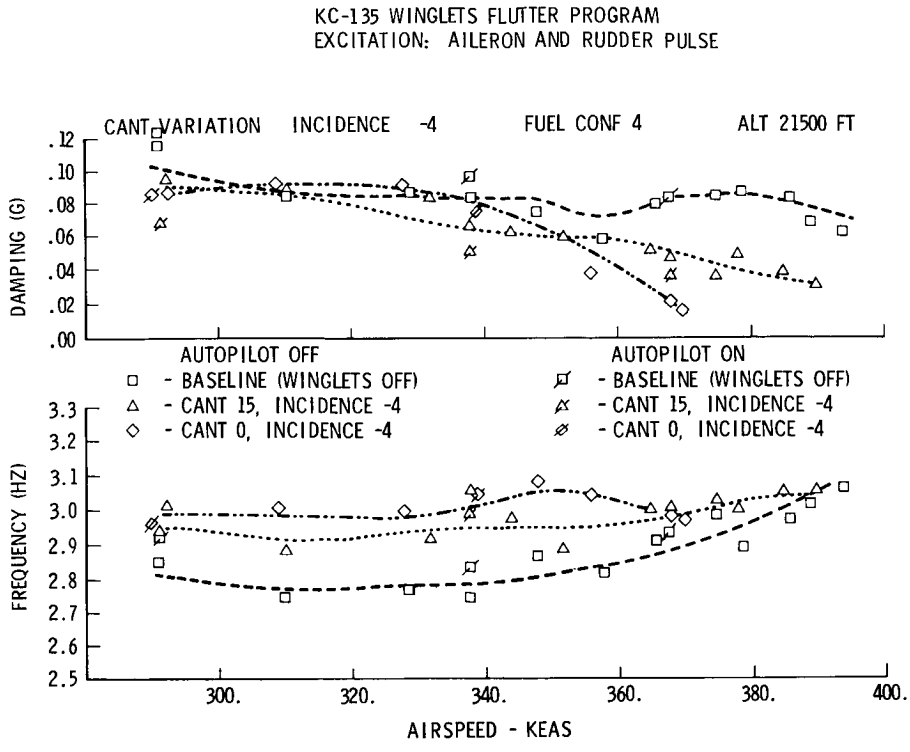

Figure 7. - Cant angle variation for aileron and rudder excitation

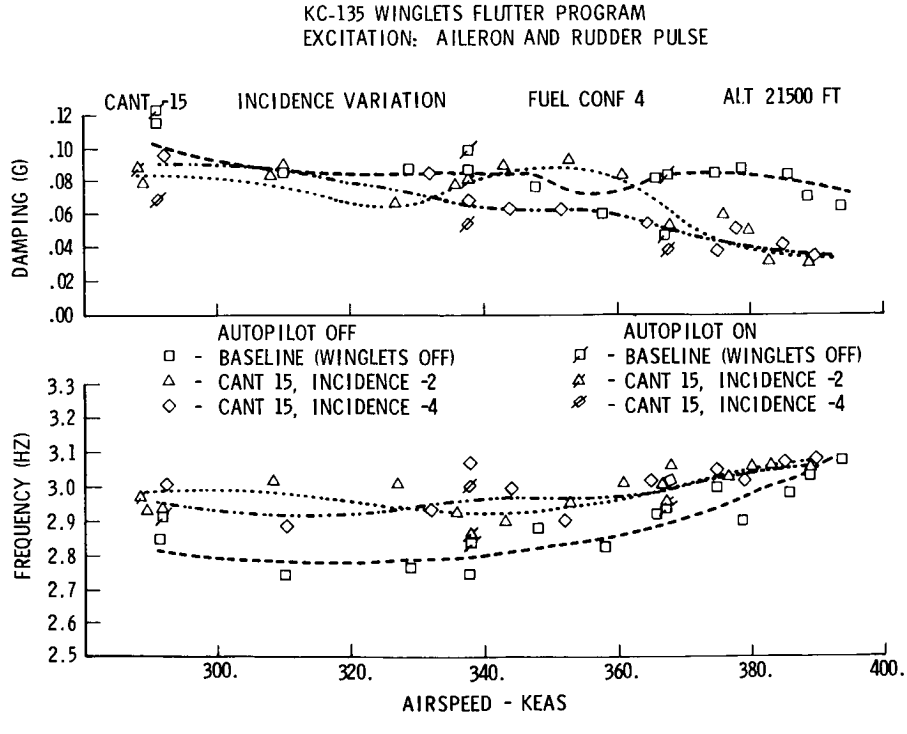

Figure 8. - Incidence angle variation for aileron and rudder excitation

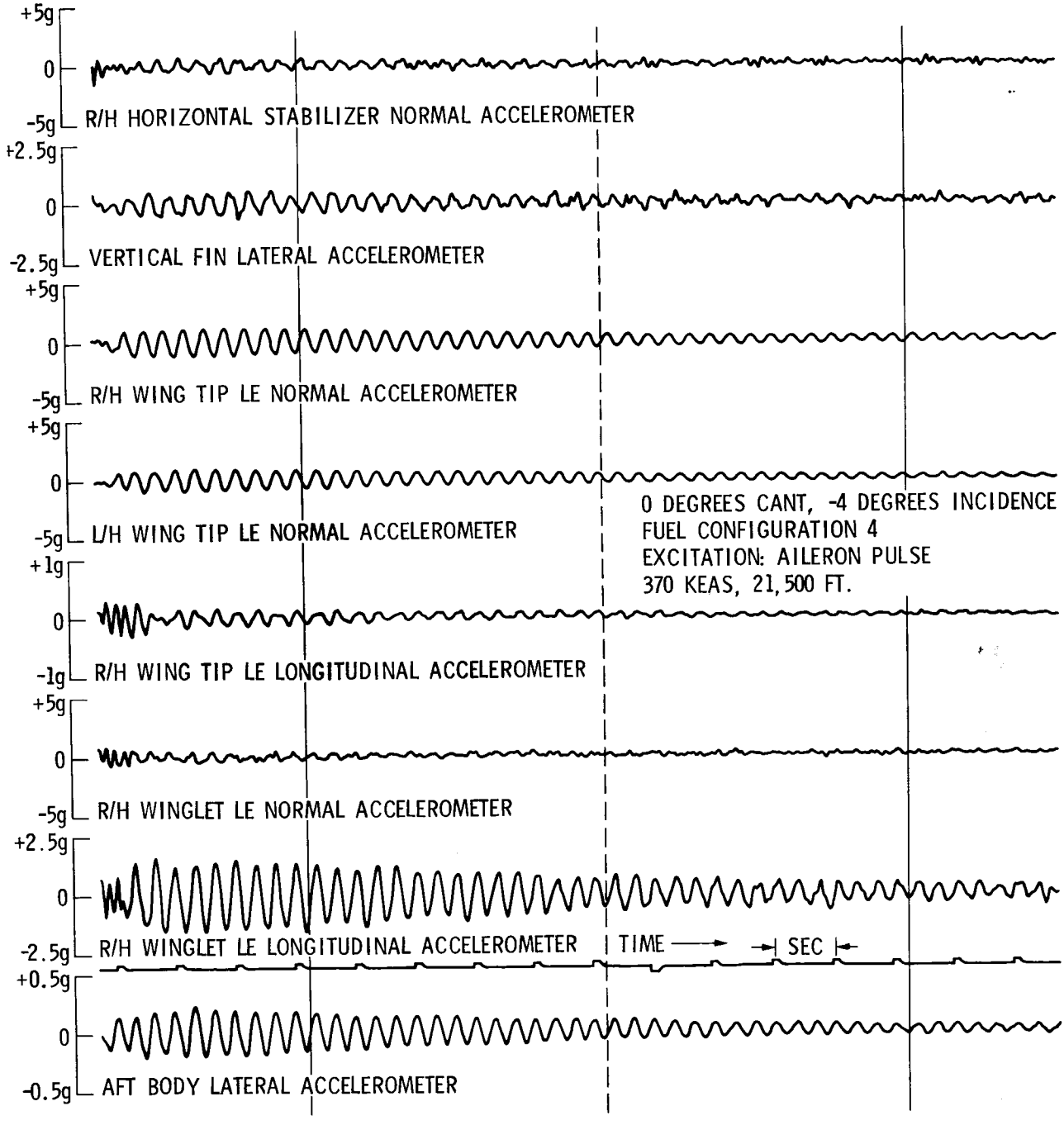

Figure 9. - Time history of 3.0 Hz antisymmetric oscillation

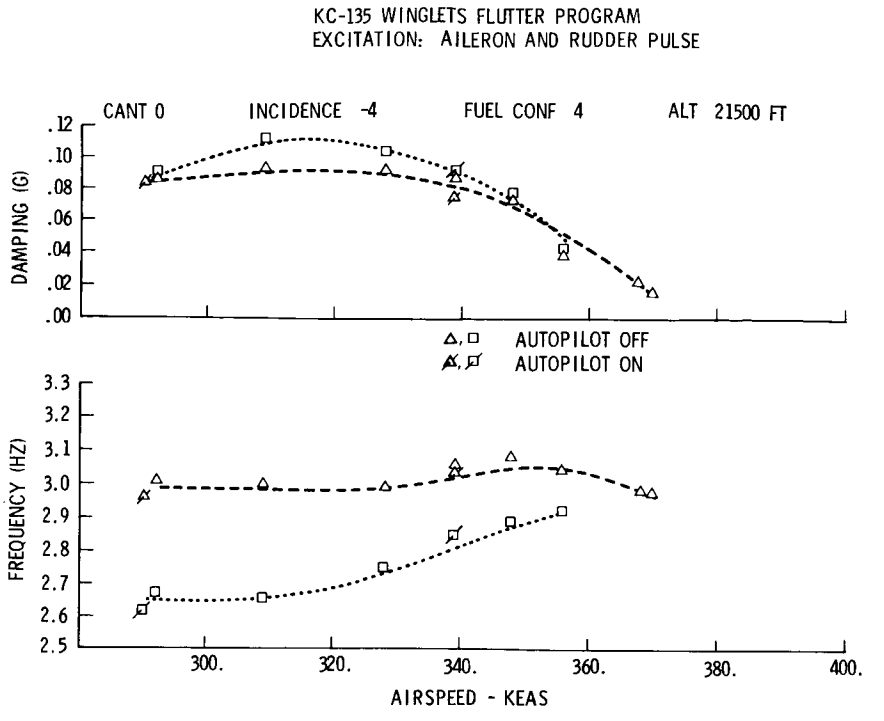

Figure 10. - Frequency and damping versus airspeed

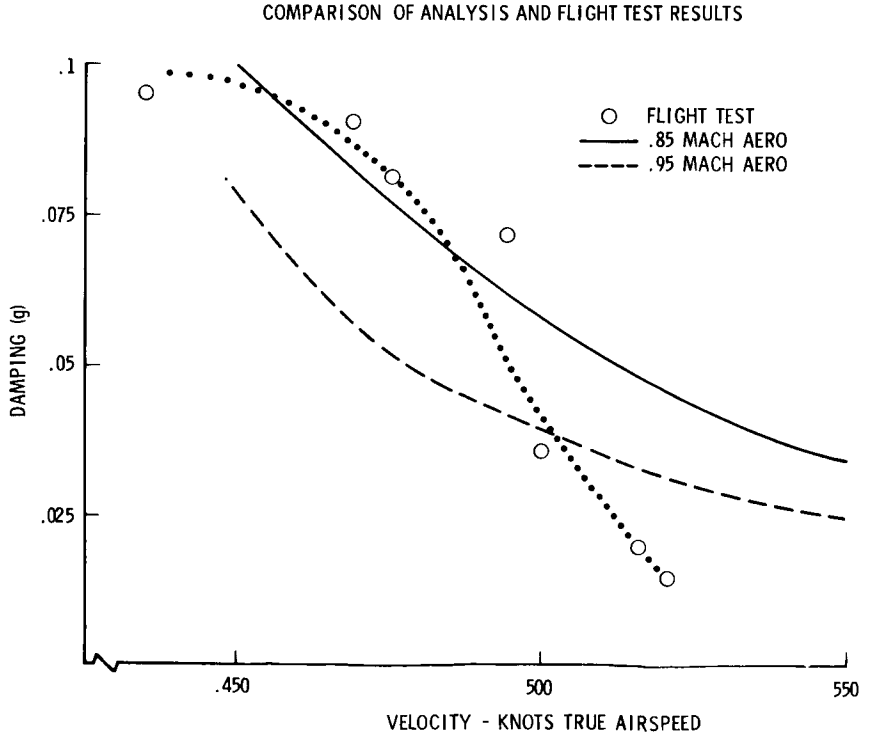

Figure 11. - Comparison of analysis and flight test results

1. Report No.	2. Government Accession No.	3. Recipient's Catalog No.
NASA CP-2211		

4. Title and Subtitle	5. Report Date
KC-135 WINGLET PROGRAM REVIEW	January 1982
	6. Performing Organization Code: 534-02-14
7. Author(s)	8. Performing Organization Report No.: H-1165
	10. Work Unit No.
9. Performing Organization Name and Address: Ames Research Center, Dryden Flight Research Facility, P.O. Box 273, Edwards, CA 93523	11. Contract or Grant No.
	13. Type of Report and Period Covered: Conference Publication
12. Sponsoring Agency Name and Address: National Aeronautics and Space Administration, Washington, D.C. 20546	14. Sponsoring Agency Code

15. Supplementary Notes

16. Abstract

A review of the results of a joint NASA/USAF program to develop and flight test winglets on a KC-135 aircraft was held at the Dryden Flight Research Center on September 16, 1981. This publication is a compilation of the results presented. The winglet development from concept through wind tunnel and flight tests is discussed. Predicted, wind tunnel, and flight test results are compared for the performance loads and flutter characteristics of the winglets. The flight test winglets had a variable winglet cant and incidence angle capability which enabled a limited evaluation of the effects of these geometry changes.

17. Key Words (Suggested by Author(s))	18. Distribution Statement
Winglets KC-135 aircraft Aerodynamics Loads Flutter Fuel mileage	FEDD distribution Subject category 02

19. Security Classif. (of this report)	20. Security Classif. (of this page)	21. No. of Pages	22. Price
Unclassified	Unclassified	192	

NASA-Langley, 1982